Harnessing the therapeutic potential of the Heme Oxygenase system

Nicole Campbell

B.Sc. Human Health and Disease

A thesis submitted to

Trinity College Dublin

for the degree of

Doctor of Philosophy

Supervisor: Prof. Aisling Dunne

Co-Supervisor: Prof. Jean Fletcher

Molecular Immunology Group

School of Biochemistry and Immunology

Trinity College Dublin

2018

Declaration of Authorship

I declare that this thesis has not been submitted as an exercise for a degree at this or any other university and it is entirely my own work, except where otherwise stated. I agree to deposit this thesis in the University's open access institutional repository or allow the library to do so on my behalf, subject to Irish Copyright Legislation and Trinity College Library conditions of use and acknowledgement.

_____

Nicole Campbell

Acknowledgements

They say it takes a village to raise a child, well the same can certainly be said of PhD students! If I were to express the depth of my gratitude to everyone who helped 'raise' me in these acknowledgements they would probably stretch to the length of this thesis, so I will have to do my best to keep it brief.

First, I would like to extend my profound thanks to my supervisor and mentor, Prof. Aisling Dunne. I have learnt so much from you these past few years, and your talent, creativity and tenacity continue to be a huge inspiration to me. Thank you so much for taking a chance on me when offering me this project, and for continuing to support me as I take the next step in my career. I am sincerely grateful for the time you have invested in me and this thesis, and for your endless patience and encouragement throughout. I would also like to thank my equally wonderful co-supervisor, Prof. Jean Fletcher, who has supported me from the earliest days in my career. Thank you for seeing potential in me as an undergraduate, and for recommending me for this PhD! It has been an honour to learn from you over the years, and I greatly appreciate your input to this project. Few people are lucky enough to have a supervisor who is equal parts brilliant, knowledgeable and kind, but somehow I have been blessed with two! I would also like to thank the Health Research Board who provided funding for this project.

To all the past and present members of the Dunne lab, thank you for making the lab feel less like work and more like a second home. Clare and Emma, you both warmly welcomed me to the lab and patiently taught me how everything works during my first few years. Thanks for bringing so much fun to the lab, and for being excellent examples to live up to! To Dónal, thank you for all the chats over a glass (or a few!) of wine, and for your frequent words of encouragement. To Sharee, who was a huge help to me as both an undergraduate and in the first year of my PhD, and who played a significant role in the shaping of this project. Thank you so much for all you have taught me, and for continuing to be an excellent role model. Thanks also to Louise and Níal, who both helped out during this project and brought a lot of laughs to the lab! Glyn, the founder of team HO-1, it has been great to have you on side. I have thoroughly enjoyed all our morning and evening conversations about politics, and our HO-1 brainstorming in the pub! A huge thanks also to Olwyn, who has been not only an ideal co-worker but also a brilliant friend throughout my time in the lab. Whether I needed someone to celebrate with, or someone to vent to, I could always rely on you. To Hannah, although you've only been in the lab a year you've already been such a great help to me as I've scrambled to finish this PhD! Thank you for your friendship, and I'm glad to know team HO-1 is in safe hands! Finally, thank you to Eva, our newest lab member, for her assistance and kindness during the last few months.

Thank you to the members of the Fletcher lab, who I also worked closely with during this PhD. To Deborah, thank you for all your help over the years, especially for teaching me everything I know about Seahorse! Jamal, thank you for always bringing life and laughter wherever you go. Thanks to Andreea for both her scientific and culinary suggestions. A big thanks also to Barry, who has always been on hand to help with flow queries, and who kindly taught me how to use SPICE. Thanks for being a great teacher and friend. Aside from my two groups, I also had the pleasure of working alongside the other labs of 3.12: a huge thank you to all members of the McLaughlin, Stevenson and Lalor labs, who have made the lab such a wonderful place to work. I'm glad to call so many of you friends and I will miss you when I'm gone! I would also like to thank Prof. Brian Kirby and his lab in St. Vincent's Hospital for providing access to the psoriasis patients' blood samples used in this project. Thanks to the Downer lab for their input during lab meetings, and to Dr. Gareth Brady for lending advice and reagents to this project. Finally, thanks to all the staff of TBSI, including everyone in the teaching lab, our tech support team Liam and Noel, and Gaby and Sara in the office. All of you have supported me at some point during this PhD, and without whom things would certainly have run a lot less smoothly. I would like to pay special tribute to David O'Beirne, who was a much beloved and talented member of the school office, and who tragically passed away near the completion of this thesis.

To my stellar group of HSD girls: thank you all so so much for your ongoing friendship, love and support. Often it feels like you're my personal cheerleading squad, so strong has your encouragement been! I know I can achieve anything with such a wonderful group of women behind me, and know I am always cheering you on too. To Em and Nix, my oldest friends, thank you for always being there for a laugh, or a shoulder to cry on, and for acting as my lab 'assistants'! Thanks to Emma Leacy, who was my first friend in college and has been a great support to me throughout. Thanks especially for all your help with my Seahorse experiments, including staying late to eat takeaway and watch Drag Race with me on those crazy 18 hour days! Unfortunately I don't have space to mention all my other amazing friends, but you know who you are; thank you for all the joy you've brought into my life.

To my family, thank you for instilling in me the value of learning, and for your love and support even through difficult times. I realise I am highly privileged to have had the opportunity to do this PhD, and I owe where I am today to the sacrifices you made to prioritise my education. A special word of thanks to my Dad, who always took an interest in my work and is probably one of the few people who will read this thesis aside from my examiners!

Lastly, to Mike, who will never admit that he deserves acknowledgement, but who has been my centre these past 8 years. Your love has taught me to believe in myself and my abilities, kept me grounded through my darkest days, and helped me find reserves of strength I did not know I had. I know you would (quite literally!) go to the end of the earth for me, and I can't wait to start this next chapter with you by my side.

Abstract

The stress response enzyme, Heme Oxygenase 1 (HO-1), has been identified as an important immunomodulator which is highly upregulated in response to cellular stress and inflammation. HO-1 catalyses the conversion of free heme into the linear tetrapyrroles (LTPs), biliverdin (BV) and bilirubin, with the concomitant release of carbon monoxide. Interestingly, HO-1 and its reaction products have been reported to be protective in various models of autoimmune and inflammatory disease. Despite the promising therapeutic potential of the HO-1 system, implementation of HO-1-based therapies is hindered by the lack of clinically suitable HO-1 inducers and products. The plant-derived polyphenols, carnosol and curcumin, have been identified as candidate HO-1 inducers, however, there has been limited investigation into their effects on human immune cells. Furthermore, the marine-derived LTP, phycocyanobilin (PCB), is a structural analogue to BV, yet their anti-inflammatory activities have not been directly compared.

In order to determine whether carnosol, curcumin and PCB are viable alternatives to currently-available HO-1 modulators, and to learn more about the HO-1 system in general, this study investigated their effects on the immunologic and metabolic functions of human dendritic cells (DC) and peripheral blood mononuclear cells (PBMC). The results demonstrate that carnosol and curcumin effectively regulate the maturation and pro-inflammatory functions of human DC, through HO-1 dependent inhibition of mitogen-activated protein kinase signalling. Additionally, PCB was found to display similar efficacy to BV as an immunomodulator in human DC, and both BV and carbon monoxide were identified as important mediators of HO-1 anti-inflammatory activity in DC. Carnosol and curcumin also regulated the metabolic reprogramming of activated DC and PBMC, and a novel signalling pathway involving AMP-activated Protein Kinase-dependent upregulation of HO-1 by these polyphenols was uncovered in the course of this study. Treatment of PBMC and $CD4^+$ T cells with carnosol or curcumin was additionally found to significantly reduce T cell proliferation and pro-inflammatory cytokine production. Finally, the anti-inflammatory effects of these polyphenols observed in healthy human PBMC was applied to the context of psoriasis through investigation of their efficacy in *ex vivo* psoriasis patient PBMC. Curcumin, but not carnosol, significantly inhibited T cell proliferation and cytokine poly-functionality, with reduced expression of the psoriasis-associated cytokines IFNγ, IL-17, GM-CSF and IL-22 observed in curcumin-treated PBMC. These results therefore describe the immunological effects of carnosol, curcumin and PCB in human immune cells, and, furthermore, provide important insight into the mechanism of action of HO-1 in human DC, and its relationship to immunometabolism. Thus, this study supports the use of these naturally-derived compounds as alternative modulators of the HO-1 system, with relevance for the treatment of autoimmune and inflammatory diseases.

Publications

Campbell, N.K., Fitzgerald H.K., Malara, A., Hambly, R., Sweeney, C.M., Kirby, B., Fletcher, J.M., & Dunne, A. Naturally derived Heme-Oxygenase 1 inducers attenuate inflammatory responses in human dendritic cells and T cells: relevance for psoriasis treatment. *Sci. Rep.* **8**:10287 (2018)

Basdeo, S.A., **Campbell, N.K.**, Sullivan, L.M., Flood, B., Creagh, E.M., Mantle, T.J., Fletcher, J.M., & Dunne, A. Suppression of human alloreactive T cells by linear tetrapyrroles; relevance for transplantation. *Transl. Res.* **178:**81–94.e2 (2016)

Campbell, N.K.*, Williams, D.G.*, Barry, P., Fitzgerald, H.K., Cunningham, C.C., Nolan, D., & Dunne, A. *Trypanosoma brucei* secreted aromatic ketoacids activate the Nrf2/HO-1 pathway and suppress pro-inflammatory responses in primary murine glia and macrophages. (Manuscript in preparation)
*Equal contribution

Campbell, N.K, Fitzgerald, H.K., Fletcher, J.M., & Dunne, A. AMPK-dependent regulation of HO-1 expression by plant-derived polyphenols. (Manuscript in preparation)

Awards

October 2017: Health Research Board "Ones 2 Watch" Competition Finalist (4 total)
http://hrbones2watch.com/competition/

September 2017: Trinity College Dublin Probe 2017 "Thesis in 3" Overall Winner

August 2016: Amgen Scholars Program Alumni Travel Award (GBP£1000)

Abbreviations

2-DG	2-deoxy-D-glucose
ADP	Adenosine Diphosphate
AICAR	5-Aminoimidazole-4-carboxamide ribonucleotide
AMP	Adenosine Monophosphate
AMPK	AMP-activated Protein Kinase
AP-1	Activator Protein 1
APC	Antigen Presenting Cell
ARE	Antioxidant Response Element
ATP	Adenosine Triphosphate
BMDC	Bone Marrow Derived Dendritic Cell
BMDM	Bone Marrow Derived Macrophage
BV	Biliverdin
BVR	Biliverdin Reductase
cAMP	Cyclic AMP
CARD	Caspase Activation and Recruitment Domain
CAPS	Cryopyrin-Associated Periodic Syndrome
cDC	Classical Dendritic Cell
CDP	Common Dendritic Cell Progenitor
CNS	Central Nervous System
CO	Carbon Monoxide
CoPP	Cobalt Protoporphyrin IX
CORM	Carbon Monoxide Releasing Molecule
CTLA4	Cytotoxic T-lymphocyte Associated Protein 4
CTV	Cell Trace Violet
DAMP	Danger Associated Molecular Pattern
DAPI	4’,6-diamidino-2-phenylindole
DC	Dendritic Cell
DMEM	Dulbecco’s Modified Eagle’s Media
DMF	Dimethyl Fumarate
DMSO	Dimethyl sulfoxide
DNA	Deoxyribonucleic Acid

DSS	Dextran Sulfate-Sodium
DQ-Ova	DQ Ovalbumin
EAE	Experimental Autoimmune Encephalitis
ECAR	Extracellular Acidification Rate
ECL	Enhanced Chemiluminescent HRP Substrate
EDTA	Ethylenediaminetetraacetic acid
ELISA	Enzyme-Linked Immunosorbent Assay
ER	Endoplasmic Reticulum
ETC	Electron Transport Chain
FBS	Foetal Bovine Serum
FCCP	Carbonyl cyanide-4-(trifluoromethoxy)phenylhydrazone
FMO	Fluorescence-Minus-One
FOXP3	Forkhead Box P3
FSC	Forward Scatter
GM-CSF	Granulocyte-Monocyte Colony-Stimulating Factor
Hb	Hemoglobin
HIF1α	Hypoxia Inducible Factor 1α
HO-1	Heme Oxygenase 1
HSLB	High Stringency Lysis Buffer
IκB	Inhibitor of κB
IBD	Inflammatory Bowel Disease
iDC	Immature Dendritic Cell
IKK	IκB Kinase
IL	Interleukin
iNOS	Inducible Nitric Oxide Synthase
IRAK	Interleukin 1 Receptor Associated Kinase
IRF	Interferon Regulatory Factor
LPS	Lipopolysaccharide
LTP	Linear Tetrapyrrole
MACS	Magnetic-Activated Cell Sorting
MAPK	Mitogen Activated Protein Kinase
MHC	Major Histocompatibility Complex

MFI	Mean Fluorescence Intensity
MS	Multiple Sclerosis
mTOR	Mammalian Target of Rapamycin
mTORC1	Mammalian Target of Rapamycin Complex 1
mTORC2	Mammalian Target of Rapamycin Complex 2
NADPH	Nicotinamide Adenine Dinucleotide Phosphate-Oxidase
NET	Neutrophil Extracellular Trap
NF-κB	Nuclear Factor κB
NFAT	Nuclear Factor of Activated T-cells
NFE2	Nuclear Factor Erythroid 2
NLR	NOD-like receptor
NO	Nitric Oxide
Nrf2	NFE2 Related Factor 2
OCR	Oxygen Consumption Rate
PAMP	Pathogen Associated Molecular Pattern
PASI	Psoriasis Area Severity Index
PBMC	Peripheral Blood Mononuclear Cell
PBS	Phosphate Buffered Saline
PCB	Phycocyanobilin
PD1	Programmed Cell Death Protein 1
pDC	Plasmacytoid Dendritic Cell
PD-L1	Programmed Death-Ligand 1
PFA	Paraformaldehyde
PGC1α	Peroxisome proliferator-activated receptor gamma coactivator 1-alpha
PI	Propidium Iodide
PI3K	Phosphatidylinositol-3 Kinase
PMA	Phorbol 12-myristate 13-acetate
PRR	Pattern Recognition Receptor
PVDF	Polyvinylidene difluoride
RA	Rheumatoid Arthritis
RLR	RIG-I-like Receptor
RNA	Ribonucleic Acid

RORγt	Retinoic Acid Related Orphan Receptor γ Thymus
ROS	Reactive Oxygen Species
RPMI	Roswell Park Memorial Institute
SD	Standard Deviation
SEM	Standard Error of the Mean
siRNA	Small Interfering RNA
SLE	Systemic Lupus Erythematosus
SnPP	Tin Protoporphyrin
SRC	Spare Respiratory Capacity
SSC	Side Scatter
TCA	Tricarboxylic acid
TCR	T Cell Receptor
TGFβ	Transforming Growth Factor β
Th cell	T-Helper Cell
TIR	Toll/Interleukin 1 Receptor
TLR	Toll-Like Receptor
TNFα	Tumour Necrosis Factor α
Treg	Regulatory T Cell
iTreg	Induced Treg
nTreg	Natural Treg
US	Unstimulated

Table of Contents

Chapter 1:
Introduction

1.1 The Immune System

The immune system is comprised of an intricate network of organs, cells and soluble mediators which are specialised to protect the host from infection and cellular damage. The mammalian immune system is described as having two main 'arms'; the innate and adaptive immune systems. The innate immune system is evolutionarily the oldest part of the modern day immune system, and represents the host's first line of defence against invading pathogens (1). Innate immune defences include physical and chemical barriers to pathogen entry and immune cells such as neutrophils, monocytes and macrophages which rapidly recognise and respond to any pathogens which overcome these barriers and gain entry to the host. The innate immune response is often sufficient to resolve minor infections, however when pathogens manage to overcome these defences, the adaptive immune system is activated.

The adaptive immune system, comprised of T and B cell lymphocytes, evolved more recently than the innate immune system and is confined to vertebrates (2,3). Although it is slower to respond to infections (typically taking days to mount an immune response after infection), it has significant advantages such as high specificity and immunological memory. The adaptive immune response is initiated after a specific pathogen-derived antigen is presented to a T or B cell by antigen-presenting cells (APCs) of the innate immune system. This confers a higher degree of specificity in the response against the pathogen, as only T or B cells with receptors to that antigen are competent to respond. Importantly, the adaptive immune response generates long lived immunological memory towards specific pathogens as responder cells remain in circulation for weeks, years or even decades, and can mount a quicker immune response in the event of reinfection (3,4).

Together, the innate and adaptive immune systems synergise to protect the host from infection and other threats such as cancer and cell damage. However, defects in the immune system can result in disease where immune responses are insufficient or mounted inappropriately against the host. Chronic infection, cancer, auto-inflammatory and autoimmune diseases are all products of a malfunctioning immune system and represent major threats to human health; it is essential, therefore, to understand how the different components of the immune system function and interact with each other, as well as how they can be modulated to develop novel treatments for immune diseases.

1.2 Regulation of the Immune Response

For an immune response to be successful it must be induced in a timely manner, be of appropriate specificity and magnitude to the threat encountered, and resolved after the threat has been

eliminated. To achieve this, the immune system has evolved numerous mechanisms to ensure it is able to rapidly recognise and distinguish between different pathogens, prevent inappropriate activation against benign or self-targets, and switch off activated immune cells once they are no longer required. These mechanisms include the development of immune cells with specialised effector and regulatory functions, signalling pathways that allow rapid and restricted immune cell activation, as well as modulation of broader cellular functions such as metabolic programming. Integration of these mechanisms is necessary to ensure appropriate regulation of the immune response.

1.2.1 Pattern recognition & signalling

In order to mount an immune response against a pathogen without inappropriately targeting the host's own healthy cells the immune system must be able to distinguish 'self' from 'non-self'. In the case of the innate immune system, which must be able to promptly recognise and react to pathogens, this distinction is performed by an array of 'pattern recognition receptors' (PRRs). PRRs detect broad molecular signatures, termed 'pathogen associated molecular patterns' (PAMPs), which are common to many different varieties of bacteria, fungi, protozoa and viruses. This allows the innate immune system to quickly initiate the correct response towards the type of pathogen detected (4). PRRs are also capable of recognising 'damage associated molecular patterns' (DAMPs) which are endogenous molecules that signal that cell damage has occurred; this allows for recruitment of immune cells to sites of cellular stress to resolve the cause of damage and facilitate tissue repair (5,6).

While there are numerous different PRRs, with each cell type expressing its own repertoire, they are broadly organised into families including Toll-like receptors (TLRs), NOD-like receptors (NLRs), RIG-I-like receptors (RLRs) and cytosolic DNA sensors (7). TLRs are the most extensive and best studied family of PRRs, expressed both on the surface of cells and within the cytoplasm, and can detect PAMPs from bacteria, fungi, protozoa and viruses, as well as DAMPs. For example, TLR4, the 'classical' TLR, is a cell surface receptor which recognises lipopolysaccharide (LPS) present on the surface of gram-negative bacteria (4,7,8). In contrast, NLRs, RLRs and cytosolic DNA sensors are only found in the cytoplasm and can recognise different microbial PAMPs and endogenous DAMPs. Together the various families of PRRs provide a wide range of mechanisms to detect pathogens and stressed cells, with multiple receptors capable of detecting the same PAMPs and DAMPs. This provides redundancy in pattern recognition resulting in greater signal amplification and protection against pathogens which manage to avoid detection by certain PRRs.

Once activated, PRRs initiate an immune response appropriate for the PAMP or DAMP detected. This can be mediated by different signalling pathways depending on the PRR activated but in most cases culminates in the activation of transcription factors including NF-κB, IRF3/7 or AP-1, which upregulate genes encoding immune mediators such as cytokines or receptors depending on the cell type. TLR signalling is primarily conducted via recruitment of adaptor proteins containing TIR domains such as MyD88, TRIF, TRAM and TIRAP to the TIR domains of the TLRs. Association of this protein scaffold around the TLR results in the activation of IRAK kinases which facilitate downstream signalling including the activation of mitogen activated protein kinases (MAPKs) and transcription factors (7–10).

Signalling via NLRs is unique, as while many NLRs activate MAPKs and transcription factors upon detection of PAMPs or DAMPs, certain NLRs instead initiate the formation of the inflammasome; a large, multi-protein complex which facilitates the cleavage of caspases to produce mature forms of IL-1 family cytokines. The inflammasome is typically composed of an NLR sensor, the adaptor molecule ASC and pro-caspase 1; the best studied and most well-known of these being the NLRP3 inflammasome. Upon association with ASC, pro-caspase 1 undergoes self-cleavage and is released as the enzymatically active caspase 1. Caspase 1 cleaves both pro-IL-1β and pro-IL-18 into IL-1β and IL-18 respectively, which are potent members of the IL-1 cytokine family that strongly induce acute inflammation and pyrexia as well as influencing immune cell recruitment and polarisation (11). NLRP3 recognises various PAMPs and DAMPs, however inflammasome formation is described as a 'two step' process, requiring two separate signals or activators. The first step requires recognition of a PAMP or DAMP by PRRs, resulting in activation of NF-κB and the upregulation of the inflammasome components NLRP3, pro-IL-1β and pro-IL-18; this is often referred to as the 'priming' event. The second step involves integration of another signal which causes the oligomerization of the inflammasome components; the exact source and transduction of this signal is debated, with DAMPs such as ATP and particulates having been identified as effective NLRP3 agonists, however most theories of NLRP3 activation agree on either K^+ efflux, reactive oxygen species (ROS) generation or other cellular damage produced by triggers acting elsewhere in the cell (11–13). In this way, NLRP3 is capable of responding to multiple different stimuli, as it does not appear to directly contact PAMPs or DAMPs, and acts as a 'master' sensor of infection and cellular stress to regulate production of the highly pro-inflammatory cytokines IL-1β and IL-18.

In summary, pattern recognition by the innate immune system is a robust mechanism of rapid detection and response to infection and cellular damage. Much of innate immune cell activation also centres on the formation of the inflammasome, which acts to regulate production of the

potent IL-1 family cytokines by requiring the convergence of multiple signals for the release of their active forms. Indeed, inappropriate activation of PRRs and the inflammasome has been implicated in many non-infectious diseases such as atherosclerosis and osteoarthritis (14,15), and auto-inflammatory diseases such as the cryopyrin-associated periodic syndromes (CAPS) (12). It is therefore important to identify mechanisms of inhibiting or limiting PRR signalling in order to develop novel inhibitors of inappropriate inflammation. An overview of the major PRR signalling pathways in innate immune cells is presented in Figure 1.1.

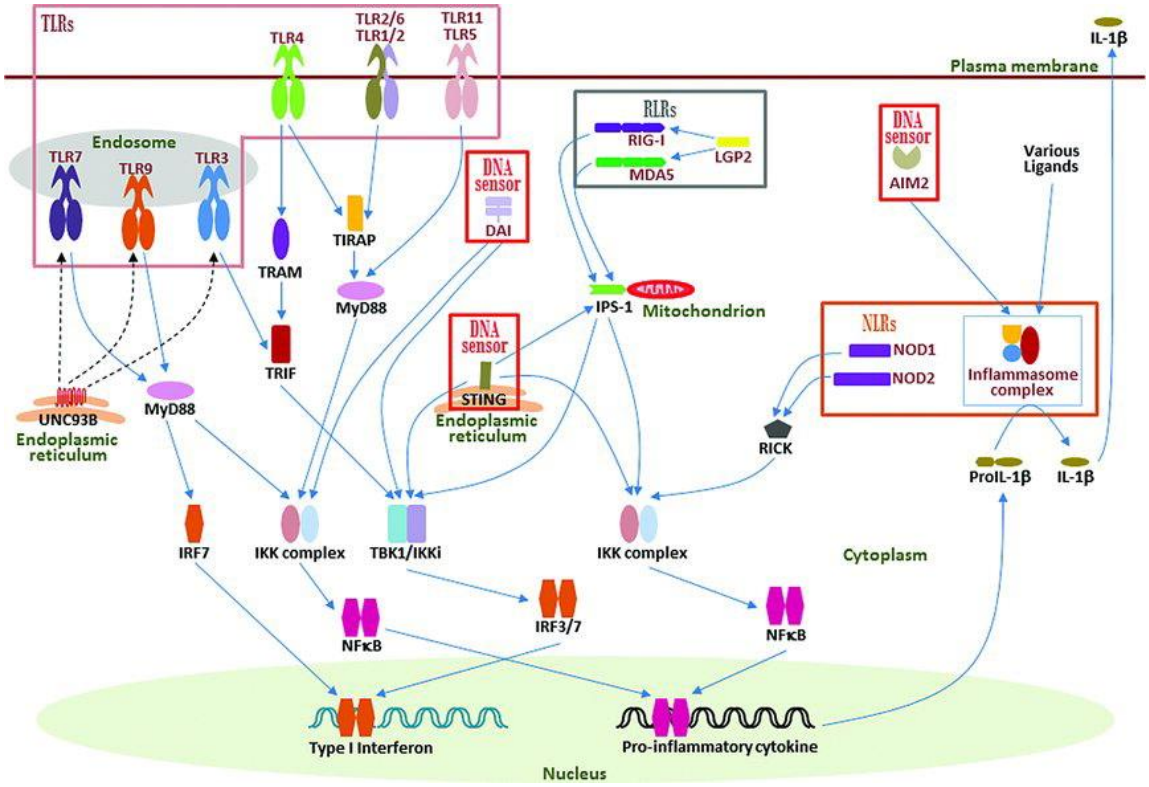

Figure 1.1. Pattern recognition and signalling in the innate immune system. Image from (7).

1.2.2 Dendritic cells

Dendritic cells (DC) are mononuclear phagocytes of the innate immune system which are specialised towards immune surveillance and antigen presentation. DC are exclusively derived from bone marrow precursor cells; macrophage and DC progenitors give rise to common DC progenitors and monocytes, both of which undergo differentiation into DC (16). There are two major DC subsets; classical DC (cDC) which populate most tissues and have an enhanced ability to capture, process and present antigens, and plasmacytoid DC (pDC) which are primarily found in blood and lymphoid tissues and have limited PRR expression and antigen capture, but are major producers of type 1 interferons in response to nucleic acid PAMPs (17,18). For the remainder of this thesis the abbreviation 'DC' will refer to classical DC only.

Due to their heightened capacity to take up and process antigens, and unique ability to prime naïve T cells, DC are widely regarded as the 'professional' APC of the immune system. Immature DC act as sentinel cells within tissues by constantly sampling antigens from their environment in order to detect PAMPs or DAMPs. Once DC are activated by an antigen they undergo extensive phenotypical and functional changes; antigen capture is significantly reduced while expression of major histocompatibility complexes (MHC), co-stimulatory molecules, chemokine receptors and cytokines are highly upregulated. This allows DC to respond to the pathogen or cell damage *in situ* while also preparing the required machinery for antigen presentation; antigens are processed within endosomes, loaded onto MHC Class I or Class II molecules and expressed on the cell surface alongside co-stimulatory receptors (19). Expression of the chemokine receptor CCR7 allows DC to receive chemotactic signals via CCL19 and CCL21 which induce migration towards tissue-draining lymph nodes (20,21). Here, mature DC are able to contact and activate naïve T cells. Full T cell activation requires the input of two separate signals; the first signal is provided by ligation of the MHC-antigen complex with the T cell receptor (TCR) and CD4 or CD8 co-receptor, and the second signal by co-stimulation between CD80 or CD86 expressed on the DC and the T cell CD28 receptor. Additionally, polarising cytokines such as IL-1β, IL-6, IL-12 and IL-23 produced by DC contribute to the differentiation of T cells into discrete T helper subsets (22). While other APCs can present antigens to activated or memory T cells, DC are the only APC capable of activating naïve T cells (23). Consequently, DC are often described as the 'bridge' between the innate and adaptive immune systems as they can respond directly to pathogens while also initiating and directing the adaptive immune response (Figure 1.2).

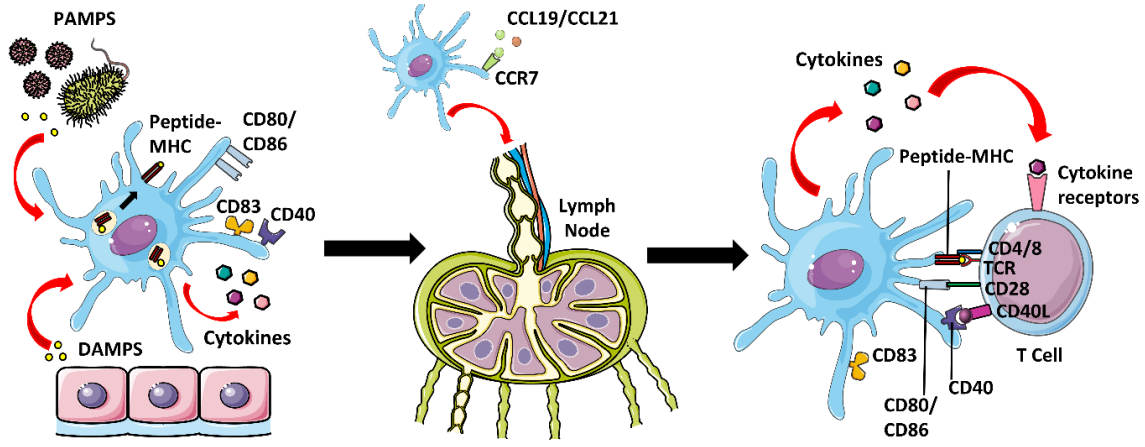

Figure 1.2. Maturation process of DC. DC uptake antigens from the surrounding tissue environment. Upon activation by PAMPs or DAMPs, DC upregulate expression of MHC molecules, co-stimulatory receptors, and cytokines. DC then migrate to the lymph node where they contact naïve T cells. Activation of T cells requires input of two signals; ligation of the MHC-peptide complex with the TCR and co-stimulation through ligation of CD80/CD86 with CD28. Cytokines produced by DC contribute to the polarisation of T cells into different effector subsets.

In addition to responding to pathogens and recruiting the adaptive immune system, DC have been recognised as important arbiters of immune tolerance. While the immune system must be competent to respond to infection and cellular damage, it is essential that it is carefully regulated to avoid excessive inflammation, allergy or autoimmunity. The majority of self-reactive T cells, which recognise self-antigens, are deleted or differentiated into anti-inflammatory regulatory T cells (Tregs) during development within the thymus, which is termed 'central tolerance' (24). However, some self-reactive T cells are released into the periphery, and therefore additional checkpoints exist to maintain 'peripheral tolerance' (25). These checkpoints aim to induce 'anergy' of self-reactive T cells, rendering them unresponsive and unable to mount an immune response to encountered self-antigens (26). DC are key mediators of peripheral tolerance; immature DC uptake and display self-antigens to T cells under steady-state conditions, but in the absence of a maturation stimulus DC lack expression of CD80 and CD86 to provide co-stimulation and cytokine production for T cell polarisation (Figure 1.3) (27–31). Activation of the self-reactive TCR by immature DC therefore results in T cell anergy, deletion, or in the presence of retinoic acid and transforming growth factor β (TGFβ) can induce differentiation into Tregs (31,32). Mature DC have also been shown to induce Tregs, lending credence to the idea that the activation and polarisation of T cells is dependent on the maturation stimuli received by DC and their environmental context, including the presence of specific soluble factors (31,33). Finally, tolerogenic DC also express ligands for the T cell checkpoint inhibitors programmed cell death 1 (PD1) and cytotoxic T lymphocyte associated protein 4 (CTLA4), which induce T cell anergy or deletion when activated (34,35).

Despite the contributions of DC to both immunity and immune tolerance, failure of these mechanisms can result in promotion of autoimmune disease or cancer by DC. TLR activation in DC during infection often precedes presentation of autoimmune diseases; this is thought to be a result of molecular mimicry, where presentation of microbial antigens closely resembling self-antigens activates autoreactive T cells, or direct activation of TLRs by self-antigens (36). Molecular mimicry has been implicated in the pathogenesis of psoriasis, as previous streptococcal infection is associated with the onset of certain types of psoriasis, although the exact antigen responsible is unknown (37). Activation of TLR7 and TLR9 by chromatin-containing immune complexes appears to be a predisposing event for development of systemic lupus erythematosus (SLE) and is particularly associated with IFN-α produced by pDC (38). Aside from initiating autoimmunity by activation of self-reactive T cells, DC within sites of inflammation can promote the differentiation of T cells into pathogenic subsets such as Th17 cells via production of pro-inflammatory cytokines (39,40). Conversely, tolerogenic DC can be exploited to promote the growth of cancers; cancer

cells cultivate anti-inflammatory tumour microenvironments and interact with tumour-infiltrating DC to downregulate expression of co-stimulatory molecules and pro-inflammatory cytokines, leading to the induction of Tregs and anergy of anti-tumour T cells (41,42). Activation of PD1 and CTLA4 on T cells by tumour infiltrating DC has recently been identified as major mechanism by which the immune response to cancer cells is inhibited; anti-PD1 and anti-CTLA4 antibodies have been met with significant success in the clinic against multiple types of cancer (43–46).

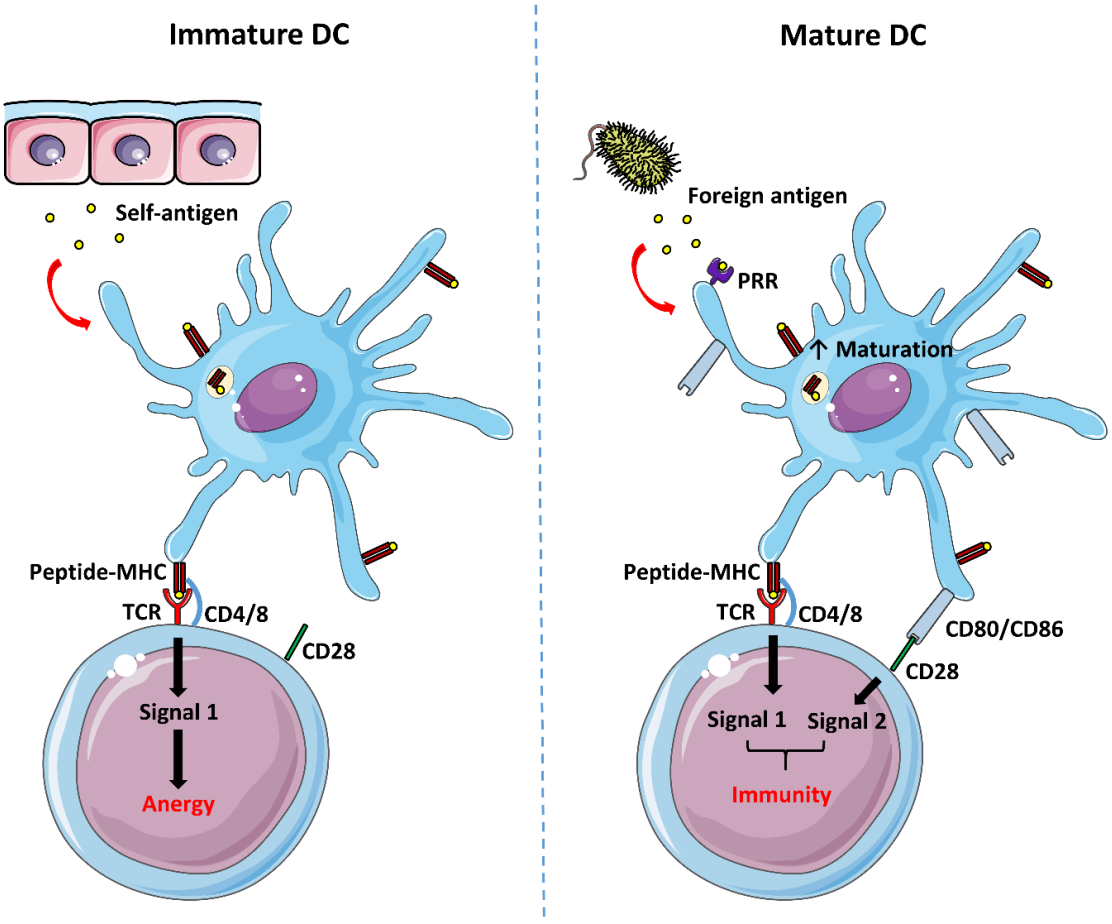

Figure 1.3. Induction of tolerance versus immunity by DC. Immature DC uptake self-antigens during the steady state and present them to T cells. T cells which recognise the self-antigen undergo anergy in the absence of co-stimulation from the DC. DC which encounter a foreign antigen are matured by PRR activation resulting in upregulation of co-stimulatory receptors. T cells which recognise the foreign antigen receive signals from both the TCR and co-stimulation and become activated.

Considering their central role within both the innate and adaptive immune system, and their involvement in the pathogenesis of many autoimmune and malignant diseases, it is unsurprising that DC have become a target for the development of novel immunotherapies. Inhibitors of DC maturation or their cytokines have been considered as treatments for autoimmune or chronic inflammatory conditions where DC promote inflammation and the expansion of pathogenic T cells; for example, antibodies against the DC cytokine IL-23 have been successful in the treatment

of psoriasis by inhibiting the polarisation of Th17 cells (47). Utilisation of DC-mediated tolerance has been suggested as a novel mechanism to reduce graft rejection in transplantation; tolerogenic DC can be generated *in vitro,* pulsed with alloantigen and injected into the host prior to transplantation in order to develop tolerance towards the alloantigen and promote Treg expansion (48). Finally, in addition to successful antibody treatments targeting PD1 and CTLA4, DC have been the focus of another experimental cancer treatment: the creation of a 'cancer vaccine'. This strategy aims to activate DC to induce anti-tumour T cell responses by either stimulating DC *in situ* with tumour antigens alongside an adjuvant, or maturing DC *ex vivo* and loading them with tumour antigens prior to reinjection into the patient (31,49). In summary, DC are involved in the mediation of both innate and adaptive immune responses, and while they contribute to the pathology of many diseases, they can also be targeted to treat disease through the development of novel immunotherapies.

1.2.3 T cells

T cells play a central role in cell-mediated immunity and are divided into numerous discrete subsets. Broad classification of T cells can be made based on their expression of cell surface markers; the majority of T cells express a TCR comprised of an α and β chain and are therefore termed αβ (alpha beta) T cells, however, a small minority of T cells instead express a TCR comprised of a γ and δ chain and are termed γδ (gamma delta) T cells. αβ T cells are further subdivided based on their expression of either the CD8 or CD4 co-receptor; $CD8^+$ T cells are known as cytotoxic T cells and recognise MHC Class I on host cells to kill virus infected or damaged cells, whereas $CD4^+$ T cells are termed 'helper' cells as they primarily manage the functions of other immune cells and thereby shape the immune response (50). $CD4^+$ T cells recognise MHC Class II on APCs and differentiate into different effector or regulatory subtypes, as described in section 1.2.2. γδ T cells are a rare population largely found at mucosal and epithelial sites and appear to be more 'innate-like' than αβ T cells as they recognise conserved non-peptide antigens directly without the need for antigen presentation by an APC, and rapidly respond once activated (51). An overview of the differentiation of the different T cell subsets is provided in Figure 1.4.

1.2.3.1 Th17 cells

Th17 cells are a T helper subset which provide immunity against extracellular pathogens such as *Candida albicans* and *Staphlyococcus aureus*. Th17 effector functions are mediated by their wide range of pro-inflammatory cytokines, including IL-17, IL-21 and IL-22. IL-17 family members, particularly IL-17A and IL-17F, are important for the recruitment and activation of neutrophils and can also act on non-immune cells in mucosa or epithelia to produce pro-inflammatory cytokines,

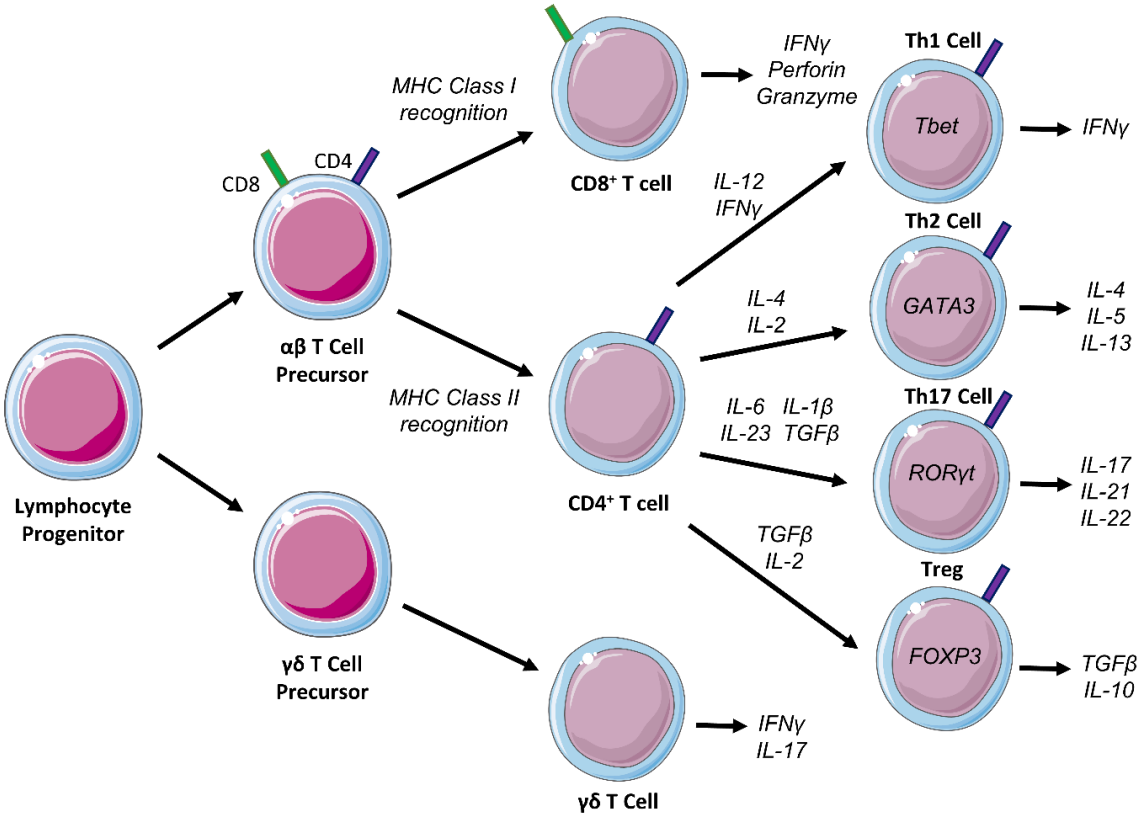

Figure 1.4. Overview of the development of different T cell subsets. Lymphocyte progenitors migrate to the thymus and develop into T cell precursors expressing either αβ or γδ TCRs. αβ T cell precursors express both CD4 and CD8 co-receptors; cells which recognise MHC Class I retain CD8 expression and become cytotoxic T cells, while cells which recognise MHC Class II retain CD4 expression and become T helper cells. $CD4^+$ T cells further differentiate into different T helper cell subsets depending on the cytokine signals received during activation.

chemokines and anti-microbial agents. IL-21 promotes Th17 cell differentiation and has a wide range of instructive effects on other immune cells, while IL-22 promotes proliferation and upregulation of anti-microbial agents in keratinocytes (52,53). Polarisation of naïve $CD4^+$ T cells to Th17 cells involves a combination of cytokines, especially TGFβ, IL-6 and IL-23. TGFβ induces the expression of the transcriptional regulators retinoic acid-related orphan receptor γ thymus (RORγt) and forkhead box P3 (FOXP3); RORγt instructs Th17 cellular programming, while FOXP3 controls Treg differentiation and inhibits RORγt activity. The addition of IL-6 and IL-23 activate STAT3 which stabilises RORγt expression, relieves inhibition by FOXP3 and promotes Th17 differentiation. As TGFβ is involved in the polarisation of both Th17 cells and Tregs the two populations are finely balanced, with the presence of pro-inflammatory cytokines determining the lineage decision (52–54).

Due to the reciprocal relationship between Th17 cells and Tregs the balance between tolerance and autoimmunity can be easily disrupted. Hence it is unsurprising that Th17 cells have been found

to be involved in the pathogenesis of numerous autoimmune diseases. The role of Th17 cells and IL-17 in autoimmunity was first described in multiple sclerosis (MS) and its murine model, experimental autoimmune encephalitis (EAE), in which autoreactive T cells degrade the myelin sheath surrounding the axons of neurons in the central nervous system (CNS), causing progressive loss of signal transmission and neuronal function. MS was originally thought to be a Th1 mediated disease, however, it is now recognised that Th17 cells are involved in at least the initiation of MS and EAE and early stages of neuroinflammation as: (i) mice with ablated Th17, but not Th1 cells, were protected from EAE induction, (ii) adoptive transfer of pathogenic Th17, but not Th1 cells, was sufficient to induce EAE in recipient mice, and (iii) neutralisation of IL-17 resulted in a less severe EAE phenotype (55–57). Th17-mediated inflammation has also been implicated in the pathology of rheumatoid arthritis (RA), a prevalent autoimmune disease characterised by progressive joint inflammation which results in painful deformity and immobility. High levels of IL-17 have been found in the inflamed synovium of RA patients and IL-17 has been shown to recruit neutrophils and monocytes to the joint and mediate destruction of synovial tissue (58). Furthermore, a novel subset of pathogenic 'ex-Th17' cells or 'non-classical Th1 cells', which are similar to Th1 cells but of a Th17 lineage, produce a wide variety of pro-inflammatory cytokines and are highly resistant to suppression by Tregs, has been described within the synovia of RA patients (59).

Finally, the contribution of Th17 cells to the pathogenesis of autoimmune diseases can be best observed in psoriasis, a skin disease characterised by extensive infiltration of immune cells and abnormal proliferation of keratinocytes, resulting in the development of painful and itchy skin lesions. IL-17 has been identified as the major cytokine responsible for the pathology of psoriasis through promotion of skin inflammation, immune cell recruitment and keratinocyte hyperproliferation. IL-17 and Th17 cells have been shown to be highly upregulated in psoriatic lesions and multiple genome-wide association studies have linked IL-17 related genes to psoriasis incidence (60,61). Other pro-inflammatory cytokines produced by Th17 cells, or induced by IL-17, such as IL-22, IL-1β and IL-36 have been shown to further drive skin inflammation and proliferation (62–65). The central role played by IL-17 and Th17 cells in psoriasis has been highlighted by the clinical success of monoclonal antibody treatments against IL-23, IL-17 and the IL-17 receptor; in many cases these new therapies have completely resolved psoriatic lesions in affected patients and appear to have long-lasting effects (66–68). Thus, further study of Th17 biology is likely to lead to new insights into autoimmune pathology and the development of novel treatment strategies.

1.2.3.2 Tregs

Tregs are a subset of T helper cells which act as the major enforcer of peripheral immune tolerance and contribute to the production of anti-inflammatory responses. Tregs are defined by expression of FOXP3 which is essential for their development and function, as well as the IL-2 receptor component CD25, as IL-2 is important for the maintenance of Treg populations (69,70). There are two major subsets of Tregs; natural Tregs (nTregs) which are derived directly from the thymus, and induced Tregs (iTregs) which arise in the periphery through differentiation of naive $CD4^+$ T cells via TGFβ. While the exact conditions required for the development of nTregs in the thymus are unclear, it is thought that they require high-affinity interactions between their TCR and self-peptide MHC complexes presented by thymic DC or medullary thymic epithelial cells alongside co-stimulation and the cytokines IL-2 and IL-7 (71). Unlike other T cell subsets, nTregs are functionally mature upon release from the thymus having undergone antigen priming in the thymus prior to encountering self-antigens in the periphery. These nTregs persist in the periphery throughout life and act to control autoreactive T cells which have escaped central tolerance mechanisms. Depletion of nTregs is associated with fatal autoimmune disease in both mice and humans (70).

Unlike nTregs, iTregs develop in peripheral tissues upon encounter of naïve $CD4^+$ T cells with self-antigens under steady-state or inflammatory conditions, and control the immune response at sites of infection or damage. iTregs also act in concert with nTregs to maintain immune tolerance and may have specialist roles such as maintenance of foetal tolerance during pregnancy and mucosal tolerance towards allergens (72). However, the primary function of iTregs appears to be the local regulation of inflammation within tissues: $CD4^+$ T cells differentiate into iTregs during inflammation in order to suppress T cell proliferation and pro-inflammatory cytokine production, thereby preventing excessive tissue damage from over-activation of the immune system (73,74). As a result of their transient role in regulating responses to infection or peripheral tolerance, iTregs have been observed to have less stable FOXP3 expression than nTregs and appear to be 'plastic', allowing them to gain characteristics and functions of other T helper subsets (72).

Tregs utilise a number of different cell- and cytokine-mediated mechanisms to exert their regulatory functions. The CTLA4 receptor is constitutively expressed by Tregs and binds the co-stimulatory molecules CD80 and CD86 on APCs, causing them to be internalised and destroyed by the Treg (75–77). This allows for the maintenance of tolerance as APCs presenting self-antigens are prevented from activating self-reactive T cells due to the absence of co-stimulation. CTLA4 has been shown to be essential for the suppressive function of Tregs (78), but is also associated with tumour promotion by suppression of anti-tumour T cells; anti-CTLA4 antibodies have been shown to improve cancer outcomes by blocking this inhibition of the immune response (43). Tregs also

suppress inflammation by the release of anti-inflammatory mediators into the surrounding microenvironment. The surface enzyme CD39 is highly expressed by Tregs and contributes to their suppressive function by catalysing the conversion of the pro-inflammatory DAMP adenosine tri-phosphate (ATP) into adenosine di-phosphate (ADP) (79–81). ADP can be further converted to adenosine by the ectoenzyme CD73, which binds the A2A purinergic receptor on inflammatory cells and upregulates intracellular levels of inhibitory cAMP (82,83). $CD39^+$ Tregs have been shown to be important in suppression of pathogenic Th17 cells in MS, but are also associated with promotion of chronic infections and cancer (84–89). Finally, production of the anti-inflammatory cytokines IL-10 and TGFβ is a major mechanism by which Tregs control immune tolerance and inflammation. TGFβ, as mentioned previously, regulates the development of iTregs, and therefore creates a positive feedback loop whereby Tregs promote the generation of further Tregs. IL-10 has wide-ranging effects on immune cells, including suppression of DC and macrophage function which results in downregulation of T cell responses. However, excessive or inappropriately released IL-10 can promote pathogen persistence and chronic infection (73,90).

In summary, Tregs are crucial for the maintenance of immune tolerance and prevention of deleterious immune responses. Both nTregs and iTregs are important in the context of autoimmunity and chronic inflammation, however they can also be exploited to create anti-inflammatory environments benefitting the expansion of pathogens or malignant cells.

1.2.4 Immunometabolism

Each living cell requires energy to function, and therefore contains cellular machinery to extract energy and biosynthetic precursors from the breakdown of different fuels. Recently it has become increasingly appreciated that cellular metabolism plays an important role in immune cell activation, and can shape the resulting immune response. Current research is now heavily focused on characterising the metabolic pathways utilised by different immune cells, and studying how altering these metabolic circuits in immune cells affects their function and the generation of pro- and anti- inflammatory immune responses.

1.2.4.1 Catabolic and anabolic metabolism

Metabolic pathways are defined as either catabolic or anabolic; catabolic metabolism involves the breakdown of complex molecules into simpler molecules with the release of energy, while anabolic metabolism uses simple molecules to build more complex molecules. Cells contain specific catabolic pathways to convert the three main fuel sources, carbohydrates, lipids and proteins, into energy, usually in the form of ATP. Carbohydrate metabolism first begins with the breakdown of complex carbohydrates into simple sugars, primarily glucose. Glucose is transported

into the cell via membrane glucose transporters, and is metabolised in the cytosol by an anaerobic pathway known as glycolysis, which catabolises glucose to pyruvate over the course of ten enzymatic reactions, generating 2 ATP and 2 NADH molecules. Pyruvate can either be converted to lactate and excreted by the cell, or transported into the mitochondria to undergo oxidative phosphorylation. Within the mitochondria, pyruvate is converted to acetyl-coA and enters the tricarboxylic acid cycle (TCA cycle, or Kreb's cycle) where it is catabolised to generate 3 NADH and 1 $FADH_2$. NADH and $FADH_2$ both provide electrons for the electron transport chain (ETC), which in the presence of oxygen creates a proton gradient across the mitochondrial inner membrane. This proton gradient is coupled to the enzyme ATP synthase, which converts ADP to ATP using the energy generated by allowing protons to travel back across the mitochondrial membrane. Each molecule of glucose can generate an additional 34 molecules of ATP during oxidative phosphorylation, making it a much more energy efficient process than glycolysis alone (91). Aside from glucose, cells can also use other fuels such as lipids and proteins as substrates for oxidative phosphorylation. Fatty acids are metabolised over a number of steps depending on the length of their aliphatic tails, eventually culminating in β-oxidation to produce large amounts of acetyl-coA, NADH, and $FADH_2$ for entry into the TCA cycle and ETC. Meanwhile, certain amino acids can be used as precursors for fatty acid synthesis and metabolism, or to produce intermediates of the TCA cycle (92).

Anabolic metabolism provides biosynthetic precursors necessary to build cellular components and energy stores. Fatty acid synthesis is an anabolic pathway opposing fatty acid oxidation, which uses intermediates from catabolic pathways including glycolysis and the TCA cycle to create *de novo* fatty acids (92). As the membranes of cells and their organelles are comprised of lipids, fatty acid synthesis supports the growth and proliferation of cells. Additionally, fatty acids can modulate cell signalling and post-translational protein modification, thereby influencing cellular responses (93). Cell growth and proliferation is also supported by the pentose phosphate pathway, which uses intermediates of glycolysis in the biosynthesis of nucleotides and amino acids. The pentose phosphate pathway also generates nicotinamide adenine dinucleotide phosphate-oxidase (NADPH), a cofactor required for the activity of numerous enzymes, including those involved in fatty acid synthesis and redox homeostasis (92,94). Finally, while protein synthesis is the primary anabolic pathway which utilises amino acids, certain amino acids can also be used as substrates for fatty acid synthesis, and contribute to the regulation of metabolic signalling (95).

While both catabolic and anabolic metabolism are necessary for the function of healthy cells, many of these processes directly oppose each other and therefore must be carefully regulated. Cells receive multiple signals from both intracellular sensors and their environment to inform

them of their energy status and nutrient availability, as well as stimuli for growth, proliferation and protein production. In order to integrate these signals to coordinate selection of a suitable metabolic response, cells have evolved 'master' sensors to regulate their metabolism. The primary anabolic sensor in mammalian cells is mechanistic target of rapamycin (mTOR), which is comprised of two complexes, mTOR Complex 1 (mTORC1) and 2 (mTORC2). Growth factors and mitogens activate signalling pathways which eventually converge to activate mTOR, which promotes synthesis of proteins, lipids and nucleotides via upregulation of their respective anabolic pathways (96,97). The increased expression of glycolytic genes by mTOR is mediated by its upregulation of the transcription factor hypoxia inducible factor 1α (HIF1α) (97), which also acts as an oxygen sensor, allowing for upregulation of anaerobic glycolysis when oxygen is limiting (98). Additionally, the activation of anabolic metabolism needs to be coupled to nutrient availability, therefore, mTOR is also positively regulated by nutrients such as glucose and amino acids (99,100). Integration of information on nutrient availability alongside growth and mitogenic signals allows for logical regulation of anabolic metabolism; the central regulatory role of mTOR in this process can be best observed in cancers where mutations in mTOR or its signalling partners often result in unrestricted cell growth and division (101).

While mTOR acts as a global regulator of anabolic metabolism, cells also require a mechanism to upregulate catabolic metabolism when energy is scarce. This role belongs to AMP-activated protein kinase (AMPK), an energy-sensing kinase which directly inhibits mTOR activity and downregulates anabolic metabolism. AMPK monitors the energy status of the cell by binding AMP, the precursor for ATP. When energy is plentiful the ratio of AMP:ATP favours ATP, resulting in low engagement of AMPK; however, during periods of starvation or cell stress the ratio of AMP:ATP increases, activating AMPK and initiating metabolic processes with the aim of increasing the cellular energy supply. AMPK activation upregulates a catabolic program which centres on oxidative phosphorylation; uptake of glucose and fatty acids into the cell is increased alongside promotion of their metabolism in the mitochondria (102). As oxidative phosphorylation is the most energy efficient metabolic pathway this allows the cell to prioritise energy production over the generation of biosynthetic precursors. To support this increase in mitochondrial activity, AMPK promotes mitochondrial biogenesis via phosphorylation of peroxisome-proliferator-activated receptor gamma coactivator 1α (PGC1α), the master regulator of mitochondrial function and metabolism (103). Furthermore, AMPK also promotes the recycling of organelles, including aberrant mitochondria, in a process known as autophagy, which functions both to improve cellular efficiency and provide fuels for catabolic metabolism (104). The upregulation of catabolic pathways and autophagy by AMPK has highlighted it as a target for the treatment of metabolic

disease (105). Interestingly, the drug metformin, an AMPK activator, is used as a first-line treatment for type II diabetes and has also been associated with reduced inflammation and incidence of cancer (106,107). A summary of the catabolic and anabolic metabolic pathways under the control of mTOR and AMPK is provided in Figure 1.5.

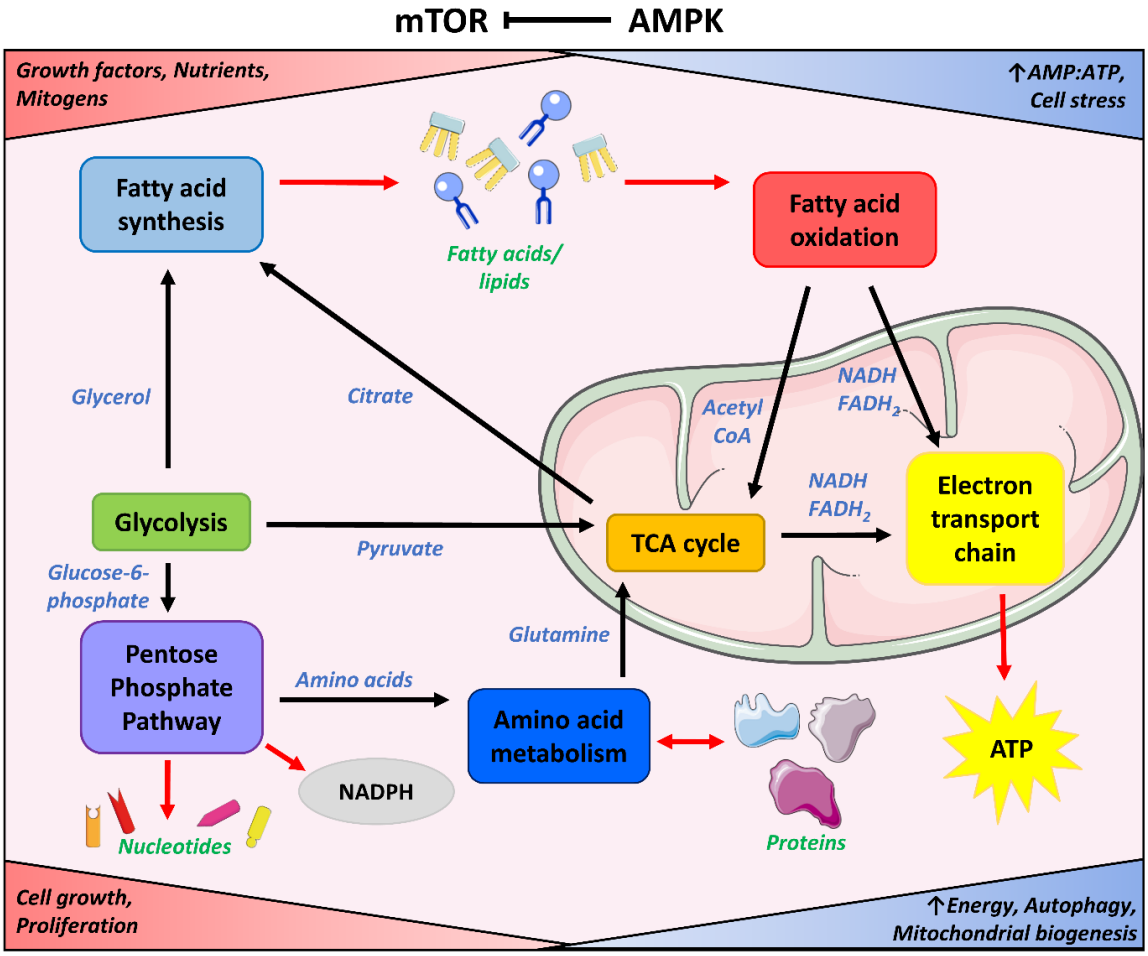

Figure 1.5. Control of anabolic and catabolic metabolism by mTOR and AMPK. mTOR signalling is upregulated in response to growth factors, mitogens and nutrient availability, resulting in increased activation of glycolysis, fatty acid synthesis and the pentose phosphate pathway. This generates biosynthetic precursors such as fatty acids and nucleotides to promote cell growth and proliferation. AMPK is activated in response to low energy availability (↑AMP:ATP ratio) and cell stress, resulting in increased fatty acid oxidation and flux through the TCA cycle and ETC. This produces large amounts of ATP as well as promoting autophagy and mitochondrial biogenesis.

1.2.4.2 Metabolism of immune cells

The specific metabolic pathways upregulated by immune cells upon engagement with different stimuli appears to underpin the type of immune response produced by that cell, with some cell types displaying an increased dependency on certain metabolic pathways over others. Fundamental studies examining the metabolism of murine bone-marrow derived macrophages (BMDM) have shown that upon activation with a pro-inflammatory stimulus such as LPS, BMDM greatly upregulate their rate of glycolysis while downregulating oxidative phosphorylation, relying

almost exclusively on glycolysis to meet their metabolic demands (108). This program of aerobic glycolysis is termed Warburg metabolism, and was first observed in cancer cells by Otto Warburg in 1956 (109). The mechanism by which this switch to Warburg metabolism occurs in BMDM is dependent on upregulation of HIF1α via mTOR activation, which promotes the expression of genes encoding both glycolytic machinery and pro-inflammatory cytokines such as pro-IL-1β (110–112). Although glycolysis produces less ATP than oxidative phosphorylation, it does confer advantages to newly activated immune cells as it can rapidly produce additional ATP and biosynthetic precursors, even in inflammatory environments where oxygen is often limiting (113,114). Downregulation of oxidative phosphorylation also allows for the activated BMDM to repurpose TCA cycle intermediates to support its heightened anabolic metabolism. For example, citrate fuels the upregulation of fatty acid synthesis in pro-inflammatory macrophages, which provides large amounts of phospholipids necessary to expand the membranes of the endoplasmic reticulum (ER) and Golgi apparatus, in support of the cell's increased requirement for protein synthesis (115). Conversely, in alternatively-activated BMDM, which are generally considered to be anti-inflammatory, oxidative phosphorylation is the dominant metabolic pathway. Oxidative phosphorylation in these anti-inflammatory macrophages is largely fuelled by fatty acid oxidation, which provides sufficient energy to support the long-term responses carried out by this class of macrophage, such as tissue repair and parasite control. IL-4, the cytokine which mediates alternative activation of macrophages, upregulates fatty acid oxidation and oxidative phosphorylation alongside anti-inflammatory immune pathways in BMDM (116–118). This metabolic program is also driven by high AMPK activity in the alternatively-activated macrophage, which suppresses pro-inflammatory responses and promotes polarisation towards an anti-inflammatory phenotype (119).

Due to the close ontological relationship between macrophages and DC, similar metabolic patterns have been observed in murine bone marrow derived DC (BMDC) as in BMDM. Activation of TLR signalling in BMDC has also been reported to trigger a switch to Warburg metabolism, which is essential for the survival of BMDC and their ability to stimulate T cells (120). Similarly, HIF1α has been observed to be highly upregulated in activated BMDC, and appears to control the increased glycolytic metabolism and pro-inflammatory immune function of these cells (121). Interestingly, it has also been reported that the upregulation of glycolysis in BMDC primarily serves to support increased fatty acid synthesis and expansion of their ER/Golgi compartment, indicating that this is a common consequence of anabolic metabolism in pro-inflammatory cells (122). Finally, similar to alternatively-activated BMDM, AMPK has been described to suppress glycolytic metabolism and pro-inflammatory responses in BMDC (120,123). Activation of AMPK also appears to contribute to

the anti-inflammatory effects of IL-10 in BMDC (120), suggesting that suppression of metabolic reprogramming plays an important role in the regulation of immune cells.

Many of the metabolic patterns seen in innate immune cells can also be observed in cells of the adaptive immune system. T cells in particular have unique metabolic demands as a result of their strong proliferative response upon activation, and generation of long-lived memory cells. Naïve and memory T cells are largely quiescent, relying on oxidative phosphorylation to meet their limited energy demands (124). However, during activation T cells switch from catabolic to anabolic metabolism to support their rapid growth, proliferation and polarisation (125,126). Similar to pro-inflammatory BMDM and BMDC, upregulation of glycolysis is observed during T cell activation upon engagement of the TCR, and is necessary for their early production of cytokines (127). Subsequently, the metabolic profile adopted by the T cell is linked to its differentiation into discrete subsets. Effector T cells including Th1, Th17 and cytotoxic T cells display high rates of aerobic glycolysis and associated mTOR signalling to fuel their extensive proliferation and effector functions (128,129). Anti-inflammatory Tregs, on the other hand, do not undergo this upregulation of glycolysis, and instead utilise fatty acid oxidation and oxidative phosphorylation to meet their metabolic demands, via activation of AMPK (129). Thus, T cell metabolism reflects the functional requirements of each T cell type: actively proliferating T cells engage anabolic metabolism to provide for their growth and effector functions, while Tregs and resting naïve and memory T cells utilise catabolic pathways to provide energy over the long-term.

One of the gaps in our understanding of immunometabolism is the species differences between murine and human immune cells. To date, much of the research within the field has been performed in mice. While there are many similarities between the immune systems of mice and humans, differences in habitat and life cycle have likely resulted in important evolutionary differences in metabolic function between the two species (130). One of the major differences between murine and human macrophages and DC is expression of inducible nitric oxide synthase (iNOS); nitric oxide (NO) produced by iNOS is an important regulator of Warburg metabolism, as it has been shown to mediate the downregulation of oxidative phosphorylation seen in pro-inflammatory BMDM and BMDC (131,132). However, expression of iNOS by human macrophages/DC is limited, thus it is unclear to what degree they engage in Warburg metabolism (133,134). Although studies in human macrophages have identified upregulation of glycolysis as an important modulator of the pro-inflammatory immune response during sepsis and tuberculosis (135,136), recent studies have reported that human macrophages and DC stimulated with LPS display increases in both glycolysis and mitochondrial respiration (137,138). Similarly, in T cells, some metabolic features remain similar between mice and humans, while others display distinct

differences. A study by Renner *et al.* has reported that like murine T cells, human $CD4^+$ and $CD8^+$ T cells upregulate glycolysis when activated; however, while this upregulation of glycolysis was required for T cell proliferation, T cells could utilise either glycolysis or oxidative phosphorylation to support cytokine production (139). Other studies have demonstrated that human T cells are capable of adapting their metabolism to compensate for nutrient deficiencies in their microenvironment (140,141), a feature which allows them to maintain their effector functions in pro-inflammatory environments where there often exists competition for limited nutrient supplies.

Through the foundational research described above, a paradigm for immunometabolism has emerged: pro-inflammatory cells are associated with anabolic metabolism, characterised by high glycolytic flux & mTOR signalling, while anti-inflammatory cells are catabolic, relying on fatty acid oxidation, oxidative phosphorylation and AMPK activation for efficient energy production. However, it appears that human immune cells may not display the same discrete activation of metabolic pathways seen in their murine equivalents, instead demonstrating greater metabolic plasticity. Furthermore, caution should be exercised when applying this paradigm to disease models, as differences between the metabolic profiles of cells activated *in vitro* versus *in vivo* have been identified (142–144). Thus, further research into the metabolic function of human immune cells, especially in disease contexts, is necessary before therapies targeting metabolic pathways can be considered.

1.3 The Heme Oxygenase System

Heme oxygenase (HO) is an enzyme which catalyses the breakdown of heme into the linear tetrapyrrole (LTP) biliverdin (BV), with the concomitant release of free iron and carbon monoxide (CO). BV can then be converted into another LTP, bilirubin (BR), by the enzyme biliverdin reductase (BVR) (Figure 1.6). Heme is an iron-containing porphyrin that is a component of many biologically important proteins, especially hemoglobin which is used to carry oxygen within red blood cells. Free heme is cytotoxic due to its iron component which can form free radicals via a Fenton reaction, thereby causing oxidative stress (145–147). Therefore, it is important that heme released from degraded hemoproteins is rapidly catabolised to prevent cellular damage. Under homeostasis, senescent red blood cells are removed from circulation in the spleen, where heme is catabolised within red-pulp macrophages by the constitutively expressed HO isozyme HO-2. The resulting LTPs, BV and BR, are typically excreted in bile as bile pigments, however they also have potent antioxidant and anti-inflammatory properties (148–151). HO-2 is also highly expressed in the brain, where it produces CO which is used as a neurotransmitter (152,153).

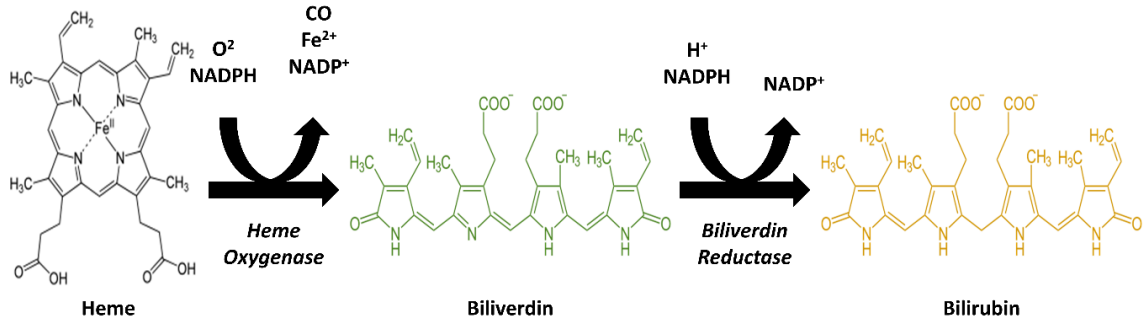

Figure 1.6. The Heme Oxygenase System. The conversion of free heme to BV, CO and iron is catalysed by the enzyme HO under aerobic conditions. BV can then be converted to BR by the enzyme BVR. Both of these enzymes utilise NADPH as a cofactor.

1.3.1 Heme oxygenase 1

HO-1 is a stress-inducible HO isozyme encoded by the gene *HMOX1,* which is an important immunomodulator and antioxidant. Unlike HO-2, which is constitutively expressed and controls the breakdown of heme under homeostasis, HO-1 is highly upregulated in response to oxidative stress and inflammation, and provides protection against cellular and tissue damage. HO-1 expression is largely under the control of the redox-sensitive transcription factor nuclear factor erythroid 2 (NFE2)-related factor 2 (Nrf2) which binds to the antioxidant response element (ARE) in the promoter region of many antioxidant genes, including *HMOX1.* Under steady-state conditions, Nrf2 is bound to the protein Keap1 (Kelch-like erythroid cell-derived protein with CNC homology-associated protein 1) in the cytoplasm, which suppresses Nrf2 activity by facilitating its ubiquitination and thereby targeting it for degradation by the proteasome (154). However, in the presence of oxidants, ROS and other Nrf2 activators, the cysteine residues of Keap1 are modified resulting in disruption of the ubiquitination, and consequent stabilisation, of Nrf2 (155,156). Nrf2 can then migrate to the nucleus and bind to the ARE to promote expression of antioxidant genes. Furthermore, another level of regulation exists for HO-1 expression; Bach1 is a transcriptional repressor and heme sensor which binds the *HMOX1* promoter, thereby blocking Nrf2 from accessing the ARE. However, in the presence of high intracellular levels of heme, Bach1 undergoes a conformational change and dissociates from the DNA. It is then exported from the nucleus, ubiquitinated and degraded, allowing *HMOX1* transcription to occur (157).

Although Nrf2 and Bach1 are the primary regulators of HO-1, other transcription factors and signalling pathways have been described to modulate HO-1 expression. Binding sites for the pro-inflammatory transcription factors NF-κB and AP-1 have been identified within the *HMOX1* promoter, suggesting that they may upregulate HO-1 expression during inflammation (158–160). Some instances of HO-1 upregulation *in vitro* have been shown to be dependent on or correlated with NF-κB or AP-1 expression; a review of these studies is provided by Alam and Cook (161). As

ROS cause cellular damage resulting in the release of DAMPs, and are frequently produced in response to infection, induction of HO-1 by NF-κB or AP-1 may be a response to cell damage or serve to protect the cell from ROS generated during inflammation (162). Additionally, it has been suggested that HO-1 may inhibit NF-κB signalling and thus prevent the expression of pro-inflammatory genes, therefore it is plausible that HO-1 may be induced by pro-inflammatory transcription factors to provide negative feedback limiting their activity (163,164).

While there appear to be multiple transcriptional regulators of HO-1 expression, most HO-1 inducers do not interact directly with transcription factors but instead activate them via an intermediate signalling pathway. Protein kinase pathways, particularly MAPKs, which are associated with responses to cellular stress have been implicated in the regulation of HO-1 expression. The MAPKs ERK, JNK and p38 have been shown to upregulate HO-1 in different cell types and cellular conditions, however p38 appears to be the most commonly associated MAPK in HO-1 induction and blockade of p38 signalling inhibits the induction of HO-1 by multiple stimuli (159,161,165). The phosphatidylinositol-3 kinase (PI3K)/Akt pathway has been reported to mediate the expression of HO-1 in response to cytokines and prostaglandins as well as some pharmacological HO-1 inducers (159,166–169). Interestingly, the cytokine IL-10 also upregulates HO-1 expression as part of its anti-inflammatory activity, and it is thought that this effect is mediated via activation of STAT3 (170,171). HO-1 is also upregulated in response to LPS in some cell types such as macrophages, which is mediated via TLR4 signalling; this may produce another negative feedback loop as HO-1 derived CO has been reported to inhibit TLR4 signalling and therefore limit inflammation (159,172,173). In summary, due to the prevalence of hemoproteins within cells and the potent antioxidant and anti-inflammatory effects of HO-1, it is unsurprising that cells possess numerous different mechanisms to upregulate HO-1 expression in response to stress, and it is likely that many stimuli which induce HO-1 expression utilise multiple signalling pathways and transcription factors to do so (Figure 1.7).

Although HO-1 can be upregulated by most cell types, it appears to have a significant role in the functioning of immune cells. As described above, HO-1 has demonstrable anti-inflammatory properties and its expression is often upregulated during inflammation. Additionally, a *HMOX1*$^{-/-}$ mouse model found that knockout mice produced significantly more IL-1β, IL-6, IL-12 and TNFα when challenged with LPS compared to wild type mice (174). In agreement with these observations, HO-1 has primarily been associated with the activity of myeloid cells, particularly in the promotion of anti-inflammatory immune responses. For instance, HO-1 is constitutively expressed by immature DC, which maintain immune tolerance as described previously, and is downregulated upon DC maturation (175–177). Pharmacological downregulation or inhibition of

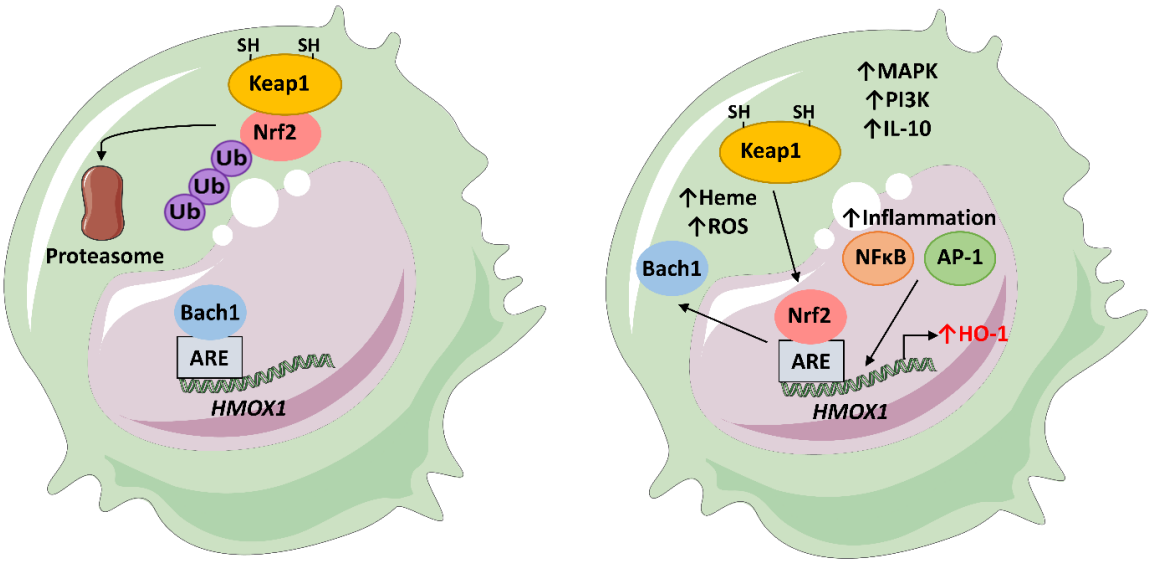

Figure 1.7. Regulation of HO-1 expression. Under homestatic conditions, Nrf2 is ubiquitinated by Keap1 and targeted by the proteosome for degradation. Bach1 binds to the ARE and inhibits *HMOX1* transcription. During cell stress, increased intracellular levels of heme cause Bach1 to dissociate from the ARE, and ROS cause Nrf2 to dissociate from Keap 1, allowing it to migrate to the nucleus and bind the ARE to promote *HMOX1* transcription. The transcription factors NF-κB and AP-1 can also bind the HO-1 promoter and promote HO-1 upregulation during inflammation. Finally, signalling through MAPKs, PI3K and IL-10 have also been reported to regulate HO-1 expression in certain cell types

HO-1 within DC *in vitro* enhances their maturation, cytokine production and activation of T cell responses, whereas HO-1 induction promotes tolerogenic DC by inhibiting their pro-inflammatory functions and maintaining them in an immature-like phenotype (176,178–180). Thus, HO-1 expression is closely associated with the maturation status of DC and appears to regulate their activity. Similar to DC, HO-1 also has immunomodulatory properties within macrophages. For example, Wegiel *et al.* observed that *HMOX1*$^{-/-}$ mice have defective macrophage populations and that macrophage differentiation is dependent on HO-1 derived CO (181). Furthermore, HO-1 expression has been demonstrated to promote the polarisation of macrophages towards an anti-inflammatory or alternatively-activated phenotype (182).

While HO-1 is strongly associated with regulation of the phenotype and function of myeloid cells, less is known of its role in T cell biology. HO-1 expression is correlated with the inhibition of effector T cell responses and promotion of Tregs, however it is unclear to what extent this is mediated by HO-1 activity in T cells or APCs. Pae *et al.* reported that HO-1 is constitutively expressed by human Tregs and that HO-1 expression inhibited T cell proliferation (183). CO derived from HO-1 has been shown to suppress T cell proliferation via inhibition of IL-2 production and caspases 3 and 8, thus limiting pro-inflammatory T cell responses (184,185). This effect was demonstrated in T cells stimulated *in vitro* in the absence of APCs, and therefore is an example of

HO-1 immunomodulatory activity within T cells. However, other reports of HO-1-mediated anti-inflammatory effects in T cells appear to be dependent on HO-1 expression by APCs rather than by T cells themselves. Activation and proliferation of T cells in response to HO-1 inhibition was observed by Burt *et al.* only when T cells were cultured in the presence of APCs (186). Furthermore, it was demonstrated that Tregs from *HMOX1*$^{-/-}$ mice are not impaired and are functionally suppressive, and that while HO-1 inhibition reduced Treg suppression, this effect was mediated by HO-1 activity in DC than in Tregs themselves (180,187,188). In support of these observations, a study by Wong *et al.* reported that DC expressing HO-1 promoted Treg differentiation and suppressed inflammation in an allergic airway model (189). Therefore, the current model suggests that HO-1 primarily modulates T cell activity through its expression in APCs; HO-1 maintains DC in an immature state which promotes Treg differentiation and inhibits pro-inflammatory T cell responses.

In summary, HO-1 is a poly-functional enzyme which is induced in response to cell stress and inflammation. HO-1 expression is associated with the maintenance of immune tolerance and inhibition of pro-inflammatory immune responses, and is especially significant in the function of myeloid cells.

1.3.2 Linear tetrapyrroles

LTPs are a class of chemical compound whose structure is comprised of four pyrrole rings linked together linearly by covalent bonds or carbon bridges. Common LTPs include the heme breakdown products and bile pigments BV and BR, and phycobilins found in cyanobacteria. BV and BR have both been demonstrated to possess antioxidant and anti-inflammatory properties, and are thought to be responsible for much of the activity of HO-1.

BV is produced as an intermediate of heme catabolism and is readily converted to BR by BVR. BV is soluble and readily excreted into bile during homeostatic heme catabolism, while BR is insoluble and must be glucuronidated by the liver in order to be excreted. BR is one of the most potent antioxidants found in mammalian cells and is particularly important in the protection against lipid peroxidation (150). However it is also extremely cytotoxic at high concentrations; hyperbilirubinemia results in jaundice and is especially dangerous in neonates, however, moderate hyperbilirubinemia in adults, termed Gilbert's syndrome, has been shown to be protective against cardiovascular disease, diabetes mellitus, metabolic syndrome and obesity (190,191). In addition to its antioxidant properties, BR has also been shown to display anti-inflammatory activity. BR treatment inhibited iNOS expression and TNFα production in response to LPS in rats (192), while HO-1 derived BR was found to downregulate IFNγ-induced MHC Class II

expression on endothelial cells (193). BR has also been reported to inhibit leukocyte trafficking by disrupting the ROS-mediated signalling of adhesion molecule VCAM1 (194). Finally, a dimethyl ester of BR was recently shown to inhibit pro-inflammatory eicosanoid signalling by inhibition of the arachidonic acid pathway enzymes phospholipase A2, lipoxygenase and cyclooxygenase (195). Thus, BR is protective during inflammation through both the neutralisation of ROS and direct inhibition of pro-inflammatory signalling.

While many of the protective effects of BV and BVR can be ascribed to the activity of BR, direct anti-inflammatory signalling by BV and BVR has been demonstrated in numerous studies. In a rat model of acute lung injury, BV administration protected rats from endotoxic shock, reduced serum levels of IL-6 and promoted IL-10 expression (196). Similarly, in a rat model of cerebral ischemia reperfusion injury BV administration reduced expression of the pro-inflammatory cytokines IL-6, TNFα , and IL-1β (197). Furthermore, in HO-2 null mice, BV administration ameliorated chronic inflammation by reducing the activation of immune cells and pro-inflammatory cytokine production (198,199). In addition to its enzymatic function, Wegiel *et al.* have reported that BVR can act as an anti-inflammatory signalling molecule upon binding of BV. It was observed that cell-surface BVR initiates a cell signalling cascade which activates PI3K and Akt to produce the anti-inflammatory cytokine IL-10, while BV was also found to inhibit TLR4 expression via NO-dependent nuclear translocation of BVR to the TLR4 promoter (200,201). BVR has also been suggested to activate the AP-1 mediated pathway of HO-1 induction, and therefore contribute to the upregulation of HO-1 expression in response to inflammation (202). Thus, BV has been established as protective in many inflammatory animal models and has multiple modes of action, acting either by itself, as a precursor for BR, or as an activator of BVR-mediated signalling and transcriptional regulation (149).

In conclusion, LTPs are versatile compounds due to their extensive antioxidant and anti-inflammatory properties, and are important effectors of HO-1 activity. Due to the insolubility and cytotoxicity of BR, BV represents a more attractive immunomodulator which has demonstrable anti-inflammatory functions both dependent and independent of BR.

1.3.3 Carbon monoxide

CO is also produced by HO during heme catabolism. At high concentrations it is considered a poison and environmental pollutant given that it strongly binds to hemoglobin and reduces the oxygen carrying capacity of red blood cells, thereby resulting in inhibition of cellular respiration. However at physiological concentrations, it is recognised as an important cellular messenger and anti-inflammatory agent.

Both HO-1 derived and exogenously delivered CO have been demonstrated to inhibit pro-inflammatory immune responses *in vitro* and *in vivo*. Studies performed by Choi *et al.* in murine macrophages have shown that both HO-1 overexpression and CO treatment inhibited TNFα, IL-1β, IL-6 and granulocyte-monocyte colony-stimulating factor (GM-CSF) production by murine macrophages in response to LPS, while increasing production of IL-10 (203–205). CO has also been shown to inhibit DC maturation and antigen presentation to T cells, and to inhibit T cell proliferation (184,185,206–208). *In vivo*, CO has been reported to improve disease outcomes in many animal models of inflammatory disease, including sepsis, EAE, Alzheimer's disease and colitis (209–212). Furthermore, CO administration during animal models of organ transplantation has been shown to limit ischemia-reperfusion injury to donor organs and suppress graft rejection (213–215). Interestingly, recent studies utilising members of a new class of CO releasing molecules (CORMs) have reported that CORM-A1 and CORM3 upregulate HO-1 and are protective in various *in vitro* and *in vivo* models of inflammation (216–218). This new method of CO administration may therefore allow for safer use of CO as a therapy in inflammatory disease.

The mechanism of action of CO appears to involve multiple different cellular targets. Modulation of MAPK signalling pathways has been proposed as a major mechanism by which CO exerts its anti-inflammatory activity. Otterbein *et al.* reported that the anti-inflammatory effects of CO in murine macrophages were dependent on activation of the p38 MAPK, while Morse *et al.* demonstrated that CO inhibits the JNK MAPK and its downstream target, AP-1 (203,219). However, it is unlikely that CO binds to MAPKs directly as they do not contain transition metals and thus it is assumed that they are downstream targets of a yet unidentified CO-binding effector protein (220,221). Additionally, Jung *et al.* recently reported that CO negatively regulated NLRP3 inflammasome activation by inhibiting caspase 1 expression, thereby limiting IL-1β and IL-18 release, and suggested that this effect is mediated by suppression of mitochondrial ROS generation (222). Downregulation of TLR4 signalling has also been observed in response to CO, however it is unknown whether CO modulates the expression or function of other PRRs (172,223). Finally, it has also been reported that CO itself can induce HO-1 expression; this provides an interesting positive feedback system by which CO promotes and sustains its own activity by upregulating HO-1 to further its generation (216,222–227).

In conclusion, CO is an intriguing cellular regulator which has wide ranging physiological and anti-inflammatory functions. Alongside BV and BR, CO mediates the cytoprotective functions of HO-1. Treatment with inhaled CO gas or with various CORMs may prove beneficial in the context of inflammation or oxidative stress (168,228).

1.4 HO-1 in Disease

Due to the extensive antioxidant and anti-inflammatory properties of the HO-1 system, it is unsurprising that HO-1 and its products have been associated with beneficial outcomes in both human disease and animal models. Free heme can contribute to the progression of many inflammatory diseases such as sepsis and malaria and hence HO-1 upregulation is a protective mechanism in heme-mediated pathologies (147). Furthermore, it has been suggested that polymorphisms in the *HMOX1* gene resulting in greater expression of HO-1 are protective against inflammatory diseases, while those resulting in impaired transcription of *HMOX1* have been associated with an increased risk of diseases such as atherosclerosis and coronary heart disease (168,229). Additionally, HO-1 expression in patients suffering from autoimmune diseases such as MS or psoriasis has been correlated with disease activity; this upregulation of HO-1 is thought to be a response to excessive inflammation (230,231). Therefore, modulation of the HO-1 system, either by induction of HO-1 expression or administration of its products CO, BV or BR, has been investigated as a novel treatment strategy in various animal models of inflammatory disease (192,211,212,232–234).

1.4.1 HO-1 in autoimmunity

Autoimmunity is associated with significant morbidity and mortality, and the global incidence and prevalence of autoimmune diseases is rising (235). Despite this trend, the majority of autoimmune diseases are incurable, and many lack effective treatments to control disease progression and symptoms. Hence, there is a significant incentive to identify new targets to treat autoimmune disease, and, for the reasons outlined above, the HO-1 system has become an important target of interest.

1.4.1.1 Multiple sclerosis

MS is a chronic, debilitating neurological disease with limited treatment options and no available cure. Research over the last number of years has identified Th17 cells as the pathological cells responsible for MS pathogenesis and pathology (discussed in section 1.2.3.1), and more recently HO-1 and its products have been identified as protective in MS and EAE. Fagone *et al.* reported that HO-1 expression is reduced in the peripheral blood mononuclear cells (PBMC) of MS patients compared to both healthy controls and patients with non-immune mediated neurological disease, and that HO-1 expression is further downregulated in MS patients experiencing disease relapse compared to those with stable disease or receiving corticosteroid treatment (230). Furthermore, HO-1 upregulation has been observed in glial cells within MS plaques, likely as a local response to neuroinflammation (236). In EAE models, both HO-1 and CO have been demonstrated to improve

disease outcomes, while administration of BVR and BR have also been shown to suppress EAE onset and progression (210,237–239). Interestingly, a recent study by Simon *et al.* reported that intradermal injection of the HO-1 inducer, cobalt protoporphyrin IX (CoPP), inhibited the induction of EAE in mice via suppression of autoreactive T cells by HO-1^+ DC (240). These studies point towards a role for free radicals in the pathogenesis of EAE and MS, and lend support for the modulation of the HO-1 system as a novel treatment strategy for MS.

1.4.1.2 Inflammatory bowel disease

Inflammatory bowel disease (IBD) is an autoimmune disease affecting the gut, and is divided into two main categories; Crohn's disease, which can affect the digestive tract anywhere proximal to the colon, and ulcerative colitis, which affects the colon and rectum. IBD is characterised by a dysregulated immune system within the gut alongside disturbances in the intestinal microbiome, resulting in chronic inflammation which causes damage to the gut over time (241). Despite the identification of pathogenic immune cells as central to the pathology of IBD, treatments aimed at controlling inflammation in the gut are limited. As a result, a significant number of patients are unable to manage their disease and often require numerous surgeries to remove affected tissue, which greatly impacts their quality of life. It has previously been observed that HO-1 expression is upregulated in the intestinal epithelium of patients with IBD (242,243). Hence, the anti-inflammatory potential of HO-1 and its products has been investigated in numerous *in vivo* models of IBD. A protective role for HO-1 has been identified in the dextran sulfate-sodium (DSS) model of colitis; Zhong *et al*. reported that induction of HO-1 via hemin administration ameliorated colitis symptoms, while the HO-1 inhibitor, tin protoporphyrin (SnPP), exacerbated disease (244). The protective effects of HO-1 in this study was accompanied by a reduction in Th17-mediated IL-17 production and expansion of Tregs. A follow up study confirmed that the improved Th17/Treg balance was dependent on HO-1, and mediated by reduced IL-6 signalling (232). Other studies have investigated the use of HO-1 products in models of IBD. For example, Berberat *et al.* reported that treatment with the HO-1 inducer CoPP or BV, but not CO, was protective in the DSS colitis model (245), while a number of studies have demonstrated that CO administration improves disease symptoms in models of IBD (246–249). Taken together, these studies suggest that administration of HO-1 inducers or reaction products may be promising potential treatments for IBD, however, further clinical investigation is necessary.

1.4.1.3 Psoriasis

Psoriasis is a chronic autoimmune disease of the skin affecting 2-3% of the population, which manifests as red, scaly plaques with associated pruritus and pain (250). It is characterised by excessive keratinocyte proliferation as well as extensive infiltration and activation of immune cells

(251). Although the causes of psoriasis are incompletely understood, important roles for DC and T cells in the pathophysiology of psoriasis have been identified, and particular emphasis has been placed on the Th17 axis cytokines, IL-23, IL-17 and IL-22 (252–254). Recently developed monoclonal antibodies against IL-23 and IL-17 have proved to be highly effective treatments against moderate to severe cases of psoriasis, while traditional therapies such as phototherapy and corticosteroids remain the primary treatments for mild to moderate disease (66–68).

Unsurprisingly, the HO-1 system has recently become a target of interest for psoriasis treatment. While keratinocytes constitutively express HO-2 to combat ROS generated from environmental stressors such as UV radiation, upregulation of HO-1 expression has been observed in psoriatic plaques (231). Keratinocytes upregulate HO-1 during terminal differentiation in the epidermis, and a role for HO-1 during cutaneous wound healing has also been described. Therefore, HO-1 induction during psoriasis may act to alleviate abnormal keratinocyte differentiation and proliferation which is a feature of psoriatic lesions (231,255,256). Furthermore, upregulation of HO-1 has been demonstrated to inhibit skin inflammation and keratinocyte proliferation in animal models of psoriasis. Ma *et al.* observed a decrease in pro-inflammatory cytokines and keratinocyte hyperproliferation upon administration of CoPP in a guinea pig model of psoriasis, while Listopad *et al.* observed similar results in a murine model of the disease. In this case, a decrease in T cell mediated skin inflammation was accompanied by increased HO-1 activity in APCs present in the skin (179,257). Zhang *et al.* also recently reported that induction of HO-1 improved symptoms in a murine model of psoriasis, and attributed this effect to negative regulation of STAT3 signalling by HO-1 (258). Interestingly, induction of HO-1 is also associated with existing treatments for psoriasis. For example, phototherapy involving exposure to UVA radiation has been shown to upregulate HO-1 expression in both *in vitro* and *in vivo* skin cells, while the immunosuppressant dimethyl fumarate (DMF), also known as Fumaderm™, used to treat both psoriasis and MS, has been identified as a potent HO-1 inducer, and at least some of its anti-inflammatory effects have been attributed to HO-1 (259–263). Whether HO-1 activity is required for the efficacy of these therapies remains unclear, however, these studies provide further support for the modulation of HO-1 expression as a potential treatment for psoriasis and other immune mediated disorders.

1.4.2 Naturally-derived HO-1 modulators

Despite the body of evidence supporting modulation of the HO-1 system as a treatment for diseases characterised by damaging inflammation or oxidative stress, clinical implementation of HO-1 based therapies faces numerous challenges. Traditional HO-1 inducers primarily include metalloporphyrins such as CoPP, which strongly upregulate HO-1 expression but are also associated with significant toxicity concerns and thus are unsuitable for clinical use (264,265). The

vast majority of animal studies examining the role of HO-1 in different disease models have utilised either metalloporphyrins, *HMOX1*$^{-/-}$ animals, or gene silencing to modify HO-1 expression, but none of these methodologies are suitable for use in humans, making the findings of these studies difficult to translate to the clinic. Furthermore, while DMF is an approved treatment for psoriasis and MS, and has been demonstrated to upregulate HO-1 expression, it is also associated with significant side effects including leukopenia and gastrointestinal disturbances, rendering it intolerable for a subset of patients (266). CO delivery via inhalation or administration of CORMs has been considered therapeutically but requires further research to determine a safe dose that will produce an effective concentration in specific tissues but without risk of CO-mediated toxicity (229). Finally, therapeutic administration of LTPs also faces challenges: BR is unsuitable for clinical use due to its potent cytotoxicity and poor solubility, while commercially available BV, whether synthetic or extracted from bovine bile, has not been approved for human use, and large scale production of biliverdin in *E.coli* or yeast expression systems has been attempted but is hindered by potential endotoxin contamination (267). Therefore, there is a great need to identify safer and better tolerated alternatives to currently available sources of HO-1 inducers and LTPs. Thus far, a number of plant- and marine-derived compounds have been identified as candidate HO-1 inducers or LTP analogues.

1.4.2.1 Curcumin

Curcumin is a yellow-coloured polyphenol with anti-inflammatory and antioxidant properties most commonly found in the turmeric plant (*Curcuma longa*). Turmeric has been used in Indian and Chinese medicine for centuries to treat disorders including gastrointestinal complaints and infections, while curcumin is widely used as a health supplement, cosmetics ingredient, and food flavouring and colouring (268). Curcumin has been investigated as a treatment for a wide variety of indications including cancer, infection and inflammation (269–272). One of the mechanisms by which curcumin is thought to exert its activity is activation of Nrf2 and consequent upregulation of HO-1; McNally *et al.* reported that curcumin activated Nrf2 in the HUH7 hepatoma cell line via a combination of ROS production, activation of the p38 MAPK and inhibition of protein phosphatases (165). Furthermore, numerous studies have reported that the protective anti-inflammatory and antioxidant effects of curcumin are attenuated in Nrf2 knockout mice or in the presence of HO-1 inhibitors (273–276).

As described in section 1.3.1, HO-1 has well-described immunomodulatory effects in DC, primarily through the regulation of DC maturation. Interestingly, a number of studies have examined the activity of curcumin in DC, and report similar effects to those seen with HO-1 induction. Kim *et al.* reported that murine DC treated with curcumin displayed reduced maturation, cytokine

production and activation of Th1 cells when stimulated with LPS, and described inhibition of MAPK signalling and NF-κB translocation as potential mechanisms (277). Furthermore, both Cong *et al.* and Rogers *et al.* have reported that curcumin-treated murine DC promote Treg differentiation (278,279). In the case of human DC, Rogers *et al.* reported that curcumin treatment arrests DC maturation and impairs their ability to induce allostimulatory T cell responses, while promoting Treg expansion (279). This is supported by Shirley *et al.* who also observed impairment of maturation, cytokine production, chemotaxis and induction of T cell responses in curcumin-treated DC stimulated with LPS or Poly I:C (280). Although the direct effects of curcumin have primarily been investigated within innate immune cells, there have been some studies into its activity in T cells. In murine lymphocytes, Gao *et al.* reported inhibition of T cell proliferation and cytokine production by curcumin, via inhibition of NF-κB (281). Curcumin was also shown to inhibit T cell proliferation and production of IFNγ and IL-17 in both *in vitro* and *in vivo* models of graft versus host disease (282). These effects have also been observed in human T cells by Kim *et al.*, who additionally reported an increased percentage of Tregs within $CD4^+$ T cells cultured with curcumin (283).

In support of its well-described anti-inflammatory effects *in vitro*, curcumin treatment has shown efficacy in many animal models of autoimmunity. Liu *et al.* reported that administration of curcumin in the DSS colitis model improved disease activity and histological scores, mediated by reduced STAT3 signalling and pro-inflammatory cytokine production (284). Another study by Zhao *et al.* investigated curcumin in a model of colitis and found that curcumin treatment ameliorated disease symptoms via inhibition of DC activation (285). Interestingly, a recent study by Brück *et al.*, which administered dietary curcumin to mice in an EAE model, observed that curcumin upregulated HO-1 expression and STAT3 signalling in DC, resulting in inhibition of IL-12 and IL-23 production by DC, reduced differentiation of pathogenic Th1 and Th17 cells, and consequently improved EAE disease scores (286). Capini *et al.* also utilised a novel delivery system by combining curcumin with antigen-loaded liposomes which were administered to mice in an antigen-specific RA model. Mice that received the curcumin liposomes displayed reduced inflammation and arthritis symptoms due to the induction of antigen-specific Tregs by APCs (287). Finally, curcumin has been investigated in two different psoriasis models; Kang *et al.* reported curcumin significantly reduced pro-inflammatory cytokines, including Th17 axis cytokines IL-23, IL-22 and IL-17, and improved psoriatic lesions in a transgenic mouse model of psoriasis (288), while Sun *et al.* found that curcumin inhibited imiquimod-induced psoriasis-like inflammation via inhibition of Th17-polarising cytokines (289). Therefore, the use of curcumin as a treatment in autoimmunity is supported by numerous pre-clinical animal models, with modulation of DC activity to control

pathogenic T cells emerging as a common feature of its effects. However, further research into the immunomodulatory effects of curcumin, and its mechanism of action, in human cells is warranted.

Despite the positive results from *in vitro* studies and animal models, clinical studies investigating curcumin have been met with mixed results (290). While curcumin is widely sold as an oral health supplement, the oral bioavailability of curcumin is limited due to poor absorption from the gut and rapid metabolic degradation; a pilot study which administered 12 g per day of oral curcumin to ten healthy subjects reported a failure to detect the presence of curcumin in the serum or HO-1 mRNA or protein in PBMC of any subject at any time point up to 48 hours (291,292). Furthermore, a small phase II clinical trial which administered oral curcumin supplements to psoriasis patients reported a low response rate; however, this study lacked a placebo group for comparison (293). Nevertheless, success has been found in clinical trials of curcumin where the target tissue was easily accessible, or through utilisation of novel curcumin preparations with greater bioavailability. For example, oral administration of curcumin was found to significantly improve the induction and maintenance of remission in ulcerative colitis compared to placebo in two randomised controlled trials (294,295); the efficacy of orally administered curcumin may be greater in conditions affecting the gut as absorption from the gastrointestinal tract is not required for curcumin to reach its target tissue. Similarly, topical application of curcumin in a clinical trial of gingivitis reported significant anti-inflammatory effects (296), while in another trial of psoriasis patients, topical curcumin reduced keratinocyte proliferation and T cell migration into the skin (297). Additionally, a lecithin-based delivery system for curcumin was utilised to improve oral bioavailability in a recent randomized controlled trial of psoriasis. When administered as an adjuvant therapy to topical corticosteroids, curcumin significantly reduced the number and severity of psoriatic plaques and downregulated serum levels of the pro-proliferation cytokine IL-22, compared to placebo (298). Further research to improve the topical delivery of curcumin is ongoing, with novel preparations of curcumin as gels, films and nanovesicles among the examples of formulations which have been tested in *in vivo* trials (299).

In conclusion, curcumin is a well-studied naturally-derived HO-1 inducer with demonstrable antioxidant and anti-inflammatory properties both *in vitro* and *in vivo*. Encouragingly, clinical studies of curcumin have reported that it is well tolerated even at reasonably high doses, however, its safety in long-term treatment is still unknown (300,301). Thus, curcumin may represent a safe option for therapeutically inducing HO-1 expression, yet more studies in human cells are warranted and bioavailability issues must also be considered.

1.4.2.2 Carnosol

Carnosol is another polyphenol primarily found in the rosemary herb (*Rosmarinus officinalis*), which also has anti-inflammatory and antioxidant properties. Although it has not been in use as ubiquitously as curcumin, carnosol is a constituent of many herbs widely consumed as part of the health-promoting Mediterranean diet, and is thought to contribute to its protective effects (302). Like curcumin, carnosol has also been identified as a natural inducer of HO-1 through activation of Nrf2 and PI3K signalling (167,303,304). Carnosol has primarily been investigated as an anti-cancer compound due to its anti-proliferative and pro-apoptotic properties at high concentrations, and has been shown to inhibit experimental carcinogenesis in both *in vitro* and *in vivo* models (302,305,306). However, little investigation into its potential as an anti-inflammatory agent has been performed to date.

In vitro studies of carnosol have observed anti-inflammatory and antioxidant effects similar to those described for HO-1. Lian *et al.* reported that carnosol inhibited NF-κB nuclear translocation and transcriptional activity, and downregulated ICAM-1 expression and monocyte adhesion in TNFα-activated endothelial cells. Furthermore, these effects were attenuated in the presence of small interfering RNA (siRNA) against either Nrf2 or HO-1, demonstrating a dependence on HO-1 for these anti-inflammatory effects (163). Lo *et al.* also observed an inhibition of NF-κB activation and iNOS expression in carnosol-treated murine macrophages stimulated with LPS, and reported that carnosol inhibited p38 and ERK MAPK signalling (307). A recent study using the HaCaT keratinocyte cell line found that carnosol treatment protected keratinocytes from UVB-mediated ROS, cell death and NF-κB activation (308). Finally, carnosol has also been reported to inhibit iNOS expression and pro-inflammatory cytokine and chemokine production by LPS-stimulated murine macrophages, and to inhibit the expression of the catabolic genes MMP-3, MMP-13, ADAMTS-4 as well as IL-6 and NO production in human chondrocytes (309,310).

Surprisingly few *in vivo* studies have investigated carnosol for its anti-inflammatory and antioxidant properties. Wang *et al.* reported that carnosol was protective in a rat model of spinal cord injury, and its effects were attributed to activation of Nrf2 and inhibition of NF-κB and COX-2 (311). Two studies reported that carnosol was effective at alleviating pain responses in a murine model of pain; both studies reported inhibition of COX-1 and COX-2 signalling as well as a reduction in eicosanoid production by carnosol (312,313). Interestingly, a study by Lee *et al.* investigated the activity of carnosol in a murine model of atopic dermatitis and found it effectively inhibited STAT3 activation, reduced the production of pro-inflammatory cytokines and improved skin inflammation (314). In terms of human studies, only one clinical trial investigating carnosol has been published to date: in a randomised controlled trial of erythema, administration of

carnosol-rich sage extract significantly reduced UV-induced erythema compared to placebo (315). These studies suggest that carnosol treatment could be protective in the context of inflammatory skin diseases such as psoriasis. Although few *in vivo* or clinical studies have investigated carnosol as an anti-inflammatory therapy, it is believed to be well-absorbed and unlikely to have significant toxicity concerns as it is regularly consumed in herb-rich diets (302). A recent study by Arranz *et al.* reported that bioavailable fractions of digested rosemary extract contained carnosol and displayed immunomodulatory activity, suggesting that carnosol may have greater bioavailability than curcumin (316). In summary, while further investigation into the bioavailability, safety and efficacy of carnosol *in vivo* is necessary before it can be utilised in the clinic, carnosol represents an attractive candidate for development as a naturally-derived HO-1 inducer and novel immunotherapeutic.

1.4.2.3 Phycocyanobilin

Therapeutic administration of BV has been considered due to its extensive anti-inflammatory and antioxidant properties, described in section 1.3.2, but progress has been limited due to toxicity concerns of bile or microbial-derived BV. However, LTPs with close structural similarities to BV, known as phycobilins, naturally occur within cyanobacteria such as *Spirulina platensis*. These phycobilins contain pigments which allow cyanobacteria to absorb light at wavelengths which are not well absorbed by the prototypical light-absorbing pigment, chlorophyll. One such phycobilin which is a structural analogue to BV is phycocyanobilin (PCB), a blue-coloured chromophore which is a component of the protein phyocyanin found in Spirulina (Figure 1.8) (317). Data from the Dunne lab has confirmed that PCB is a potent antioxidant in human cells and is also a substrate for human BVR, causing it to be reduced to phycocyanorubin (318).

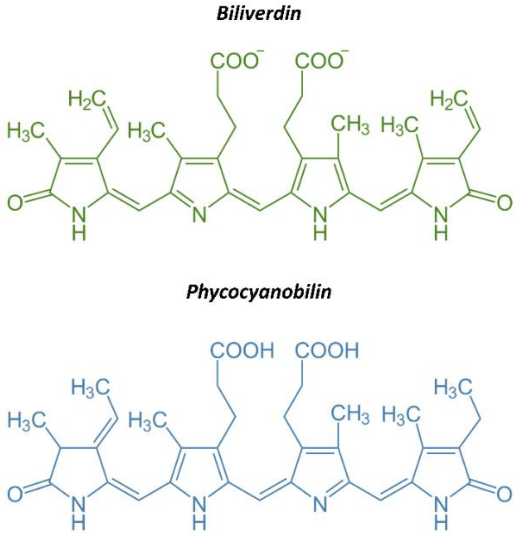

Figure 1.8. Structural similarities between BV and PCB.

Spirulina is widely consumed as a dietary protein source and health supplement due to its anti-inflammatory and 'immune boosting' properties (319–322). However, there has been little investigation into the use of purified PCB, or other phycobilins, as an anti-inflammatory treatment. Oral administration of PCB was shown to be protective in murine models of diabetic nephropathy and liver injury as a result of its antioxidant activity (323,324). PCB was also reported to prevent cellular injury due to oxidative stress in an *in vitro* neuronal cell line, as well as restore oxidative imbalance and inhibit inflammation in a rat model of acute cerebral hypoperfusion (325). Interestingly, there have been a few studies investigating PCB in the context of EAE; Pentón-Rol *et al.* reported that treatment of rats with phycocyanin improved symptoms of EAE, and in two recent follow up studies also observed that phycocyanin induces re-myelination in rats and mice affected by EAE, and that PCB can also ameliorate EAE and reduce pro-inflammatory cytokines in mice (326–328). Additionally, data from the Dunne lab has shown that PCB limits allogeneic immune responses and has anti-inflammatory properties in human PBMC *in vitro* (318). Both Spirulina and PCB have been reported by Strasky *et al.* to increase HO-1 expression in an endothelial cell line and murine model of atherosclerosis, potentially allowing for HO-1 induction as a positive feedback mechanism in certain cells (329). Finally, digestion of phycocyanin by gastric pepsin has been reported to yield biologically active chromopeptides, supporting oral consumption as an effective route of administration (330).

In conclusion, while there has been a limited number of investigations into the therapeutic use of PCB to date, there is sufficient evidence to suggest it can exert anti-inflammatory and antioxidant activity, and to support further investigation into its use as an immunotherapy. Furthermore, due to its structural similarity to BV and ability to act as a substrate for BVR, it is likely that PCB preparations can mimic the beneficial effects of BV in inflammation and oxidative stress, but without the toxicity concerns of currently available sources of BV.

1.5 Research Question

The identification of anti-inflammatory drugs with minimal side effects, yet which are effective in blocking pathways leading to damaging inflammation is much sought-after. As outlined above, the induction of HO-1 or administration of the HO reaction products has clear protective effects in several models of autoimmune or inflammatory disease, making HO-1 inducers and LTPs ideal candidates for use in preventative medicines, or as therapeutics which could potentially complement current immunosuppressants and biologics. Existing HO-1 inducers such as CoPP and DMF, as well as commercial preparations of BV, are associated with intolerable side effects or toxicity concerns. Therefore, identification of alternative modulators of the HO-1 system which can be used to harness the therapeutic properties of HO-1 is of considerable interest. Furthermore, increased understanding of the mechanism(s) by which HO-1 exerts its anti-inflammatory effects will inform the development of novel anti-inflammatories. The plant-derived polyphenols, carnosol and curcumin, are candidate HO-1 inducers yet there has been little research into their effects on human immune cells. Similarly, PCB represents a promising analogue of BV, yet there has been no direct comparison of their anti-inflammatory effects in innate immune cells. Therefore, the goal of this study is to explore the potential of these naturally-derived HO-1 inducers and products as immunomodulators in human immune cells, through investigation of their effects on different mediators of immune regulation, including DC, T cells and metabolic signalling.

1.5.1 Aims

- To determine if carnosol, curcumin or PCB treatment can modulate the maturation and function of human DC.
- To assess whether carnosol or curcumin can inhibit pro-inflammatory T cell responses and promote Tregs, in human PBMC and $CD4^+$ T cells.
- To characterise the effects of carnosol and curcumin on metabolic activity and signalling within human DC and PBMC.
- To investigate the effects of carnosol and curcumin in human keratinocytes and *ex vivo* psoriasis patient PBMC

Chapter 2:
Materials and Methods

2.1 Materials

2.1.1 Cell culture

Lymphoprep was purchased from Axis-Shield poC. MagniSort Human CD14 Positive Selection Kit and Human CD4 Positive Selection Kit were purchased from eBioscience. The following were all purchased from Sigma-Aldrich: Dulbecco's Phosphate-Buffered Saline (PBS), Roswell Park Memorial Institute (RPMI)-1640 Medium, Dulbecco's Modified Eagle's Media (DMEM), L-Glutamine, Penicillin-Streptomycin solution, Foetal Bovine Serum (FBS), Ethylenediaminetetraacetic Acid (EDTA), Trypsin-EDTA solution, Trypan Blue solution and Dimethyl Sulfoxide (DMSO). Human recombinant Granulocyte-Monocyte Colony-Stimulating Factor (GM-CSF) and IL-4 were purchased from Miltenyi Biotec.

2.1.2 Reagents

Biliverdin hydrochloride (BV; microbial source), phycocyanobilin (PCB; microbial source) and Sn(IV) Protoporphyrin IX dichloride (SnPP) were all purchased from Frontier Scientific. Carnosol (from *Rosemarinus officinalis*) and curcumin (from *Curcuma longa*) were purchased from Sigma-Aldrich and dissolved in DMSO. Human hemoglobin (Hb) was purchased from Sigma-Aldrich and dissolved in fresh RPMI before use. Compound C (also known as dorsomorphin) was purchased from Sigma-Aldrich and dissolved in DMSO. 5-Aminoimidazole-4-carboxamide ribonucleotide (AICAR) was purchased from Sigma-Aldrich and dissolved in water. Ultrapure lipopolysaccharide (LPS) from E. Coli O111:B4 was purchased from Enzo Life Sciences. Human monoclonal anti-CD3 and anti-CD28 antibodies were purchased from eBioscience. AlamarBlue was purchased from BioRad.

2.1.3 Western blotting

All chemicals used were purchased from Sigma-Aldrich unless otherwise stated. Acrylamide was purchased from Fisher. SeeBlue Plus2 Pre-Stained Protein Standard was purchased from Invitrogen. Immobilon polyvinylidene difluoride (PVDF) membrane and Enhanced Chemiluminescent (ECL) Horseradish-Peroxidase (HRP) Substrate were purchased from Merck Millipore.

2.1.4 Primary antibodies

Anti-phospho-MEK, anti-MEK, anti-phospho-p38, anti-p38, anti-phospho-ERK (1/2), anti-ERK (1/2), anti-IκB, anti-phospho-AMPK and anti-AMPK were all purchased from Cell Signalling

Technology. Anti-HO-1 was purchased from Enzo Life Sciences. Anti-pro-IL-1β was purchased from R&D Systems. Anti-β-actin-peroxidase was purchased from Sigma-Aldrich.

2.1.5 Secondary antibodies

Anti-rabbit IgG (whole molecule)-peroxidase, anti-mouse IgG (whole molecule)-peroxidase and anti-goat IgG (whole molecule)-peroxidase were purchased from Sigma-Aldrich.

2.1.6 Flow cytometry

Phorbol 12-myristate 13-acetate (PMA), ionomycin and brefeldin were purchased from Sigma. Anti-mouse Ig CompBeads were purchased from BD. Fix & Perm kit, FITC-conjugated DQ-Ovalbumin and Mitotracker Green™ were purchased from Invitrogen. CellTraceViolet (CTV) was purchased from Life Technologies. Fixable Viability Dye eFluor506 and eFluor780, Propidium Iodide (PI), Annexin V Binding Buffer and Foxp3 Staining Buffer Kit were all purchased from eBioscience. Brilliant Stain Buffer was purchased from BD Horizon. The following fluorochrome-conjugated antibodies were purchased from eBioscience, BioLegend and BD Horizon as specified in Table 2.1.

Table 2.1. Fluorochrome-Conjugated Antibodies

Specificity	Clone	Fluorochrome	Volume used (µl/ test)	Supplier
CD3	UCHT1	BV711	1.25	BD Horizon
CD4	RPAT4	PE-CF594	1.25	BD Horizon
CD161	DX12	PE-Cy5	5	BD Horizon
TCRγδ	B1	BV650	1.25	BD Horizon
CD8	SK1	APC eFluor 780	1.25	eBioscience
CD25	BC96	PE-Cy7	1.5	eBioscience
CD127	eBioRDRS	APC-eFluor 780	1.25	eBioscience
CD39	24DMS1	PerCP-e710	1.25	eBioscience
Foxp3	236AIE7	PE	1.5	eBioscience
CTLA4	L3D10	APC	1.25	Biolegend
Ki67	SolA15	V450	1.5	eBioscience
IL-2	5344.111	PE-CF594	1.25	BD Horizon
IL-17	BL168	Alexa488	1.5	Biolegend
IFNγ	4S.B3	APC	0.5	Biolegend
TNFα	MAb11	PerCP-Cy5.5	1.25	eBioscience
GM-CSF	MP1-22E9	PE	1.25	eBioscience
IL-22	22URTI	PE-Cy7	1.25	eBioscience
CD209	9E9A8	PE-Cy7	1.5	BioLegend
CD14	61D3	FITC	1.5	eBioscience

	HCD14	FITC	1.5	BioLegend
CD40	5C3	BV510	1.25	eBioscience
CD80	2D10.4	FITC	1.5	eBioscience
CD83	HB15e	PE	1.25	eBioscience
CD86	IT2.2 IT2.2	PerCP-e710 APC	0.5 0.5	eBioscience Biolegend
Annexin V	n/a n/a	APC FITC	1.25 1.25	eBioscience Biolegend

2.1.7 Seahorse XF analyser

Seahorse XF/XFe 24 well cell culture microplates, extracellular flux assay kits, XF calibrant and XF assay media was purchased from Agilent Technologies. Oligomycin A was purchased from Cayman Chemicals. Carbonyl cyanide-p-trifluoromethoxyphenylhydrazone (FCCP) was purchased from Santa Cruz Biotechnology. Rotenone, antimycin A and 2-deoxy-D-glucose (2-DG) were purchased from Sigma-Aldrich. Cell-Tak™ was purchased from Fisher Scientific.

2.1.8 Confocal microscopy

Light-protective cell culture microplates were purchased from iBidi. Anti-p65 antibody was purchased from Santa Cruz Biotechnology. Fluorochrome-conjugated secondary anti-mouse antibody was purchased from Abcam. 4',6-diamidino-2-phenylindole (DAPI) and phalloidin stains were purchased from VWR.

2.1.9 siRNA

On-Target Plus non-targeting siRNA pools and SMARTpool siRNA oligonucleotides targeting HO-1 were purchased from Dharmacon. Oligofectamine was purchased from Invitrogen.

2.2 Methods

2.2.1 Preparation of protoporphyrins and linear tetrapyrroles

SnPP, BV and PCB were dissolved in 50 mM Tris HCl buffer pH 8.6 and adjusted to pH 7.4 for use in cell culture. Where there was incomplete dissolution of solute the concentrations of obtained solutions were determined by spectrophotometry using the Beer Lambert law. The molar extinction coefficient for SnPP at 407 nm was 36800 $M^{-1}cm^{-1}$. The molar extinction coefficients for BV and PCB at 650 nm were 12500 $M^{-1}cm^{-1}$ and 13087 $M^{-1}cm^{-1}$, respectively. Stock solutions were prepared and then diluted as required.

2.2.2 Cell culture

Cells were cultured at 37°C with an atmosphere of 95% humidity and 5% CO_2. RPMI and DMEM cell culture media were supplemented with 10% FBS, 2 mM L-Glutamine, 100 U/ml penicillin and 100 µg/ml streptomycin. Cell numbers and viability were determined by performing cell counts in trypan blue. Cells were diluted in trypan blue and 10 µl was loaded onto a Hycor KOVA Glastic cell counter slide and viewed under a light microscope. Cell viability was assessed by dye exclusion. The number of viable cells was determined using the following formula:

$$Number\ of cells/ml = \#\ cells\ counted\ \times\ dilution\ factor\ \times\ 10^4$$

2.2.3 HaCaT cell culture

The HaCaT keratinocyte cell line was stored cryopreserved in liquid nitrogen, at a concentration of 3 x 10^6 cells/ml in freezing medium (FBS supplemented with 10% DMSO) in plastic cryovials. HaCaTs were cultured in DMEM supplemented with 10% FBS, 2 mM L-glutamine, 100 U/ml penicillin and 100 µg/ml streptomycin. HaCaTs were grown in 75 cm^2 flasks and passaged every 3-4 days by trypsinisation. For use in *in vitro* assays HaCaTs were seeded at 40,000 cells/ml one day prior to treatment and left to adhere overnight. Prior to use in cytokine or proliferation assays the cell culture media was replaced with DMEM containing 1% FBS for 12-18 hours, after which the media was returned to complete DMEM.

2.2.4 PBMC isolation

This study was approved by the research ethics committee of the School of Biochemistry and Immunology, Trinity College Dublin and is in accordance with the Declaration of Helsinki. PBMC were isolated from leukocyte-enriched buffy coats obtained from anonymous healthy donors with consent from the Irish Blood Transfusion Service, St James' Hospital, Dublin. Blood was diluted in sterile PBS and centrifuged at 1250 g for 10 minutes at room temperature, with the brake off. The buffy coat layer was removed and diluted in sterile PBS. 25 ml of diluted buffy coat was layered over 20 ml LymphoPrep and PBMC were isolated by density-gradient centrifugation at 800 g for 20 minutes at room temperature, with the brake off. The PBMC layer was removed from the interface of the gradient and washed twice in sterile PBS by centrifugation at 650 g for 10 minutes at room temperature. Isolated PBMC were re-suspended and cultured in RPMI.

2.2.5 Isolation of psoriasis patient PBMC

Written informed consent was obtained from participants attending a specialist psoriasis out-patient clinic at St Vincent's University Hospital, Dublin. This study received ethical approval from St. Vincent's University Hospital Ethics and Medical Research Committee and was conducted in

accordance with the Declaration of Helsinki. Blood samples were taken from consenting patients (n=9; mean Psoriasis Area Severity Index [PASI] 6.6 ± 3.3), PBMC were isolated as described above and stored cryopreserved at -80°C in freezing medium.

2.2.6 Isolation of CD14⁺ monocytes and CD4⁺ T Cells

$CD14^+$ monocytes and $CD4^+$ T cells were isolated from PBMC by magnetic-activated cell sorting (MACS), using the Magnisort CD14 or CD4 positive selection kits (eBioscience). PBMC were washed in MACS buffer (PBS supplemented with 2% FBS and 2 mM EDTA) and pelleted by centrifugation at 300 g for 5 minutes. PBMC were re-suspended in MACS buffer at 1 x 10^8 cells/ml in a 12 x 75 mm 5ml tube and incubated with anti-CD14 biotin (10 µl per 100 µl cells) for 10 minutes at room temperature. Cells were then washed in 4 ml MACS buffer and pelleted by centrifugation at 300 g for 5 minutes. Supernatant was discarded, cells were re-suspended in their original volume of MACS buffer and incubated with MagniSort positive selection beads (15 µl per 100 µl cells) for 10 minutes at room temperature. The volume was then adjusted to 2.5 ml and the tube placed inside the magnetic field of a Magnisort magnet for 5 minutes. The negative fraction was then poured off by inverting the tube while held inside the Magnisort magnet, and the remaining cells were re-suspended in 2.5 ml MACS buffer. This step was repeated three times and then the positive fraction containing the $CD14^+$ monocytes was re-suspended in RPMI and counted. $CD14^+$ monocyte purity was confirmed by flow cytometry and was routinely greater than 90% (Figure 2.1). For $CD4^+$ T cell isolation the CD14 negative fraction was collected and counted and the above protocol was followed using anti-CD4 biotin. $CD4^+$ T cell purity was confirmed by flow cytometry and was routinely greater than 95% (Figure 2.2).

2.2.7 Culture of monocyte derived dendritic cells

Primary human DCs were cultured from $CD14^+$ monocytes isolated from healthy human PBMCs. Purified $CD14^+$ monocytes were cultured at 1 x 10^6 cells/ml in 6 well plates in RPMI supplemented with human recombinant GM-CSF (50 ng/ml) and IL-4 (40 ng/ml). On the third day of culture half the media was carefully removed from the wells and replaced with fresh media containing GM-CSF and IL-4. On the sixth day of culture non-adherent cells were gently removed from the wells and pelleted by centrifugation at 300 g. DCs were re-suspended in RPMI and counted. The purity of DCs was determined by expression of CD14 and CD209 (DC-SIGN) by flow cytometry; $CD14^-$ $CD209^{hi}$ cells were defined as immature DCs and were routinely greater than 95% (Figure 2.3)

2.2.8 Flow cytometry

2.2.8.1 Extracellular staining

For staining of cells with fluorochrome-conjugated antibodies against extracellular markers, cells were harvested and washed in PBS. Cells were first stained with an amine-binding viability dye which stains dead cells by incubating them in 30 µl Fixable Viability Dye (diluted 1:1000 in PBS) for 30 minutes at 4^{o}C, protected from light. Cells were then washed in PBS and centrifuged at 300 g for 5 minutes. The supernatant was discarded and cells were incubated in 30 µl PBS (or Brilliant Stain buffer diluted 1:2 in PBS where two or more Brilliant Violet dyes were used) containing fluorochrome-conjugated antibodies at the test volumes indicated in Table 2.1, for 15 minutes at room temperature, protected from light. Following extracellular staining, cells were washed in PBS, centrifuged at 300 g and re-suspended in PBS for acquisition.

2.2.8.2 Intracellular staining

For analysis of cytokine production by flow cytometry, cells were incubated with PMA (50 ng/ml) and ionomycin (500 ng/ml) in the presence of brefeldin A (5 µg/ml) for 6 hours prior to staining. After surface staining, cells were treated with 50 µl Fix & Perm solution A for 15 minutes in the dark at room temperature. Cells were washed in PBS and centrifuged at 300 g for 5 minutes at room temperature. Cells were then stained with intracellular fluorescently labelled antibodies in 30 µl Fix & Perm solution B (or Brilliant Stain buffer diluted 1:2 in Fix & Perm solution B where two or more Brilliant Violet dyes were used) and incubated for 15 minutes in the dark at room temperature. Cells were washed again and re-suspended in PBS for acquisition.

2.2.8.3 Intranuclear staining

For staining of intranuclear markers, cells were treated with 250 µl FOXP3 fixation and permeabilisation buffer for 30 minutes in the dark at 4^{o}C following surface staining. Cells were then washed twice with 1 ml 1X FOXP3 permeabilisation buffer and centrifuged at 300 g for 5 minutes. Cells were then stained with intranuclear fluorescently labelled antibodies in 30 µl permeabilisation buffer and incubated for 30 minutes at 4^{o}C in the dark. Cells were washed in PBS and centrifuged at 300 g for 5 minutes at room temperature. Cells were then re-suspended in PBS and analysed by flow cytometry.

2.2.8.4 CTV labelling

In order to label CD4^{+} T cells with CTV to assess cellular proliferation, CD4^{+} cells were isolated as described in section 2.2.6. Cells were washed in PBS and centrifuged at 300 g. Cells were re-

suspended in 10 ml warm PBS containing 1 µM CTV and incubated at 37°C for 10 minutes. In order to stop CTV uptake into the cells, 10 ml of RPMI or 1 ml FBS was added and the cells were incubated on ice for 15 minutes. The cells were then centrifuged at 300 g, re-suspended in RPMI and counted. Stained and unstained cell samples were fixed with 4% paraformaldehyde (PFA) for use as compensation controls.

2.2.8.5 Annexin V & PI staining

For assessment of apoptosis, cells were stained with fluorochrome-conjugated anti-Annexin V and PI. Cells were washed in 1X Annexin V binding buffer and pelleted by centrifugation at 300 g. Supernatant was discarded and cells were incubated in 30 µl 1X binding buffer containing 1.25 µl fluorochrome-conjugated anti-Annexin V for 15 minutes at room temperature, protected from light. Cells were then washed in 1X binding buffer and centrifuged at 300 g. Supernatant was discarded and cells were re-suspended in 200 µl 1X binding buffer containing 5 µl PI, and immediately acquired.

2.2.8.6 DQ-Ovalbumin

The model antigen DQ-Ova, which fluoresces upon processing by proteases inside the cell, was used to assess antigen uptake. DQ-Ova was prepared to a stock concentration of 1 mg/ml. Cells were incubated with fresh media containing 500 ng/ml DQ-Ova for 20 minutes at 37°C, followed by incubation at 4°C for 10 minutes. Cells were then washed in PBS, centrifuged at 300 g, re-suspended in PBS and immediately acquired. Cells treated with media containing no DQ-Ova were used as a gating control for DQ-Ova positive cells.

2.2.8.7 Mitotracker Green labelling

In order to analyse mitochondrial mass, cells were stained with Mitotracker Green. Cells were washed in warm PBS and centrifuged at 300 g for 5 minutes. Supernatants were removed and cells were stained with Mitotracker Green at a final concentration of 4 nM in PBS. Cells were incubated for 30 minutes at 37°C. Cells were washed in warm PBS and centrifuged at 300 g for 5 minutes. Supernatants were removed and cells were acquired immediately.

2.2.8.8 Acquisition, compensation and analysis

Where flow cytometry experiments contained more than one fluorochrome, single-stained controls were prepared for each fluorochrome using BD CompBeads in order to calculate spectral compensation. Samples were acquired on either a BD FACSCanto II or LSRFortessa flow cytometer. All flow cytometry data analysis was performed using FlowJo v10 (Treestar Inc) software.

Polyfunctionality of T cells from psoriasis patient PBMC was analysed using SPICE software (National Institute of Allergy and Infectious Diseases, National Institutes of Health). Cells were gated on according to the gating strategies presented in Appendix 4.

2.2.9 Enzyme-Linked Immunosorbent Assay

The concentrations of cytokines present in supernatants collected from cell cultures were measured by Enzyme-Linked Immunosorbent Assay (ELISA) using eBioscience Ready-Set-Go ELISA kits for IL-8, TNF-α, IL-12p70, IL-23p19, IL-10, IFN-γ and IL-17. 96-well high binding plates were coated with 75 µl of capture antibody diluted in PBS (1:250 dilution) and incubated overnight at 4°C. The capture antibody was removed and 75 µl 1X assay diluent was added to the plates and incubated for 1 hour at room temperature. The plates were then washed 3 times by submerging in ELISA wash buffer (PBS, 0.0005% Tween-20). 100 µl of serially-diluted protein standards (recombinant cytokines of known concentrations) were prepared in 1X assay diluent and added to the plates in triplicate. Between 50 – 100 µl of supernatants were added to the plates either undiluted or diluted in 1X assay diluent and incubated overnight at 4°C. The next day the plates were washed 3 times with ELISA wash buffer and 75 µl of detection antibody diluted in 1X assay diluent (1:250 dilution) was added to the plates, which were then incubated for 2 hours at room temperature. The plates were washed 3 times with ELISA wash buffer and 75 µl of HRP-conjugated streptavidin diluted in 1X assay diluent (1:250 dilution) was added and incubated for 20 minutes at room temperature, protected from light. The plates were then thoroughly washed in ELISA wash buffer and 75 µl of TMB solution was added. The plates were allowed to develop protected from light and the reaction was stopped by the addition of 35 µl 1 M sulphuric acid. The OD value of each well was determined at 450 nm using a microplate reader. A standard curve was generated using the serially diluted protein standards and used to determine the concentration of cytokine in the supernatant.

2.2.10 SDS-PAGE and Western blotting

2.2.10.1 Sample preparation

Cell lysates were prepared by removing cell supernatants and washing cells in PBS prior to addition of high stringency lysis buffer (HSLB; 1 mM EDTA, 10% Glycerol, 50 mM HEPES, 100 mM NaCl, 1% NP-40, pH 7.5) containing 1% phosphatase inhibitor cocktail 3. The samples were centrifuged at 16,000 g for 5 minutes, and the lysates were transferred to new Eppendorf tubes and stored at -20°C until use.

2.2.10.2 SDS-PAGE

Either 10% or 12% polyacrylamide gels were prepared (Table 2.2) depending on the size of the protein of interest, and placed in 1X running buffer (25 mM Tris, 250 mM Glycine, 1% SDS, pH 8.3). Samples were thawed and diluted in Laemmli buffer containing 5% β-mercaptoethanol, and boiled at 100°C for 5 minutes. Samples and a pre-stained molecular weight ladder were loaded onto the gels. Electrophoresis was carried out at 120 volts (V) for 90 minutes.

Table 2.2. Composition of SDS-polyacrylamide gel (2 gels)

	10% Resolving Gel	**12% Resolving Gel**	**Stacking Gel**
30% Acrylamide	5 ml	6 ml	0.67 ml
H_2O	5.9 ml	4.9 ml	2.7 ml
1.5 M Tris-HCl	3.8 ml	3.8 ml	-
1 M Tris-HCl	-	-	0.5 ml
10% SDS	0.15 ml	0.15 ml	40 µl
10% APS	0.15 ml	0.15 ml	40 µl
Temed	6 µl	6 µl	6 µl

2.2.10.3 Transfer of proteins onto PVDF membrane

The resolved proteins were transferred onto a PVDF membrane. The gel was removed and placed onto a sheet of filter paper soaked in 1X transfer buffer (39 mM Glycine, 48 mM Tris, 20% methanol, pH 8.0). The PVDF membrane was soaked in methanol and placed carefully over the gel. An additional filter paper soaked in 1X transfer buffer was then placed on top of the PVDF membrane. The system was then pressed tightly together to ensure there were no air bubbles between the gel and the membrane. The proteins were transferred for 75-90 minutes at 200 milliamperes (mA) in 1X transfer buffer.

2.2.10.4 Immunodetection of proteins

PVDF membranes contained resolved proteins were incubated for 1 hour at room temperature in either 5% Marvel in TBST (2 mM Tris, 50mM NaCl, 0.05% Tween-20, pH 7.6) or 3% BSA in TBST. The membrane was then incubated in primary antibody (diluted according to Table 2.3) overnight at 4°C. The following day, the membrane was washed 3 times for 5 minutes with TBST, and then incubated for 2 hours in secondary antibody (Table 2.3) at room temperature. The membrane was then washed a further 3 times and developed using freshly prepared ECL on a BioRad ChemiDoc

system. Densitometry analysis was performed using ImageLab software (BioRad). Examples of full-length blots are provided in Appendix 3.

Table 2.3. Dilutions for Western blot antibodies

Primary Antibody	Dilution	Secondary Antibody	Dilution
Anti-HO-1	1:1000	Anti-Rabbit	1:2000
Anti-phospho-MEK	1:1000	Anti-Rabbit	1:2000
Anti- MEK	1:2000	Anti-Rabbit	1:2000
Anti-phospho-ERK (1/2)	1:2500	Anti-Rabbit	1:2000
Anti-ERK (1/2)	1:5000	Anti-Rabbit	1:2000
Anti-phospho-p38	1:1000	Anti-Rabbit	1:2000
Anti-p38	1:1000	Anti-Rabbit	1:2000
Anti-phospho-AMPK	1:1000	Anti-Rabbit	1:2000
Anti-AMPK	1:1000	Anti-Rabbit	1:2000
Anti-IκB	1:1000	Anti-Mouse	1:1000
Anti-Pro-IL-1β	1:500	Anti-Goat	1:1000
Anti-β-actin-peroxidase	1:50,000	-	-

2.2.11 Seahorse XF/XFe 24 analyser

The Seahorse XF/XFe 24 analyser simultaneously measures in real time the oxygen consumption rate (OCR), a measure of the rate of oxidative phosphorylation, and extracellular acidification rate (ECAR), a measure of the rate of glycolysis, in the medium directly surrounding a single layer of cells. The Seahorse cartridge plate, consisting of the sensors for O_2 and pH, was hydrated prior to use by the addition of 1 ml XF calibrant fluid per well and incubated in a no-CO_2 incubator at 37°C for a minimum of 8 hours prior to use.

2.2.11.1 PBMC Seahorse experiments

Seahorse 24-well microplates were pre-treated with 50 µl/well Cell-Tak™ (22.4 µg/ml) dissolved in 0.1 M sodium bicarbonate (pH 8.0) and incubated at room temperature for a minimum of 30 minutes. Following incubation, the wells were washed twice with sterile water. PBMC were counted, washed and re-suspended in complete XF assay medium (supplemented with 10 mM glucose, 1 mM sodium pyruvate, 2 mM L-glutamine and pH adjusted to 7.4) and seeded into the microplate at 5 x 10^5 cells/well, in an initial volume of 100 µl/well. Blank wells (XF assay medium only) were left without PBMC for subtracting background OCR and ECAR during Seahorse analysis. The microplate was briefly pulse centrifuged, rotated and pulse centrifuged a second time to ensure cells were adhered to the bottom of the plate. The plate was incubated in a no-CO_2

incubator at 37°C for 15 minutes. An additional 400 µl/well of complete assay medium was gently added to each well and the plate was incubated for a further 15 minutes.

Metabolic compounds were prepared in XF assay medium and loaded into the appropriate injection ports on the cartridge plate (75 µl/port) and incubated for 10 minutes in a no-CO_2 incubator at 37°C. The cartridge was then placed into the XF/XFe analyser and the machine was calibrated. Following calibration the cell plate was added to the XF/XFe analyser and the OCR and ECAR were measured over time as detailed in Table 2.4. Upon completion of the assay the XF assay medium was removed and HSLB was added to each well. Protein concentration was determined by the Pierce BCA assay (ThermoFisher) to ensure protein content was similar between all treatment wells.

2.2.11.2 DC Seahorse experiments

DC were washed and re-suspended in complete RPMI and seeded at 2 x 10^5 cells/well into the Seahorse 24 well microplate. DC were cultured with relevant experimental conditions in the Seahorse microplate for up to 24 hours prior to Seahorse analysis. 30-60 minutes prior to placement into the XF/XFe analyser the culture medium was replaced with complete XF assay medium and incubated in a no-CO_2 incubator at 37°C. Blank wells (XF assay medium only) were left without DC for subtracting background OCR and ECAR during Seahorse analysis.

Metabolic compounds were prepared in XF assay medium and loaded into the appropriate injection ports on the cartridge plate (75 µl/port) and incubated for 10 minutes in a no-CO_2 incubator at 37°C. The cartridge was then placed into the XF/XFe analyser and the machine was calibrated. Following calibration the cell plate was added to the XF/XFe analyser and the OCR and ECAR were measured over time as detailed in Table 2.4. Upon completion of the assay the XF assay medium was removed and HSLB was added to each well. Protein concentration was determined by the Pierce BCA assay (ThermoFisher) to ensure protein content was similar between all treatment wells.

Table 2.4. Seahorse protocol

Step	Action
1	Equilibrate
2	Mix (3 mins)
3	Wait (2 mins)
4	Measure (3 mins)
5	Repeat steps 2-4 x2
6	Inject Port A
7	Repeat steps 2-4 x3
8	Inject Port B
9	Repeat steps 2-4 x3
10	Inject Port C
11	Repeat steps 2-4 x3
12	Inject Port D
13	Repeat steps 2-4 x3
14	End protocol

2.2.11.3 Seahorse analysis

Analysis of results was performed using Wave software (Agilent Technologies). The rates of basal glycolysis, max glycolysis, glycolytic reserve, basal respiration, max respiration, ATP production and respiratory reserve were calculated as detailed in Table 2.5:

Table 2.5. Seahorse calculations

Rate	Calculation
Non-glycolytic ECAR	Average ECAR values after 2-DG treatment.
Basal glycolysis	Average ECAR values prior to oligomycin treatment – non-glycolytic ECAR
Max glycolysis	Average ECAR values after oligomycin & before FCCP treatment
Glycolytic reserve	Max glycolysis – basal glycolysis
Non-mitochondrial OCR	Average OCR values after rotenone/antimycin A & before 2-DG treatment
Basal respiration	Average OCR values prior to oligomycin treatment – non-mitochondrial OCR
Max respiration	Average OCR values after FCCP & before rotenone/antimycin A treatment
Non-ATP respiration	Average of OCR values after oligomycin & before FCCP treatment
ATP production	Basal respiration – non-ATP respiration
Respiratory reserve	Max respiration – basal respiration

2.2.12 Confocal microscopy

2.2.12.1 NF-κB nuclear translocation

Translocation of the active subunit of NF-κB, p65, from the cytosol to the nucleus during LPS activation of DC was imaged by confocal microscopy. DC were seeded at 1 x 10^6 cells/ml in a light-protective microplate (iBidi) and cultured with relevant experimental conditions. The microplate was spun at 110 g for 5 minutes and cells were fixed with 4% PFA in PBS for 15 minutes at room temperature. Cells were permeabilised by incubation in 100% methanol for 5 minutes at -20^{o}C. Following fixation and permeabilisation, cells were incubated with blocking buffer (5% BSA, 0.005% Tween-20 in PBS) for 1 hour at room temperature. After blocking, cells were incubated with anti-p65 antibody in blocking buffer (1:300) for 3 hours at room temperature, followed by incubation with a fluorochrome-conjugated secondary anti-mouse antibody in blocking buffer (1:500) for 1 hour at room temperature. Finally, nuclei were stained with DAPI in PBS (1:2000) for 5 minutes at room temperature, and washed in PBS. Images were taken on a Leica SP8 scanning confocal microscope at X63 magnification.

2.2.12.2 HaCaT proliferation

Proliferation of HaCaT keratinocytes was analysed by confocal microscopy. HaCaTs were seeded at 40,000 cells/ml in a light-protective microplate (iBidi) and left to adhere for 24 hours. After 24 hours cell culture medium was replaced with DMEM containing 1% FBS for 12-18 hours to synchronise the cell cycle. HaCaTs were then cultured in relevant experimental conditions for 24 hours. Cells were fixed with 4% PFA in PBS for 15 minutes at room temperature. Cells were permeabilised by incubation with 0.5% Triton X in PBS for 10 minutes at room temperature. Cells were then washed with PBS and incubated with phalloiden solution (1:2000) in PBS for 2 hours at room temperature, in the dark. Cells were washed with PBS and nuclei were stained with DAPI in PBS (1:2000) for 5 minutes at room temperature. Tile scan images were taken on a Leica SP8 scanning confocal microscope at X10 magnification. The number of cells per image was counted using ImageJ software. Each experimental condition was run in duplicate and the average cell count from both duplicates was reported for each experiment.

2.2.13 siRNA transfection

Oligonucleotides were solubilised in RNase-free water to a final concentration of 20 μM. Further dilutions of oligonucleotides and oligofectamine were made according to Table 2.6. After 5 minutes, diluted oligofectamine was added dropwise onto the diluted oligonucleotides, and incubated for 15-20 minutes at room temperature to allow complexes to assemble. The cells were

washed in pre-warmed serum- and antibiotic- free medium and then the appropriate volume of serum- and antibiotic-free medium was added to the wells, as detailed in Table 2.6. The complexes were then added dropwise onto the cells, and mixed by gently swirling the cell culture plate. Cells were incubated for 6 hours prior to addition of cell culture medium containing 2X concentrations of FBS and L-glutamine. Cells were cultured for a further 24-72 hours to complete transfection.

Table 2.6. Components and volumes required for siRNA transfection

	Component	**6-well plate**	**24-well plate**
Oligonucleotide dilution (1:10; volume per well)	Oligonucleotides	10 µl	2.5 µl
	Serum & antibiotic free medium	90 µl	22.5 µl
Oligofectamine dilution (1:5; volume per well)	Oligofectamine	4 µl	1 µl
	Serum & antibiotic free medium	16 µl	4 µl
Volume per well	Serum & antibiotic- free medium	880 µl	220 µl
Volume per well	2X medium	1 ml	250 µl

2.2.14 AlamarBlue viability assay

Viability of HaCaTs was measured by reduction of alamarBlue reagent. A volume of alamarBlue equal to 10% of the cell culture volume was added to each well and the plate was swirled gently to mix. Cells were incubated at 37^{o}C for 18 hours and then absorbance was read at 570 nm and 600 nm. The 600 nm absorbance values were subtracted from the 570 nm values, and cellular viability was expressed as a percentage of the untreated control.

2.2.15 Statistical analysis

All statistical analysis was performed on GraphPad Prism 6 software. Comparison of two treatment groups was made by a two-tailed Student's t test. ≥ 3 groups were analysed by one-way ANOVA with either Tukey's multiple comparisons post hoc test to compare the means of all groups with each other, Dunnett's multiple comparisons post hoc test to compare the means of treatment groups to a control group, or Sidak's multiple comparisons post hoc test to compare the means of preselected treatment group pairs. Resulting p values ≤ 0.05 were considered significant and denoted with asterisks or hash marks in the figures.

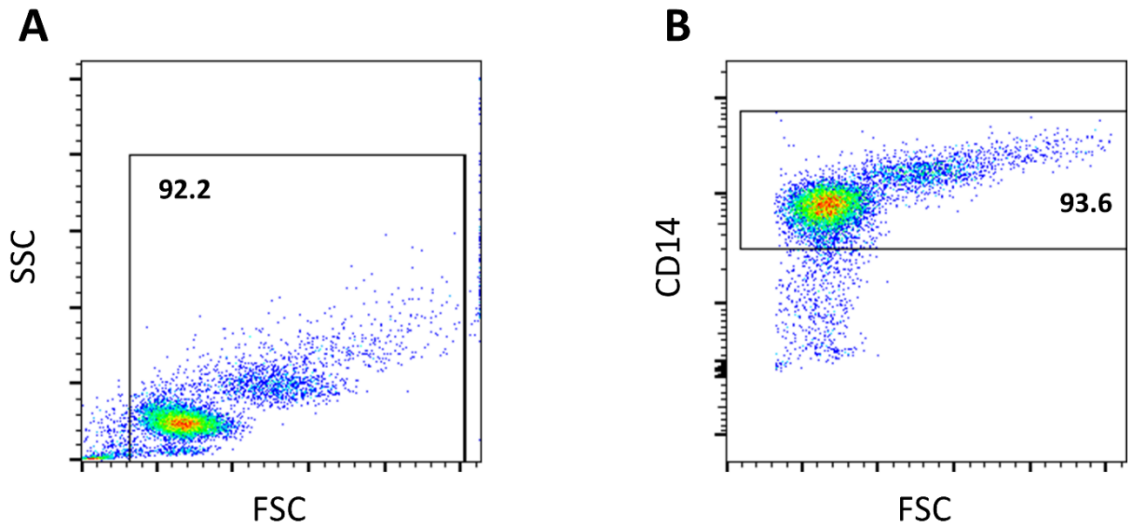

Figure 2.1. Analysis of monocyte purity by flow cytometry. Purified monocytes were identified as $CD14^{+}$ by flow cytometry. **(A)** Dead cells and cellular debris were excluded on the basis of size (forward scatter; FSC) and granularity (side scatter; SSC). **(B)** Viable cells were then gated for CD14 expression.

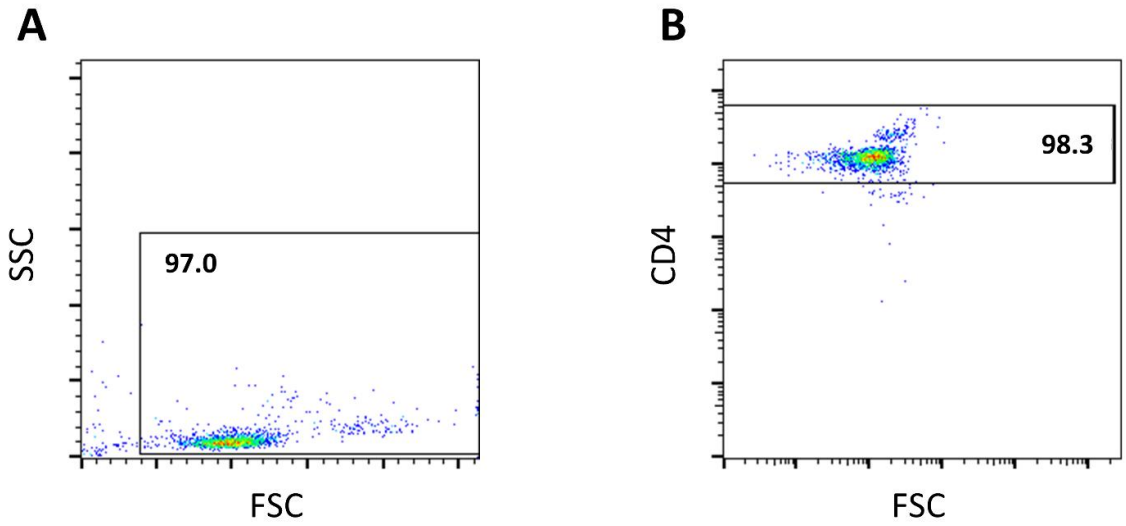

Figure 2.2. Analysis of CD4⁺ T cell purity by flow cytometry. Purified CD4⁺ T cells were identified as CD4⁺ by flow cytometry. **(A)** Dead cells and cellular debris were excluded on the basis of size (FSC) and granularity (SSC). **(B)** Viable cells were then gated for CD4 expression.

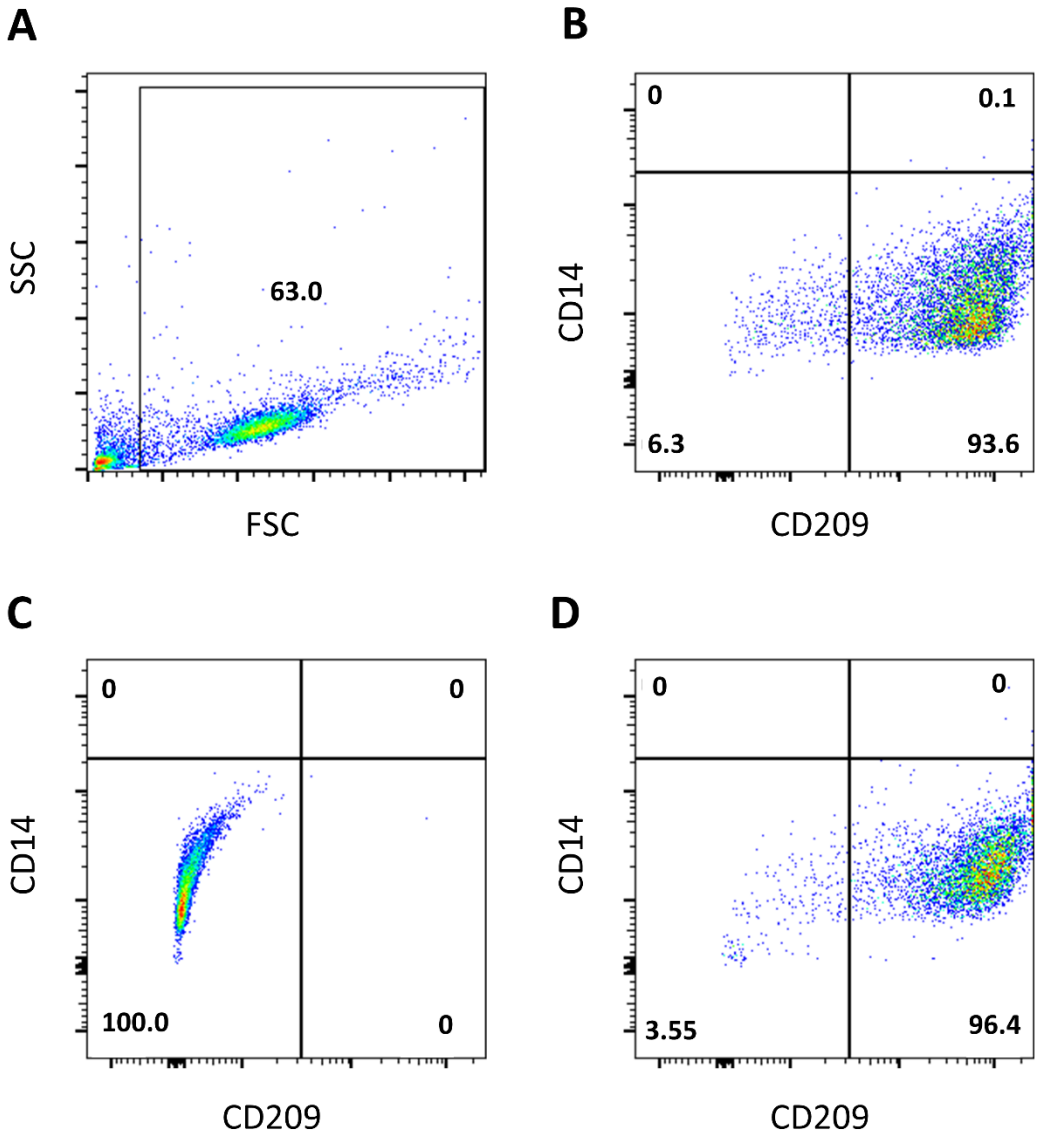

Figure 2.3. Analysis of DC purity by flow cytometry. Human monocyte-derived DC were identified as $CD14^{-}CD209^{+}$ by flow cytometry. **(A)** Dead cells and cellular debris were excluded on the basis of size (FSC) and granularity (SSC). Viable cells were then gated for **(B)** CD14 and **(C)** CD209 expression using fluorescence-minus-one (FMO) controls. **(D)** FMO defined CD14 vs CD209 gate was then applied to DC sample to determine purity of the DC population.

Chapter 3:
Modulation of the HO-1 system in human DC

3.1 Introduction

DC play a central role in the generation of both pro- and anti-inflammatory immune responses due to their position as the 'professional' APC of the immune system. Therefore, drugs which modulate the phenotype and function of DC are highly sought after as new treatment strategies for diseases in which the immune response is dysregulated. In the case of autoimmunity, DC can either instigate or protect against self-directed inflammation. In EAE & MS, DC have been implicated in the induction of pathogenic Th17 cells and neuroinflammation (331–337). However, tolerogenic DC have been found to be protective against EAE. For example, Yogev *et al.* observed that depletion of DC prior to induction of EAE aggravates disease symptoms due a reduction of Treg numbers (338), while the beneficial effects of TGF-β and IFN-β in EAE have been attributed to the activity of DC (339,340). Similarly, in psoriasis, the immunological synapse between DC and T cells has become a target of interest for disease treatment. Enrichment of pro-inflammatory DC has been observed in psoriatic plaques (341,342), where they contribute to local inflammation of the skin and promote differentiation of Th17 cells. Specifically, the pro-inflammatory cytokines TNFα and IL-23 produced by DC have been shown to be key contributors to the pathology of psoriasis, as evident by the clinical efficacy of treatments targeting these cytokines (343–345). Meanwhile, Langerhans cells, a DC subset resident in the epidermis, act to suppress inflammation in psoriatic lesions via production of the anti-inflammatory cytokine IL-10 and upregulation of PD-L1 expression (346). Thus, there is solid rationale to target DC in autoimmunity, with the overall aim of re-balancing their immunogenic and tolerogenic activities.

HO-1 is a stress response protein which has been described to promote tolerogenic DC. Chauveau *et al.* were the first to report that HO-1 is constitutively expressed by immature DC, and is downregulated upon DC maturation. Furthermore, they found that DC treated with the HO-1 inducer, CoPP, were refractory to maturation by LPS, and displayed reduced pro-inflammatory cytokine production (176). Following this, it was found that HO-1 expression by DC is required for the suppressive activity of Tregs, and that DC which express HO-1 actively inhibit effector T cell responses (177,188). These results are supported by a recent study from Wong *et al.* which found that DC treated with CoPP were capable of inducing Treg differentiation, and were protective in a model of airway inflammation (189). Mechanistically, it is not well established how HO-1 modulates the activity of DC. Inhibition of p38 MAPK signalling by HO-1 has been suggested by Al-Huseini *et al.* as one mechanism by which HO-1 regulates DC function (178). Additionally, while treatment of DC with SnPP, a metalloporphyrin which inhibits the enzymatic activity of HO-1, has been shown to oppose the effects of HO-1 expression in DC (177,178), it has yet to be elucidated which products of HO-1 mediate its immunomodulatory effects. Rémy *et al.* reported that

treatment with the CO-donor CORM2 produced similar immunomodulatory effects in DC as HO-1 (207). In support of a role for CO in the activity of HO-1 in DC, Riquelme *et al.* reported that CO impairs antigen presentation and activation of T cells by DC, via inhibition of DC mitochondrial function (208). Thus, while there exists some evidence that CO is at least partially responsible for the activity of HO-1 in DC, the contributions of HO-1 derived LTPs, and the cellular pathways involved in these effects, remain unclear.

Despite the mounting evidence that upregulation of HO-1 promotes tolerogenic DC and anti-inflammatory immune responses, translation of these studies to the clinic has been hindered by the lack of suitable HO-1 inducers. HO-1 inducers used *in vitro* or in pre-clinical *in vivo* studies are typically metalloporphyrins such as CoPP and hemin, but these are difficult to administer and are associated with potential toxicities. Hence, the identification of alternative inducers of HO-1, or HO-1 products, which can be used to modulate the HO-1 system in DC, and which are more appropriate for clinical use, is required before HO-1 can be used therapeutically. Aside from metalloporphyrins, polyphenols are another class of compound whose members frequently display the capacity to upregulate HO-1. Through a review of the literature, the plant-derived polyphenols curcumin and carnosol were identified as candidate HO-1 inducers which are likely to be well tolerated as they are derived from common foods (303,304,347). Curcumin has previously been shown to inhibit the maturation and function of DC, although these studies have largely been performed in murine cells (277–280). Furthermore, while upregulation of HO-1 by curcumin has been linked to some of its anti-inflammatory effects in murine DC (286), it remains unclear to what extent its activity in human DC is mediated by HO-1. Unlike curcumin, there have been no studies to date investigating the effects of carnosol in either murine or human DC.

Finally, although BV is known to mediate some of the antioxidant and anti-inflammatory effects of HO-1 *in vivo* (196,201,245,348), it remains unknown to what extent it contributes to the activity of HO-1 in DC. Rémy *et al.* previously reported that CO, but not other HO-1 products, was responsible for the immunomodulatory activity of HO-1 in human DC (207). However this study tested only one concentration of BV (10 μM), and a non-significant trend towards reduced maturation and cytokine production with BV treatment can be observed on assessment of their results. Therefore, it is possible that higher concentrations of BV may replicate some of the activity seen with HO-1 inducers in DC. Clinically, however, BV faces similar challenges to metalloporphyins as commercially available preparations of BV are not approved for use in humans due to contamination and toxicity concerns. Interestingly, a structural analogue to BV, PCB, has been identified as a component of phycocyanin, a chromoprotein found in Spirulina (317). Furthermore, data from the Dunne lab has confirmed that PCB acts as a substrate for human

BVR, lending credence to the hypothesis that it may replicate the activity of BV (318). Little research into the anti-inflammatory effects of PCB has been carried out to date, and there are currently no studies investigating its use in DC.

In summary, the HO-1 system is known to have immunomodulatory activity in DC, and to promote the generation of tolerogenic DC that may be useful in the context of autoimmunity. However, it is unclear how HO-1 achieves its anti-inflammatory effects in DC, and which of its reaction products contribute to these effects. Furthermore, currently available HO-1 inducers and products are unsuitable for clinical use, therefore it is necessary to identify whether alternative HO-1 inducers, such as carnosol and curcumin, or LTPs such as PCB, can also be used to modulate the phenotype and function of DC.

3.2 Aims

- To characterise the immunomodulatory effects of the polyphenols, carnosol and curcumin, and the LTP, PCB, in primary human DC.
- To determine the contribution of the HO-1 reaction products, BV and CO, to its immunomodulatory activity in human DC.
- To elucidate the molecular mechanism(s) by which the HO-1 inducers, carnosol and curcumin, modulate the phenotype and function of human DC.

3.3 Results

3.3.1 Carnosol and curcumin are non-toxic to primary human DC

The polyphenols carnosol and curcumin are poorly soluble in water, therefore DMSO was chosen as the vehicle for these compounds. However, DMSO is known to be potentially toxic to cell cultures even at low concentrations (349). Stock solutions were prepared to ensure that the final concentration of DMSO in cell cultures was not greater than 0.5%. In order to confirm that the preparations of carnosol and curcumin were non-toxic to primary human DC at the concentrations used in this study, DC were treated with carnosol or curcumin (2.5-10 μM) and cell viability was examined after 24 hours. Apoptotic cell death was measured by Annexin V & PI staining, with no increase in apoptosis observed in carnosol or curcumin treated DC compared to the vehicle control (Figure 3.1A). Total viability was measured using an amine-binding viability dye, and again no differences were seen between carnosol or curcumin treated DC and the vehicle control (Figure 3.1B). The viability of DC after 24 hours was typically in the range of 80-90% with all treatments, therefore carnosol and curcumin were determined to be well tolerated by primary human DC at the concentrations used in this study.

3.3.2 BV and PCB are non-toxic to primary human DC

As the only previous study to examine BV treatment in human DC used just one concentration (10 μM) (207), the viability of human DC treated with higher concentrations of BV (25-100 μM) was assessed. Furthermore, as PCB has not been investigated using human DC before, the viability of DC treated with various concentrations of PCB (12.5-50 μM) was also measured. Both BV and PCB are soluble in aqueous buffers, therefore DMSO toxicity was not a concern. DC were treated with BV or PCB and cell viability was measured after 24 hours. Apoptotic cell death was measured by Annexin V & PI staining, with no increase in apoptosis observed in BV or PCB treated DC compared to the vehicle control (Figure 3.2A). Total viability was measured using an amine-binding viability dye, and again no differences were seen between BV or PCB treated DC and the vehicle control (Figure 3.2B). As previously observed, the viability of DC after 24 hours was typically in the range of 80-90% with all treatments, therefore BV and PCB were also well tolerated by primary human DC at the concentrations used in this study.

3.3.3 Carnosol and curcumin induce HO-1 expression in both immature and LPS-treated DC

Carnosol and curcumin have previously been described to induce HO-1 in other cell types (303,304), and it was confirmed that they are non-toxic to human DC up to 10 μM, therefore it

was next examined whether they were capable of upregulating HO-1 in DC at these concentrations. DC were treated with carnosol or curcumin (2.5-10 μM) for 24 hours and HO-1 expression was assessed by Western blot. Immature DC constitutively expressed HO-1 (Figure 3.3A, lane 1), and consistent with previous reports (176,177), LPS-stimulated mature DC downregulated HO-1 expression (Figure 3.3A, lane 2). Conversely, treatment with carnosol or curcumin alone enhanced HO-1 expression (Figure 3.3A, lanes 4-9). Next it was determined whether this upregulation of HO-1 by carnosol and curcumin would be seen in the presence of a maturation stimulus such as LPS. DC were treated with carnosol or curcumin (2.5-10 μM) for 6 hours, to allow for the upregulation of *HMOX1* gene transcription and protein translation, prior to treatment with LPS (100 ng/ml), and HO-1 expression was assessed by Western blot after 24 hours. As before, the basal expression of HO-1 was reduced in LPS-stimulated DC (Figure 3.3B, lane 2), however this was overcome in the presence of carnosol or curcumin (Figure 3.3B, lanes 3-8).

3.3.4 Treatment with carnosol or curcumin inhibits LPS-mediated maturation of human DC

Mature DC are capable of activating naïve T cells and initiating pro-inflammatory immune responses which contribute to the pathology of autoimmune diseases. HO-1 overexpression with CoPP has previously been shown to arrest the maturation of DC via inhibition of surface co-stimulatory and maturation marker upregulation (176,178,350). Similar observations have been reported in curcumin-treated DC in response to LPS stimulation (279,280). Having confirmed that both carnosol and curcumin upregulate HO-1 expression in human DC, it was next investigated whether they could also inhibit DC maturation in response to a pro-inflammatory stimulus such as LPS. Immature DC were incubated with increasing concentrations of carnosol or curcumin for 6 hours prior to stimulation with LPS. Expression of the co-stimulatory molecules CD80 and CD86, and the maturation markers CD40 and CD83 was measured by flow cytometry after 24 hours. Both carnosol and curcumin significantly downregulated expression of all markers tested compared to control DC, and these effects were observed to be dose-dependent ($p<0.05$ – $p<0.001$; Figure 3.4).

3.3.5 Treatment with BV and PCB moderately reduces LPS-mediated DC maturation

Despite previous reports that HO-1 expression inhibits DC maturation in response to pro-inflammatory stimuli (176,178,350), it is unclear which HO-1 products mediate this effect. Although it was reported that CO, but not BV, was capable of reducing expression of CD80, CD83 and CD86 in LPS-stimulated DC (207), the concentration of BV used was much lower than the concentrations selected for use in this study. Additionally, the effects of PCB on human DC

maturation have yet to be investigated. Therefore, it was next examined whether BV or PCB could reduce LPS-mediated DC maturation. Immature DC were incubated with increasing concentrations of BV or PCB for 6 hours (in accordance with incubation times used for polyphenol experiments) prior to stimulation with LPS. Expression of the co-stimulatory molecules CD80 and CD86, and the maturation markers CD40 and CD83 was measured by flow cytometry after 24 hours. There was a trend towards reduced expression of all markers in BV and PCB treated DC, however significant reductions were seen only for CD83 in DC treated with 100 µM BV ($p<0.01$) and for CD40 in DC treated with 50 µM PCB ($p<0.05$; Figure 3.5). This suggests that BV can contribute to the reduction of DC maturation by HO-1, and furthermore, indicates that PCB possesses similar activity to BV in this regard, at least in an *in vitro* context.

3.3.6 Carnosol and curcumin treatment maintains the phagocytic capacity of LPS-stimulated DC in a HO-1-dependent manner

Upon maturation, DC lose their capacity to take up/phagocytose antigens as their role switches from tissue surveillance to antigen presentation (19,351). As it was previously observed that carnosol and curcumin reduced the phenotypic maturation of DC, it was next investigated whether they might also maintain the capacity of DC to uptake antigens after LPS stimulation. To test this, immature DC were pre-treated with carnosol (10 µM) or curcumin (10 µM) for 6 hours prior to stimulation with LPS. After 24 hours, DC were incubated with FITC-conjugated DQ-Ovalbumin (DQ-Ova; a model antigen) at 500 ng/ml and analysed for antigen uptake by flow cytometry. As expected, immature DC displayed high DQ-Ova uptake, and this was significantly reduced in LPS-stimulated DC ($p<0.001$). However, both carnosol and curcumin treatment maintained the phagocytic capacity of LPS-treated DC, with DQ-Ova uptake levels observed to be similar to that of immature DC (Figure 3.6A,B). In order to determine if this effect is dependent on HO-1 activity, immature DC were treated with carnosol or curcumin in the presence or absence of SnPP, a HO-1 enzymatic inhibitor, prior to LPS stimulation and DQ-Ova treatment as before. The observed increase in DQ-Ova uptake in carnosol- and curcumin-treated DC stimulated with LPS was significantly attenuated in the presence of SnPP confirming that HO-1 activity is indeed required for this effect ($p<0.05$; Figure 3.6A,C).

3.3.7 BV and PCB do not modulate the phagocytic capacity of LPS-stimulated DC

Having observed that the maintenance of antigen uptake in LPS-stimulated DC by carnosol and curcumin was dependent on HO-1 activity, and that BV and PCB displayed some capacity to limit DC maturation, it was hypothesised that BV could modulate antigen uptake by DC downstream of

HO-1. DC were incubated with BV or PCB for 6 hours prior to LPS stimulation and DQ-Ova treatment as previously described. Unlike carnosol and curcumin treated DC, neither BV nor PCB treatment increased the antigen uptake capacity in LPS stimulated DC (Figure 3.7). Therefore, it can be concluded that the HO-1 dependent activity of carnosol and curcumin on DC antigen capture is not mediated by BV or other LTPs, and is instead likely mediated by CO.

3.3.8 Carnosol and curcumin reduce pro-inflammatory cytokine production by LPS-stimulated human DC

Cytokine production by DC plays a significant role in the pathology of autoimmune diseases. For example, TNFα contributes to local inflammation, while IL-12 and IL-23 instruct T cell polarisation towards the pro-inflammatory Th1 and Th17 phenotypes, respectively (36,352). Upregulation of HO-1 expression has previously been described to reduce cytokine production by LPS-stimulated DC (176,178). Furthermore, curcumin has been reported to reduce IL-12 production by DC, but its effects on other pro-inflammatory cytokines have not been assessed (277,280). To examine the effect of carnosol and curcumin on cytokine production by human DC, immature DC were pre-treated with carnosol or curcumin and stimulated with LPS for 24 hours as before. Supernatants were collected and analysed by ELISA for IL-12p70, IL-23p19, TNFα and IL-10. Both carnosol and curcumin treatment reduced IL-12p70 and IL-23p19 to almost undetectable levels, even at the lowest concentrations tested ($p<0.05$ – $p<0.001$). Curcumin also significantly decreased the concentration of TNFα ($p<0.05$), while there was a non-significant trend towards reduced TNFα in carnosol-treated DC. A decrease in the anti-inflammatory cytokine, IL-10, was also observed with both carnosol and curcumin treatment, however the ratio of IL-10 to pro-inflammatory cytokines remained favourable (Figure 3.8).

IL-1β plays a crucial role in innate immune responses and is also associated with Th17 differentiation (353). Unlike the cytokines listed above, IL-1β is not secreted into DC cell supernatants by LPS stimulation alone as the immature cytokine (pro-IL-1β) must be processed by caspase-1 and the inflammasome complex prior to secretion. It is, however, possible to detect the intracellular pro-form of IL-1β by Western blot. To examine production of pro-IL-1β, immature DC were pre-treated with carnosol (10 μM) or curcumin (10 μM) for 6 hours prior to stimulation with LPS for 3-6 hours. Pro-IL-1β expression was upregulated in whole cell lysates from DC treated with LPS in comparison to unstimulated DC, however this effect was reduced in LPS-treated DC that had been pre-treated with either carnosol or curcumin (Figure 3.9).

3.3.9 Cytokine production by DC is reduced following treatment with BV or PCB

It is currently unclear whether BV contributes to the inhibitory effects of HO-1 on DC cytokine production (207). Furthermore, PCB treatment has not been investigated in the context of DC cytokine production. Given that both BV and PCB displayed some capacity to limit DC maturation, it was next investigated whether they could also modulate DC function. DC were incubated with BV or PCB for 6 hours prior to stimulation with LPS for 24 hours as previously described. Supernatants were collected and analysed by ELISA for IL-12p70, IL-23p19, and IL-10. Both BV and PCB significantly reduced the production of IL-12p70 and IL-23p19 ($p<0.05$ – $p<0.0001$), with PCB treatment showing greater potency over BV in the reduction of IL-23 (Figure 3.10). A trend towards reduced IL-10 was also observed with BV and PCB treatment, however, similar to carnosol and curcumin treated DC, the ratio of IL-10 to pro-inflammatory cytokines was favourable.

3.3.10 Carnosol and curcumin-treated DC have a reduced capacity to stimulate proliferation of allogeneic CD4⁺ T cells

The immune synapse between DC and $CD4^+$ T cells is central to the generation of harmful adaptive immune responses in autoimmunity, thus, the overall goal in modulating DC maturation and function in the context of autoimmunity is to limit the activation of pathogenic T cells. It has previously been reported that HO-1-overexpressing DC have an impaired ability to drive adaptive T cell responses (176,177). In order to assess the impact of carnosol and curcumin treatment on the ability of DC to activate T cells, immature DC were pre-treated with carnosol or curcumin prior to stimulation with LPS as previously described. After 24 hours, cells were washed in fresh RPMI and added to purified allogeneic $CD4^+$ T cells labelled with CTV. After 5 days, $CD4^+$ T cell proliferation was measured by CTV fluorescence and supernatants were analysed for IFNγ production as an indicator of T cell activation. Analysis of $CD4^+$ T cell proliferation revealed that T cells cultured with allogeneic DC, previously matured with LPS, demonstrated a higher level of proliferation compared to T cells cultured with immature DC. However, $CD4^+$ T cells cultured with LPS-stimulated DC, previously treated with carnosol or curcumin, showed significantly lower levels of proliferation, and this effect was observed to be dose-dependent ($p<0.05$ – $p<0.001$; Figure 3.11). Similarly, the concentration of IFNγ in the supernatants of T cells cultured with carnosol- or curcumin-treated DC was lower than that from T cells cultured with control DC (Figure 3.12). Taken together, these results suggest that carnosol and curcumin reduce the capacity of DC to stimulate allogeneic T cells.

3.3.11 Immunomodulation of DC phenotype and function by carnosol and curcumin is dependent on HO-1 activity

Curcumin has previously been reported to have immunomodulatory effects in murine and human DC similar to those seen in CoPP-treated DC (277,279,280), yet it has not been tested whether the effects of curcumin in DC are directly dependent on its ability to upregulate HO-1. Having observed that both curcumin and carnosol act as strong inducers of HO-1 in human DC, and that the maintenance of antigen uptake capacity in LPS-stimulated DC by these polyphenols was dependent on HO-1 activity, it was next investigated whether the reduction of DC maturation and cytokine production by curcumin and carnosol would also be dependent on HO-1. Silencing of HO-1 expression in human DC was attempted but unfortunately was unfeasible due to difficulties in maintaining HO-1 knockdown alongside carnosol and curcumin treatment without comprising cellular viability (Appendix 1). Therefore, the contribution of HO-1 to the immunomodulatory effects of DC was examined using the HO-1 enzymatic inhibitor, SnPP.

DC were incubated with carnosol or curcumin, in the presence or absence of SnPP, for 6 hours prior to stimulation with LPS for 24 hours. The expression of the maturation marker CD83, and co-stimulatory receptor CD86, was measured by flow cytometry. As previously observed, carnosol and curcumin treatment reduced CD83 and CD86 expression in LPS stimulated DC, however, this effect was attenuated in the presence of SnPP (Figure 3.13A,B). Furthermore, addition of SnPP prevented the previously observed reduction of TNFα production in LPS-stimulated DC by curcumin (Figure 3.13C). Taken together, these results indicate that at least some of the immunomodulatory activity of curcumin and carnosol is mediated by their upregulation of HO-1 and its subsequent enzymatic activity.

3.3.12 The carbon monoxide scavenger, hemoglobin, reduces the anti-inflammatory effects of carnosol and curcumin in human DC

Having confirmed that the effects of carnosol and curcumin in human DC are at least partially dependent on the enzymatic activity of HO-1, it was of interest to determine which HO-1 reaction product(s) were mediating these effects. Previous experiments investigating the use of BV in human DC indicated that while it does possess some immunomodulatory activity, this does not account for all the observed HO-1-dependent effects of carnosol and curcumin. CO has previously been demonstrated to inhibit DC maturation and antigen presentation to T cells (206–208). To test whether CO generation contributes to the activity of carnosol and curcumin, DC were treated with carnosol and curcumin, as before, with the addition of hemoglobin (Hb; 10 μM), which

strongly binds CO and has been used previously as a scavenger of CO *in vitro* (170,184). Expression of the co-stimulatory receptors CD80 and CD86 was measured by flow cytometry. Addition of Hb resulted in a reversal of the previously observed reduction in CD86 expression in LPS-stimulated DC pre-treated with carnosol ($p<0.01$; Figure 3.14A). In curcumin-treated DC, Hb partially reversed reductions in both CD80 and CD86 expression after LPS stimulation ($p<0.05$; Figure 3.14B).

It was previously observed that, while the promotion of antigen-uptake in human DC by carnosol and curcumin was dependent on HO-1 activity, BV was not responsible for this effect. Having confirmed that Hb treatment partially reversed the reduction of DC maturation by carnosol and curcumin, it was next investigated whether Hb treatment would also inhibit antigen uptake in carnosol- and curcumin-treated DC. DC were treated with carnosol or curcumin, with or without the addition of Hb, and stimulated with LPS as before. Similar to HO-1 inhibition with SnPP, Hb treatment significantly attenuated DQ-Ova uptake in carnosol-treated DC suggesting that CO is at least partially responsible for maintaining DC in an immature state post HO-1 induction ($p<0.001$). Hb also modestly reduced curcumin-mediated DQ-Ova uptake, however the effects were not as potent as those observed in carnosol-treated DC (Figure 3.15).

Finally, the effect of Hb on cytokine production by carnosol- and curcumin-treated DC was assessed. As previously seen, carnosol and curcumin treatment reduced the expression of IL-23p19 by LPS-stimulated DC. However, carnosol-treated DC displayed significantly higher IL-23 production when cultured in the presence of Hb ($p<0.01$), and a trend towards increased IL-23 production was also observed in curcumin-treated DC (Figure 3.16). In summary, scavenging of CO by Hb partially reversed some of the immunomodulatory effects of carnosol and curcumin in human DC, indicating that CO contributes to the HO-1 dependent activity of these polyphenols.

3.3.13 Curcumin, but not carnosol, partially inhibits NF-κB signalling in human DC

Although HO-1 is known to promote tolerogenic DC, the mechanism by which it modulates the immunogenicity of DC is unclear. NF-κB is the master transcription factor which regulates expression of pro-inflammatory genes in DC, and it has previously been suggested that HO-1 can inhibit NF-κB signalling in a cancer cell line (164). Therefore, it was hypothesised that the anti-inflammatory effects of carnosol and curcumin seen in DC could result from inhibition of NF-κB signalling. Activation of NF-κB is regulated by the inhibitory protein complex IκB; upon integration of a pro-inflammatory stimulus, IκB kinase (IKK) phosphorylates IκB, causing it to disassociate from the active subunits of NF-κB. IκB is then targeted for degradation and the active NF-κB subunits

can translocate to the nucleus (354). Therefore, measurement of IκB degradation acts as an indicator of NF-κB activation.

To assess IκB degradation in response to LPS stimulation, DC were treated with carnosol (10 μM) or curcumin (10 μM) for 6 hours prior to simulation with LPS for 15 minutes up to 3 hours. Expression of IκB was detected by Western blot. Control DC showed significant downregulation of IκB expression as early as 15 minutes post-LPS stimulation, which was restored by 3 hours post-LPS. Neither carnosol nor curcumin treatment appeared to prevent the degradation of IκB in LPS-stimulated DC (Figure 3.17).

Despite failing to observe inhibition of NF-κB activation in carnosol- and curcumin-treated DC, it is possible for NF-κB signalling to be obstructed downstream of its activation. Previous studies have reported that carnosol and curcumin can inhibit the nuclear translocation of the active NF-κB subunit, p65 (163,279). Therefore, it was next determined whether a similar effect would be observed in carnosol- and curcumin-treated DC. To measure nuclear translocation of p65, DC were treated with carnosol or curcumin for 6 hours prior to simulation with LPS for 30 minutes. DC were stained with anti-p65 and DAPI, and detection of p65 localisation was performed by confocal microscopy. LPS stimulation strongly upregulated p65 nuclear translocation, and again no effect was observed with carnosol treatment. Interestingly, LPS-induced translocation of p65 was inhibited with curcumin treatment suggesting that the two compounds may differentially affect NF-κB signalling in human DC (Figure 3.18).

3.3.14 Carnosol and curcumin inhibit MAP Kinase activation in LPS-stimulated human DC

Despite the indication that curcumin can inhibit NF-κB signalling in DC, no effect on NF-κB was observed with carnosol treatment. Therefore, inhibition of NF-κB is unlikely to be the mechanism by which HO-1, and the polyphenols carnosol and curcumin, achieve the majority of their immunomodulatory effects in DC. Signalling through MAPKs such as MEK/ERK and p38 mediates some of the functional and phenotypic changes arising from the maturation of human DC in response to pro-inflammatory stimuli (355). Furthermore, it has previously been suggested that HO-1 can inhibit p38 MAPK signalling in DC (178). To investigate whether carnosol or curcumin could inhibit MAPK activation, DC were pre-treated with carnosol (10 μM) or curcumin (10 μM) for 6 hours prior to stimulation with LPS over time. Phosphorylation, and therefore, activation of MEK, ERK and p38 MAPK was assessed by Western blotting. Both carnosol and curcumin treatment reduced LPS induced activation of MEK and ERK, while a modest reduction of p38 activation was also observed (Figure 3.19).

To ensure the observed reduction of MAPK activation was not due to early activation of MAPKs by carnosol and curcumin, and therefore tolerance to LPS stimulation, activation of MEK (which acts upstream of ERK) and p38 was assessed after addition of carnosol, curcumin or LPS as a positive control. As expected, LPS induced activation of both MEK and p38, however there was no observed effect with either carnosol or curcumin (Figure 3.20). Therefore, the observed inhibition of MAPK signalling by carnosol and curcumin is a result of the anti-inflammatory activity of these compounds, and does not represent 'exhaustion' of the MAPKs.

3.3.15 Inhibition of MAP Kinase signalling in LPS-stimulated DC by carnosol and curcumin is dependent on HO-1 activity

Finally, having observed that both carnosol and curcumin effectively inhibit MAPK signalling in LPS-stimulated DC, it was next investigated whether this inhibition was dependent on HO-1. DC were pre-treated with carnosol or curcumin, in the presence or absence of the HO-1 inhibitor SnPP, for 6 hours prior to stimulation with LPS for 30 minutes. Phosphorylation of MEK and p38 MAPK was assessed by Western blotting. As before, both carnosol and curcumin inhibited LPS-induced activation of both MAPKs; however, this effect was attenuated in the presence of SnPP (Figure 3.21). Taken together with previous results demonstrating that the immunomodulatory functions of carnosol and curcumin in DC are dependent on HO-1 activity, this result suggests that HO-1 upregulation by carnosol and curcumin acts to inhibit MAPK signalling in response to pro-inflammatory stimuli, thereby limiting the downstream immune response.

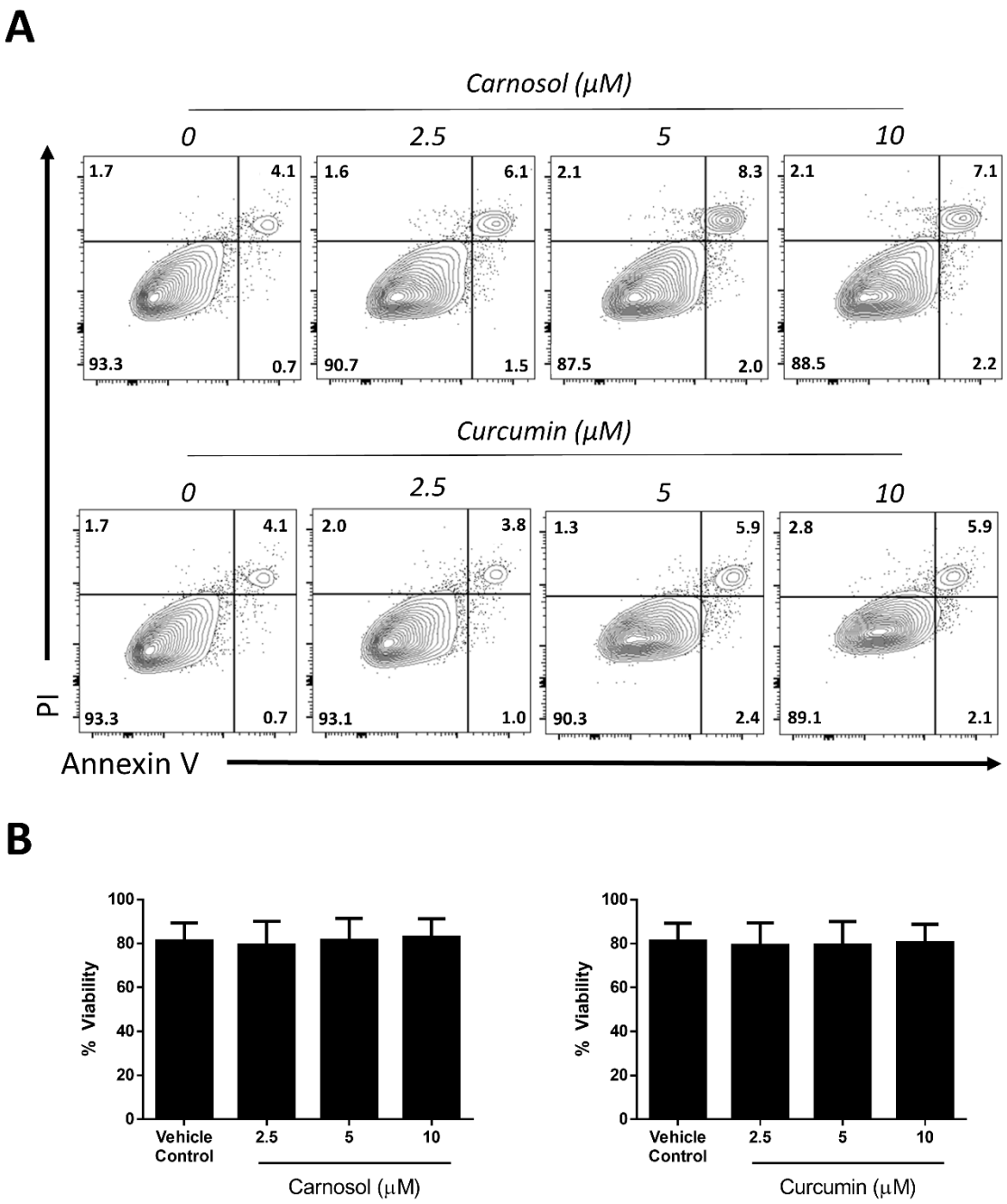

Figure 3.1. Carnosol and curcumin are non-toxic to human DC. (A) Primary human DC were incubated with a vehicle control, carnosol or curcumin (2.5-10 μM). After 24 hours, cells were stained for Annexin V and PI uptake and analysed by flow cytometry. Viable cells were designated as Annexin V^- PI^- (non-apoptotic cells). Results shown are from one healthy donor and are representative of data from four independent experiments. **(B)** DC from healthy donors (n=6) were incubated with increasing doses of carnosol (2.5-10 μM) or curcumin (2.5-10 μM) for 6 hours prior to stimulation with LPS (100 ng/ml). Cells were stained with an amine-binding viability dye after 24 hours and analysed by flow cytometry. Pooled data (n=6) depicts the mean (±SEM) percentage viable cells of total DC (gated by forward and side scatter).

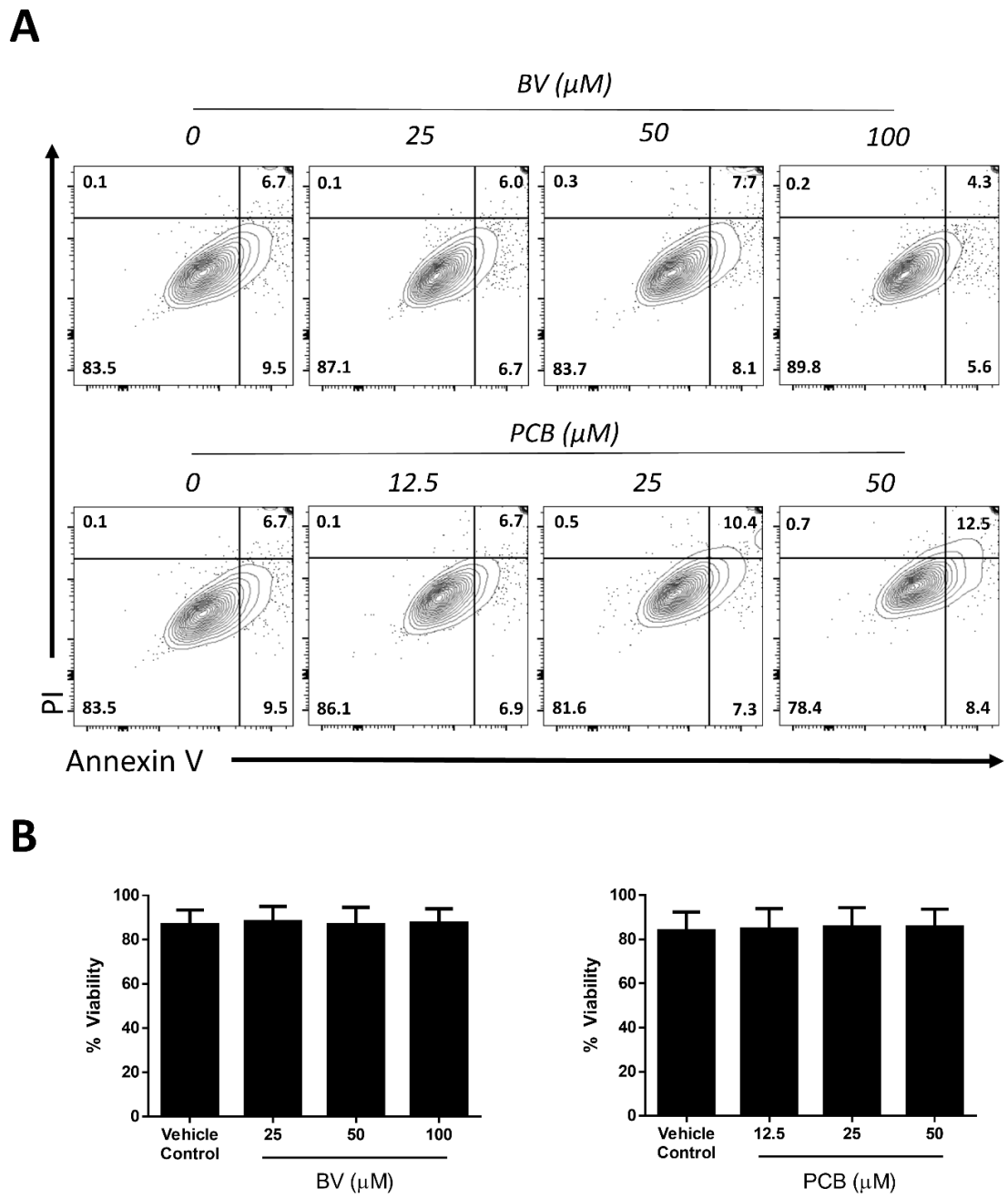

Figure 3.2. BV and PCB are non-toxic to human DC. (A) Primary human DC were incubated with a vehicle control, BV (25-100 μM) or PCB (12.5-50 μM). After 24 hours, cells were stained for Annexin V and PI uptake and analysed by flow cytometry. Viable cells were designated as Annexin V^- PI^- (non-apoptotic cells). Results shown are from one healthy donor and are representative of data from four independent experiments. **(B)** DC from healthy donors (n=6) were incubated with increasing doses of BV (25-100 μM) or PCB (12.5-50 μM) for 6 hours prior to stimulation with LPS (100 ng/ml). Cells were stained with an amine-binding viability dye after 24 hours and analysed by flow cytometry. Pooled data (n=6) depicts the mean (±SEM) percentage viable cells of total DC (gated by forward and side scatter).

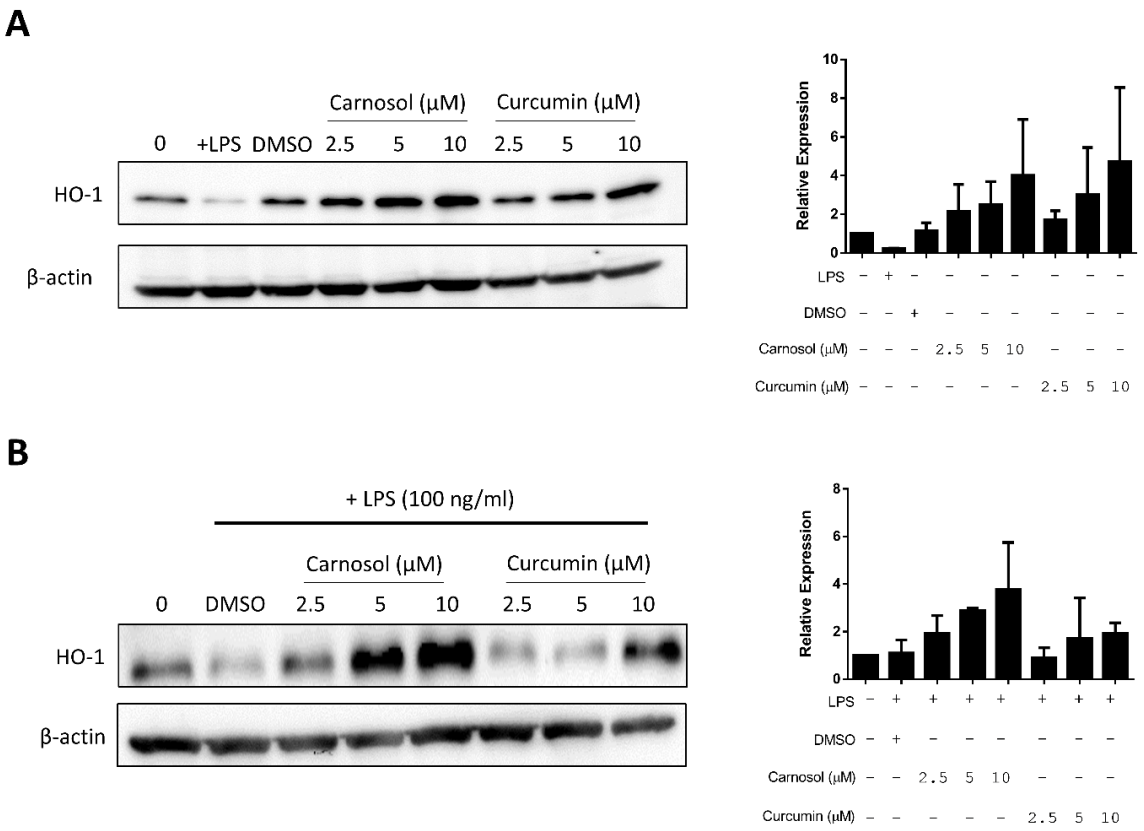

Figure 3.3. Carnosol and curcumin upregulate HO-1 expression in human DC. (A) Immature DC from healthy donors (n=2-4) were treated with vehicle control, LPS (100 ng/ml), carnosol or curcumin (2.5-10 μM) for 24 hours or **(B)** treated with carnosol or curcumin for 6 hours prior to stimulation with LPS for 24 hours. HO-1 expression was detected by Western blot. All blots depict an individual donor and are representative of 2-4 independent experiments. Densitometric analysis was performed using ImageLab (Bio-Rad) software (n=2-4).

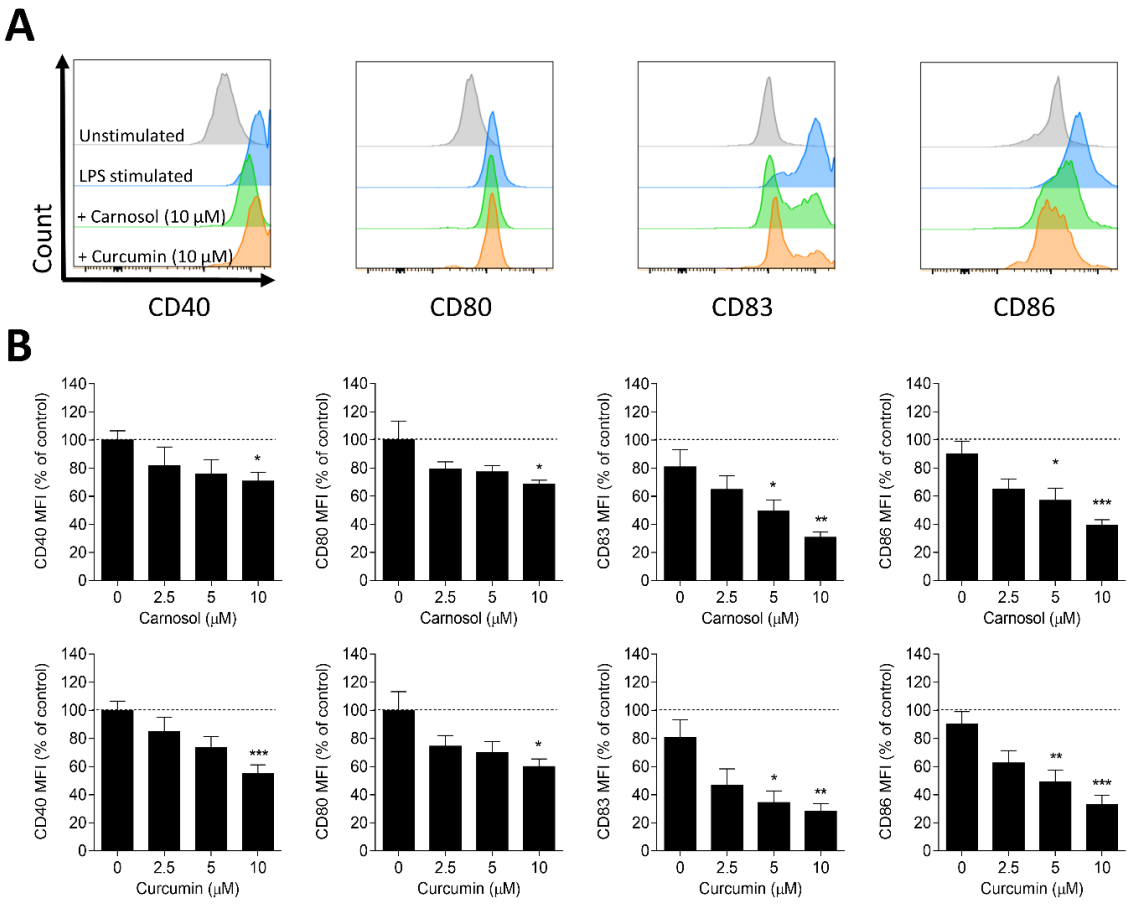

Figure 3.4. Treatment with carnosol or curcumin inhibits LPS-mediated maturation of human DC. DC from healthy donors (n=6) were incubated with increasing doses of carnosol (2.5-10 µM) or curcumin (2.5-10 µM) for 6 hours prior to stimulation with LPS (100 ng/ml). Cells were stained with fluorochrome conjugated antibodies specific for CD40, CD80, CD83 and CD86 after 24 hours and analysed by flow cytometry. **(A)** Histograms depicting expression of maturation markers by viable cells in carnosol and curcumin treated DC compared to vehicle control from one representative experiment. **(B)** Pooled data (n=6) depicting expression of CD40, CD80, CD83 and CD86 in carnosol and curcumin treated DC. Results shown are mean (± SEM) of the measured Mean Fluorescence Intensities (MFI), expressed as percentages of the vehicle controls. Statistical significance was determined by one-way ANOVA, with Dunnett's multiple comparisons post hoc test to compare treatment groups against the control group (***p<0.001, **p<0.01, *p<0.05).

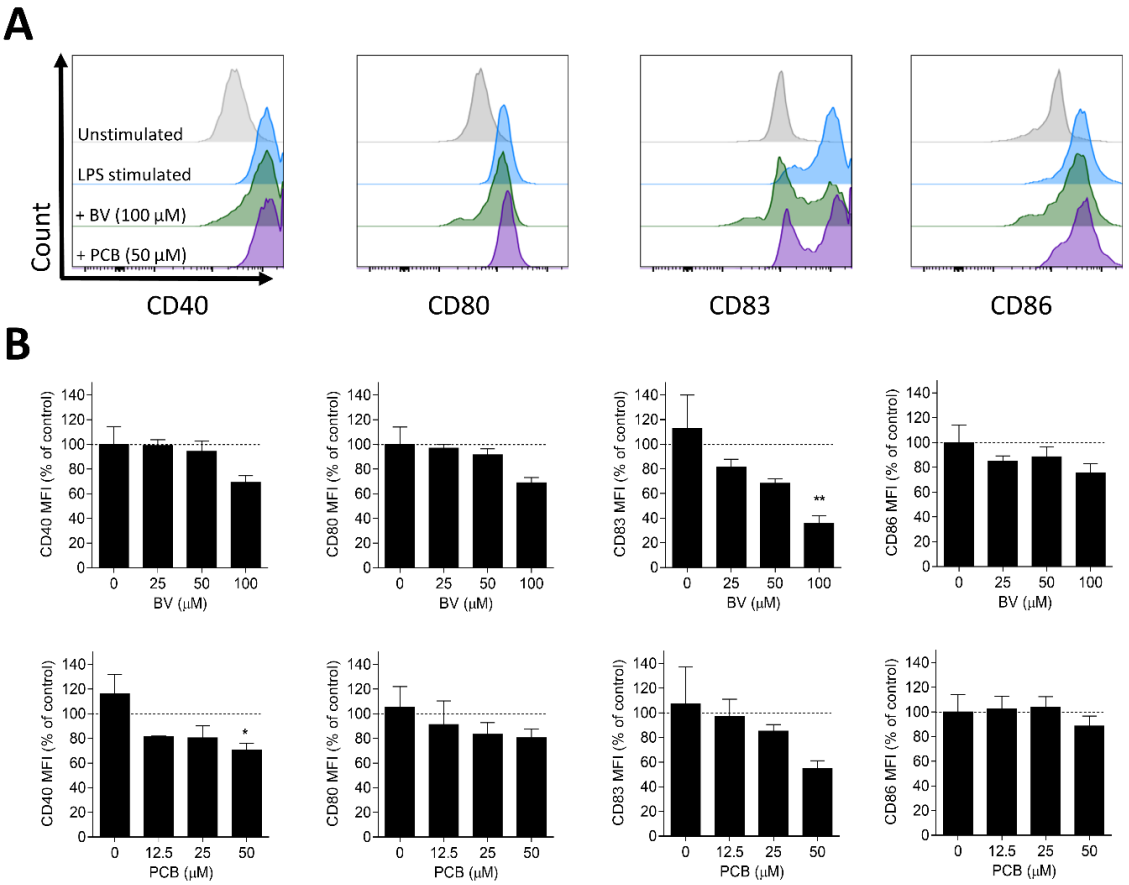

Figure 3.5. Treatment with BV and PCB moderately reduces LPS-mediated DC maturation. DC from healthy donors (n=6) were incubated with increasing doses of BV (25-100 µM) or PCB (12.5-50 µM) for 6 hours prior to stimulation with LPS (100 ng/ml). Cells were stained with fluorochrome conjugated antibodies specific for CD40, CD80, CD83 and CD86 after 24 hours and analysed by flow cytometry. **(A)** Histograms depicting expression of maturation markers by viable cells in BV and PCB treated DC compared to vehicle control from one representative experiment. **(B)** Pooled data (n=6) depicting expression of CD40, CD80, CD83 and CD86 in BV and PCB treated DC. Results shown are mean (± SEM) of the measured Mean Fluorescence Intensities (MFI), expressed as percentages of the vehicle controls. Statistical significance was determined by one-way ANOVA, with Dunnett's multiple comparisons post hoc test to compare treatment groups against the control group (**p<0.01, *p<0.05).

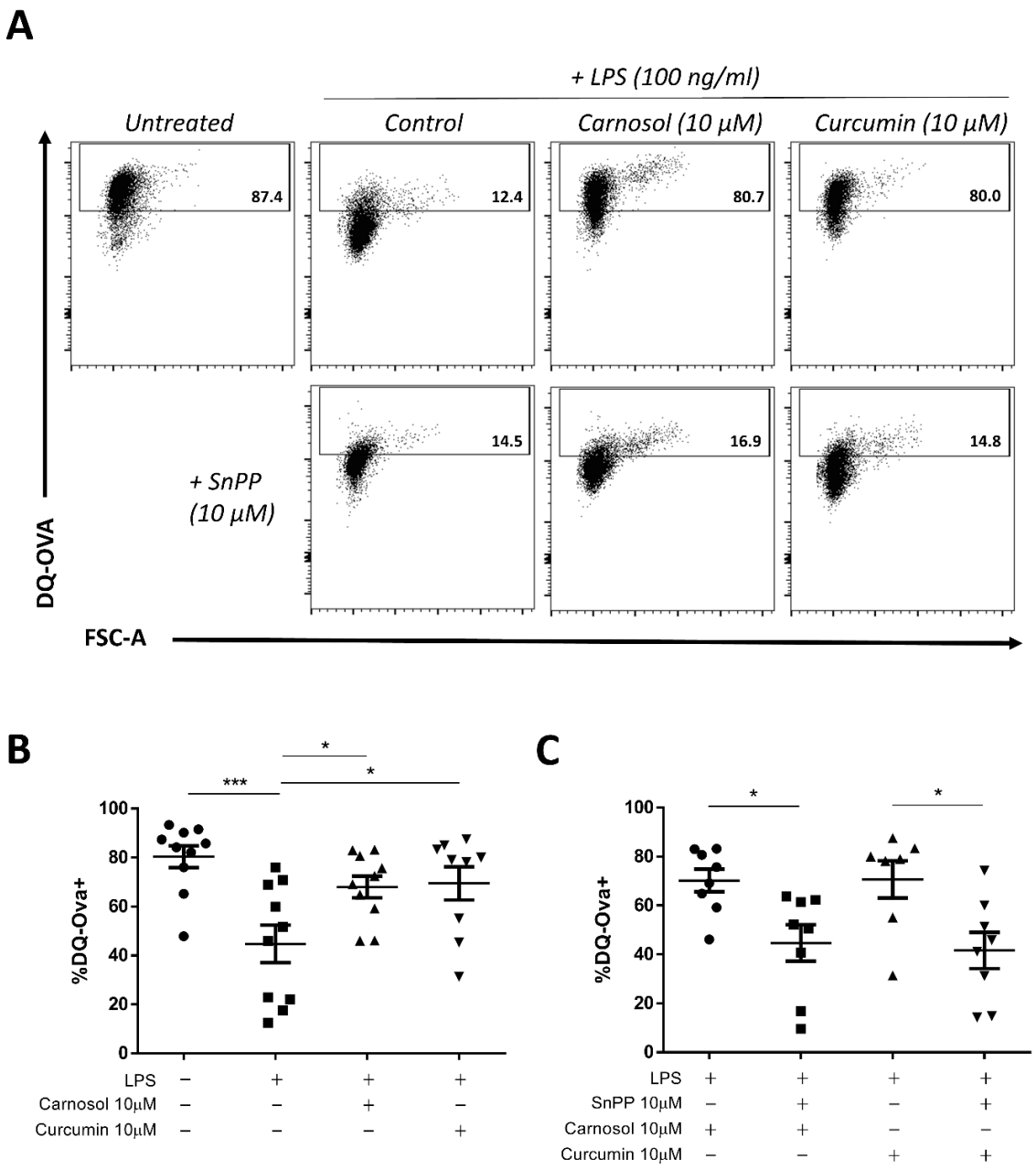

Figure 3.6. Maintenance of antigen uptake by carnosol and curcumin in LPS-treated DC is dependent on HO-1. DC from healthy donors (n=8-10) were incubated with carnosol (10 µM) or curcumin (10 µM), with or without SnPP (10 µM), for 6 hours prior to stimulation with LPS for 24 hours. DC were then incubated with DQ-Ovalbumin (DQ-Ova; 500 ng/ml) for 20 minutes prior to analysis by flow cytometry. **(A)** Representative dot plots depicting DQ-Ova uptake by DC (gated by forward and side scatter) treated with carnosol, curcumin and SnPP from one donor. **(B)** Pooled data depicting percentage DQ-Ova uptake of DC treated with carnosol and curcumin alone and **(C)** in the presence of SnPP. Results shown are mean (± SEM) of the percentage DQ-Ova uptake in carnosol- and curcumin-treated DC, with or without SnPP. Statistical significance was determined by one-way ANOVA, with either Tukey's multiple comparisons post hoc test to compare means of all groups, or Sidak's multiple comparisons post hoc test to compare means of pre-selected group pairs (***p<0.001, *p<0.05).

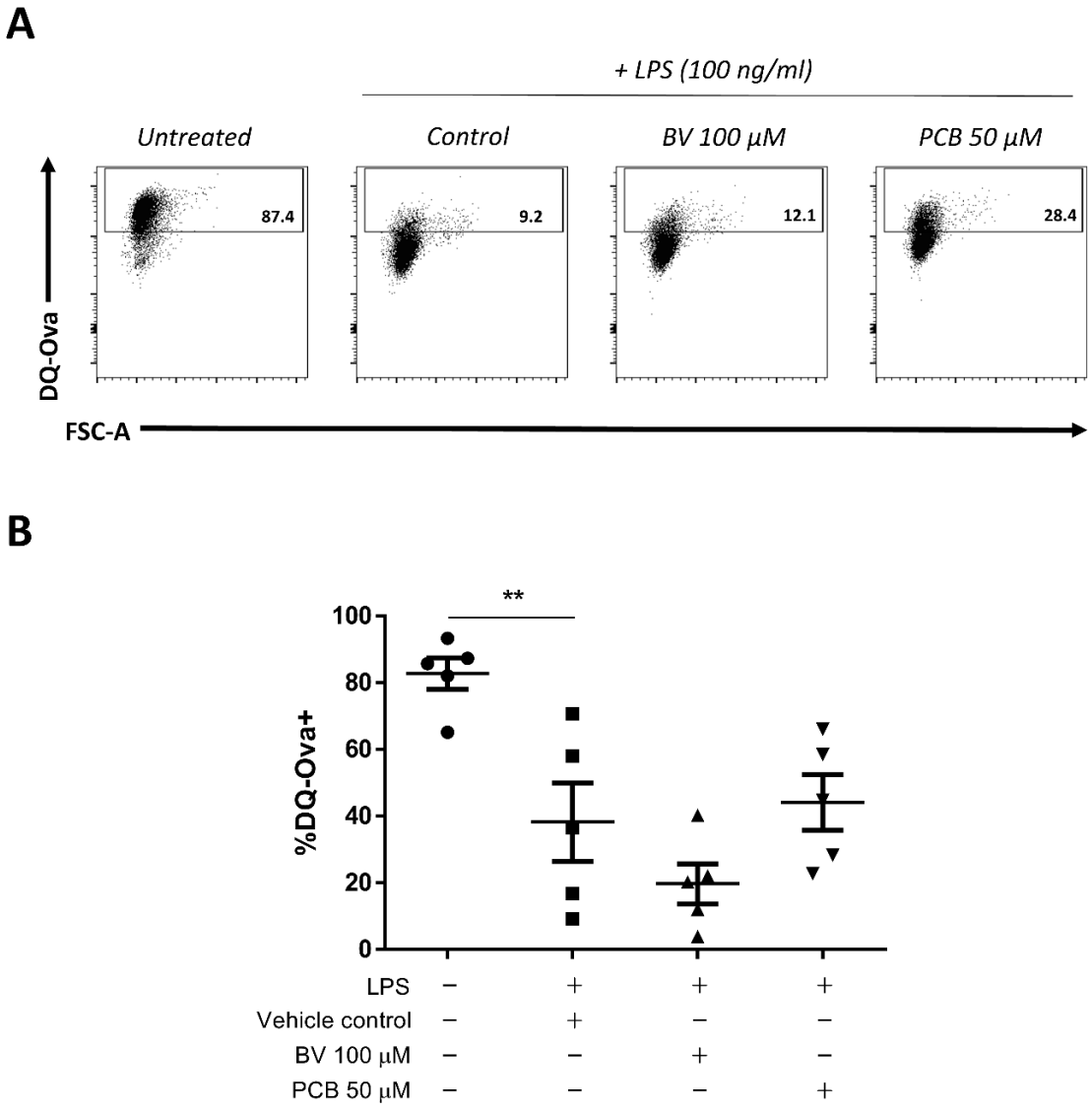

Figure 3.7. Neither BV nor PCB modulate the antigen uptake capacity of LPS-stimulated DC. DC from healthy donors (n=5) were incubated with a vehicle control, BV (100 µM) or PCB (50 µM) for 6 hours prior to stimulation with LPS for 24 hours. DC were incubated with DQ-Ovalbumin (DQ-Ova; 500 ng/ml) for 20 minutes prior to analysis by flow cytometry. **(A)** Representative dot plots depicting DQ-Ova uptake by DC (gated by forward and side scatter) treated with BV or PCB from one donor. **(B)** Results shown are mean (± SEM) of the percentage DQ-Ova uptake in BV and PCB treated DC. Statistical significance was determined by one-way ANOVA, with Tukey's multiple comparisons post hoc test to compare means of all groups (**p<0.01).

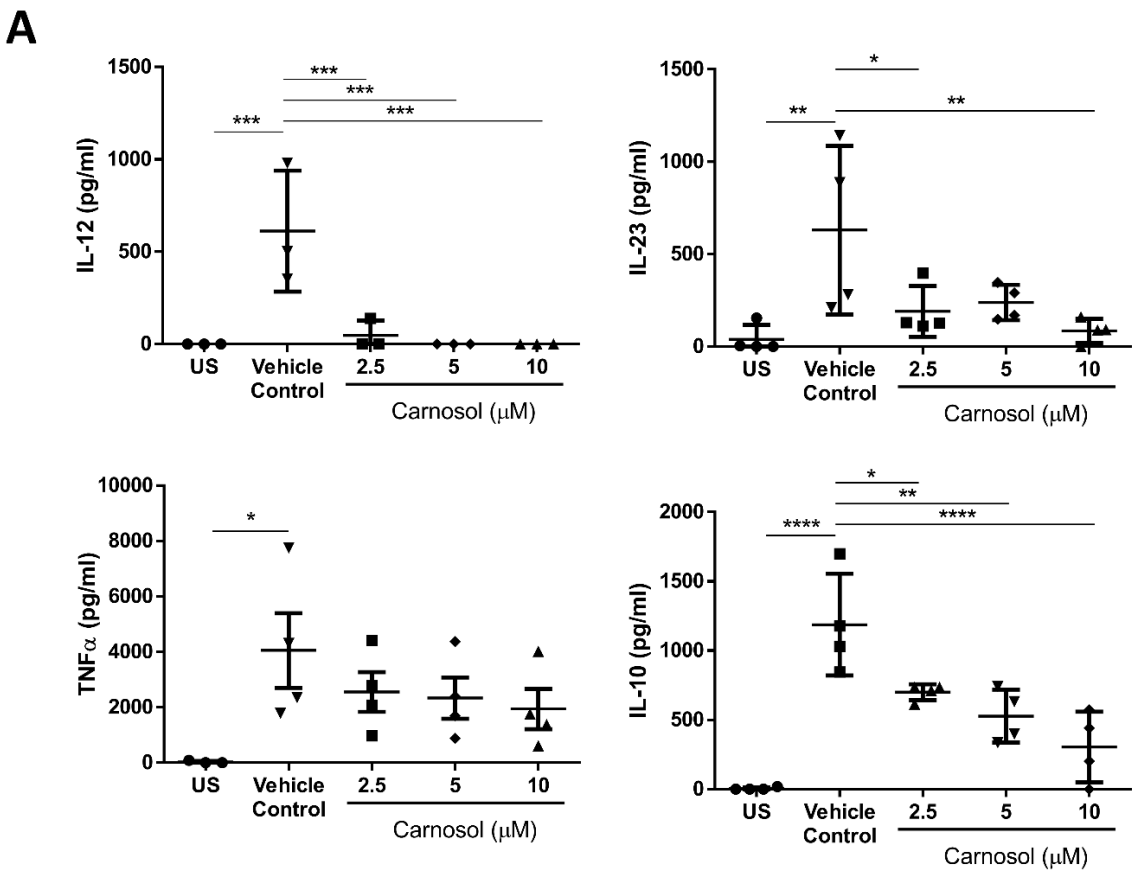
A
IL-12 (pg/ml)
IL-23 (pg/ml)
TNFα (pg/ml)
IL-10 (pg/ml)
US
Vehicle Control
2.5
5
10
Carnosol (μM)

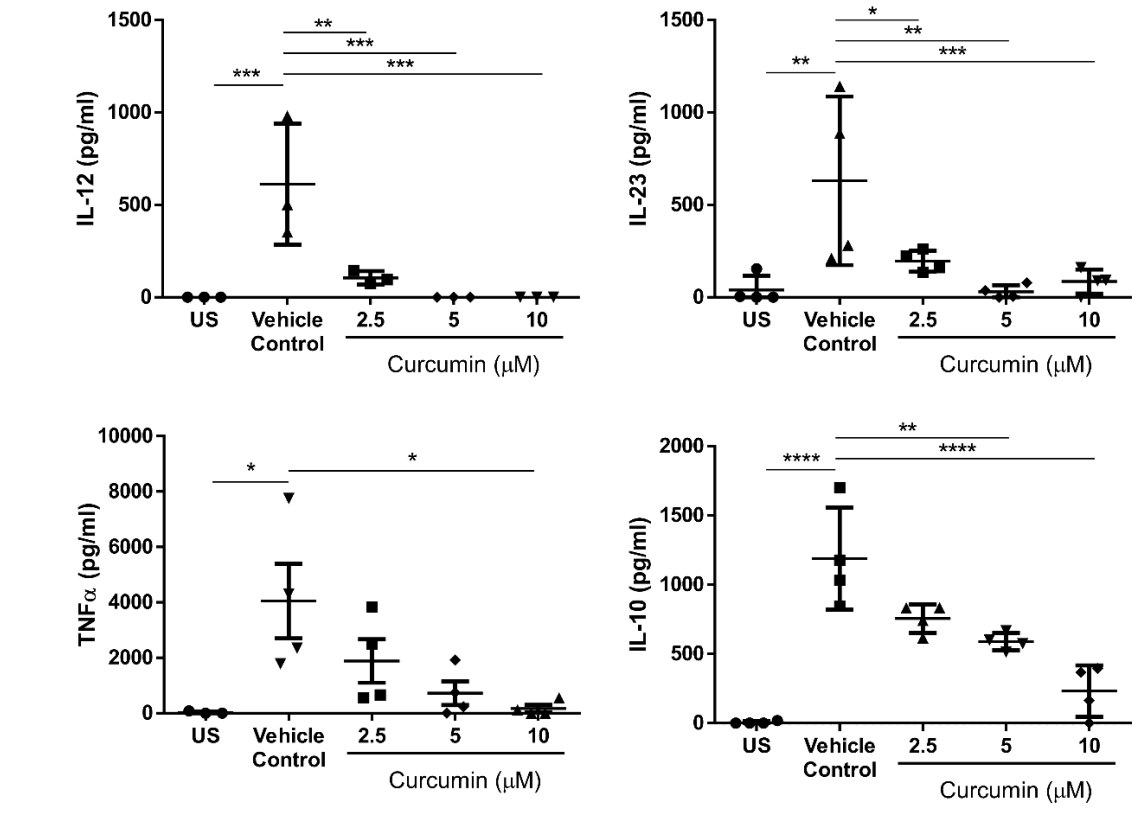
B
IL-12 (pg/ml)
IL-23 (pg/ml)
TNFα (pg/ml)
IL-10 (pg/ml)
US
Vehicle Control
2.5
5
10
Curcumin (μM)

Figure 3.8. Carnosol and curcumin inhibit cytokine production by LPS-treated DC. DC from healthy donors (n=4) were incubated with increasing doses of **(A)** carnosol (2.5-10 μM) or **(B)** curcumin (2.5-10 μM) for 6 hours prior to stimulation with LPS. Supernatants were collected after 24 hours and IL-12p70, IL-23p19, TNFα, and IL-10 production was measured by ELISA. Results shown are mean (± SEM) of the pooled cytokine concentrations (means of three technical replicates per donor). Statistical significance was determined by one-way ANOVA, with Dunnett's multiple comparisons post hoc test to compare means of treatment groups to the control group (****$p<0.0001$, ***$p<0.001$, ** $p<0.01$, *$p<0.05$).

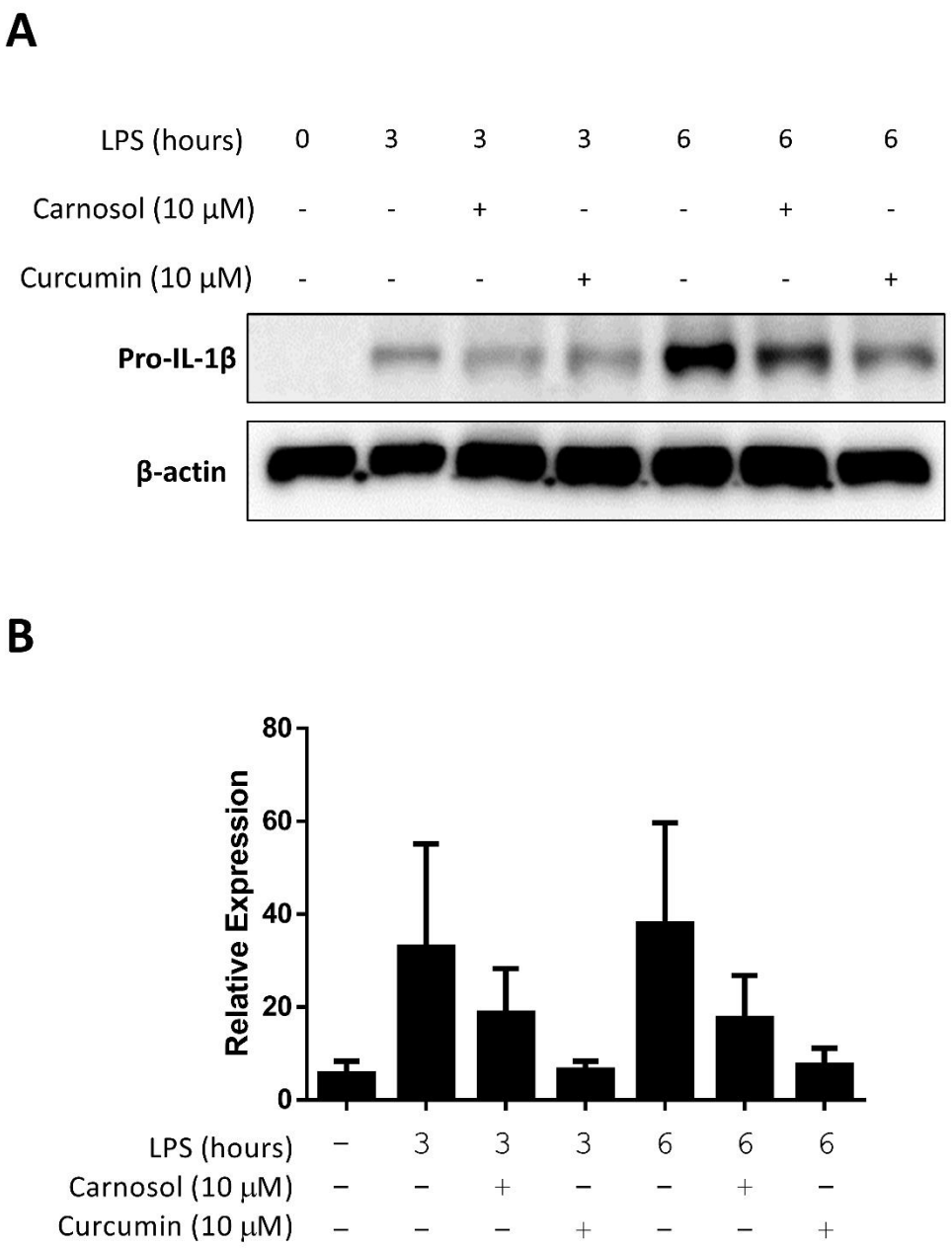

Figure 3.9. Carnosol and curcumin inhibit pro-IL-1β expression by LPS-treated DC. DC from healthy donors (n=3) were treated with either carnosol (10 μM), curcumin (10 μM) or a vehicle control for 6 hours prior to stimulation with LPS. Cell lysates were harvested at 3 hours and 6 hours post LPS (100 ng/ml) stimulation and expression of pro-IL-1β was detected by Western blotting. **(A)** Representative blot of three independent experiments is shown. **(B)** Densitometric analysis was performed using ImageLab (Bio-Rad) software (n=3).

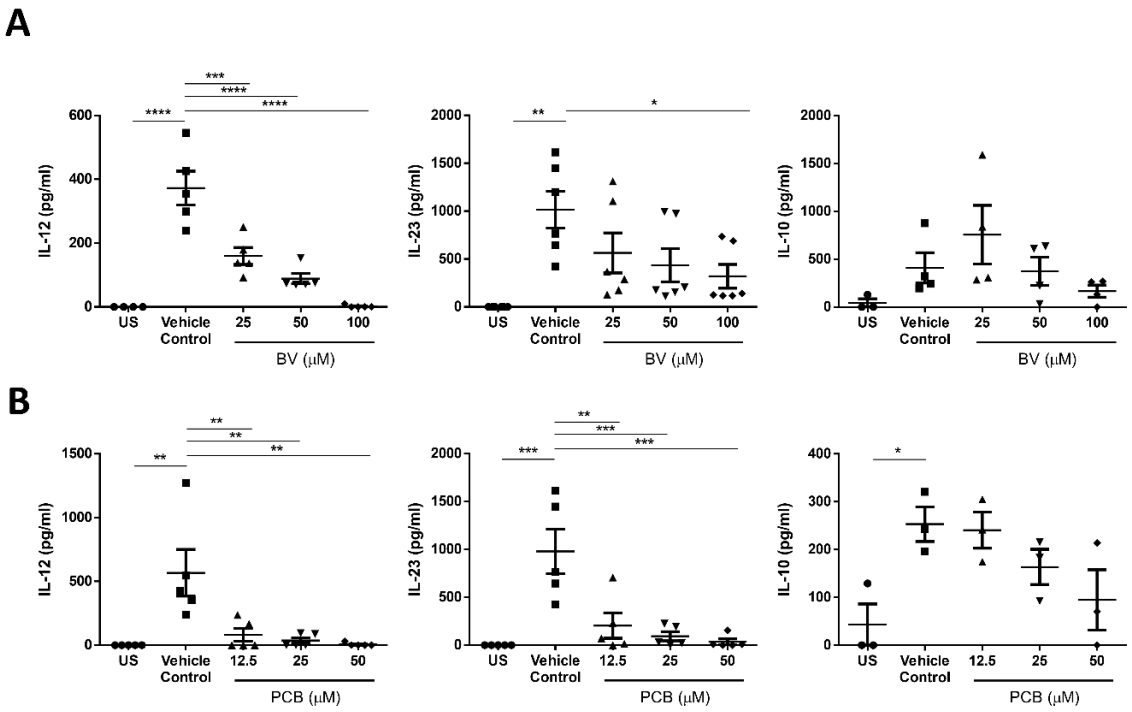

Figure 3.10. BV and PCB inhibit cytokine production by LPS-treated DC. DC from healthy donors (n=3-6) were incubated with a vehicle control or increasing doses of **(A)** BV (25-100 μM) or **(B)** PCB (12.5-50 μM) for 6 hours prior to activation with LPS. Supernatant was collected after 24 hours and analysed for IL-12p70, IL-23p19 and IL-10 secretion by ELISA. Results shown are means ± SEM of the pooled cytokine concentrations (means of three technical replicates per donor). Statistical significance was determined by one-way ANOVA, with Dunnett's multiple comparisons post hoc test to compare means of treatment groups to the control group (****p<0.0001, ***p<0.001, ** p<0.01, *p<0.05).

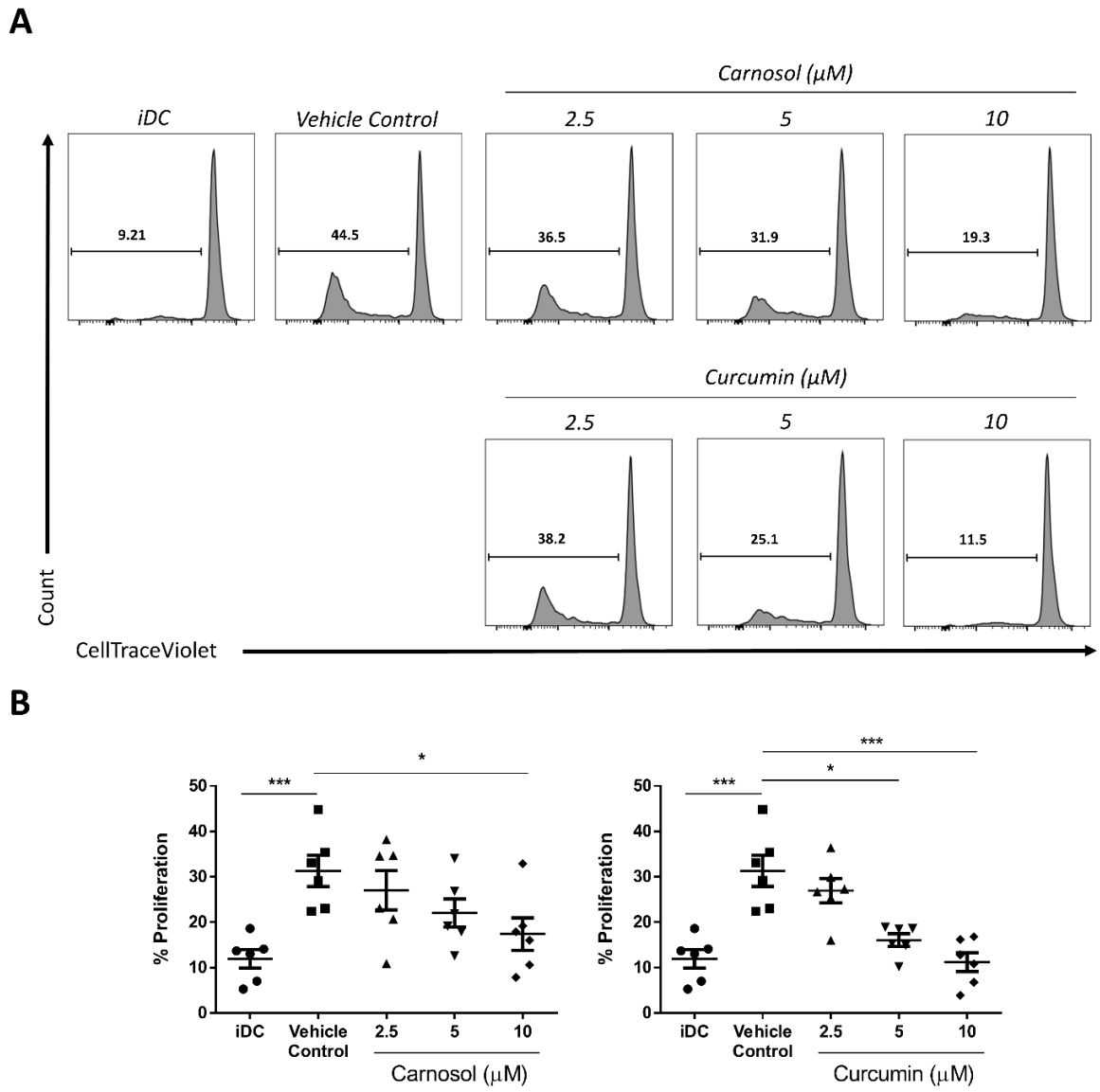

Figure 3.11. Carnosol- and curcumin-treated DC have a reduced capacity to stimulate allogeneic CD4⁺ T cells. DC from healthy donors (n=6-7) were treated with carnosol or curcumin (2.5-10 μM) for 6 hours prior to stimulation with LPS. After 24 hours, DC were washed and cultured at a 1:10 ratio with allogeneic purified CD4⁺ T cells. Immature DC (iDC) were also cultured with CD4⁺ T cells as an allogeneic control. After 5 days CD4⁺ T cells were analysed for proliferation by flow cytometry. **(A)** Histograms depicting proliferation of CD4⁺ T cells (gated by forward and side scatter) co-cultured with either control, carnosol or curcumin treated allogeneic DC, as measured by CTV fluorescence. Data shown is from one healthy donor. **(B)** Pooled data depicting mean (± SEM) percentage proliferation of CD4⁺ T cells cultured with control DC or DC treated with different concentrations of carnosol or curcumin. Statistical significance was determined by one-way ANOVA, with Tukey's multiple comparisons post hoc test to compare means of all groups (***p<0.001, *p<0.05).

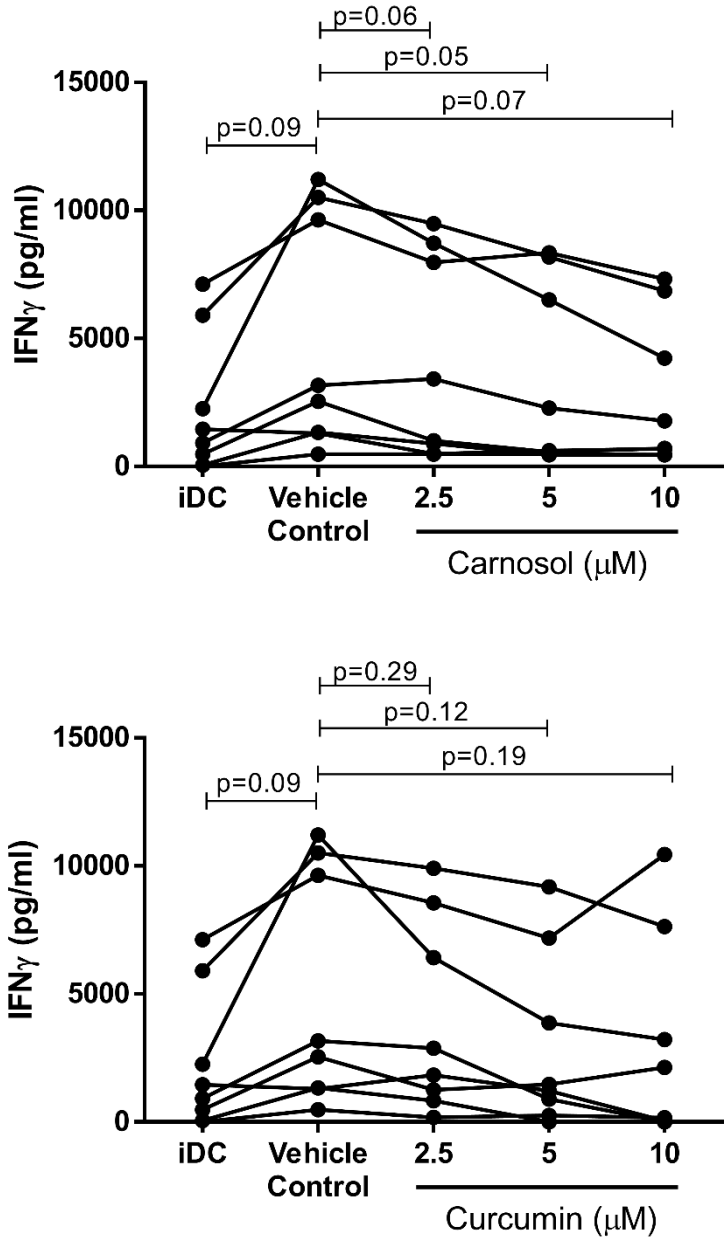

Figure 3.12. Carnosol- and curcumin-treated DC have a reduced capacity to induce IFNγ production by allogeneic CD4⁺ T cells. DC from healthy donors (n=8) were treated with carnosol or curcumin (2.5-10 μM) for 6 hours prior to stimulation with LPS. After 24 hours, DC were washed and cultured at a 1:10 ratio with allogeneic purified CD4⁺ T cells. After 5 days supernatants were measured for IFNγ concentration by ELISA. Pooled data (n=8) depicting mean (± SEM) percentage reduction in IFNγ in CD4⁺ T cells cultured with curcumin- or carnosol-treated DC matured with LPS. Statistical significance was determined by one-way ANOVA, with Dunnett's multiple comparisons post hoc test to compare means of all treatment groups to the control group.

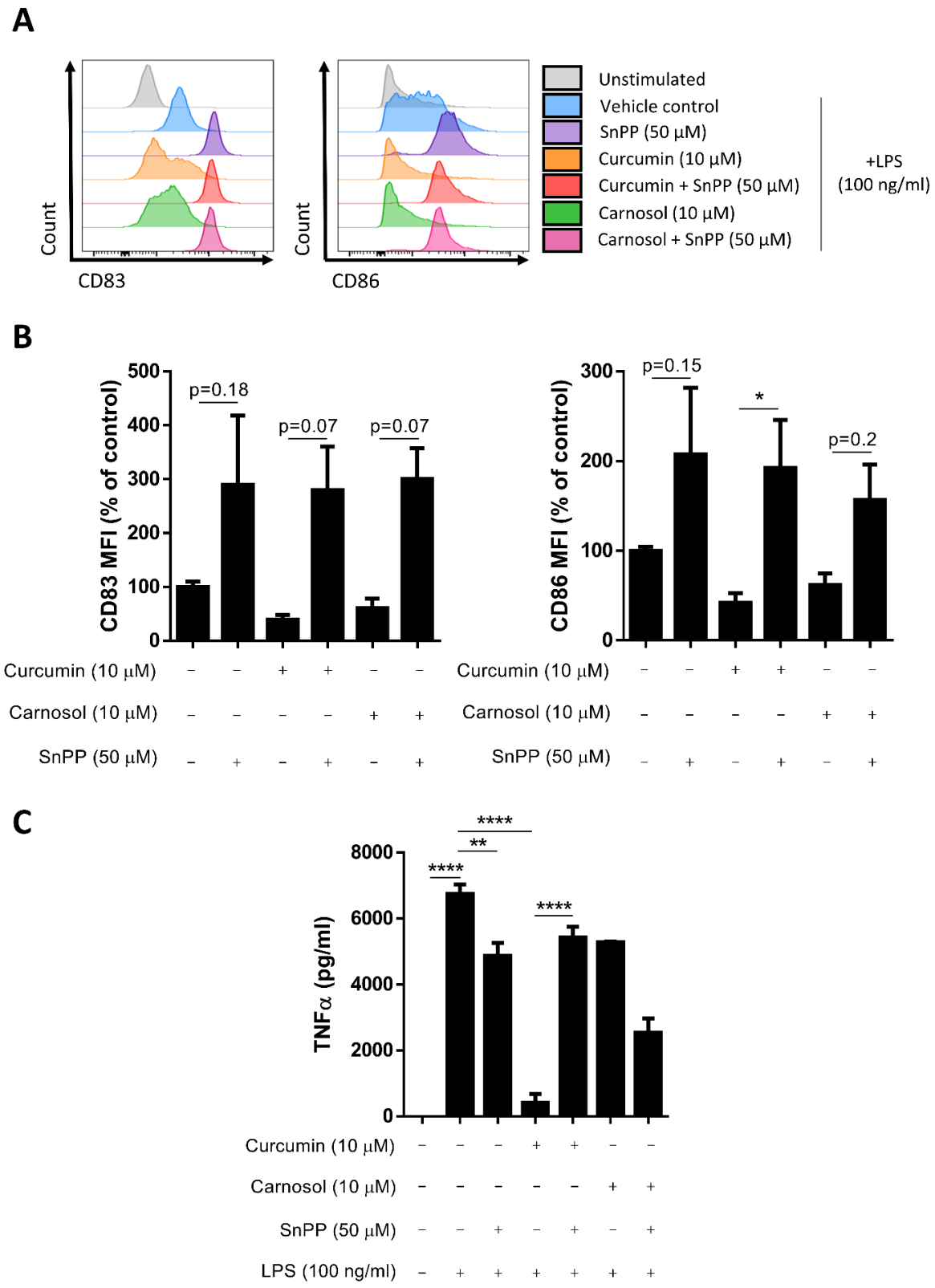
A
Count
CD83
Count
CD86
Unstimulated
Vehicle control
SnPP (50 µM)
Curcumin (10 µM)
Curcumin + SnPP (50 µM)
Carnosol (10 µM)
Carnosol + SnPP (50 µM)
+LPS
(100 ng/ml)
B
CD83 MFI (% of control)
p=0.18
p=0.07
p=0.07
CD86 MFI (% of control)
p=0.15
*
p=0.2
Curcumin (10 µM)
Carnosol (10 µM)
SnPP (50 µM)
C
TNFα (pg/ml)
****
**
****
****
Curcumin (10 µM)
Carnosol (10 µM)
SnPP (50 µM)
LPS (100 ng/ml)

Figure 3.13. Immunomodulation of DC by carnosol and curcumin is dependent on HO-1 activity. DC from healthy donors (n=5) were incubated with carnosol (10 µM), curcumin (10 µM), with or without SnPP (50 µM), or a vehicle control for 6 hours prior to stimulation with LPS (100 ng/ml). Cells were stained with fluorochrome conjugated antibodies specific for CD83 and CD86 after 24 hours and analysed by flow cytometry. **(A)** Histograms depicting expression of CD83 and CD86 by viable cells in DC treated with carnosol or curcumin, with or without SnPP, compared to controls from one representative experiment. **(B)** Pooled data (n=5) depicting expression of CD83 and CD86 in carnosol and curcumin treated DC, with or without SnPP. Results shown are mean (± SEM) of the measured Mean Fluorescence Intensities (MFI), expressed as percentages of the vehicle controls. **(C)** The concentration of TNFα in cell culture supernatants was measured by ELISA. Results shown are mean (± SD) of two technical replicates from one healthy donor, and is representative of four independent experiments. Statistical significance was determined by one-way ANOVA, with Sidak's multiple comparisons post hoc test to compare preselected treatment group pairs (****$p<0.0001$, **$p<0.01$, *$p<0.05$).

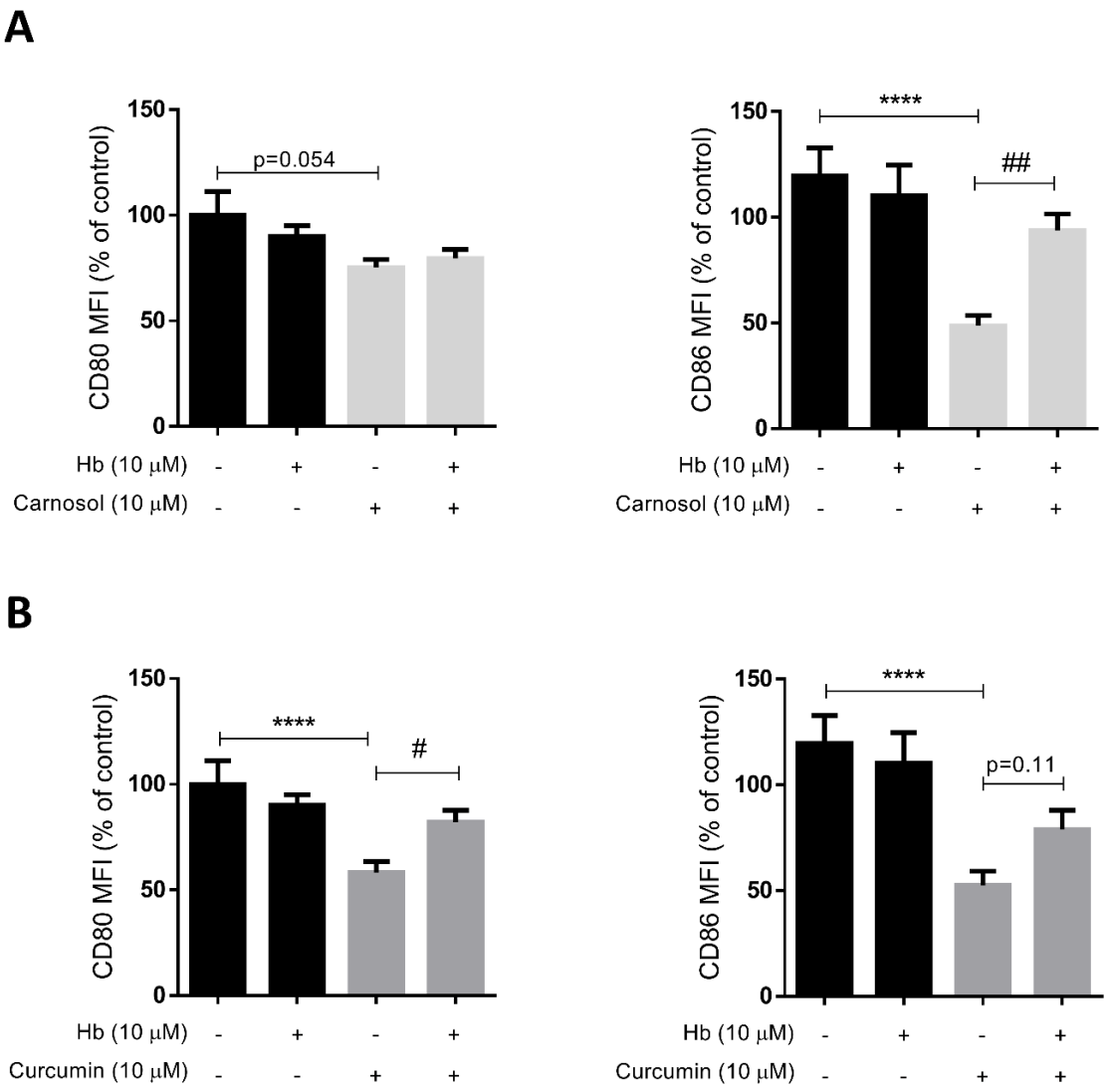

Figure 3.14. Hemoglobin, a CO scavenger, inhibits the reduction of DC maturation by carnosol and curcumin. DC from healthy donors (n=3) were treated with carnosol (10 μM) or curcumin (10 μM) either alone or in the presence of the CO scavenger hemoglobin (Hb; 10 μM) for 6 hours prior to stimulation with LPS. Cells were stained with fluorochrome conjugated antibodies specific for CD80 and CD86 after 24 hours and analysed by flow cytometry. Pooled data depicting expression of CD80 and CD86 in **(A)** carnosol- and **(B)** curcumin-treated DC. Results shown are mean (± SEM) of the measured Mean Fluorescence Intensities (MFI), expressed as percentages of the vehicle control. Statistical significance was determined by one-way ANOVA, with Dunnett's multiple comparisons post hoc test to compare treatment groups against the control group (denoted by asterisks) and Sidak's multiple comparisons post hoc test to compare the means of preselected pairs of groups (denoted by hash marks). (****p<0.0001, *p<0.05, ##p<0.01, #p<0.05).

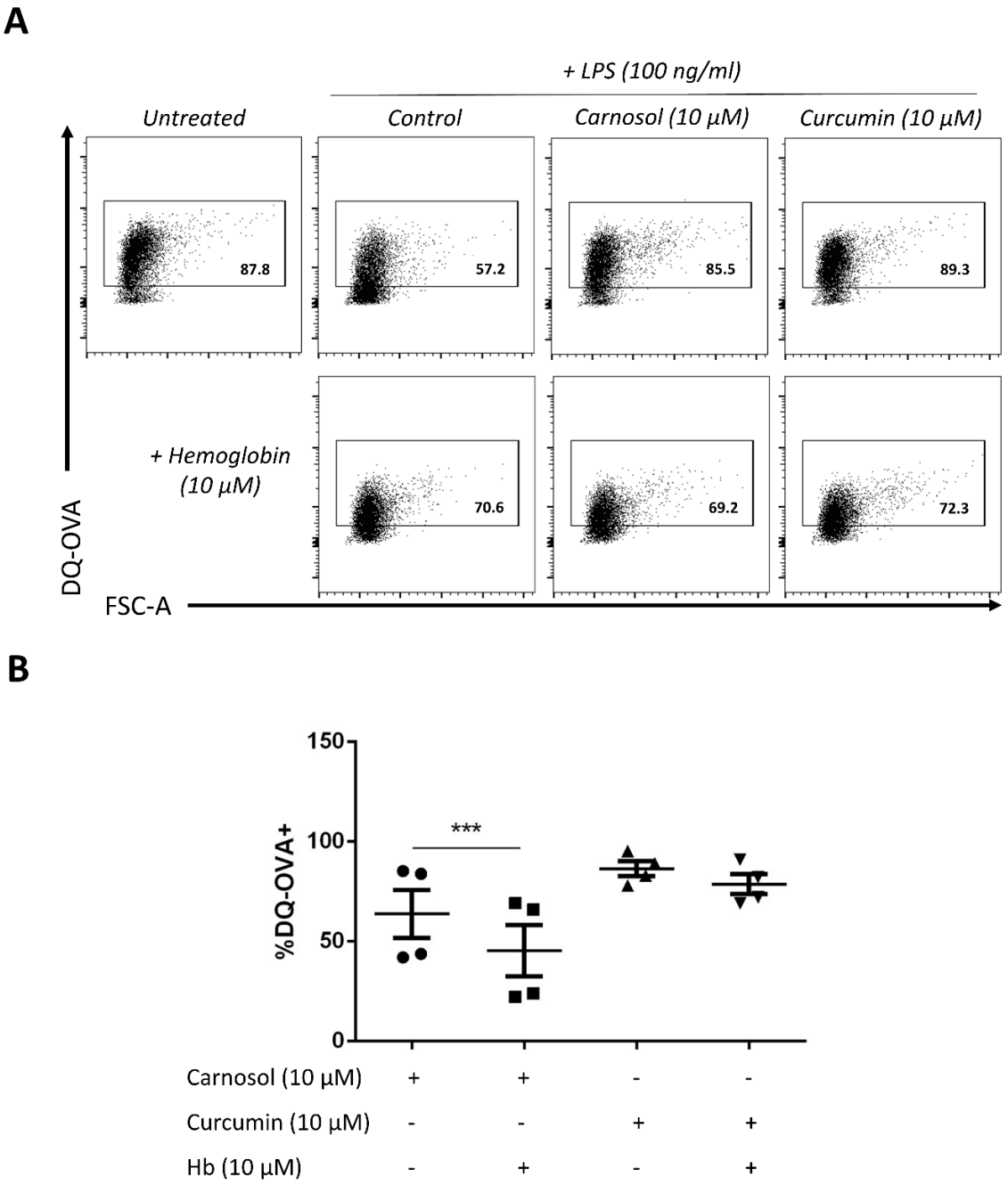

Figure 3.15. Hemoglobin partially inhibits the maintenance of antigen uptake capacity by carnosol in LPS-stimulated DC. DC from healthy donors (n=4) treated with carnosol (10 µM) or curcumin (10 µM), with or without Hb (10 µM), were incubated with DQ-OVA as described previously. **(A)** Representative dot plots depicting DQ-Ova uptake by DC (gated by forward and side scatter) treated with carnosol, curcumin and Hb from one donor. **(B)** Pooled data (n=4) depicting mean (± SEM) percentage DQ-Ova uptake of DC treated with carnosol and curcumin either alone or in the presence of Hb. Statistical significance was determined by one-way ANOVA, with Sidak's multiple comparisons post hoc test to compare the means of preselected group pairs (***p<0.001).

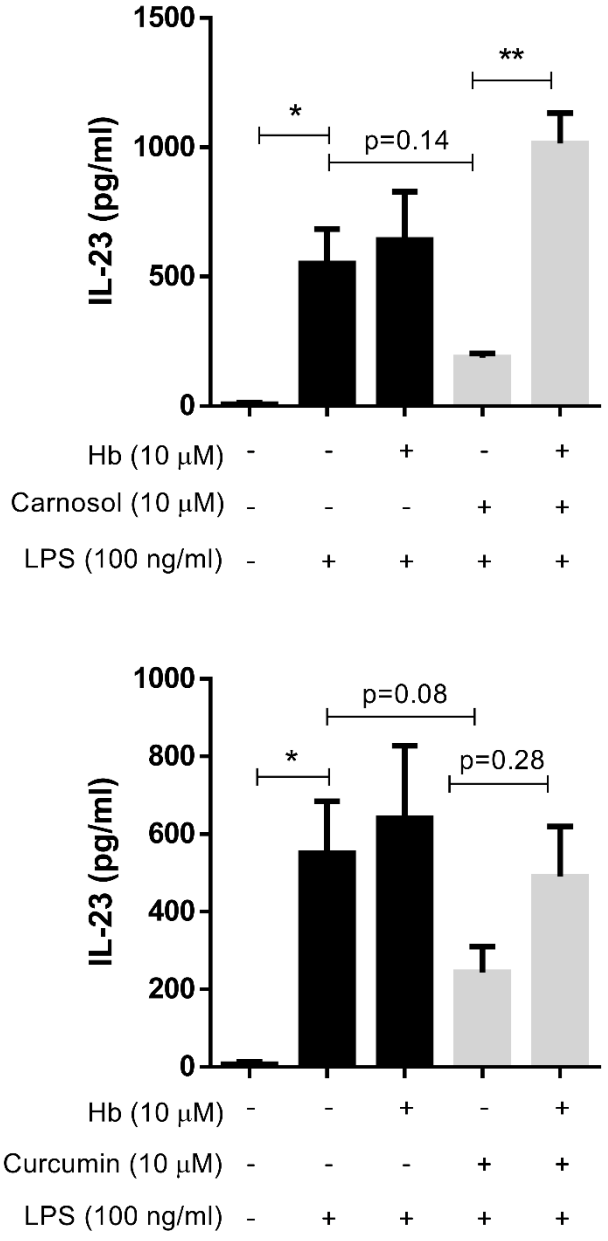

Figure 3.16. Hemoglobin partially inhibits the reduction of IL-23 production by carnosol and curcumin in LPS-stimulated DC. DC from healthy donors (n=3) were treated with carnosol (10 μM) or curcumin (10 μM) either alone or in the presence of the CO scavenger hemoglobin (Hb; 10 μM) for 6 hours prior to stimulation with LPS. Pooled data (n=3) depicts the mean (± SEM) concentration of IL-23p19 in supernatants of DC treated with carnosol, curcumin and Hb. Statistical significance was determined by one-way ANOVA, with Dunnett's multiple comparisons post hoc test to compare treatment groups against the control group (**p<0.01, *p<0.05).

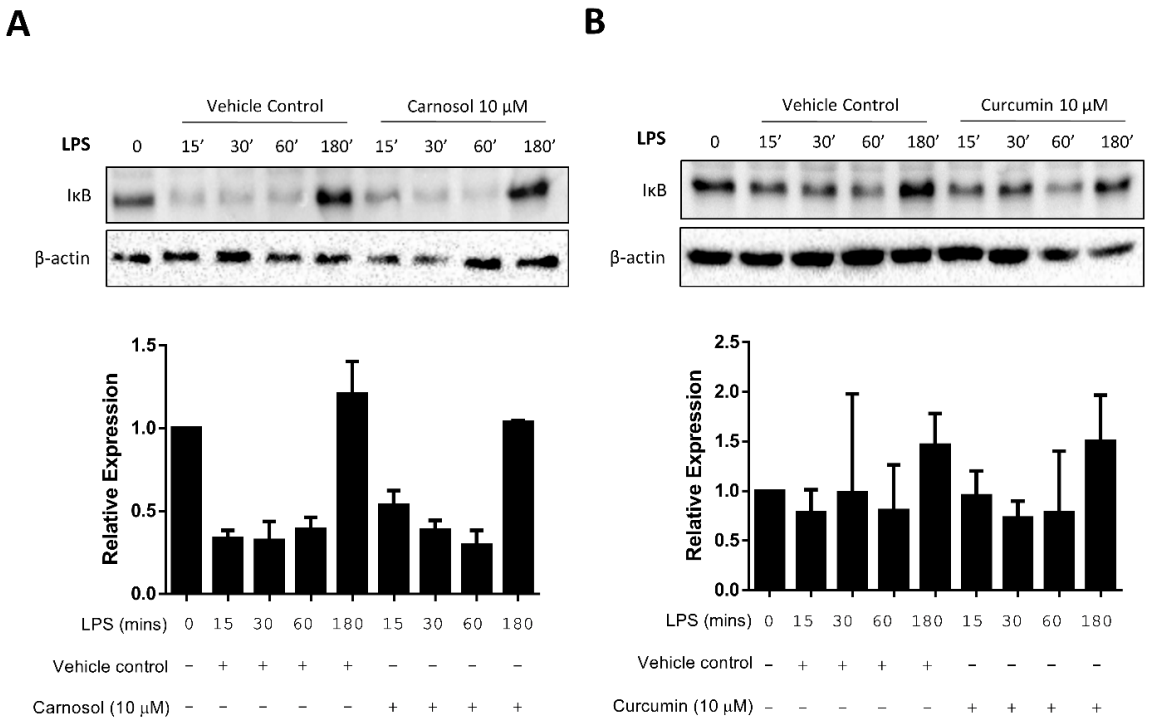

Figure 3.17. Carnosol and curcumin do not inhibit IκB degradation in LPS-stimulated DC. DC from healthy donors (n=3) were incubated with **(A)** carnosol (10 μM), **(B)** curcumin (10 μM) or a vehicle control for 6 hours prior to stimulation with LPS (100 ng/ml) for 15 minutes to 3 hours. The degradation of IκB was measured by Western blot. All blots depict an individual donor and are representative of three independent experiments. Densitometric analysis was performed using ImageLab (Bio-Rad) software (n=3).

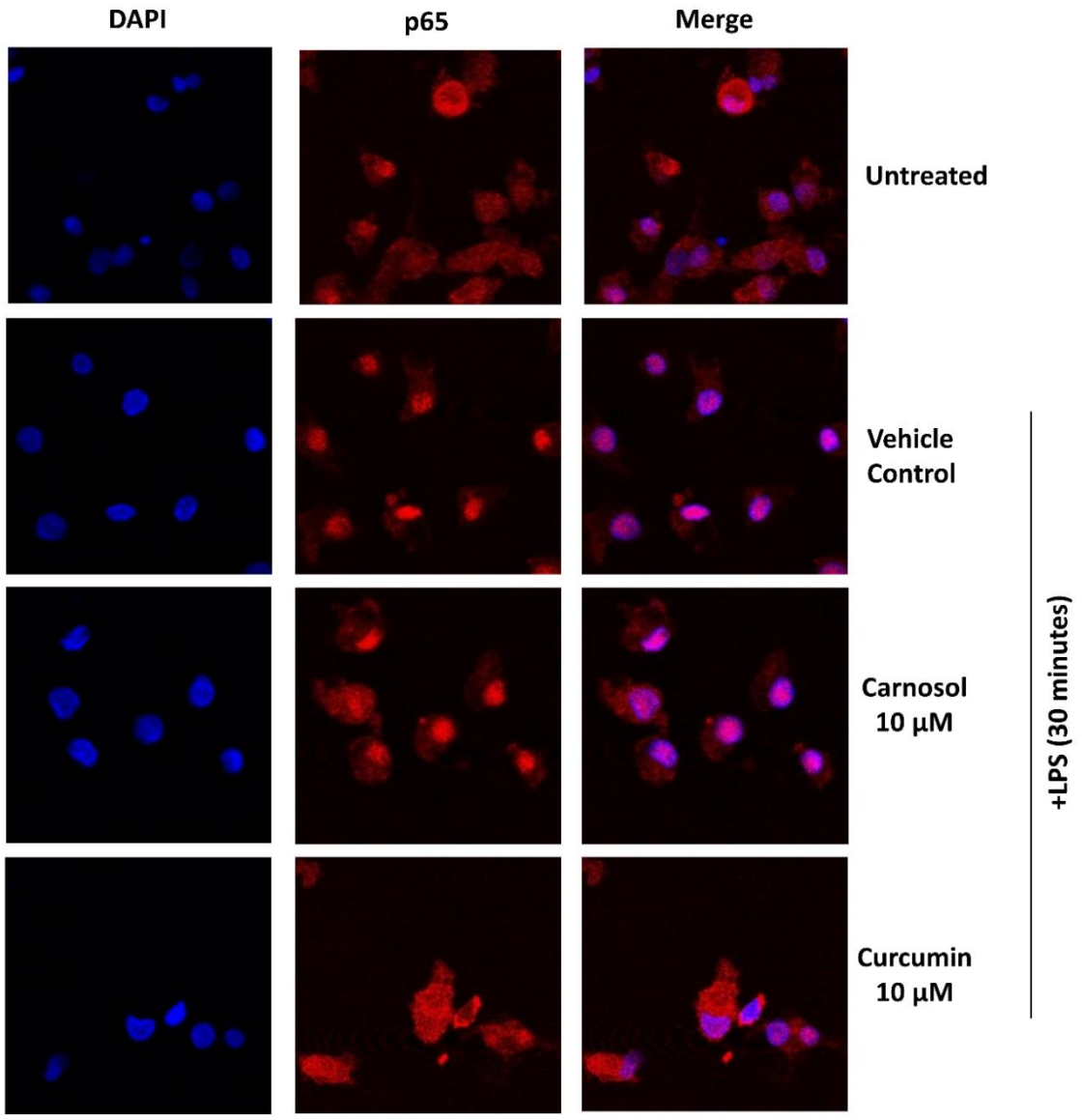

Figure 3.18. Curcumin reduces nuclear translocation of the NF-κB subunit p65 in LPS-stimulated DC. DC from healthy donors (n=4) were incubated with carnosol (10 µM), curcumin (10 µM) or a vehicle control for 6 hours prior to stimulation with LPS for 30 minutes. The nuclear translocation of the NF-κB subunit p65 was assessed by confocal microscopy. Data shown is from one healthy donor and is representative of experiments performed in four healthy donors.

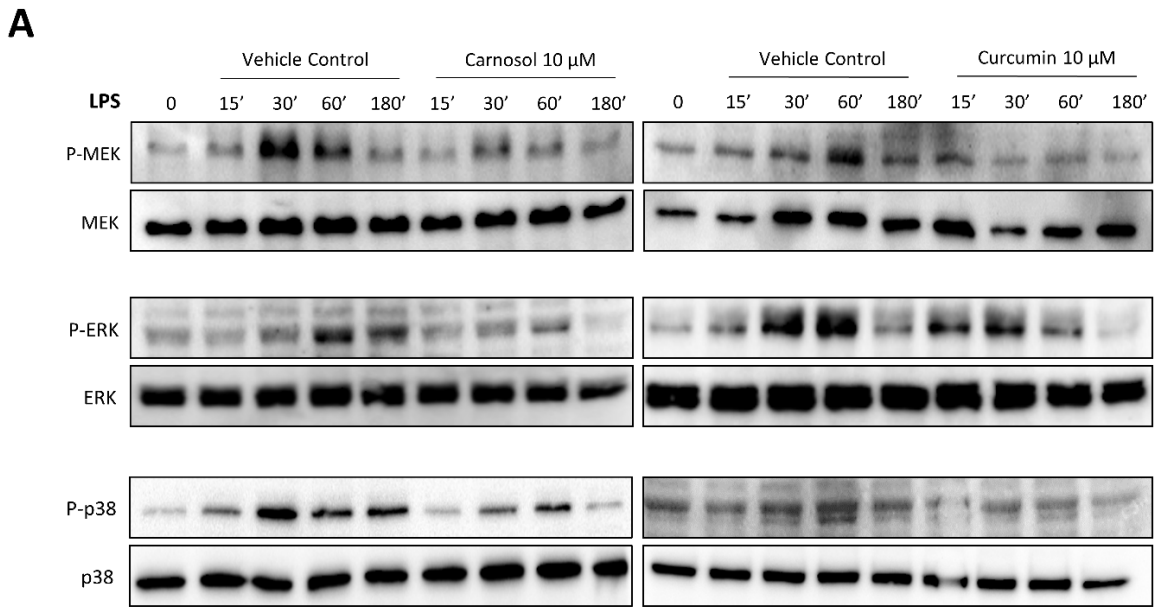
A
Vehicle Control
Carnosol 10 μM
Vehicle Control
Curcumin 10 μM
LPS
0
15′
30′
60′
180′
15′
30′
60′
180′
0
15′
30′
60′
180′
15′
30′
60′
180′
P-MEK
MEK
P-ERK
ERK
P-p38
p38

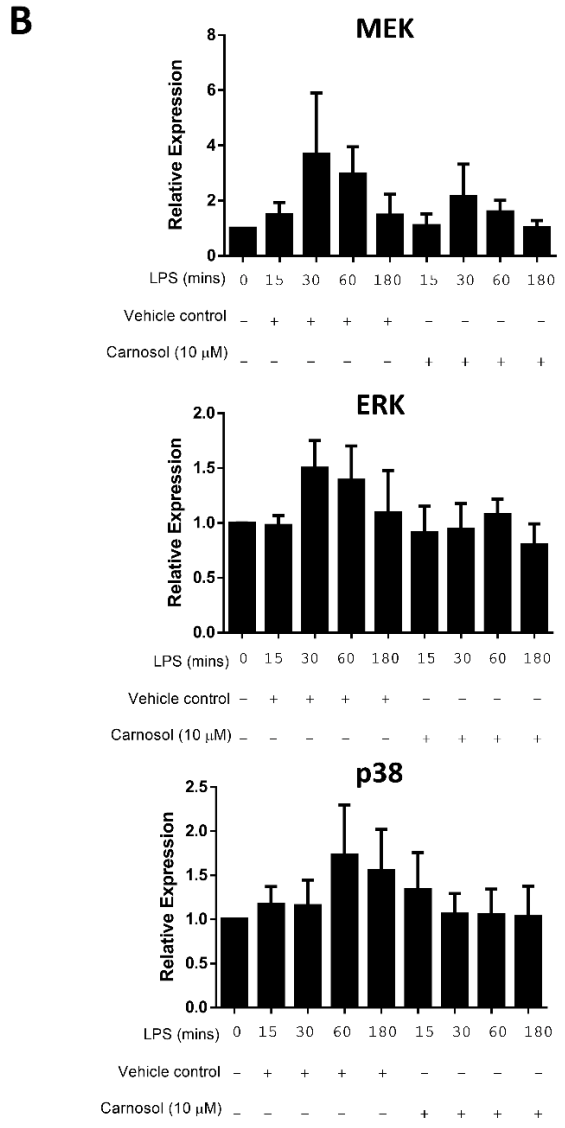
B
MEK
Relative Expression
LPS (mins) 0 15 30 60 180 15 30 60 180
Vehicle control – + + + + – – – –
Carnosol (10 μM) – – – – – + + + +
ERK
Relative Expression
LPS (mins) 0 15 30 60 180 15 30 60 180
Vehicle control – + + + + – – – –
Carnosol (10 μM) – – – – – + + + +
p38
Relative Expression
LPS (mins) 0 15 30 60 180 15 30 60 180
Vehicle control – + + + + – – – –
Carnosol (10 μM) – – – – – + + + +

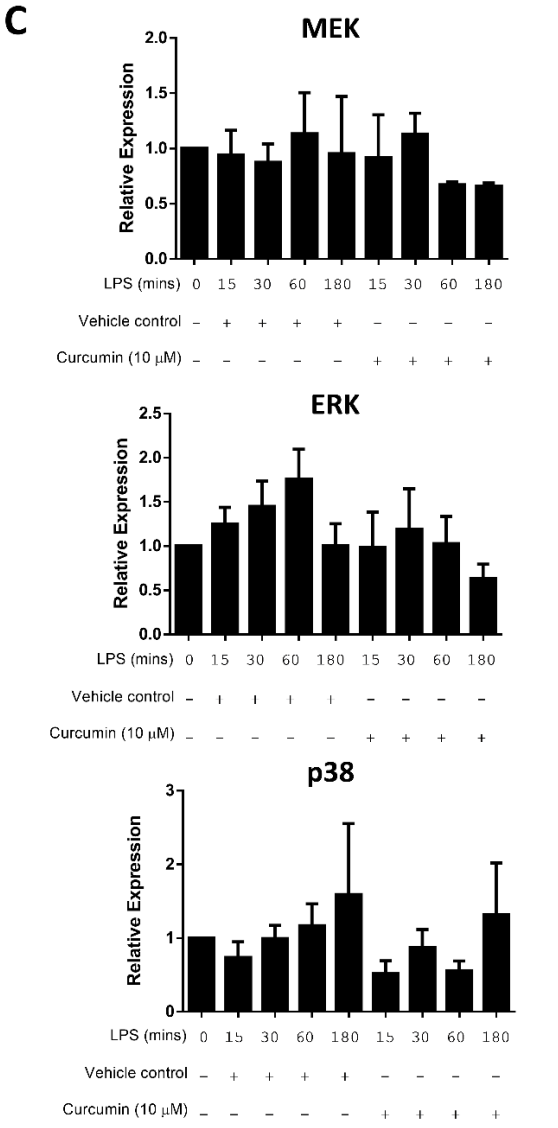
C
MEK
Relative Expression
LPS (mins) 0 15 30 60 180 15 30 60 180
Vehicle control – + + + + – – – –
Curcumin (10 μM) – – – – – + + + +
ERK
Relative Expression
LPS (mins) 0 15 30 60 180 15 30 60 180
Vehicle control – + + + + – – – –
Curcumin (10 μM) – – – – – + + + +
p38
Relative Expression
LPS (mins) 0 15 30 60 180 15 30 60 180
Vehicle control – + + + + – – – –
Curcumin (10 μM) – – – – – + + + +

Figure 3.19. Carnosol and curcumin reduce activation of MAP Kinases in LPS-stimulated DC. DC from healthy donors (n=2-6) were incubated with carnosol (10 µM), curcumin (10 µM) or a vehicle control for 6 hours prior to stimulation with LPS (100 ng/ml) for 15 minutes to 3 hours. **(A)** The activation of the MAPKs MEK, ERK and p38 was measured by Western blot. All blots depict an individual donor and are representative of 2-6 independent experiments. Densitometric analysis of **(B)** carnosol and **(C)** curcumin treated DC was performed using ImageLab (Bio-Rad) software (n=2-6).

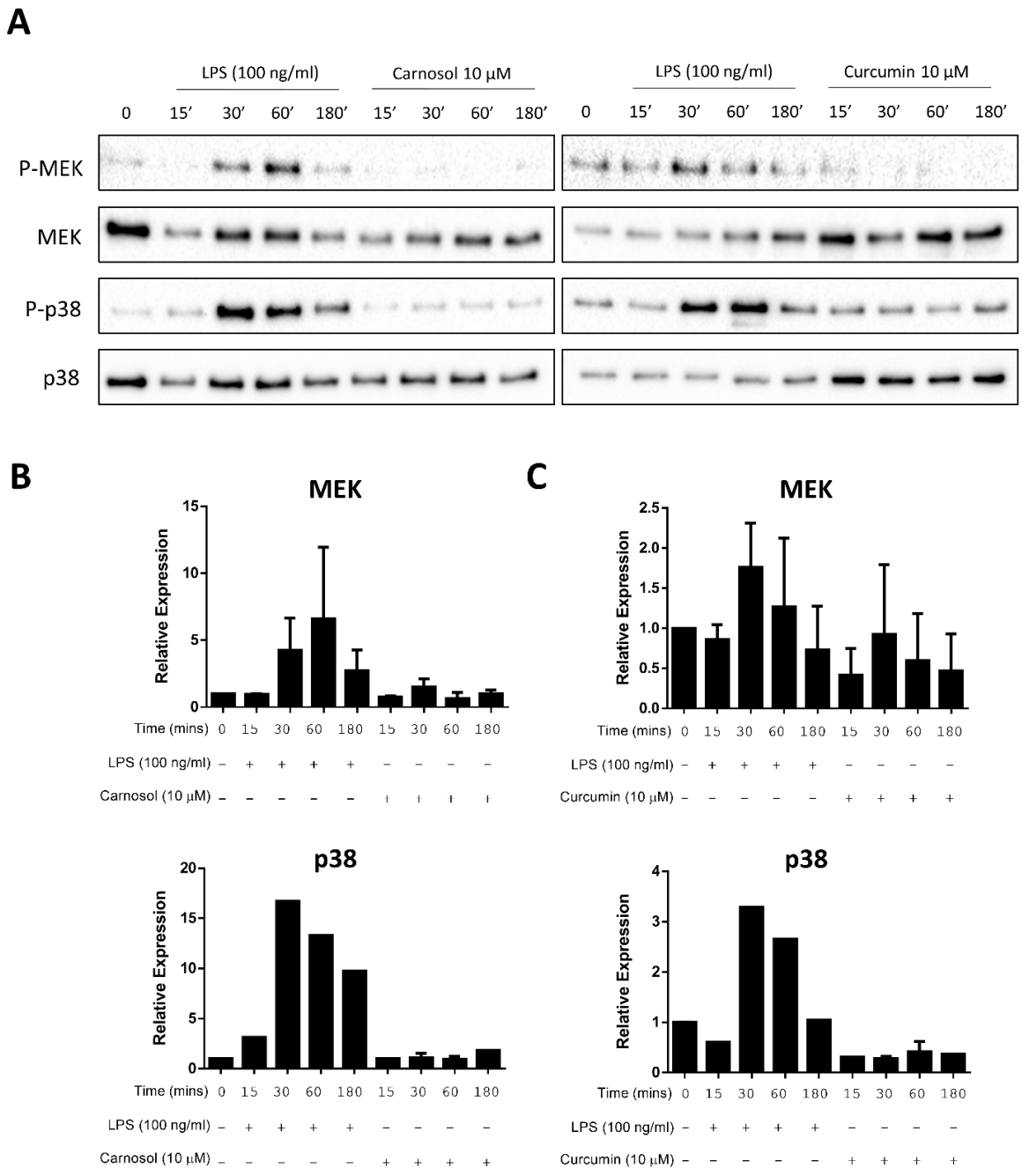

Figure 3.20. Carnosol and curcumin do not activate MAP Kinases in human DC. DC from healthy donors (n=2-3) were incubated with LPS (100 ng/ml), carnosol (10 µM) or curcumin (10 µM) for 15 minutes to 3 hours. **(A)** The activation of the MAPKs MEK and p38 was measured by Western blot. All blots depict an individual donor and are representative of 2-3 independent experiments. Densitometric analysis of **(B)** carnosol and **(C)** curcumin treated DC was performed using ImageLab (Bio-Rad) software (n=2-3).

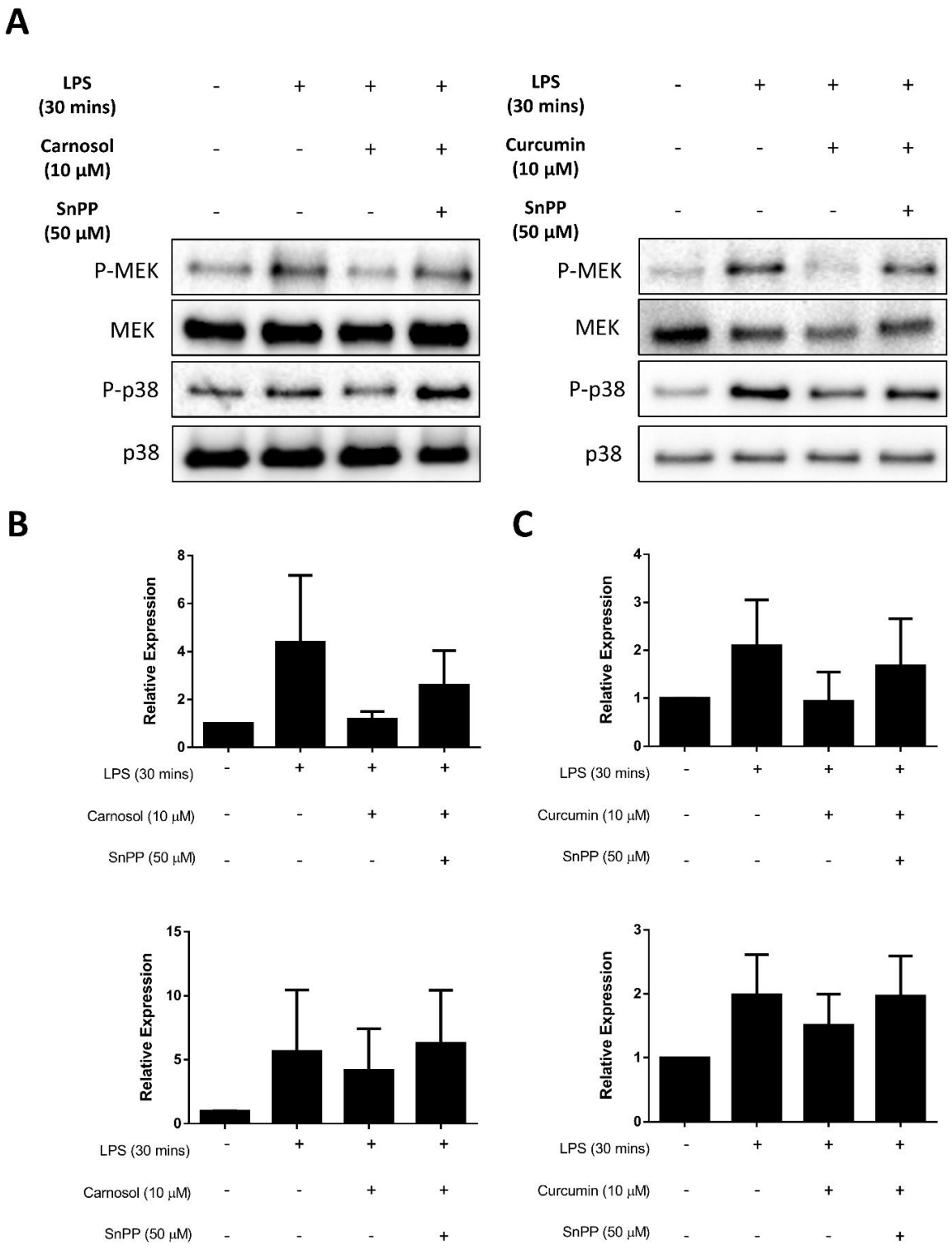

Figure 3.21. Inhibition of MAPK activation by carnosol and curcumin is dependent on HO-1 activity. DC from healthy donors (n=3) were incubated with carnosol (10 µM), curcumin (10 µM), with or without SnPP (50 µM), or a vehicle control for 6 hours prior to stimulation with LPS (100 ng/ml) for 30 minutes. **(A)** The activation of the MAPKs MEK and p38 was measured by Western blot. All blots depict an individual donor and are representative of three independent experiments. Densitometric analysis of **(B)** carnosol and **(C)** curcumin treated DC was performed using ImageLab (Bio-Rad) software (n=3).

3.4 Discussion

The HO-1 system has emerged as an important immunomodulatory pathway in DC, which can promote the development of tolerogenic DC and shape resulting immune responses. Unlike most other cell types, where HO-1 is expressed as a response to oxidative stress or inflammation (356), immature DC constitutively express HO-1, and downregulate this expression upon receipt of a pro-inflammatory stimulus (176,177). Overexpression of HO-1 renders DC refractory to maturation, while knockdown or inhibition of HO-1 is sufficient to promote DC maturation and activation (176,178,189,350). Therefore, HO-1 is intimately related to the maturation status of the DC, and its expression appears to regulate DC function by suppressing pro-inflammatory responses. Pharmacological upregulation of HO-1 expression in DC has potential as a novel approach to modify DC activity, especially in the context of autoimmunity where aberrant DC activation can promote pathogenic T cells. However, the pursuit of this approach has been limited by a lack of HO-1 inducers which are suitable for clinical use. Administration of HO-1 products could also aim to replicate the immunomodulatory effects of HO-1 induction, however it is currently unclear which of the HO-1 products are responsible for its activity in DC. Furthermore, application of these products is associated with its own set of challenges, including difficulties in delivery and toxicity concerns.

The results of this chapter aim to address the above challenges by investigating both the use of novel plant- and marine-derived HO-1 inducers/products and their mechanism of action in human DC. Two polyphenols, curcumin and carnosol, which are naturally-occurring within common foods, were selected for investigation as potential HO-1 inducers in human DC. The data presented herein confirms that curcumin and carnosol are potent inducers of HO-1 expression in DC; both compounds strongly upregulated HO-1 in immature DC, and this upregulation was maintained even after the addition of a maturation stimulus. As the role of HO-1 in DC has been best described in the context of DC maturation (176,177,188,189), it was next determined whether curcumin and carnosol treatment would replicate these effects in DC. Curcumin has previously been shown to reduce expression of DC maturation markers in murine BMDC (277) and human monocyte-derived DC (279,280). Consistent with this, a dose-dependent reduction in expression of the co-stimulatory receptors, CD80 and CD86, and the maturation markers, CD40 and CD83, was observed in curcumin-treated DC stimulated with LPS. Carnosol treatment also displayed similar efficacy to curcumin in the reduction of DC surface markers. Therefore, both polyphenols were found to regulate the phenotypic maturation of human DC, closely mimicking the previously reported activity of traditional HO-1 inducers in this cell type. This immature phenotype observed in carnosol- and curcumin-treated DC is supported by functional analyses which demonstrated

that treated DC possess a greater capacity for antigen capture and reduced pro-inflammatory responses. Antigen capture capacity reflects the maturation status of the DC, as DC which have undergone maturation switch from a tissue-surveillance role towards antigen presentation, and migrate to the lymph node to contact T cells (19,351). There have been mixed reports regarding the effects of curcumin on antigen capture with Shirley *et al.* reporting a decrease in antigen uptake after curcumin treatment (280), while Kim *et al.* demonstrated an increase in phagocytosis (277). There have been no studies, to date, examining the effect of carnosol on antigen capture. In the present study, antigen uptake and processing of the model antigen, DQ-Ova, was significantly increased in LPS-stimulated DC which were pre-treated with carnosol or curcumin and reflected that of immature DC. This result confirms that carnosol- and curcumin-treated DC are functionally immature as well as phenotypically immature.

The cytokines released by DC reflect their status as immunogenic or tolerogenic, as their downstream activity functions to shape the resulting immune response. IL-12 and IL-23 are important cytokines which polarise T cells into Th1 and Th17 effector subsets, respectively, and have been associated with the pathology of autoimmune diseases such as MS and psoriasis (56,336,337,346,357). Expression of both of these cytokines by human DC was reduced to almost undetectable levels with carnosol and curcumin treatment. IL-1β is involved in the differentiation of Th17 cells (353), the primary pathogenic T cell in MS and psoriasis, and a reduction in expression of the pro-form of this cytokine was also observed. Interestingly, despite reports that HO-1 induction by CoPP conserves IL-10 expression in DC (176,189), a decrease in IL-10 was observed with both carnosol and curcumin treatment. However, these results are in agreement with previous studies that have shown reductions of both IL-12 and IL-10 in curcumin-treated DC (277,280). Finally, the observed tolerogenicity of curcumin- and carnosol- treated DC was further demonstrated in a co-culture system with allogeneic $CD4^+$ T cells; both compounds effectively limited the ability of DC to initiate an adaptive immune response, as measured by T cell proliferation and IFNγ production. Again, this is in agreement with other studies which have described the reduced capacity of DC treated with HO-1 inducers or curcumin to activate T cells (177,278–280,283). Therefore, these data support previous studies which have characterised the anti-inflammatory properties of curcumin in DC, while also describing a novel role for carnosol as a modulator of DC maturation and function.

This study reports for the first time that carnosol and curcumin are effective HO-1 inducers in human DC, and that they are capable of modulating DC maturation and function in a similar fashion to traditional HO-1 inducers. However, whether the effects of these polyphenols in DC were dependent on their upregulation of HO-1 had yet to be elucidated. Attempts to address this

question initially utilised a gene-silencing approach, with the aim of preventing the upregulation of HO-1 expression by carnosol and curcumin in order to identify their HO-1-specific and non-specific effects. Unfortunately, this strategy proved too technically difficult to deliver useful results: it was not possible to achieve sufficient RNA interference to counteract the strong induction of HO-1 by carnosol and curcumin without negatively impacting cellular viability. Instead, a commonly used enzymatic inhibitor of HO-1, SnPP, was added to DC alongside carnosol and curcumin to assess the contribution of HO-1 activity to their effects in DC. Encouragingly, addition of SnPP limited the ability of carnosol and curcumin to inhibit the maturation of DC; SnPP reversed the reduction of CD83 and CD86 expression seen in carnosol- and curcumin-treated DC, and abrogated their increased antigen capture capacity. Additionally, SnPP partially reversed the ability of curcumin to inhibit cytokine production by LPS-stimulated DC, as an increase of TNFα production was observed in curcumin-treated DC in the presence of SnPP. These results provide some insight into the mechanism of action of carnosol and curcumin, indicating that the activity of HO-1 contributes to their anti-inflammatory activities in DC. Interestingly, a recent study by Mucha *et al.* which sought to compare different mechanisms of HO-1 inhibition identified similar obstacles as those that were faced during the course of this study. RNA interference was found to be ineffective at inhibiting HO-1 upregulation by inducers such as hemin, and while SnPP did effectively inhibit the enzymatic activity of HO-1, it also increased HO-1 expression (358). This confounding factor may mask some of the effects of SnPP-mediated inhibition of HO-1. The authors conclude that currently the most reliable strategy for inhibition of HO-1 is knockdown via CRISPR-Cas9 gene editing; should this approach prove to be effective in primary human DC, it is hoped that it can be used to build on the results presented in this chapter and further define the contributions of HO-1 to the immunomodulatory activity of carnosol and curcumin.

Although it has been known for a number of years that HO-1 can regulate the maturation and function of DC, it remains unclear which components of the HO-1 pathway affect this regulation. BV is the primary product of heme catabolism by HO-1, yet its effects in DC have been largely unexplored. Additionally, PCB has been identified as a structural analogue to BV and as a substrate for human BVR (318), therefore the effects of PCB in human DC were assessed alongside that of BV. Interestingly, both BV and PCB treatment moderately reduced the expression of DC maturation and co-stimulatory markers, although this reduction was not as potent as that observed with carnosol and curcumin. Furthermore, while the increased capacity for antigen capture in LPS-stimulated DC treated with carnosol or curcumin was observed to be HO-1 dependent, neither BV nor PCB displayed any ability to replicate this effect. Conversely, both BV and PCB strongly inhibited the production of pro-inflammatory cytokines IL-12 and IL-23 by LPS-

stimulated DC, and to a similar extent to that seen with carnosol and curcumin. Therefore, it can be concluded that while BV may contribute in part to the regulation of DC maturation and function by HO-1, it does not fully account for all the observed effects seen with HO-1 inducers, making involvement of other HO-1-related factors likely. Nonetheless, this study presents evidence for the first time that BV can exert anti-inflammatory effects within human DC. Moreover, these results indicate that PCB compares favourably to BV, and displays similar, if not greater, efficacy in its immunomodulatory activity. Interestingly, work carried out in the Dunne laboratory has demonstrated that PCB is also a more potent antioxidant than BV (318), and may therefore represent an attractive alternative to BV as an antioxidant and anti-inflammatory therapy.

Although this study has determined that BV does have some anti-inflammatory activity in human DC, this does not fully account for the HO-1 dependent effects of carnosol and curcumin, thus it was investigated whether CO, another HO-1 product, might play a role. Hemoglobin is a hemoprotein which is usually involved in the transport of oxygen, but which has a much higher affinity for CO. Thus, hemoglobin can act as a scavenger of CO, and in this context, has been used as a CO inhibitor (170,184). In the present study, hemoglobin was used to scavenge CO in carnosol- and curcumin-treated DC in order to assess its contribution to their immunomodulatory effects. Hemoglobin partially attenuated the reduction of DC maturation by carnosol and curcumin; the expression of the co-stimulatory receptors CD80 and CD86 by carnosol- and curcumin-treated DC was increased in the presence of hemoglobin, while the antigen uptake of carnosol, but not curcumin, treated DC was decreased. Additionally, hemoglobin was found to inhibit the reduction of IL-23 production by both polyphenols. These results are in agreement with Rémy *et al.* who found that DC treated with CORM2 displayed reduced maturation and cytokine production in response to LPS (207). However, while CO has been shown to promote phagocytosis in macrophages (209), other studies have reported that CO does not affect antigen uptake by DC (206,208). Discrepancies between the results presented herein and previous studies may have arisen due to differences in assessing CO activity; other investigations into the effects of CO in DC have administered CO, either directly or via CORMs, rather than scavenge CO as performed in this investigation. While use of hemoglobin as a scavenger of CO better assesses the role of CO in the context of HO-1 induction, it does have limitations; in the current study it was not possible to measure the concentration of CO within DC in order to assess the extent of CO scavenging by hemoglobin, therefore it is possible that CO may have only been weakly, or transiently, inhibited. Furthermore, through the course of this study it was found that hemoglobin, as a heme-containing protein, can also cause some upregulation of HO-1 expression in DC, which may confound some of its observed effects. Notwithstanding these limitations, the use of hemoglobin in the present

study provides some insight into the contribution of CO to the effects of HO-1 inducers carnosol and curcumin. As was the case with BV, CO does display some anti-inflammatory activity in human DC, yet does not account for all effects observed with traditional HO-1 inducers or the polyphenols, carnosol and curcumin. It is therefore hypothesised that no single HO-1 product mediates all observed immunomodulatory effects, but that each product partially contributes, with likely redundancy or overlap between them. Interestingly, HO-1 itself may directly interact with transcription factors to regulate DC function; Lin *et al.* previously reported that a cleaved HO-1 protein without enzymatic activity can localise to the nucleus and directly bind transcription factors (359). Indeed, a recent study also reported that HO-1 can directly bind STAT3 and inhibit its activation, thereby limiting Th17 cell differentiation (360). Although in this study it was not possible to explore whether HO-1 displays similar activity within human DC, this possibility is an interesting avenue for future research.

Finally, although it was determined that the activity of carnosol and curcumin in DC is dependent on HO-1 activity, mediated in part by BV and CO, the mechanism of action responsible for these immunomodulatory effects remained to be elucidated. NF-κB is activated as a result of PRR signalling, and controls the immune response of DC by upregulating expression of genes including surface maturation markers and pro-inflammatory cytokines (361,362). Inhibition of NF-κB has previously been suggested as a mechanism of action by HO-1 (164,350), therefore it was of interest to determine whether carnosol and curcumin might affect signalling through NF-κB. It was observed that neither carnosol nor curcumin prevented degradation of IκB in LPS-stimulated DC, indicating that they do not modulate the engagement of TLR4 or the signalling intermediates upstream of IKK activation. This is in contrast with early studies which reported that curcumin can inhibit IKK activation & subsequent degradation of IκB (363,364); however these studies were performed in various cell lines, and therefore may diverge from the activity of curcumin in primary human DC. NF-κB signalling can also be regulated downstream of its activation by IKK. Interestingly, curcumin, but not carnosol, was found to inhibit translocation of the active NF-κB subunit, p65, to the nucleus of LPS-stimulated DC. This result is supported by Rogers *et al.* who also reported that curcumin can inhibit nuclear translocation of p65 in human DC (279). However, it is in contrast with previous studies that have observed inhibition of NF-κB with carnosol treatment in RAW264.7 macrophages (307), and human chondrocytes (309). Taken together, the results of the present study suggest that carnosol and curcumin differentially regulate NF-κB depending on cell-type. As only curcumin, and not carnosol, displayed NF-κB regulatory activity in primary human DC this effect is unlikely to be dependent on HO-1, as both polyphenols were observed to similarly upregulate HO-1 expression. However, the inhibition of NF-κB by curcumin

may regulate DC maturation and function independently of its HO-1 dependent effects, and contribute to differences in activity observed between the two polyphenols. Further research is required to delineate these differential activities of carnosol and curcumin in human DC, and to determine which of the anti-inflammatory effects of curcumin are dependent on its inhibition of NF-κB signalling.

The differential regulation of NF-κB by carnosol and curcumin in human DC, while interesting, did not explain the shared HO-1 dependent immunomodulatory effects of these polyphenols. Alongside activation of transcription factors such as NF-κB, pro-inflammatory stimuli also trigger signalling pathways which culminate in the activation of MAPKs. MAPKs can phosphorylate both cytoplasmic targets and nuclear transcription factors, and thereby regulate the resulting DC immune response (365,366). Furthermore, signalling via the MAPKs, ERK and p38, in murine DC has been shown to contribute to the differentiation of Th17 cells, and inhibition of these MAPKs is protective against EAE (333,337). HO-1 has previously been reported to inhibit the p38 MAPK in murine DC and endothelial cells (178,367), therefore it was investigated whether carnosol or curcumin might regulate MAPK activation. Both carnosol and curcumin were found to inhibit activation of the MAPKs ERK, its upstream kinase MEK, and p38, in LPS-stimulated human DC. Signalling via ERK regulates pro-inflammatory cytokine production by DC, while p38 signalling is particularly important in the generation of immunogenic DC, as it positively regulates expression of surface maturation markers and the cytokines IL-12 and IL-23, and negatively regulates antigen capture (355). Therefore, inhibition of these MAPKs by carnosol and curcumin represents a likely explanation for their observed immunomodulatory effects in human DC. These results are supported by Kim *et al.* who previously reported that curcumin inhibits activation of ERK and p38 in murine DC (277). Conversely, although it has been reported that curcumin can upregulate HO-1 via p38 activation in a hepatoma cell line (165), in the present study no activation of MEK or p38 was observed with either curcumin or carnosol treatment alone, ruling out this mechanism of action in human DC. In order to integrate the observed inhibition of MAPK signalling by these polyphenols with their HO-1 dependent anti-inflammatory effects in DC, the activation of MAPKs in curcumin- and carnosol-treated DC was assessed in the presence of SnPP. The inhibition of MEK and p38 activation by curcumin and carnosol was abrogated in the presence of SnPP, confirming a link between polyphenol-induced HO-1 expression and regulation of MAPK signalling. Therefore, this study reports for the first time that curcumin and carnosol inhibit MAPK activation in human DC, in a HO-1 dependent manner. Precisely which of the HO-1 products mediate the inhibition of MAPKs, and how they achieve this inhibition, remains to be determined in future studies.

In summary, the results presented in this chapter contribute to our current understanding of the role of HO-1, and its products BV and CO, in the generation of tolerogenic DC. The data presented herein supports a model whereby upregulation of HO-1 in DC can suppress MAPK signalling in response to pro-inflammatory stimuli, resulting in the maintenance of DC in an immature state (Figure 3.22). It also provides further evidence to support the use of the plant-derived polyphenols, carnosol and curcumin, and the marine-derived LTP, PCB, as potential drug candidates to treat autoimmune and inflammatory disease. Carnosol and curcumin therefore represent promising alternatives to currently available metalloporphyrins as HO-1 inducers suitable to modulate immune responses in human DC, while PCB may replicate the activity of BV in human DC with greater potency and efficacy.

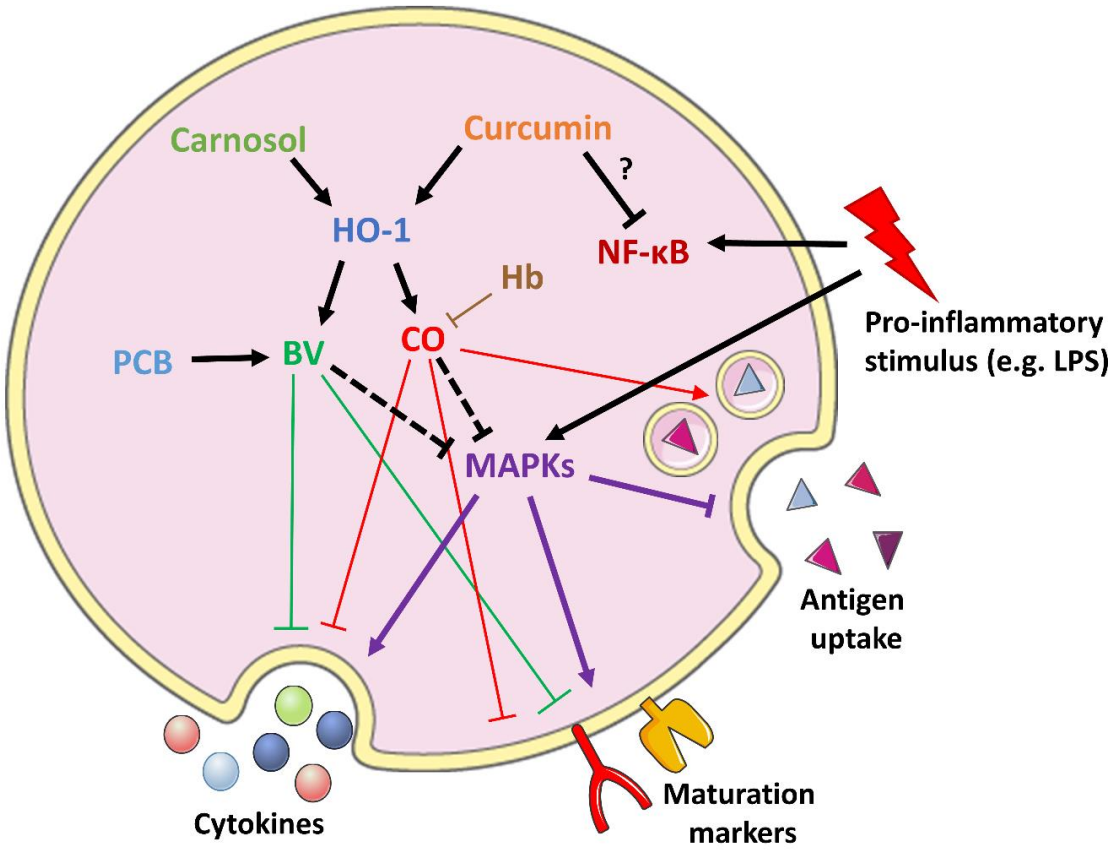

Figure 3.22. Model of HO-1 mediated inhibition of DC maturation and pro-inflammatory functions. Pro-inflammatory stimuli act on DC to activate NF-κB and MAPKs, which upregulate DC cytokine production, expression of surface maturation markers and inhibit antigen uptake (purple arrows). Carnosol and curcumin both upregulate expression of HO-1, which catabolises heme to produce BV and CO. BV inhibits pro-inflammatory cytokine production and DC maturation (green arrows), which is replicated by PCB. CO inhibits pro-inflammatory cytokine production and DC maturation, and promotes antigen uptake (red arrows). These effects may be mediated by inhibition of MAPK signalling by BV and/or CO (dashed arrows). Additionally, curcumin can inhibit NF-κB signalling through an unknown mechanism.

Chapter 4:
The relationship between immunometabolism and the anti-inflammatory effects of carnosol and curcumin

4.1 Introduction

The emerging field of immunometabolism has highlighted the significance of metabolic function in the regulation of immune cell activity. Under certain conditions, anabolic and catabolic metabolism have become associated with pro- and anti-inflammatory immune cells, respectively. Thus, modulation of specific metabolic pathways in immune cells may represent a novel strategy to downregulate inflammation while maintaining the activity of anti-inflammatory immune cells. Indeed, altered metabolic activity in immune cells has been observed in the context of autoimmunity, both in animal models and human patients, lending further support to the potential targeting of metabolic pathways to restore immune balance during disease (368,369). DC and T cells are the predominant immune cell types which mediate autoimmunity, therefore identification of immunomodulators which can modify the metabolic profiles of these cells is of considerable interest.

Each of the discrete T cell subsets have been described to employ metabolic programs which provide support for their specific needs and effector functions. Within helper T cell populations, effector T cells are dependent on mTOR signalling after activation to support their differentiation and expansion via upregulation of aerobic glycolysis (129,370). The requirement for this metabolic reprogramming during T cell activation is starkly evident in anergic T cells. For example, Zheng *et al.* observed that anergic T cells (which have received signal 1 in the absence of signal 2) failed to upregulate metabolite transporters and activate mTOR, while inhibition of cellular metabolism & mTOR signalling was sufficient to induce anergy even in the presence of both signals (371). Conversely, Tregs are less dependent on mTOR and glycolysis, instead displaying high AMPK activity with associated engagement of lipid oxidation and oxidative phosphorylation (129). Of note, metabolic programming appears to regulate the lineage decision-making between Th17 cells and Tregs; a study by Shi *et al.* reported that Th17 cell differentiation is dependent on upregulation of glycolysis via HIF1α and mTOR, with inhibition of either glycolysis or HIF1α/mTOR resulting in a decreased frequency of Th17 cells and concomitant increase of Tregs. Importantly, blockade of glycolysis was protective in the transfer model of EAE, due to the expansion of Tregs over Th17 cells (372). Furthermore, Dang *et al.* reported that HIF1α itself can regulate the differentiation of Th17 cells and Tregs through activation of RORγt transcription (373). Interestingly, in addition to glycolysis, Th17 cells also depend on *de novo* fatty acid synthesis, while Tregs take up exogenous fatty acids to support their metabolism. In support of this, inhibition of fatty acid synthesis was also found to be protective in the EAE model (374). Alteration of cellular metabolism may therefore represent a novel mechanism to restore the Th17/Treg balance in autoimmune diseases such as MS and psoriasis. However, caution should be exerted in the translation of these studies

to human disease. To date, the majority of studies investigating T cell metabolism have been performed in murine cells. Recent studies performed in human cells have suggested that while human Th17 cells are similarly dependent on the mTOR-HIF1α-glycolysis pathway for their differentiation and function, development of human Tregs is also contingent on glycolysis (375). Further research is therefore required to define the influence of immunometabolism on the reciprocal relationship of human Th17 cells and Tregs.

DC execute a number of specialist functions at different stages of the immune response, from immunosurveillance within tissues to antigen presentation in the lymph node. The metabolic requirements of DC are therefore dependent on their activation state and environment, and it is now recognised that coordination of both immunological and metabolic signalling pathways is required for DC maturation. Similar to BMDM, BMDC also engage Warburg metabolism upon activation via TLR signalling, with an upregulation of aerobic glycolysis and downregulation of oxidative phosphorylation observed in mature BMDC. Conversely, this metabolic program is suppressed in immature BMDC by high AMPK activity (120). Stimulation of BMDC with LPS was found by Jantsch *et al.* to increase expression of HIF1α, which mediated upregulation of the glucose transporter GLUT1 and DC maturation markers (121). Furthermore, Everts *et al.* reported that increased glycolysis occurred within minutes of DC activation, and that its purpose was to produce metabolites required for *de novo* fatty acid synthesis, which allowed for the expansion of ER and Golgi membranes to support the increased demand for protein synthesis and transport in the maturing DC (122). Everts *et al.* also found that, similar to BMDM, the downregulation of oxidative phosphorylation in BMDC resulted from suppression of mitochondrial activity by iNOS-derived NO (132); however, human DC do not generally express iNOS, therefore, it is doubtful whether they engage Warburg metabolism like their murine counterparts. Indeed, a recent study by Malinarich *et al.* found that while mature human DC are more glycolytic than immature DC, they do not entirely downregulate oxidative phosphorylation, and instead display a more 'balanced' switch to glycolysis (138). As this is the only study published to date which has investigated the metabolism of human DC, it remains unclear to what extent human DC metabolism reflects that of murine DC, and what the relationship is between metabolism, maturation and function in human DC.

Finally, although HO-1 is known to modulate cellular bioenergetics via its role in heme/iron metabolism and redox homeostasis (376), its relationship to the metabolism of immune cells has, so far, been unexplored. Many of the effects of HO-1 on cellular and systemic metabolism have been attributed to the activity of its products: CO has been shown to inhibit glycolysis and improve mitochondrial function in cardiac tissue (377–379), and to promote oxidative phosphorylation in

astrocytes (380). Meanwhile, Gilbert's syndrome (adult hyperbilirubinemia) is believed to be protective against metabolic syndrome, diabetes mellitus and obesity (190,191), and an iron-rich diet has been reported to improve glucose tolerance in mice via activation of AMPK (381). Interestingly, metabolic signalling has also been described to regulate HO-1 expression. Blockade of fumarase, the TCA cycle enzyme which converts fumarate to malate, has been shown to increase HO-1 expression (382), as has the fumarate-derivative DMF (262,383), which is used in the treatment of psoriasis and MS. Itaconate, a metabolite produced by activated macrophages has also been shown to upregulate HO-1 expression (384). Additionally, the protective effects of the adipokine, adiponectin, in iron-induced liver damage, has been ascribed to HO-1 induction via activation of AMPK and PPARα (385). Given that both HO-1 and metabolic signalling are known to regulate immune function, particularly in DC, it is of interest to determine whether cross-talk exists between the HO-1 system and immunometabolism.

In summary, characterisation of the metabolic pathways utilised by immune cells in different contexts may provide new insights into their biology, and could potentially lead to the development of new treatment strategies for immune-mediated diseases. However, the majority of research informing the current understanding of immunometabolism has been performed in murine systems, therefore it is imperative that this field of study is extended to human immune cells. Moreover, although there is evidence that the HO-1 system is interrelated to metabolic function, its role in immunometabolism has not been explored. Therefore, the purpose of this chapter is to explore the metabolic effects of the HO-1 inducers, carnosol and curcumin, in human immune cells.

4.2 Aims

- To characterise the effects of the HO-1 inducers, carnosol and curcumin, on metabolic pathways in human PBMC and DC.
- To determine whether metabolic signalling regulates HO-1 expression in human DC.

4.3 Results

4.3.1 Curcumin, but not carnosol, slightly reduces the viability of human PBMC

Carnosol and curcumin were previously found to be non-toxic to human DC, however, the activation of adaptive immune cells requires longer exposure to treatments *in vitro*. First, it was confirmed that anti-CD3 stimulation of human PBMC resulted in effective activation of T cells. PBMC were either left unstimulated or stimulated with anti-CD3, and after 3-4 days the concentration of the T cell cytokines, IFNγ and IL-17, in cell culture supernatants was measured by ELISA. There was no detectable production of either IFNγ or IL-17 by unstimulated PBMC, however, anti-CD3 stimulation resulted in a significant upregulation of both cytokines ($p<0.05$ – $p<0.01$; Figure 4.1). Hence, stimulation of PBMC with anti-CD3 for 3-4 days was found to effectively activate T cells.

To determine whether PBMC would tolerate carnosol or curcumin treatment over this timeframe, PBMC were treated with carnosol (2.5-10 µM) or curcumin (1-5 µM) for 6 hours prior to stimulation with anti-CD3. After 3-4 days the viability of PBMC was assessed by flow cytometry, using an amine-binding viability dye. Carnosol was well tolerated by PBMC up to 10 µM, while curcumin treatment produced an approximate ~10% decrease in viability at 5 µM (Figure 4.2). Therefore carnosol and curcumin were judged to be largely well tolerated by PBMC, albeit, in the case of curcumin, at lower concentrations than those used previously in DC.

4.3.2 Carnosol and curcumin upregulate HO-1 expression in human PBMC

Having confirmed that carnosol and curcumin are tolerated by PBMC up to 5 µM, it was next determined whether they could induce HO-1 expression in PBMC at these concentrations. PBMC were treated with carnosol or curcumin (1-5 µM) for 24 hours, and HO-1 expression was detected by Western blot. Unlike DC, PBMC do not basally express HO-1, however, both carnosol and curcumin were found to increase HO-1 expression at 2.5 and 5 µM (Figure 4.3). Thus, it was confirmed that these polyphenols can induce HO-1 expression in PBMC at the concentrations used in this study.

4.3.3 Carnosol and curcumin inhibit the upregulation of glycolysis in stimulated PBMC

Activation of both murine and human T cells has been observed to result in a marked increase in glycolysis (386,387). Furthermore, effector T cells, particularly Th17 cells, have been shown to be particularly dependent on glycolysis for their differentiation and function (129,372,373). Although some evidence exists to suggest that the HO-1 system can regulate cellular bioenergetics (376),

the effects of HO-1 inducers on the metabolism of immune cells has not been investigated. The polyphenols, carnosol and curcumin, were confirmed to be effective, non-toxic, HO-1 inducers in PBMC. Therefore, it was next assessed whether treatment with carnosol or curcumin could limit the upregulation of glycolysis in activated T cells.

PBMC were treated with carnosol (5 µM) or curcumin (5 µM) for 6 hours prior to stimulation with anti-CD3. After 4 days, PBMC were re-seeded into a Seahorse microplate for assessment of metabolic activity. PBMC were placed into a Seahorse XFe24 analyser and their glycolytic activity was determined by the measured ECAR after addition of oligomycin (an inhibitor of mitochondrial complex V), FCCP (a mitochondrial uncoupler), rotenone and antimycin A (inhibitors of the mitochondrial complexes I & III, respectively), and 2-DG (an inhibitor of glycolysis). The ECAR of anti-CD3 stimulated PBMC was observed to be greater than unstimulated PBMC, while PBMC which were treated with carnosol or curcumin prior to stimulation displayed an ECAR similar to unstimulated PBMC (Figure 4.4A). Analysis of the glycolytic profiles of control, carnosol- and curcumin-treated PBMC revealed that the basal rate of glycolysis was significantly increased in anti-CD3 stimulated PBMC compared to unstimulated PBMC ($p<0.05$), while a trend towards reduced basal glycolysis was observed in stimulated PBMC previously treated with carnosol or curcumin. Similarly, a trend towards an increased max glycolytic rate and glycolytic reserve was observed in anti-CD3 stimulated compared to unstimulated PBMC, which was again reduced in carnosol- and curcumin-treated PBMC (Figure 4.4B). These results confirm that mitogen-stimulated PBMC significantly upregulate glycolytic metabolism compared to resting PBMC. Furthermore, treatment of PBMC with the polyphenols, carnosol and curcumin, appears to limit this upregulation of glycolysis after anti-CD3 stimulation.

4.3.4 PBMC treated with carnosol or curcumin display reduced oxidative phosphorylation

Following the observation that the glycolytic profiles of carnosol- and curcumin-treated PBMC, stimulated with anti-CD3, resembled that of unstimulated PBMC, the effects of these polyphenols on oxidative phosphorylation was next examined. PBMC were treated with carnosol or curcumin, stimulated with anti-CD3 and placed in a Seahorse XFe24 analyser as before. Engagement of oxidative phosphorylation was determined by the measured OCR after addition of oligomycin, FCCP, rotenone/antimycin A and 2-DG. The OCR of anti-CD3 stimulated PBMC was observed to be greater than that of unstimulated, carnosol- and curcumin-treated PBMC, all of which remained mostly quiescent (Figure 4.5A). Analysis of the respiratory profiles of control, carnosol- and curcumin-treated PBMC showed that the basal respiratory rate and ATP production of all treatment groups were comparable. However, anti-CD3 stimulated PBMC possessed a

significantly higher max respiratory rate and respiratory reserve compared to unstimulated PBMC ($p<0.05$), which was absent in PBMC treated with carnosol or curcumin (Figure 4.5B). Therefore, stimulated PBMC were observed to have a greater respiratory capacity than unstimulated PBMC, although the basal respiratory rate of stimulated and unstimulated PBMC were largely similar. Moreover, carnosol and curcumin treatment appeared to abrogate this increased spare respiratory capacity (SRC) in stimulated PBMC.

4.3.5 Unstimulated PBMC preferentially utilise oxidative phosphorylation over glycolysis

The metabolic analysis of control, carnosol- and curcumin-treated PBMC demonstrated that PBMC stimulated with anti-CD3 display an increased rate of glycolysis and greater respiratory reserve over unstimulated PBMC, which was inhibited when PBMC were treated with carnosol or curcumin prior to activation. In order to assess whether these metabolic changes reflected a preference towards glycolysis or oxidative phosphorylation by PBMC, the ratio of basal OCR:ECAR was calculated from matched experimental data. Unstimulated PBMC were observed to have the highest OCR:ECAR ratio, reflecting a preferential use of oxidative phosphorylation over glycolysis in resting PBMC. Conversely, control, carnosol- and curcumin- treated PBMC, which were stimulated with anti-CD3, had similar OCR:ECAR ratios that were lower than that observed for unstimulated PBMC (Figure 4.6). Taken together, these data indicate that carnosol and curcumin may inhibit glycolysis and oxidative phosphorylation to a similar degree in anti-CD3 stimulated PBMC.

4.3.6 Carnosol and curcumin reduce the expansion of mitochondria following anti-CD3 stimulation in human PBMC

T cell activation via TCR stimulation has previously been reported to increase mitochondrial biogenesis (388–390), and mitochondria are required for a number of different processes important for T cell differentiation and function (391). Having observed that PBMC stimulated with anti-CD3 possessed a greater SRC than unstimulated, carnosol- and curcumin-treated PBMC, it was next investigated whether this may be a result of altered mitochondrial biogenesis. PBMC were treated with carnosol or curcumin and stimulated with anti-CD3 as before. After 4 days, PBMC were stained with Mitotracker Green and mitochondrial mass was measured by flow cytometry. PBMC stimulated with anti-CD3 were found to have significantly increased mitochondrial mass compared to unstimulated PBMC ($p<0.001$). However, this increase was inhibited in stimulated PBMC which were previously treated with carnosol or curcumin ($p<0.05$ – $p<0.01$; Figure 4.7). This result indicates that the diminished SRC observed in carnosol- and

curcumin-treated PBMC may be a result of reduced mitochondrial expansion following TCR stimulation.

4.3.7 Human DC temporally upregulate glycolysis and oxidative phosphorylation after LPS stimulation

Carnosol and curcumin were found to alter the metabolic function of PBMC, with reductions in both glycolysis and SRC observed in anti-CD3 stimulated PBMC treated with either polyphenol. Carnosol and curcumin were previously observed to limit the maturation and function of DC, therefore it was of interest to investigate whether they would also affect DC metabolism. The current understanding of DC metabolism is largely based on murine studies, which have demonstrated that murine DC strongly upregulate aerobic glycolysis and downregulate oxidative phosphorylation upon TLR stimulation (120–122). However, this engagement of Warburg metabolism is mediated by NO produced by iNOS in murine DC (132). Human monocyte-derived DC do not express iNOS, and therefore likely produce a different metabolic response when activated. A recent study investigating the metabolism of tolerogenic vs immunogenic human DC confirmed that LPS-matured DC do not undergo a switch to Warburg metabolism (138). However, the metabolism of human DC was only assessed 24 hours after stimulation. As the metabolic changes of murine DC have been observed to occur rapidly after TLR stimulation (122), it was of interest in the present study to first characterise the metabolic changes of LPS-stimulated DC over time.

Human DC were seeded into a Seahorse microplate and stimulated with LPS for 0, 1, 3, 6 or 24 hours prior to placement into a Seahorse XF24 analyser. The rate of glycolysis and oxidative phosphorylation were determined by the measured ECAR and OCR, respectively, after treatment with metabolic inhibitors as described before. The ECAR of LPS-stimulated DC was highest at 3 and 6 hours post-LPS treatment, while the ECAR of DC 24 hours post-LPS treatment was observed to be similar to that of unstimulated DC (Figure 4.8A). The glycolytic profile of unstimulated vs LPS-stimulated DC was assessed, and it was observed that the basal rate of glycolysis was increased in LPS-treated DC at all timepoints. However, the maximum rate of glycolysis increased in LPS-stimulated DC after 1 hour, and peaked at 3-6 hours before returning to the unstimulated-DC baseline by 24 hours post-LPS. This was reflected in the calculated glycolytic reserve of LPS-stimulated DC, which was greatest in DC 3-6 hours post-LPS, whereas at 24 hours post-LPS stimulation, DC displayed a glycolytic reserve similar to unstimulated DC (Figure 4.8B). Therefore, while stimulation of human DC with LPS results in a small but mostly sustained increase in the

basal glycolytic rate, the increased glycolytic potential of LPS-stimulated DC appears to be transient, peaking at 3-6 hours post-activation.

The respiratory profiles of DC appeared to mirror their observed glycolytic activity; DC stimulated with LPS for 6 hours displayed the highest OCR, while smaller increases in the OCR of DC 1, 3, and 24 hours post-LPS were seen compared to unstimulated DC (Figure 4.9A). The basal respiratory rate of LPS-stimulated DC was higher than that of unstimulated DC at all timepoints, and was significantly increased in DC 6 hours post-LPS treatment ($p<0.05$). Interestingly, the maximal respiratory rate and respiratory reserve were significantly increased in DC stimulated with LPS for 6 hours compared to both unstimulated DC and DC treated with LPS for 1 or 24 hours ($p<0.05$). Additionally, the rate of ATP production was also observed to be significantly increased in DC after 6 hours LPS stimulation ($p<0.05$; Figure 4.9B). Taken together, these data indicate that, unlike murine DC, human DC significantly upregulate both glycolytic metabolism and oxidative phosphorylation upon LPS-stimulation. However, this observed increase in DC metabolism peaks approximately 6 hours post-activation.

4.3.8 Carnosol and curcumin treatment significantly limits the upregulation of glycolysis in LPS-stimulated DC

Human DC were observed to undergo significant metabolic activation during LPS stimulation, characterised by an increased basal rate of glycolysis and oxidative respiration, and a temporary increase in glycolytic and respiratory capacity. It was next of interest to determine whether carnosol and curcumin could limit this increase in DC metabolism, as was seen in PBMC. As the greatest upregulation of glycolysis and oxidative phosphorylation was seen at 6 hours post LPS stimulation, this timepoint was chosen to assess the action of carnosol and curcumin on DC metabolism. Human DC were seeded into a Seahorse microplate and treated with carnosol (10 µM) or curcumin (10 µM) for 6 hours prior to stimulation with LPS for a further 6 hours. DC were then placed into a Seahorse XFe24 analyser and their glycolytic activity was determined by the measured ECAR in response to metabolic inhibitors, as described before.

As previously observed, the ECAR of LPS-stimulated DC was higher than that of unstimulated DC, whereas LPS-stimulated DC previously treated with either carnosol or curcumin displayed an ECAR similar to unstimulated DC (Figure 4.10A). This was reflected in the basal rate of glycolysis, which was significantly reduced in curcumin-treated DC compared to control DC ($p<0.05$), and a trend towards reduced basal glycolysis was also seen in carnosol-treated DC. The observed inhibition of glycolysis in carnosol- and curcumin-treated DC was more pronounced in the maximal rate of

glycolysis and glycolytic reserve, which were significantly reduced with both polyphenols compared to control DC ($p<0.05$ – $p<0.001$; Figure 4.10B). Therefore, carnosol and curcumin treatment prevented the upregulation of glycolysis in LPS-stimulated DC, resulting in reductions of both basal glycolysis and the spare glycolytic capacity of maturing DC.

4.3.9 Carnosol and curcumin treatment reduces the spare respiratory capacity of LPS-stimulated DC

Treatment of DC with either carnosol or curcumin was found to inhibit the upregulation of glycolysis in response to LPS stimulation. However, it was previously observed that LPS-stimulated human DC also increase oxidative phosphorylation in addition to glycolysis. Therefore, the effect of these polyphenols on oxidative phosphorylation within LPS-stimulated DC was also examined. DC were treated with carnosol or curcumin and stimulated with LPS as before. DC were then placed into a Seahorse XFe24 analyser and their rate of oxidative phosphorylation was determined by the measured OCR after treatment with metabolic inhibitors, as previously described. The OCR of LPS-stimulated DC was observed to be greater than that of unstimulated DC, and of carnosol- and curcumin-treated DC (Figure 4.11A). A slight reduction in the basal respiratory rate was observed in carnosol and curcumin treated DC compared to control DC, but this was not significant. Unlike previous experiments, the rate of ATP production was similar between unstimulated and LPS-stimulated DC, and was unaffected by either carnosol or curcumin treatment. Conversely, a trend towards an increased maximal respiratory rate and respiratory reserve was observed in LPS-stimulated DC compared to unstimulated DC, which was reduced in DC previously treated with carnosol or curcumin (Figure 4.11B). Taken together, these data suggest that carnosol and curcumin inhibit the increased SRC of LPS-stimulated DC, but without much effect on their basal respiratory rate or ATP production.

4.3.10 Curcumin-treated DC preferentially utilise oxidative phosphorylation over glycolysis

Analysis of the metabolism of carnosol- and curcumin-treated DC revealed that both polyphenols inhibited the upregulation of basal glycolysis, reserve glycolysis, and SRC in response to LPS stimulation. As a greater inhibitory effect was observed on the glycolytic vs respiratory profile of LPS-stimulated DC with carnosol and curcumin treatment, the overall preference for oxidative phosphorylation or glycolysis in these cells was determined via calculation of the basal OCR:ECAR ratio from matched experiments. Consistent with previous studies in murine and human DC which have suggested that immature DC preferentially utilise oxidative phosphorylation to meet their

metabolic requirements (120,138), unstimulated DC displayed a slightly greater OCR:ECAR ratio than LPS-stimulated DC. Interestingly, the OCR:ECAR ratio of curcumin-treated DC was significantly increased compared to control DC, which was also higher than that of unstimulated DC ($p<0.01$). Conversely, the OCR:ECAR ratio of carnosol-treated DC was similar to that of control DC (Figure 4.12). These results indicate that LPS-stimulated DC are more glycolytic than immature DC, and that curcumin inhibits the upregulation of glycolysis to a greater degree than oxidative phosphorylation. As carnosol treatment was also observed to inhibit both the increase in glycolysis and respiratory reserve after LPS stimulation, the lower OCR:ECAR ratio of carnosol-treated DC may reflect a similar level of inhibition of both glycolysis and oxidative phosphorylation in these cells.

4.3.11 Activation of AMPK regulates the induction of HO-1 by carnosol and curcumin in human DC

Previous work demonstrated that carnosol and curcumin exert extensive immunomodulatory and anti-inflammatory effects in human DC, as a result of their upregulation of HO-1 expression. The cellular energy sensor and master regulator of catabolic metabolism, AMPK, has previously been implicated in the induction of HO-1 expression in other cell types (385,392,393). Upon observation that carnosol and curcumin significantly inhibit the metabolic changes which arise as a result of DC activation and are capable of maintaining DC in an immature state (a function also ascribed to AMPK), it was hypothesised that metabolic signalling via AMPK may regulate the induction of HO-1, and associated anti-inflammatory effects, by these polyphenols. To determine whether carnosol or curcumin treatment results in the activation of AMPK in human DC, DC were treated with carnosol (10 μM), curcumin (10 μM), or AICAR (1 mM), an AMPK agonist, for 1 hour. Phosphorylation, and therefore activation, of AMPK was detected by Western blot. Treatment with AICAR, carnosol and curcumin were all found to increase the activation of AMPK compared to control DC (Figure 4.13A).

Having confirmed that carnosol and curcumin can activate AMPK, it was next investigated whether AMPK can regulate the expression of HO-1 in human DC. First, human DC were treated with increasing concentrations of AICAR for 24 hours, after which the expression of HO-1 was detected by Western blot. A dose-dependent increase of HO-1 expression was observed in AICAR-treated DC, with the greatest upregulation observed at 0.5 mM and 1 mM (Figure 4.13B). Following this, the contribution of AMPK to the upregulation of HO-1 by carnosol and curcumin was investigated. DC were treated with compound C, a pharmacological inhibitor of AMPK, for one hour prior to treatment with carnosol (10 μM) or curcumin (10 μM). After 24 hours, the expression of HO-1 was

detected by Western blot. As previously observed, carnosol and curcumin increased the expression of HO-1 by DC, however, this increase was diminished in the presence of compound C (Figure 4.13C). Taken together, these results suggest that the upregulation of HO-1 by carnosol and curcumin is mediated by their activation of AMPK in human DC.

4.3.12 Compound C, an inhibitor of AMPK, inhibits cytokine production by human DC

Treatment of human DC with carnosol or curcumin was previously found to significantly inhibit the production of pro-inflammatory cytokines in response to LPS, which was at least partially dependent on the activity of HO-1. Having observed that the induction of HO-1 by carnosol and curcumin appears to be dependent on their activation of AMPK, it was of interest to investigate whether inhibition of AMPK signalling would also block the previously observed effects on cytokine production. An attempt was made to assess the contribution of AMPK signalling in the inhibition of cytokines by carnosol and curcumin, via addition of the AMPK inhibitor, compound C. Surprisingly, as AMPK activation has previously been reported to inhibit IL-12/IL-23p40 production in murine DC (120), treatment of DC with compound C alone was sufficient to significantly inhibit the production of pro-inflammatory cytokines in response to LPS ($p<0.05$ – $p<0.0001$; Figure 4.14). Therefore, it was not possible to assess whether blockade of AMPK signalling could reverse the effects of carnosol and curcumin on DC cytokine production using pharmacological inhibition of AMPK.

4.3.13 Inhibition of AMPK attenuates the reduction of DC maturation by carnosol and curcumin

HO-1 is a known promoter of tolerogenic DC, as it is highly expressed in immature DC and limits their maturation in response to pro-inflammatory stimuli (176–178). In the present study, upregulation of HO-1 by carnosol and curcumin was previously observed to limit the maturation of human DC stimulated with LPS. As inhibition of AMPK via compound C was found to attenuate the induction of HO-1 by both carnosol and curcumin, it was next investigated whether AMPK inhibition could also reverse the effects of these polyphenols on DC maturation. Human DC were treated with compound C for one hour before addition of either carnosol (10 µM) or curcumin (10 µM) for a further 6 hours prior to stimulation with LPS. After 24 hours, expression of the maturation markers CD40 and CD83, and co-stimulatory molecules CD80 and CD86 was measured by flow cytometry. Consistent with previous experiments, carnosol treatment significantly reduced expression of CD83 and CD86 by LPS-stimulated DC ($p<0.05$), with a trend towards reduced CD40 also observed. However, this effect was attenuated in the presence of compound

C ($p<0.05$ – $p<0.001$; Figure 4.15). Similarly, curcumin treatment significantly reduced the expression of CD40 and CD86 in LPS stimulated DC ($p<0.05$), with a trend towards reduced CD83 also observed. Again, this inhibition of surface marker expression by curcumin was reversed with the addition of compound C ($p<0.05$; Figure 4.16). Treatment of LPS-stimulated DC with compound C alone did not significantly increase the expression of DC surface markers. These results indicate that signalling via AMPK is required for the modulation of DC maturation by carnosol and curcumin.

4.3.14 Inhibition of AMPK attenuates the increased phagocytic capacity of LPS-stimulated DC treated with carnosol or curcumin

Finally, the inhibition of DC surface marker expression by carnosol and curcumin had been supported by further experiments which demonstrated that carnosol- and curcumin-treated DC also maintained their capacity to uptake antigen after LPS stimulation. Having observed that inhibition of AMPK signalling via compound C reversed the effects of carnosol and curcumin on the phenotypic maturation of DC, it was next determined whether their effects on functional DC maturation would also be attenuated. DC were treated with compound C, carnosol or curcumin, and stimulated with LPS as before. After 24 hours, DC were incubated with DQ-Ova for 20 minutes, and analysed for antigen uptake by flow cytometry. As expected, stimulation of DC with LPS dramatically reduced their capacity to uptake antigen compared to immature DC ($p<0.0001$). Furthermore, both carnosol and curcumin treatment maintained the phagocytic capacity of LPS-stimulated DC similar to that of immature DC ($p<0.05$ – $p<0.001$), as was observed previously. However, addition of compound C to carnosol- and curcumin-treated DC significantly abrogated this effect ($p<0.01$ – $p<0.001$), resulting in antigen uptake similar to mature DC (Figure 4.17). Treatment of DC with compound C alone did not significantly alter their antigen uptake capacity following LPS stimulation. Taken together, these results confirm that the immunomodulatory effects of carnosol and curcumin on both phenotypic and functional DC maturation are dependent on their activation of AMPK.

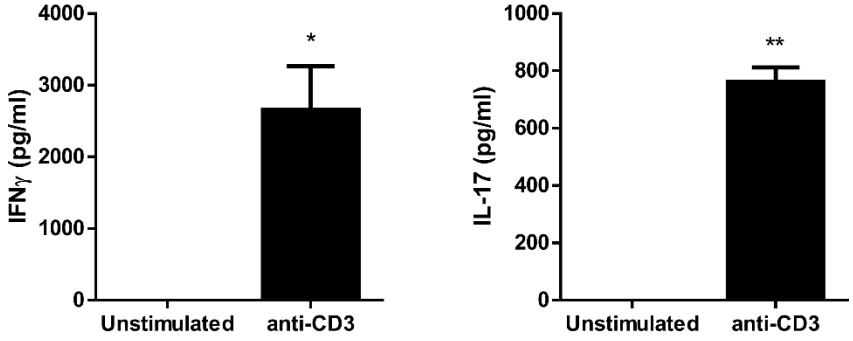

Figure 4.1. Stimulation of PBMC with anti-CD3 for 3-4 days effectively activates T cells. PBMC were left unstimulated or stimulated with anti-CD3 for 3-4 days. The concentration of IFNγ and IL-17 in cell culture supernatants was measured by ELISA. Results shown are mean (± SD) of three technical replicates from one healthy donor, and is representative of three independent experiments. Statistical significance was measured by paired t-test (**$p<0.01$, *$p<0.05$).

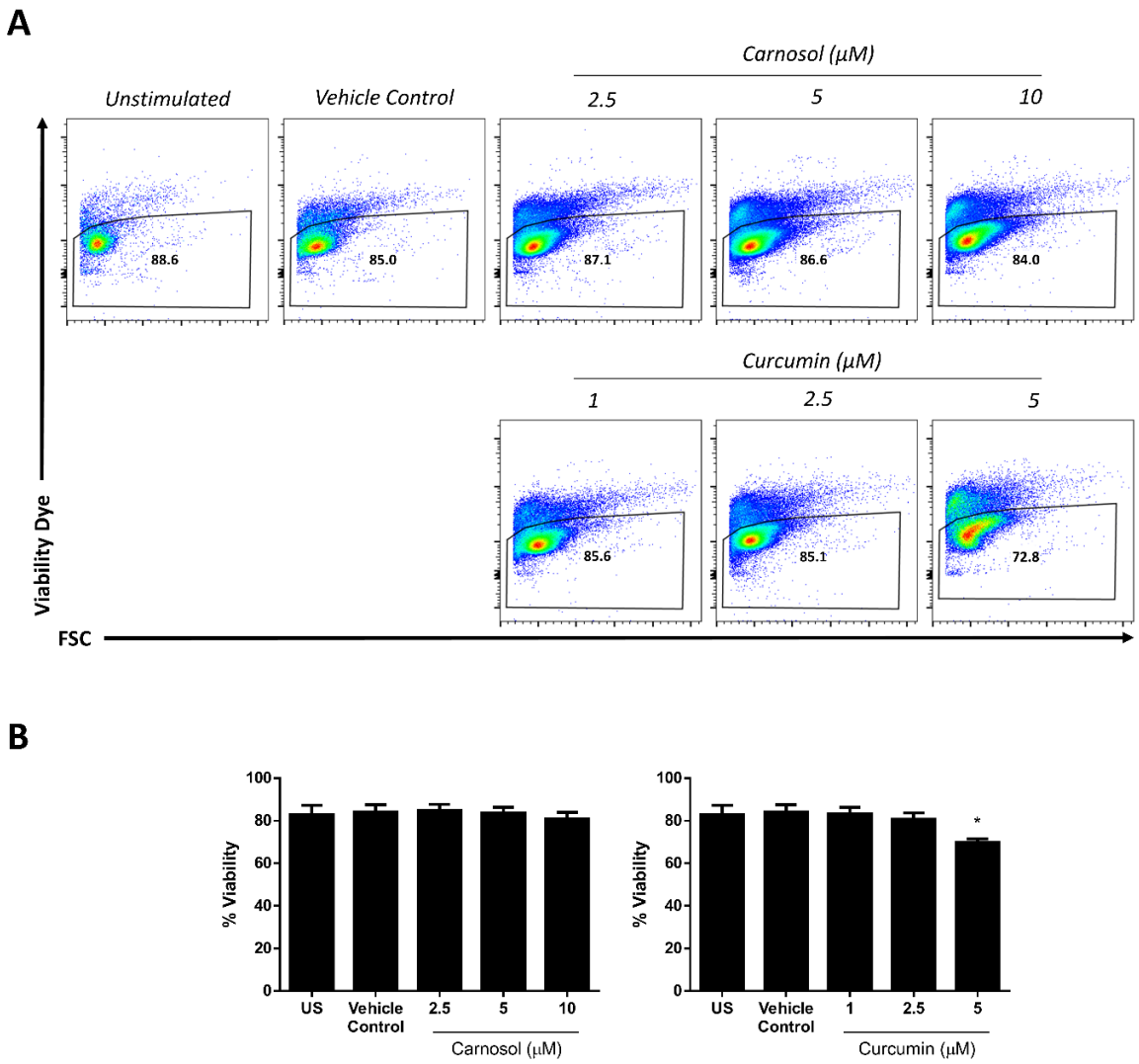

Figure 4.2. Curcumin, but not carnosol, slightly reduces viability of human PBMC. PBMC were either left unstimulated (US) or treated with carnosol (2.5-10 μM), curcumin (1-5 μM) or a vehicle control for 6 hours prior to stimulation with anti-CD3 for 3-4 days. Cells were stained with an amine-binding viability dye and analysed by flow cytometry. **(A)** Dot plots depicting viability dye uptake of control-, carnosol- and curcumin-treated PBMC. Data is from one donor and representative of five independent experiments. **(C)** Pooled data (n=5) depicting the mean (±SEM) percentage viable cells of lymphocytes (gated by forward and side scatter). Statistical significance was determined by one-way ANOVA, with Dunnett's multiple comparisons post hoc test to compare treatment groups against the control group (*p<0.05).

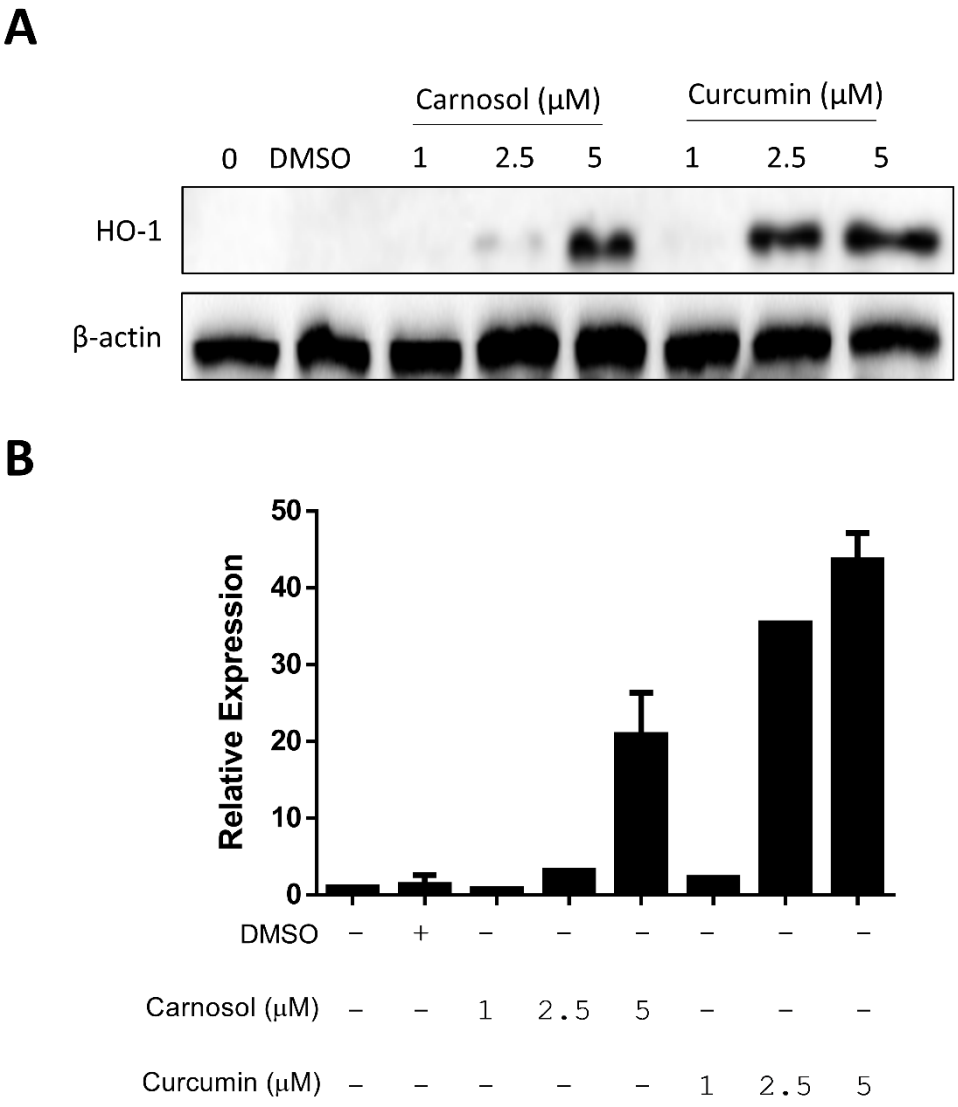

Figure 4.3. Carnosol and curcumin induce HO-1 expression in human PBMC. (A) PBMC were treated with a vehicle control, carnosol or curcumin (1-5 μM) for 24 hours. HO-1 expression was detected by Western blot; blot depicts one donor and is representative of two independent experiments. **(B)** Densitometric analysis was performed using ImageLab (Bio-Rad) software (n=2). Blot was performed with assistance from Hannah Fitzgerald.

A

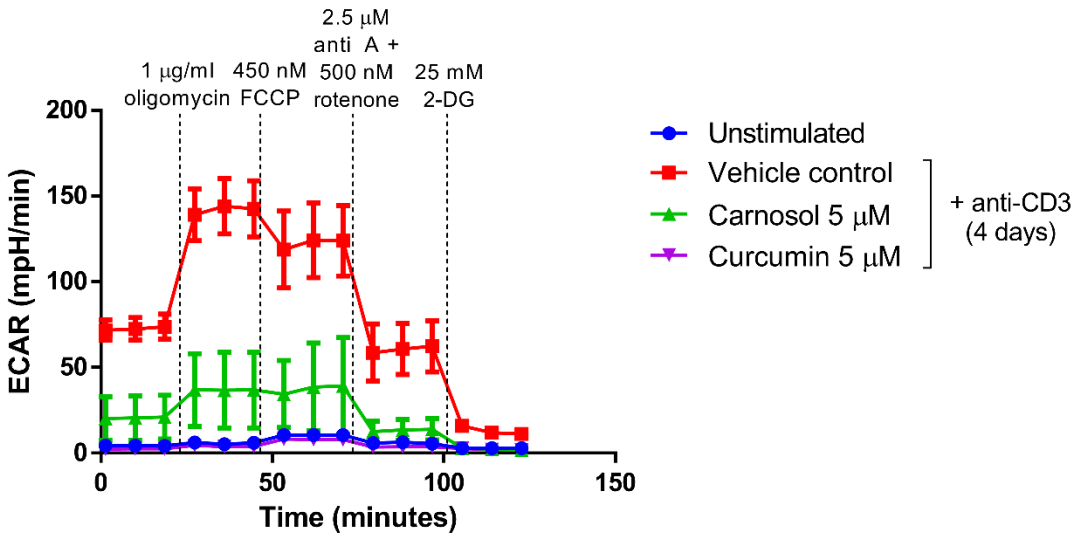
1 µg/ml oligomycin
450 nM FCCP
2.5 µM anti A + 500 nM rotenone
25 mM 2-DG
ECAR (mpH/min)
Time (minutes)
Unstimulated
Vehicle control
Carnosol 5 µM
Curcumin 5 µM
+ anti-CD3 (4 days)

B

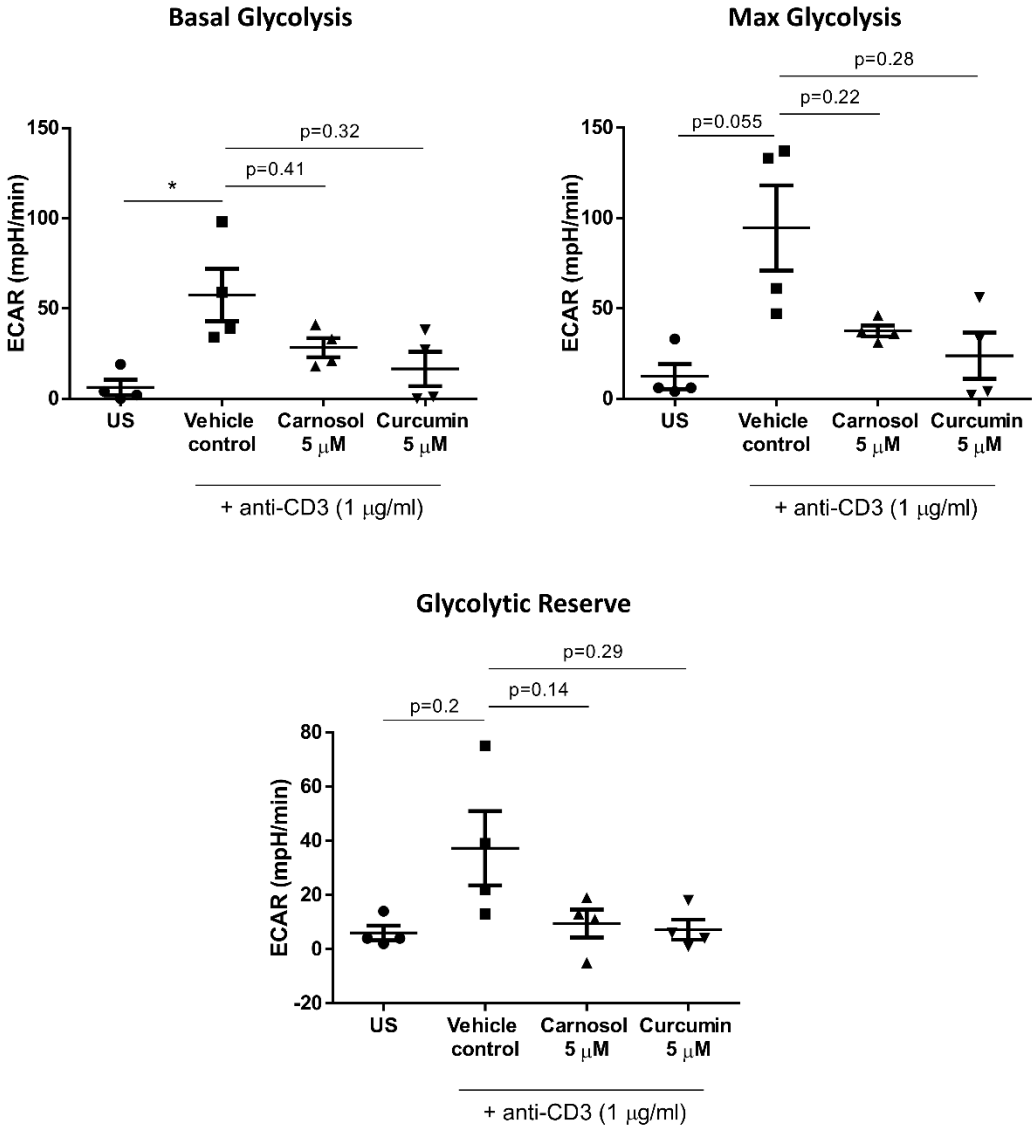
Basal Glycolysis
Max Glycolysis
Glycolytic Reserve
ECAR (mpH/min)
US
Vehicle control
Carnosol 5 µM
Curcumin 5 µM
+ anti-CD3 (1 µg/ml)
p=0.32
p=0.41
*
p=0.28
p=0.22
p=0.055
p=0.29
p=0.14
p=0.2

Figure 4.4. Carnosol- and curcumin-treated PBMC show a reduced induction of glycolysis in response to anti-CD3 stimulation. PBMC (n=4) were either left unstimulated (US) or treated with carnosol (5 µM), curcumin (5 µM) or a vehicle control for 6 hours prior to stimulation with anti-CD3 (1 µg/ml). After 4 days, PBMC were placed into a Seahorse XF24e analyser. The extracellular acidification rate (ECAR) was measured before and after the addition of oligomycin (1 µg/ml), FCCP (450 nM), antimycin A (2.5 µM) and rotenone (500 nM), and 2-DG (25 mM). **(A)** ECAR measurements over time for each treatment group. Data depicts one representative experiment. **(B)** Pooled data (n=4) depicting the calculated mean (± SEM) basal glycolytic rate, max glycolytic rate and glycolytic reserve for each treatment group. Statistical significance was determined by one-way ANOVA with Dunnett's multiple comparisons post hoc test to compare treatment groups against the control group (*$p<0.05$).

A

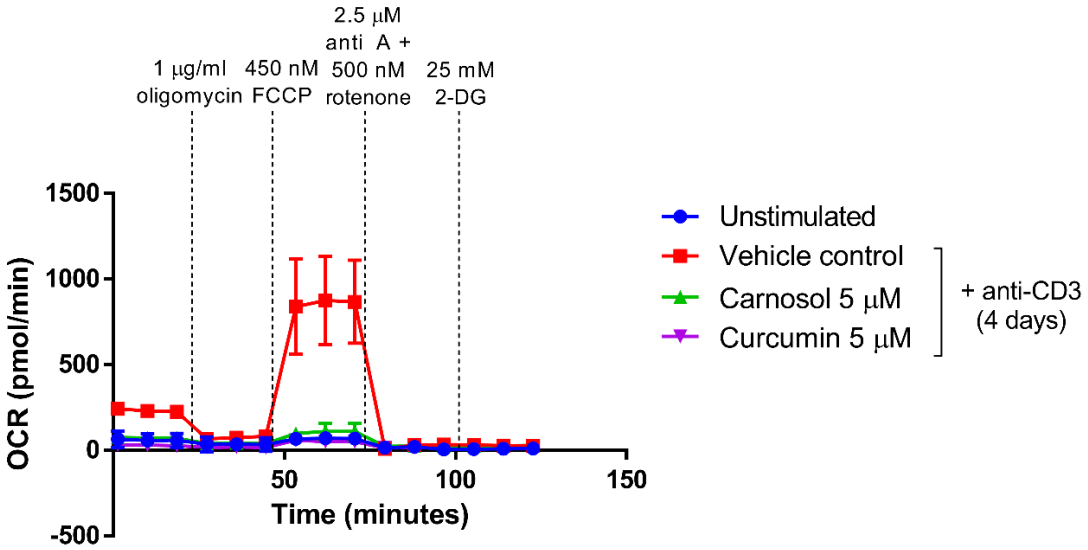
1 μg/ml oligomycin
450 nM FCCP
2.5 μM anti A + 500 nM rotenone
25 mM 2-DG
OCR (pmol/min)
Time (minutes)
Unstimulated
Vehicle control
Carnosol 5 μM
Curcumin 5 μM
+ anti-CD3 (4 days)

B

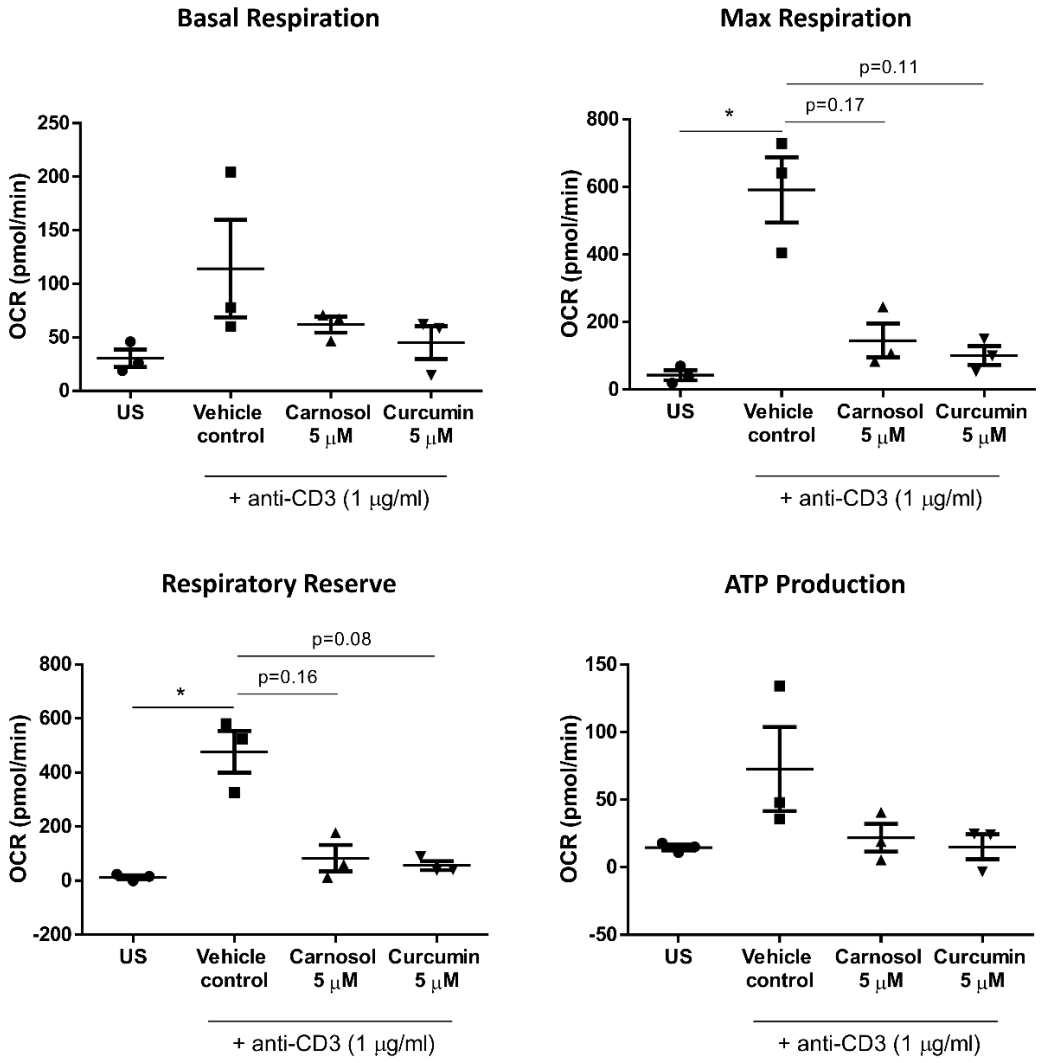
Basal Respiration
Max Respiration
Respiratory Reserve
ATP Production
OCR (pmol/min)
US
Vehicle control
Carnosol 5 μM
Curcumin 5 μM
+ anti-CD3 (1 μg/ml)
p=0.11
p=0.17
p=0.08
p=0.16
*

Figure 4.5. Carnosol- and curcumin-treated PBMC show a reduced induction of oxidative phosphorylation in response to anti-CD3 stimulation. PBMC (n=3) were either left unstimulated (US) or treated with carnosol (5 μM), curcumin (5 μM) or a vehicle control for 6 hours prior to stimulation with anti-CD3 (1 μg/ml). After 4 days, PBMC were placed into a Seahorse XF24e analyser. The oxygen consumption rate (OCR) was measured before and after the addition of oligomycin (1 μg/ml), FCCP (450 nM), antimycin A (2.5 μM) and rotenone (500 nM), and 2-DG (25 mM). **(A)** OCR measurements over time for each treatment group. Data depicts one representative experiment **(B)** Pooled data (n=3) depicting the calculated mean (± SEM) basal respiratory rate, max respiratory rate, respiratory reserve and ATP production rate for each treatment group. Statistical significance was determined by one-way ANOVA with Dunnett's multiple comparisons post hoc test to compare treatment groups against the control group (*$p<0.05$).

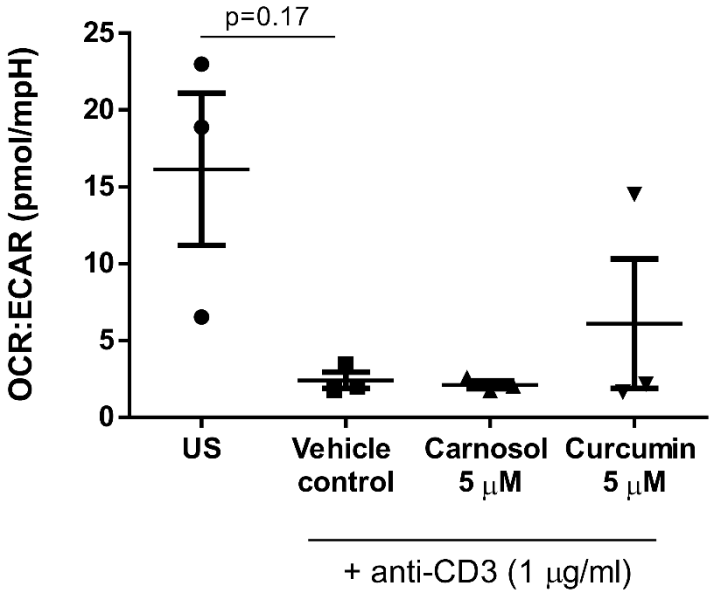

Figure 4.6. Unstimulated PBMC preferentially utilise oxidative phosphorylation over glycolysis. PBMC (n=3) were either left unstimulated (US) or treated with carnosol (5 μM), curcumin (5 μM) or a vehicle control for 6 hours prior to stimulation with anti-CD3 (1 μg/ml). After 4 days, PBMC were placed into a Seahorse XF24e analyser. Basal rates of oxidative phosphorylation and glycolysis were measured by OCR and ECAR, respectively. Pooled data (n=3) depicting the calculated mean (± SEM) ratio of OCR:ECAR for each treatment group. Statistical significance was determined by one-way ANOVA with Dunnett's multiple comparisons post hoc test to compare treatment groups against the control group.

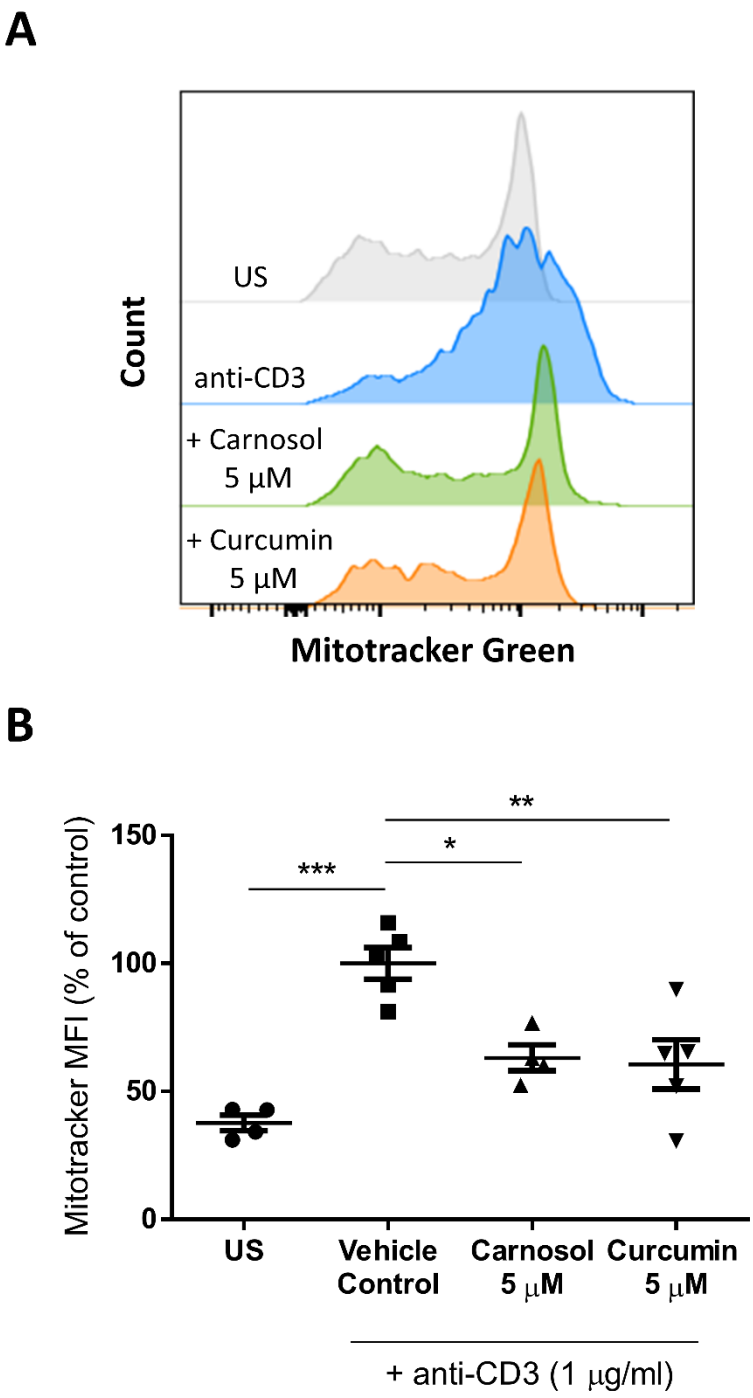

Figure 4.7. Carnosol and curcumin reduce mitochondrial expansion in anti-CD3 stimulated PBMC. PBMC (n=5) were either left unstimulated (US) or treated with carnosol (5 µM), curcumin (5 µM) or a vehicle control for 6 hours prior to stimulation with anti-CD3 (1 µg/ml) for 4 days. PBMC were then stained with Mitotracker Green and mitochondrial biomass was measured by flow cytometry. **(A)** Histogram depicting Mitotracker Green staining in control-, carnosol- and curcumin-treated PBMC from one representative experiment. **(B)** Pooled data (n=5) depicting Mitotracker Green staining in control-, carnosol- and curcumin-treated PBMC. Results shown are mean (± SEM) of the measured Mean Fluorescence Intensities (MFI), expressed as percentages of the vehicle control. Statistical significance was determined by one-way ANOVA, with Tukey's multiple comparisons post hoc test to compare means of all groups (***p<0.001, **p<0.01, *p<0.05).

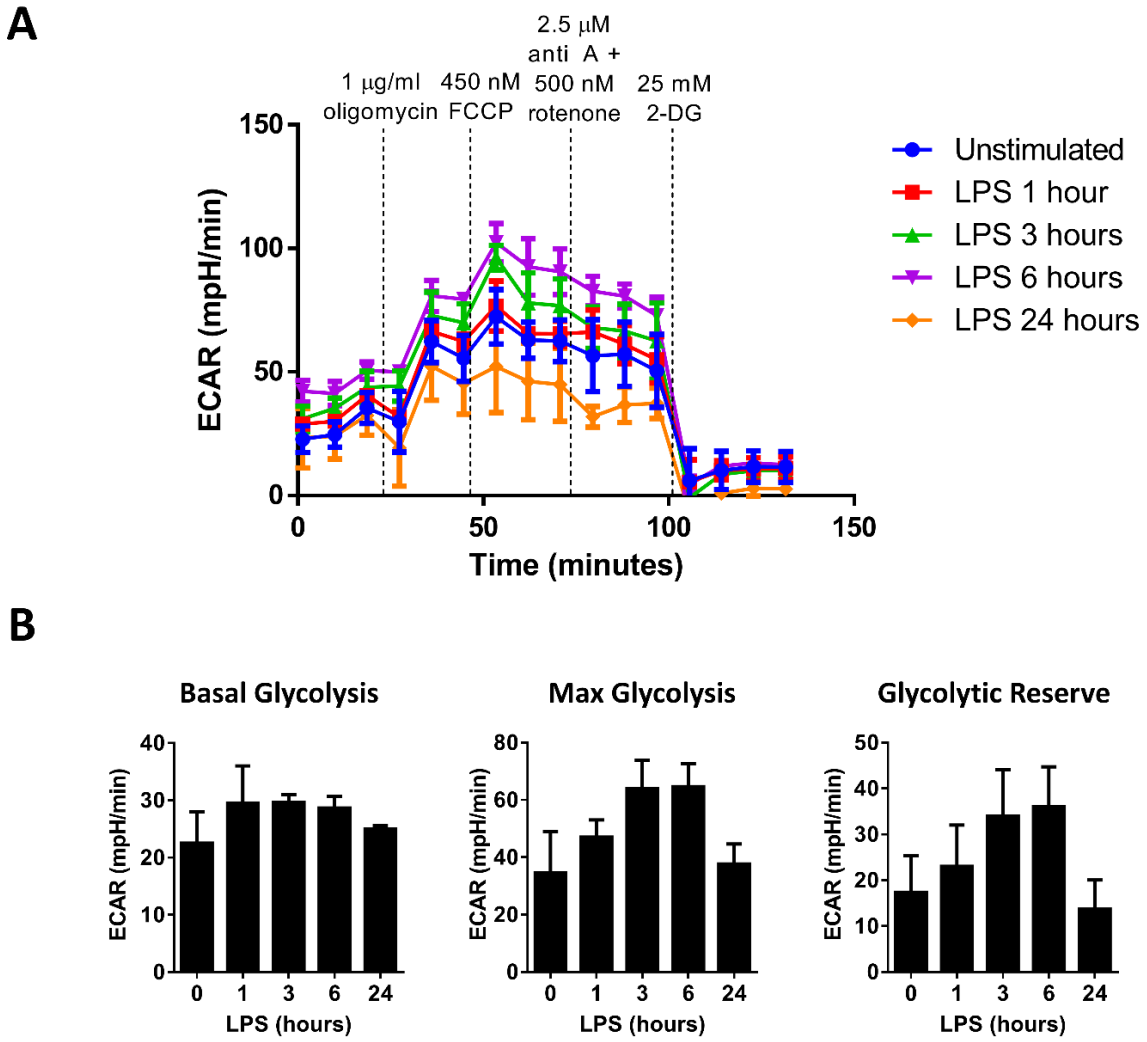

Figure 4.8. Human DC temporally increase glycolytic metabolism after LPS stimulation. Primary human DC (n=3) were stimulated with LPS (100 ng/ml) for 1, 3, 6 or 24 hours prior to placement in a Seahorse XF24 analyser. The extracellular acidification rate (ECAR) was measured before and after the addition of oligomycin (1 µg/ml), FCCP (450 nM), antimycin A (2.5 µM) and rotenone (500 nM), and 2-DG (25 mM). **(A)** ECAR measurements over time for each LPS stimulation time-point. Data depicts one representative experiment **(B)** Pooled data (n=3) depicting the calculated mean (± SEM) basal glycolytic rate, max glycolytic rate and glycolytic reserve for each LPS stimulation time-point.

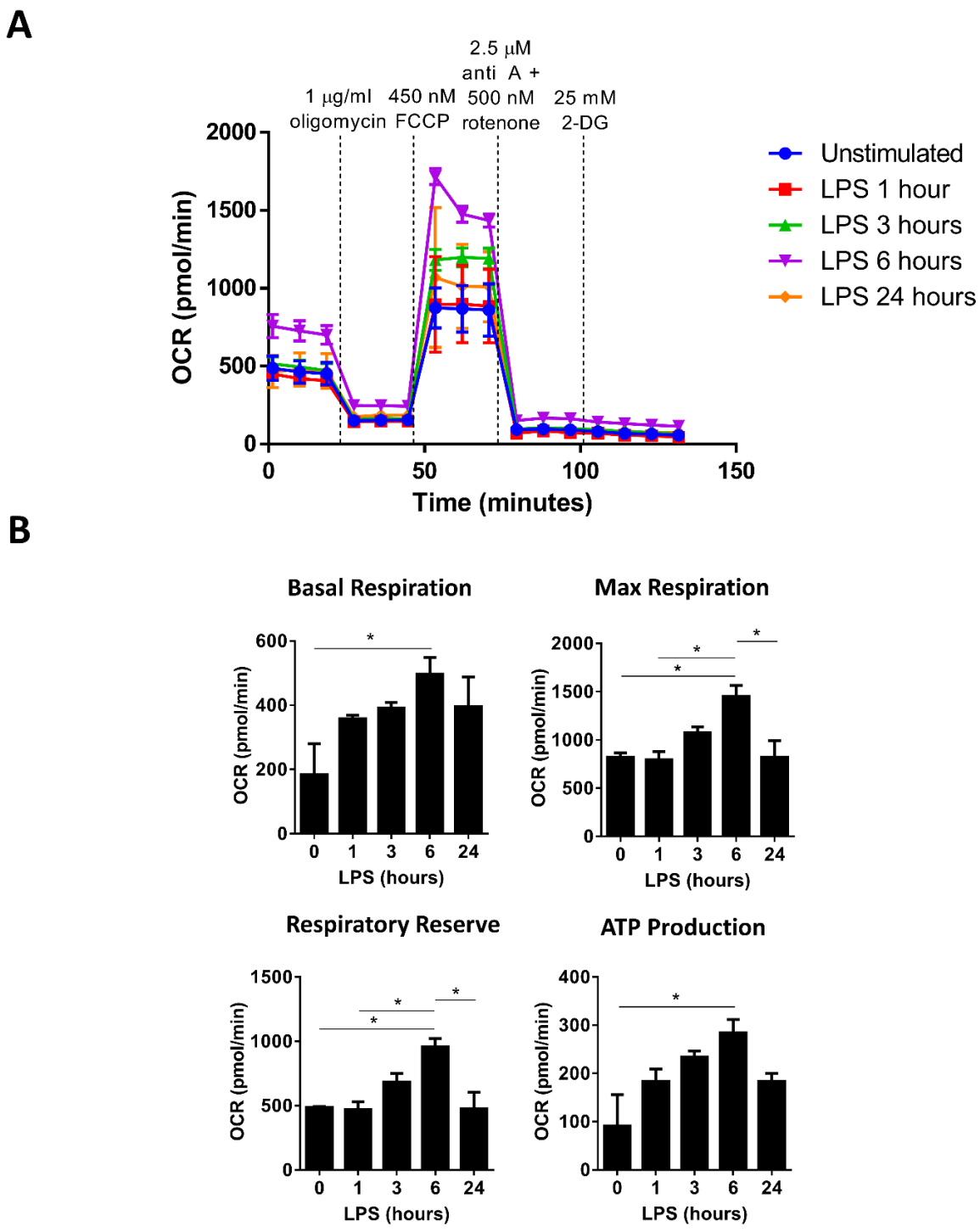

Figure 4.9. Determination of the increase in oxidative phosphorylation over time by LPS-stimulated human DC. Primary human DC (n=3) were stimulated with LPS (100 ng/ml) for 1, 3, 6 or 24 hours prior to placement in a Seahorse XF24 analyser. The oxygen consumption rate (OCR) was measured before and after the addition of oligomycin (1 µg/ml), FCCP (450 nM), antimycin A (2.5 µM) and rotenone (500 nM), and 2-DG (25 mM). **(A)** OCR measurements over time for each LPS stimulation time-point. Data depicts one representative experiment. **(B)** Pooled data (n=3) depicting the calculated mean (± SEM) basal respiratory rate, max respiratory rate, respiratory reserve and ATP production rate for each LPS stimulation time-point. Statistical significance was determined by one-way ANOVA with Tukey's multiple comparisons post hoc test to compare the means of all treatment groups (*p<0.05).

A

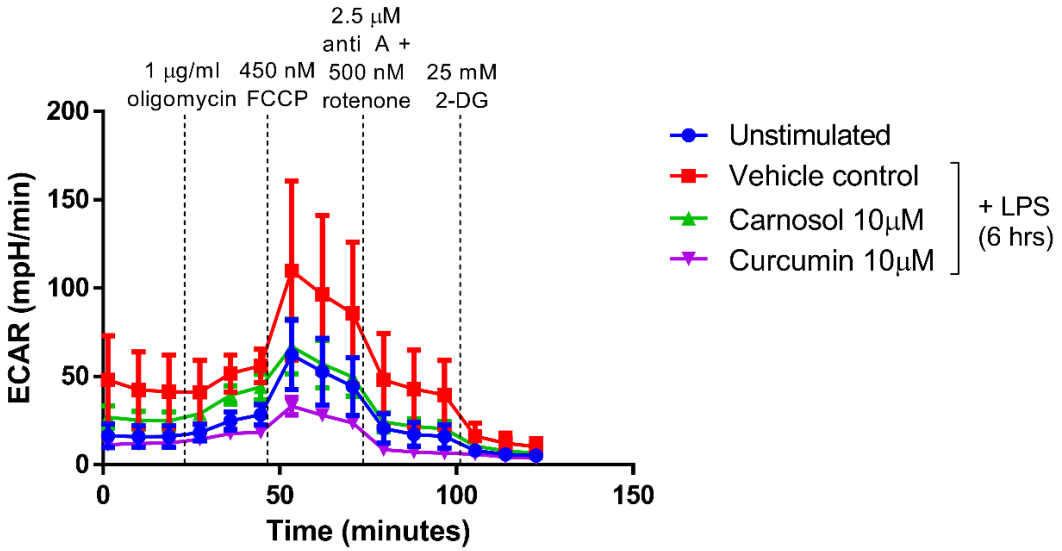
2.5 μM
anti A +
500 nM
rotenone
25 mM
2-DG
1 μg/ml
oligomycin
450 nM
FCCP
ECAR (mpH/min)
Time (minutes)
Unstimulated
Vehicle control
Carnosol 10μM
Curcumin 10μM
+ LPS
(6 hrs)

B

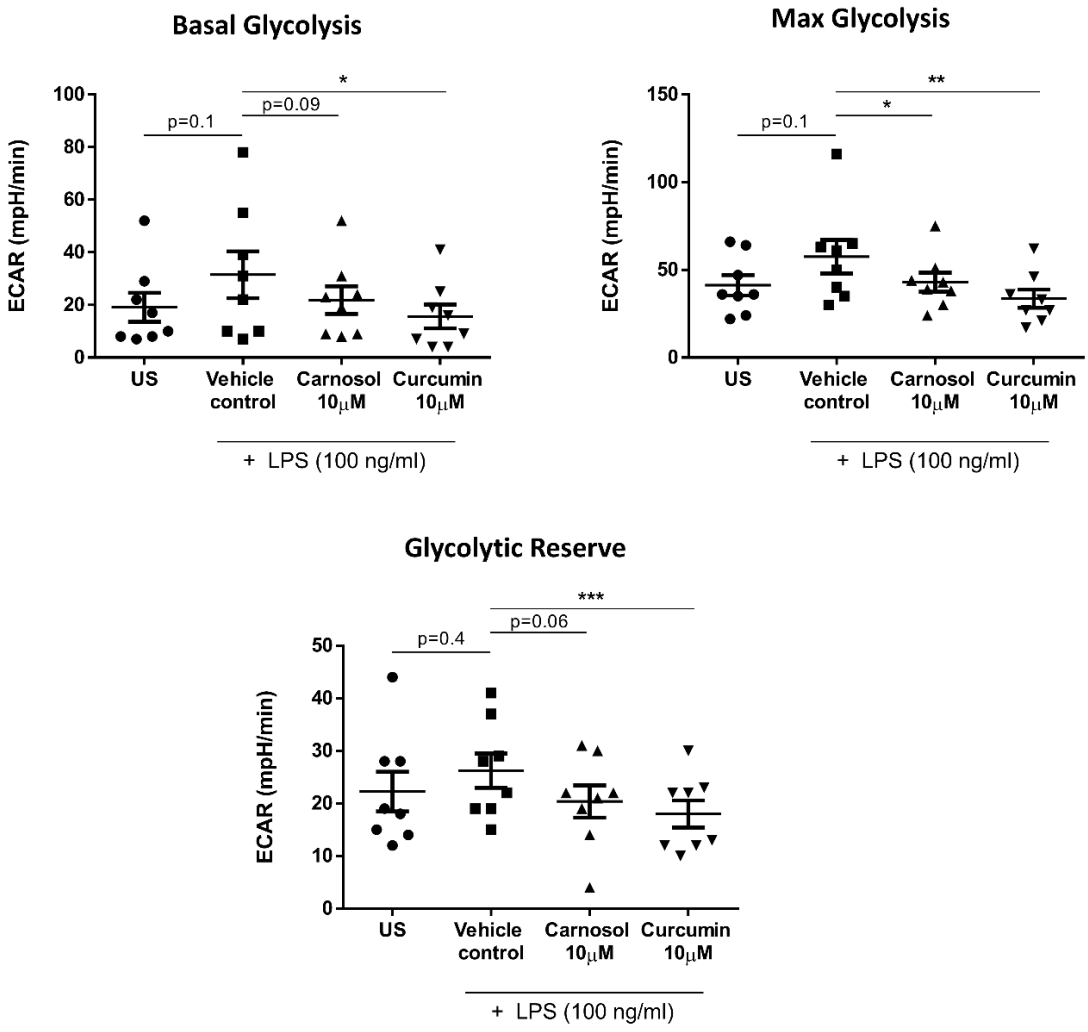
Basal Glycolysis
Max Glycolysis
Glycolytic Reserve
ECAR (mpH/min)
p=0.1
p=0.09
p=0.4
p=0.06
*
**
***
US
Vehicle control
Carnosol 10μM
Curcumin 10μM
+ LPS (100 ng/ml)

Figure 4.10. Carnosol- and curcumin-treated DC show a reduced induction of glycolysis in response to LPS stimulation. Primary human DC (n=8) were either left unstimulated (US), or treated with carnosol (10 μM), curcumin (10 μM) or a vehicle control for 6 hours, then stimulated with LPS (100 ng/ml) for 6 hours prior to placement in a Seahorse XF24e analyser. The extracellular acidification rate (ECAR) was measured before and after the addition of oligomycin (1 μg/ml), FCCP (450 nM), antimycin A (2.5 μM) and rotenone (500 nM), and 2-DG (25 mM). **(A)** ECAR measurements over time for each treatment group. Data depicts one representative experiment. **(B)** Pooled data (n=8) depicting the calculated mean (± SEM) basal glycolytic rate, max glycolytic rate and glycolytic reserve for each treatment group. Statistical significance was determined by one-way ANOVA with Dunnett's multiple comparisons post hoc test to compare treatment groups against the control group (***p<0.001, **p<0.01, *p<0.05).

A

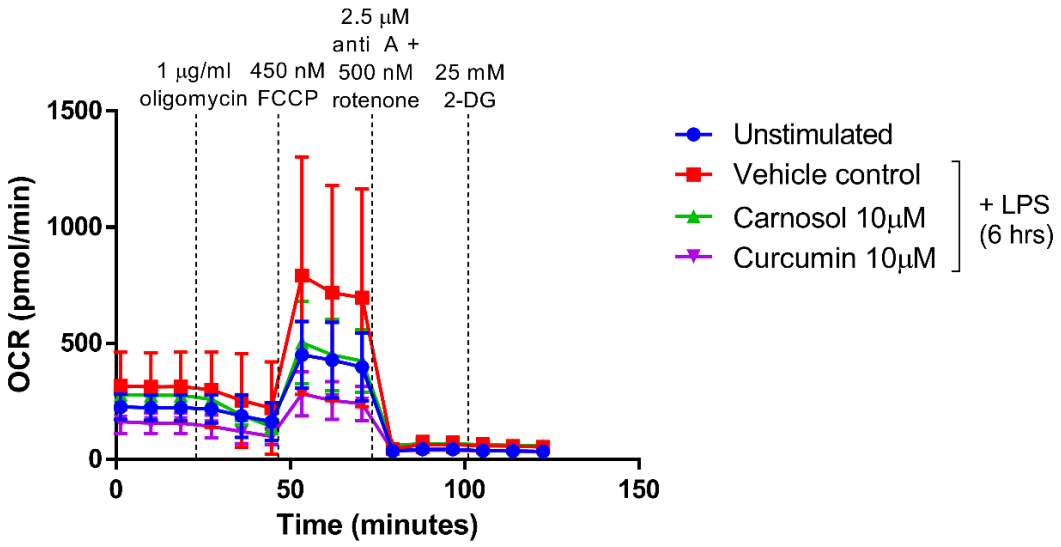
1 μg/ml oligomycin
450 nM FCCP
2.5 μM anti A + 500 nM rotenone
25 mM 2-DG
OCR (pmol/min)
Time (minutes)
Unstimulated
Vehicle control
Carnosol 10μM
Curcumin 10μM
+ LPS (6 hrs)

B

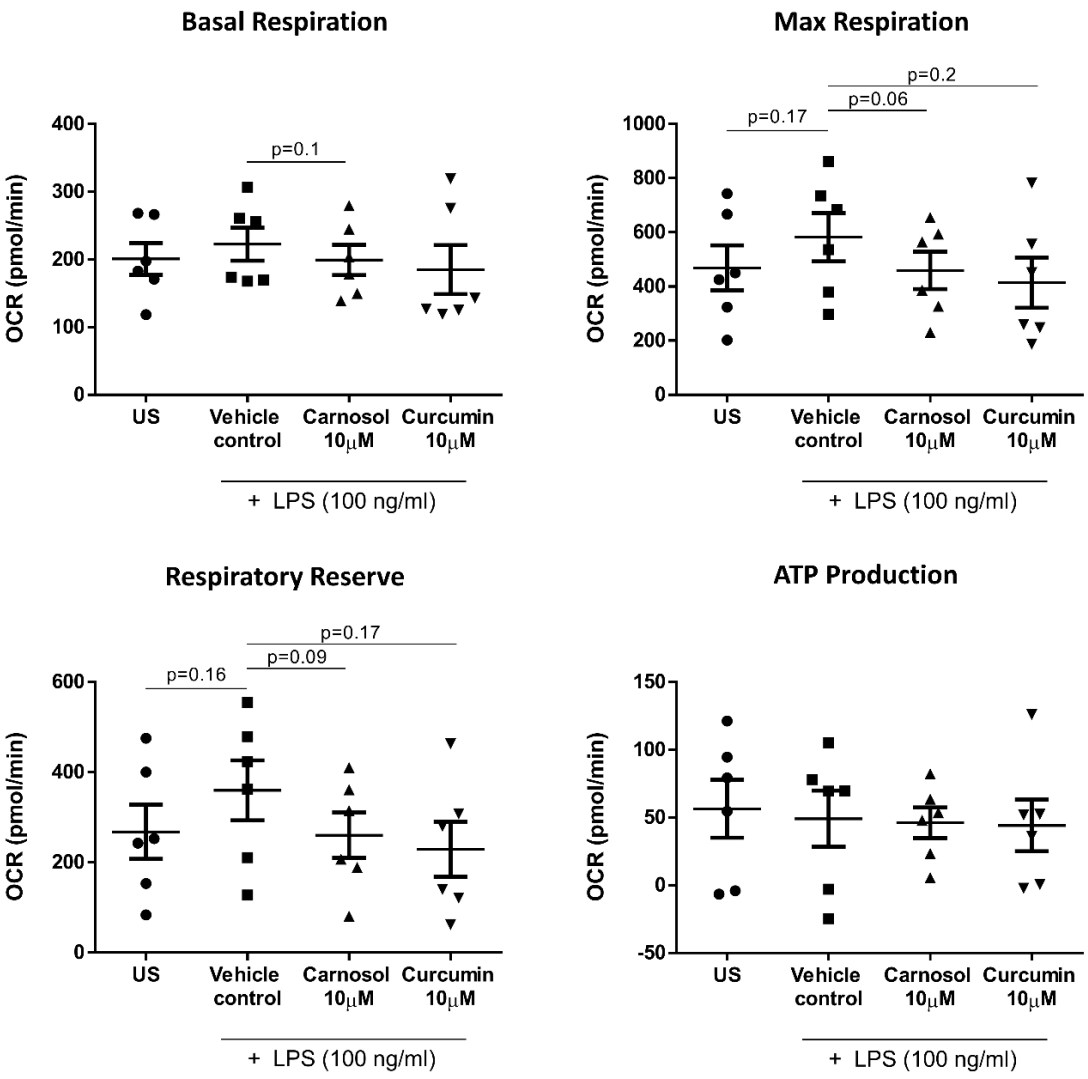
Basal Respiration
Max Respiration
Respiratory Reserve
ATP Production
OCR (pmol/min)
US
Vehicle control
Carnosol 10μM
Curcumin 10μM
+ LPS (100 ng/ml)
p=0.1
p=0.17
p=0.06
p=0.2
p=0.16
p=0.09
p=0.17

Figure 4.11. Carnosol and curcumin treatment reduces the spare respiratory capacity of LPS-stimulated DC. Primary human DC (n=6) were either left unstimulated (US), or treated with carnosol (10 μM), curcumin (10 μM) or a vehicle control for 6 hours, then stimulated with LPS (100 ng/ml) for 6 hours prior to placement in a Seahorse XF24e analyser. The oxygen consumption rate (OCR) was measured before and after the addition of oligomycin (1 μg/ml), FCCP (450 nM), antimycin A (2.5 μM) and rotenone (500 nM), and 2-DG (25 mM). **(A)** OCR measurements over time for each treatment group. Data depicts one representative experiment. **(B)** Pooled data (n=6) depicting the calculated mean (± SEM) basal respiratory rate, max respiratory rate, respiratory reserve and ATP production rate for each treatment group. Statistical significance was determined by one-way ANOVA with Dunnett's multiple comparisons post hoc test to compare treatment groups against the control group.

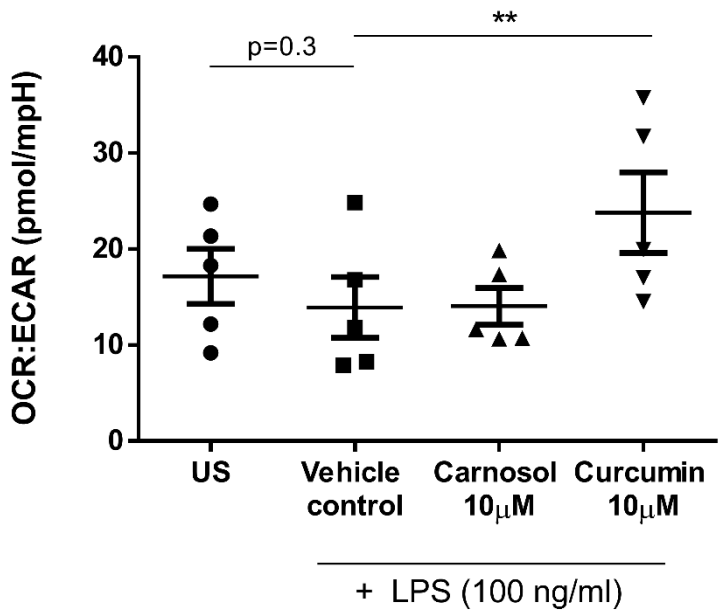

Figure 4.12. Curcumin treated DC favour oxidative phosphorylation over glycolysis. Primary human DC (n=5) either left unstimulated (US), or were treated with carnosol (10 μM), curcumin (10 μM) or a vehicle control for 6 hours, then stimulated with LPS (100 ng/ml) for 6 hours prior to placement in a Seahorse XF24e analyser. Basal rates of oxidative phosphorylation and glycolysis were measured by OCR and ECAR, respectively. Pooled data (n=5) depicting the calculated mean (± SEM) ratio of OCR:ECAR for each treatment group. Statistical significance was determined by one-way ANOVA with Dunnett's multiple comparisons post hoc test to compare treatment groups against the control group (**p<0.01).

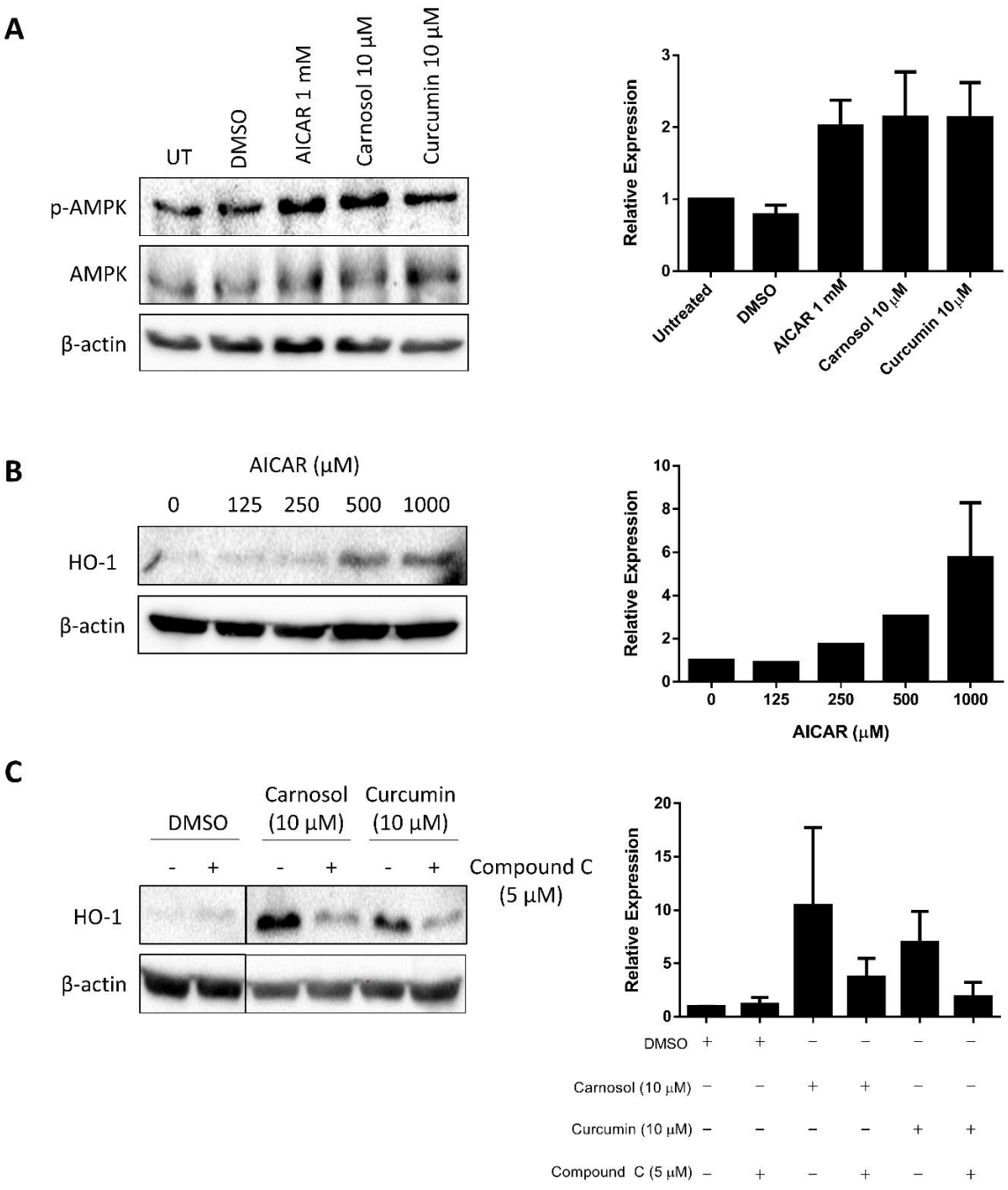

Figure 4.13. Activation of AMPK regulates the induction of HO-1 by carnosol and curcumin in human DC. (A) Primary human DC (n=7) were incubated with AICAR (1 mM), carnosol (10 μM), curcumin (10 μM), or a vehicle control for 1 hour. The activation of AMPK was measured by Western blot. **(B)** Primary human DC (n=3) were incubated with AICAR (125-1000 μM) for 24 hours. Expression of HO-1 was detected by Western blot. **(C)** Primary human DC (n=3) were incubated with compound C (5 μM) for 1 hour prior to treatment with carnosol (10 μM) or curcumin (10 μM), or a vehicle control for 24 hours. Expression of HO-1 was detected by Western blot. Dividing lines indicate where blots have been cropped; all bands shown are derived from the same blot. All blots depict an individual donor and are representative of 3-7 independent experiments. Densitometric analysis was performed using ImageLab (Bio-Rad) software (n=3-7).

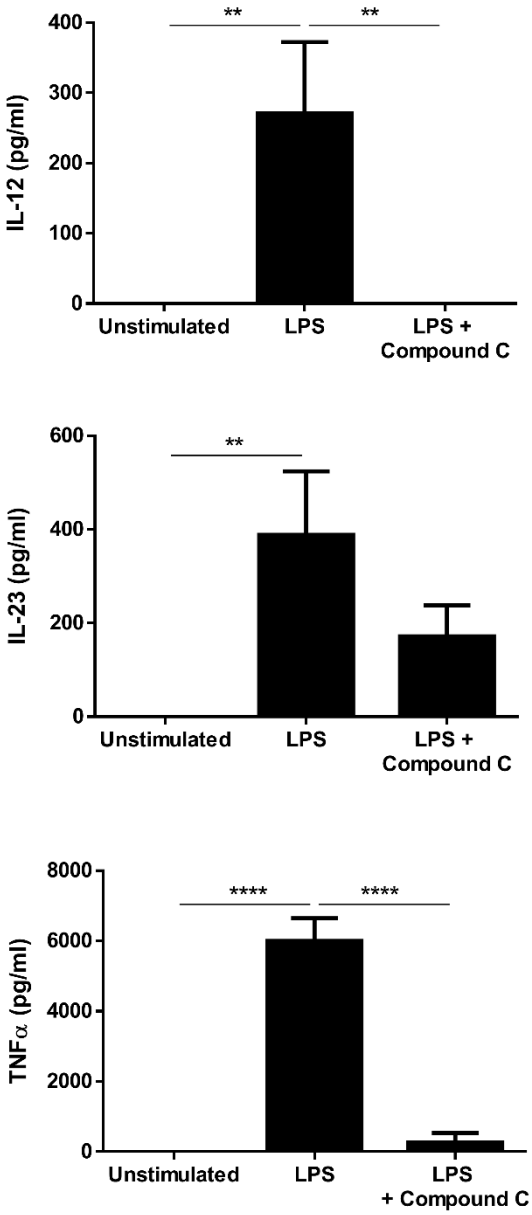

Figure 4.14. Compound C, an inhibitor of AMPK, inhibits cytokine production by human DC. Primary human DC (n=4) were treated with compound C (5 µM) for 6 hours prior to stimulation with LPS (100 ng/ml) for 24 hours. The concentration of IL-12p40, IL-23p19 and TNFα in cell culture supernatants was measured by ELISA. Results shown are mean (± SEM) of the pooled cytokine concentrations (means of two or three technical replicates per donor). Statistical significance was determined by one-way ANOVA, with Tukey's multiple comparisons post hoc test to compare means of all treatment groups (****p<0.0001, ** p<0.01).

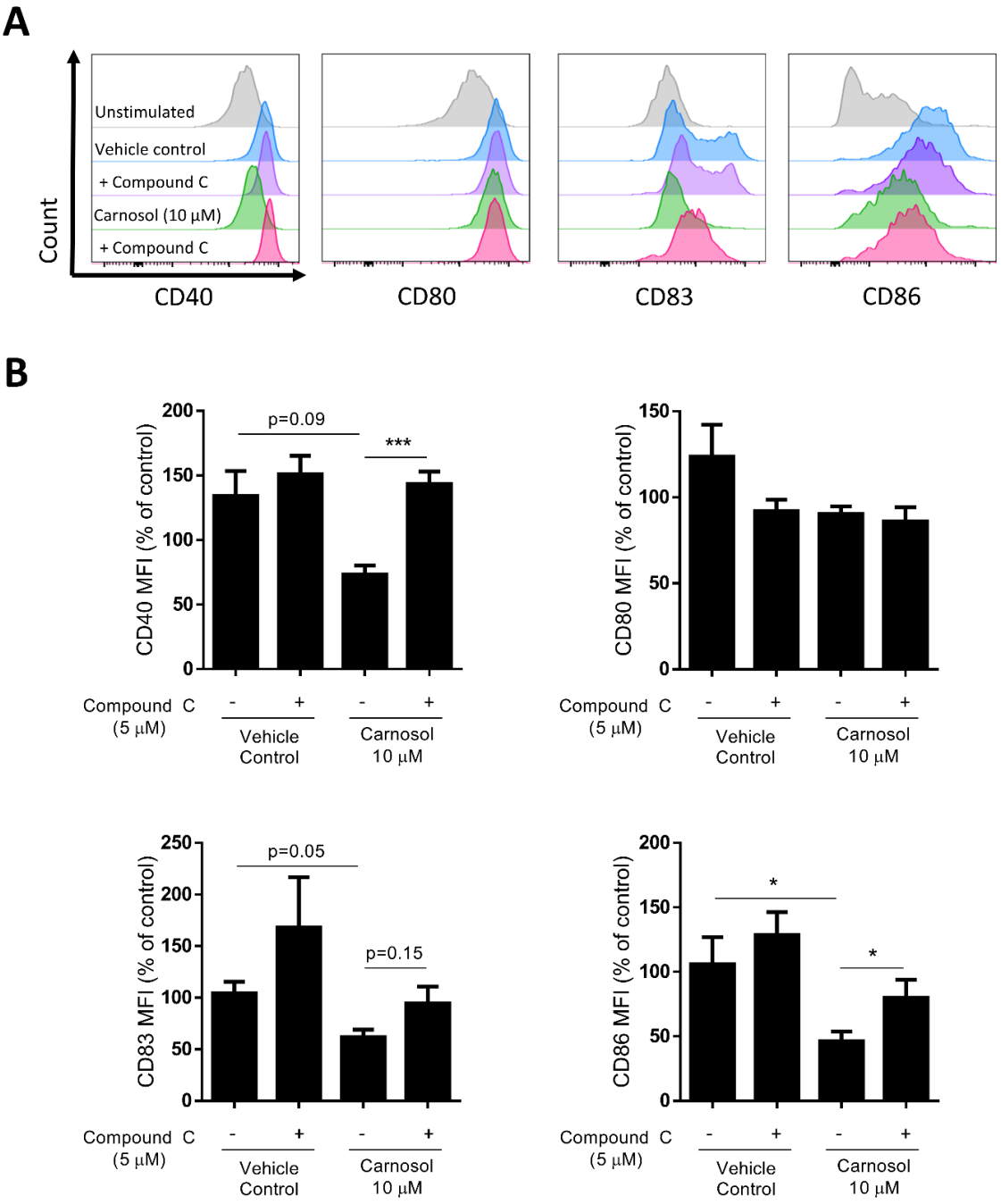

Figure 4.15. Inhibition of AMPK attenuates reduction of DC maturation markers by carnosol. Primary human DC (n=7) were incubated with or without compound C (5 µM) for 1 hour prior to treatment with carnosol (10 µM) or a vehicle control for 6 hours. DC were then stimulated with LPS (100 ng/ml) and expression of maturation markers was determined after 24 hours by flow cytometry. **(A)** Histograms depict expression of maturation markers by viable cells in carnosol-treated DC, with or without compound C, compared to controls from one representative experiment. **(B)** Pooled data (n=7) depicting expression of CD40, CD80, CD83 and CD86 in carnosol-treated DC, with or without compound C. Results shown are mean (± SEM) of the measured Mean Fluorescence Intensities (MFI), expressed as percentages of the vehicle control. Statistical significance was determined by one-way ANOVA, with Tukey's multiple comparisons post hoc test to compare the means of all groups (***p<0.001, *p<0.05).

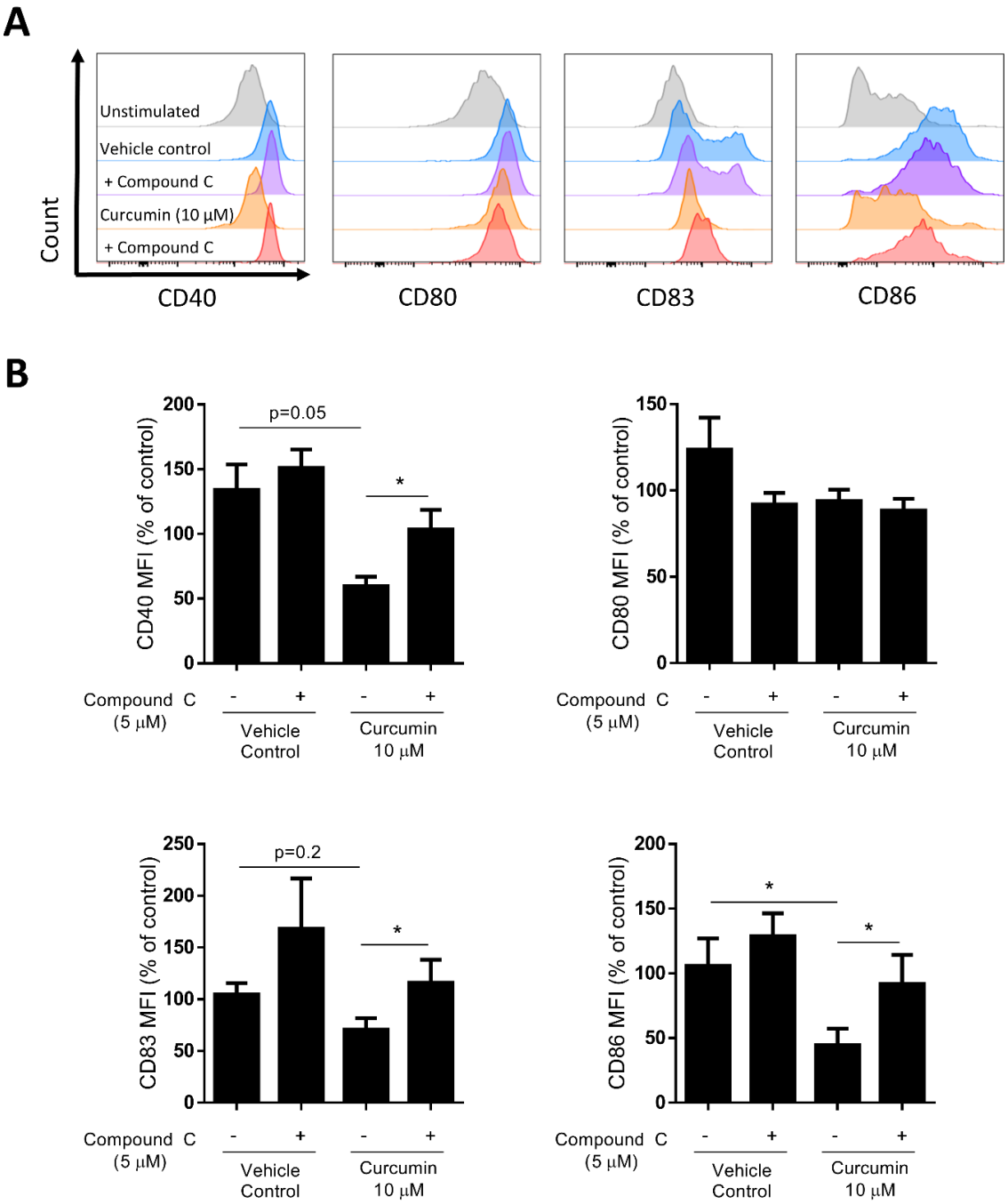

Figure 4.16. Inhibition of AMPK attenuates reduction of DC maturation markers by curcumin. Primary human DC (n=7) were incubated with or without compound C (5 µM) for 1 hour prior to treatment with curcumin (10 µM) or a vehicle control for 6 hours. DC were then stimulated with LPS (100 ng/ml) and expression of maturation markers was determined after 24 hours by flow cytometry. **(A)** Histograms depict expression of maturation markers by viable cells in curcumin-treated DC, with or without compound C, compared to controls from one representative experiment. **(B)** Pooled data (n=7) depicting expression of CD40, CD80, CD83 and CD86 in curcumin-treated DC, with or without compound C. Results shown are mean (± SEM) of the measured Mean Fluorescence Intensities (MFI), expressed as percentages of the vehicle control. Statistical significance was determined by one-way ANOVA, with Tukey's multiple comparisons post hoc test to compare the means of all groups (*p<0.05).

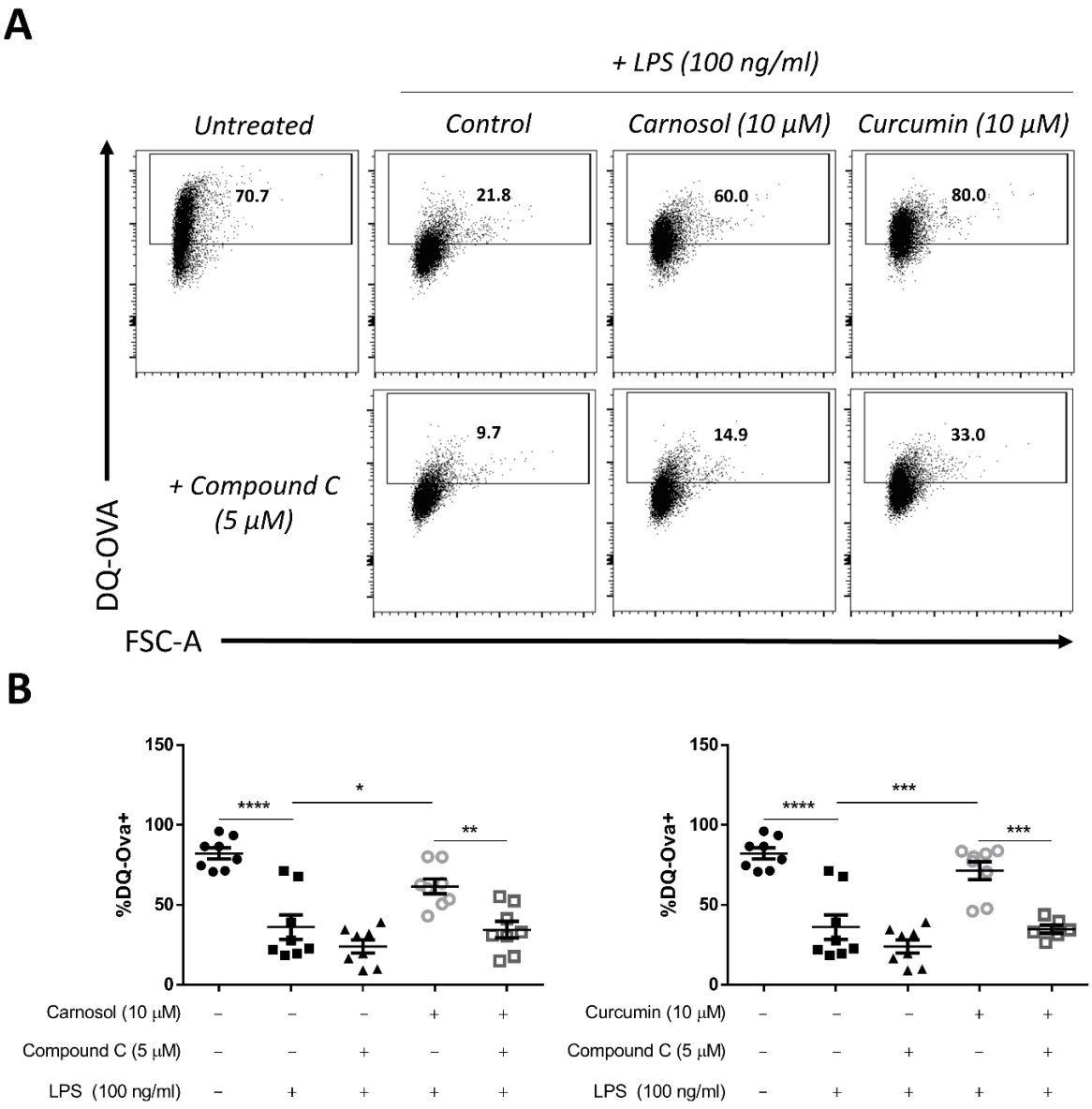

Figure 4.17. Inhibition of AMPK attenuates the increased phagocytic capacity of LPS-stimulated DC treated with carnosol or curcumin. Primary human DC (n=7) were incubated with or without compound C (5 μM) for 1 hour, then treated with carnosol (10 μM), curcumin (10 μM) or a vehicle control for 6 hours prior to stimulation with LPS (100 ng/ml) for 24 hours. DC were then incubated with DQ-Ovalbumin (DQ-Ova; 500 ng/ml) for 20 minutes prior to analysis by flow cytometry. **(A)** Representative dot plots depicting DQ-Ova uptake by DC (gated by forward and side scatter) treated with carnosol, curcumin and compound C from one representative experiment. **(B)** Pooled data (n=7) depicting percentage DQ-Ova uptake of DC treated with carnosol and curcumin, with or without compound C. Results shown are mean (± SEM) percentages of DQ-Ova uptake in control-, carnosol- and curcumin-treated DC, with or without compound C. Statistical significance was determined by one-way ANOVA, with Tukey's multiple comparisons post hoc test to compare means of all groups (****p<0.0001, ***p<0.001, **p<0.01, *p<0.05).

4.4 Discussion

Historically, cellular metabolism has been largely overlooked in the study of immunology, often dismissed as simple energy bookkeeping with little significance outside the context of metabolic diseases such as diabetes and obesity. However, in recent years, interest in the metabolism of immune cells has exploded, as the intricacies between metabolic signalling and immunological function have started to be revealed. It is now acknowledged that immune cells can be characterised by their use of distinct metabolic programs which support their specific bio-energetic requirements. Furthermore, the development, differentiation and maturation of immune cells is frequently dependent on accompanying changes to their metabolism, while cross-talk between metabolic and immunologic signalling pathways allows for the coordination of immune function and cellular metabolism. Due to the relative infancy of the field, much of the current understanding of immunometabolism is grounded in seminal studies performed in mice; it is now important that these studies are extended to human immune cells in order to expand our knowledge of human immune function during homeostasis and disease. Additionally, the relationships between known immunomodulators, such as HO-1, and immunometabolism remain a largely unexplored area of research, which could potentially yield new strategies to restore immune balance via metabolic reprogramming. Therefore, the purpose of the work described in this chapter was to explore the metabolism of activated human T cells and DC, and the metabolic effects of the HO-1 inducers carnosol and curcumin in these cells.

T cell activation is accompanied by extensive proliferation and differentiation that requires significantly increased biosynthesis and energy production. Although upregulation of aerobic glycolysis is characteristic of certain effector T cell subsets, and is important for T cell cytokine production (127,129), upregulation of oxidative phosphorylation has also been shown to be required for the activation of murine T cells (394,395). Consistent with this, in the present study activation of human PBMC with anti-CD3 was observed to result in greatly increased rates of both glycolysis and oxidative phosphorylation. This is in agreement with a previous study by Renner *et al.*, who reported that activated human $CD4^+$ and $CD8^+$ T cells display increased glucose and oxygen consumption (139). However, as expected, the ratio of oxidative phosphorylation to glycolysis usage remained higher in unstimulated PBMC compared to anti-CD3 stimulated PBMC. The increased SRC of activated T cells was supported by a significant increase in mitochondrial mass; this observation is in agreement with previous studies which have demonstrated that mitochondrial biogenesis is upregulated upon activation in murine T cells (389–391). Therefore, these results indicate that, similar to murine T cells, human T cells also upregulate metabolic machinery and display elevated metabolic activity compared to resting T cells. This is the first

study to report this effect in human PBMC, through direct measurement of glycolysis and oxidative phosphorylation using Seahorse analysis. Further research is required to establish whether different human T cell subsets display distinct metabolic profiles, as has previously been demonstrated in murine systems.

Modulation of T cell metabolism has been suggested as a potential strategy to limit harmful pro-inflammatory immune responses (396). However, there have been no studies to date investigating the effects of HO-1 inducers on T cell metabolism. In this study, the polyphenols carnosol and curcumin were confirmed as non-toxic and capable of inducing HO-1 in human PBMC, therefore, their effects on T cell metabolism were assessed. Treatment of PBMC with either carnosol or curcumin attenuated the upregulation of both glycolysis and oxidative phosphorylation seen after stimulation with anti-CD3. The quiescent metabolism of carnosol- and curcumin-treated PBMC appears to reflect that previously observed in anergic T cells, which display a failure to upregulate the metabolic machinery necessary for activation. However, inhibition of metabolic signalling in T cells was also found to be sufficient to induce anergy (371). Interestingly, curcumin has previously been reported to inhibit Ca^{2+} mobilisation and the translocation of nuclear factor of activated T cells (NFAT), an important transcription factor which mediates T cell activation, after TCR stimulation (397). Therefore, it remains to be elucidated whether the effects of these polyphenols on T cell metabolism are a result of regulation of metabolic signalling by carnosol or curcumin, or rather inhibition of T cell activation upstream of the engagement of metabolic pathways. Additionally, the effects of carnosol and curcumin on the metabolism of specific T cell subsets was not assessed in this study; it would be of interest to determine whether the inhibition of T cell metabolism by these polyphenols suppresses the function of certain T cell subsets over others, particularly in the case of Th17 cells and Tregs whose differentiation has previously been described to be regulated via metabolic signalling (372–374).

In support of the observed reduction of metabolic activity in carnosol- and curcumin-treated PBMC, both polyphenols also significantly inhibited the expansion of mitochondria in activated PBMC. Although AMPK has well-defined roles in mitochondrial biogenesis (398,399), it has been reported that the increased mitochondrial biogenesis observed in activated T cells is at least partially dependent on mTOR signalling, and that inhibition of AMPK actually results in heightened, uncoordinated mitochondrial proliferation (390). Furthermore, activation of AMPK with AICAR has been reported to induce T cell anergy via inhibition of mTOR (371), and AMPK-deficient T cells display elevated levels of glycolysis (400). As carnosol and curcumin were observed to activate AMPK in human DC, it is possible that increased AMPK activity could limit mTOR signalling in T cells, accounting for the inhibition of mitochondrial biogenesis, and reduced

metabolic activity of carnosol- and curcumin-treated PBMC. It will be interesting to determine if carnosol and/or curcumin themselves can inhibit mTOR. Conversely, AMPK has also been reported to promote the metabolic plasticity required for primary T cell responses *in vivo* (401), and TCR stimulation activates AMPK in murine and human T cells, yet without concomitant inhibition of mTOR (371,402). Therefore, future research should determine if carnosol and curcumin activate AMPK in human PBMC, and whether AMPK signalling mediates the metabolic effects of these compounds in human T cells. Additionally, although carnosol and curcumin were both found to increase expression of HO-1 in human PBMC, the contribution of HO-1 to their observed inhibition of T cell metabolism remains to be elucidated. HO-1 and its product CO have previously been reported to modulate T cell function (184–186), and it is possible that regulation of T cell metabolism is a potential mechanism for these effects. However, it is currently thought that the modulation of T cell responses by HO-1 is primarily mediated by its activity in APCs (180,187,188), therefore the observed inhibition of T cell metabolism by carnosol and curcumin may be a result of HO-1 induction in the APCs which provide co-stimulation to T cells within PBMC, thereby limiting T cell activation. Further research is required to establish the role of HO-1 in the metabolic effects of carnosol and curcumin in PBMC, and to determine whether they are a result of direct action on T cells, or via modulation of APCs.

Although there are a number of studies which have investigated the metabolism of murine DC, studies which have focused on human DC metabolism are comparatively scarce; therefore, this chapter also aimed to characterise the metabolic changes in human DC after stimulation with LPS. LPS-stimulated BMDC have previously been observed to strongly upregulate aerobic glycolysis, and simultaneously downregulate oxidative phosphorylation via the action of iNOS-derived NO (120–122,132). The results presented here demonstrate that human DC stimulated with LPS upregulate both glycolysis and oxidative phosphorylation within hours of activation. Furthermore, a transient increase in the glycolytic reserve and SRC of human DC was observed within 6 hours post-LPS stimulation, which was absent at 24 hours post-LPS. Therefore, it can be ascertained that while human DC also display increased glycolytic metabolism after activation, unlike BMDC, they also upregulate oxidative phosphorylation. This disparity between murine and human DC is likely a result of their differing expression of iNOS, as human monocyte-derived DC do not readily express iNOS; however, some evidence suggests that certain human DC subsets can express iNOS *in vivo*, therefore the metabolic profile of these DC may differ from what is observed *in vitro* (403). Consistent with the results presented in this chapter, Malinarich *et al.* recently reported that human DC matured with LPS are more glycolytic than immature DC, and do not downregulate oxidative phosphorylation (138). However, they also observed a reduced glycolytic reserve and

SRC in mature compared to immature DC; a finding which, in fact, agrees with these results, as the metabolism of DC was assessed 24 hours after maturation with LPS, by which time the increased glycolytic reserve and SRC observed in this study was absent. Interestingly, Everts *et al*. also observed an increase in the SRC of murine DC stimulated with LPS for 1 hour, which was mediated by enhanced glycolytic flux into the TCA cycle (122). This increased flow of pyruvate into the TCA cycle was found to produce citrate necessary for *de novo* fatty acid synthesis in the maturing DC, providing lipids required to expand the ER and Golgi membranes in anticipation of increased protein production (122). Therefore, the transient increase in the glycolytic reserve and SRC of LPS-stimulated DC observed in this study may represent an early adaption of maturing DC to their new immunogenic functions, which is downregulated once adequate cellular remodelling has taken place. Meanwhile, the mature DC continues to display higher basal rates of glycolysis and oxidative phosphorylation to meet its increased energy demands. In summary, this study expands the current understanding of human DC metabolism, and also underscores the importance of accounting for temporal changes when analysing the metabolism of immune cells.

The results of this chapter support previous data which described the anti-inflammatory properties of carnosol and curcumin in human DC. The upregulation of glycolysis by DC in response to LPS has been demonstrated to promote their maturation, cytokine production and activation of T cells (120–122). Interestingly, DC treated with carnosol or curcumin displayed a reduced basal rate of glycolysis, and failed to upregulate their glycolytic reserve after 6 hours of LPS stimulation. This reduced glycolytic flux was also manifest in the mitochondrial activity of carnosol- and curcumin-treated DC, as both polyphenols inhibited the increased SRC seen in response to LPS. Malinarich *et al.* previously reported that tolerogenic human DC possess a greater capacity for oxidative phosphorylation and fatty acid oxidation, and are less glycolytic than mature DC (138). Previously, carnosol and curcumin were observed to promote tolerogenic DC, and in support of this, curcumin-treated DC were found to preferentially utilise oxidative phosphorylation over glycolysis. Therefore, it is possible that the anti-inflammatory effects of carnosol and curcumin in human DC are at least partly mediated by their inhibition of glycolysis, resulting in a diminished glycolytic reserve and SRC and failure to meet the bio-energetic requirements of maturation. It would be of additional interest in future research to determine whether carnosol or curcumin treatment promotes fatty acid oxidation in DC. As was the case in PBMC, the contribution of either AMPK activation or HO-1 upregulation by carnosol and curcumin to their metabolic effects in DC remains unclear. Krawczyk *et al.* previously reported that AMPK signalling antagonises the maturation of BMDC and inhibits their upregulation of glycolysis in response to LPS (120), while Carroll *et al.* found that AMPK-deficient BMDC display enhanced maturation and pro-

inflammatory functions (123). Therefore, the observed activation of AMPK by carnosol and curcumin could explain their modulation of the metabolic and immunological function of human DC. Further work is required to investigate if inhibition of either AMPK or HO-1 attenuates the effects of carnosol and curcumin on DC metabolism.

Although the HO-1 inducers carnosol and curcumin were found to limit the metabolic reprogramming of human DC in response to LPS, it was not determined whether this effect was a result of HO-1 activity. However, a relationship between metabolic signalling and the upregulation of HO-1 in DC by these polyphenols was uncovered in the course of this study. Signalling via AMPK has previously been implicated in the upregulation of HO-1 by certain drugs (392,393,404), but there have been no such reports in human immune cells. Furthermore, both carnosol and curcumin have been reported to activate AMPK in skeletal muscle and cancer cell lines (405–408). In this study, carnosol and curcumin were both found to activate AMPK in human DC. Moreover, AMPK activation was found to upregulate expression of HO-1 in human DC, and inhibition of AMPK attenuated the induction of HO-1 by carnosol and curcumin. This study is therefore the first to report an association between AMPK signalling and HO-1 expression in human DC, and that the upregulation of HO-1 by carnosol and curcumin is at least partially dependent on their activation of AMPK. Interestingly, a number of xenobiotics, including various polyphenols, have been reported to activate AMPK via an increase in the AMP:ATP ratio; this is achieved by inhibition of the mitochondrial ETC complexes (398). Curcumin, in particular, has been shown to inhibit ATP synthase in mitochondrial preparations, thereby limiting ATP production and increasing the ratio of AMP to ATP (409). Given that a number of polyphenols also appear to inhibit ATP synthase or complex I (410,411), it is likely that carnosol acts in a similar fashion. Therefore, elevation of AMP levels represents a probable mechanism by which carnosol and curcumin activate AMPK in human DC, however, further research is required to confirm this.

Finally, the results of this chapter demonstrate that AMPK activation by carnosol and curcumin is required to mediate their immunomodulatory effects in human DC. Pharmacological inhibition of AMPK was found to reverse the observed reduction of DC maturation by these polyphenols; the addition of compound C to carnosol- and curcumin-treated DC significantly increased their expression of surface markers, and reduced their antigen uptake capacity. The inhibition of DC maturation by carnosol and curcumin was previously found to be dependent on the activity of HO-1, and inhibition of AMPK was observed to reduce the upregulation of HO-1 by both polyphenols. Taken together, these results suggest that the AMPK-dependent immunomodulatory effects of carnosol and curcumin in human DC are mediated by its upregulation of HO-1 in these cells. Mechanistically, the upregulation of HO-1 by AMPK appears to be transcriptionally regulated as a

number of studies have identified cross-talk between AMPK and Nrf2, the major transcription factor in control of HO-1 expression (393,404,412). Phosphorylation of Nrf2 at its serine 550, resulting in increased nuclear accumulation of the transcription factor, has been proposed by Joo *et al.* as a potential mechanism by which AMPK regulates Nrf2 activity (413). Interestingly, Nrf2 activation may contribute to the role of AMPK in mitochondrial biogenesis and metabolism: Nrf2 has been associated with improved efficiency of oxidative phosphorylation and ATP production, enhanced fatty acid oxidation, and reduced mitochondrial ROS (414). PGC1α, the AMPK-regulated transcription factor which promotes mitochondrial biogenesis, has been shown to activate Nrf2 and upregulate genes involved in redox homeostasis, presumably to counteract the ROS produced as a result of increased mitochondrial activity (415,416). Furthermore, both Nrf2 itself and HO-1-derived CO can also promote mitochondrial biogenesis, therefore, Nrf2 activation by PGC1α serves to both support its expansion of mitochondria, and also protect against oxidative stress (417,418). The role of AMPK in the antioxidant response was also demonstrated by Zmijewski *et al.* who found that exposure to the pro-oxidant hydrogen peroxide activated AMPK independently of the cellular AMP:ATP ratio (419). Together, the AMPK-PGC1α-Nrf2-HO-1 axis appears to integrate mitochondrial biogenesis and function with redox homeostasis, ensuring that the increased ROS produced by oxidative metabolism is compensated by increased antioxidant activity. The results of this study add to this paradigm by suggesting that signalling between AMPK and HO-1 also coordinates catabolic metabolism with tolerogenic immune responses in human DC. Additionally, this study indicates that the previously observed anti-inflammatory effects of AMPK in BMDC could be mediated by increased HO-1 expression (120,123). It will be of interest to further explore the relationships between AMPK, HO-1 and the metabolism and function of DC in the future.

In conclusion, the results of this chapter describe the metabolic changes arising from the activation of human PBMC and DC, and characterise a hitherto-unidentified role for the HO-1 system in immunometabolism. Furthermore, this study provides evidence that the polyphenols carnosol and curcumin may be useful as modulators of cellular metabolism, however, further research is required to determine how they regulate metabolic activity. The data presented here supports a model whereby activation of AMPK by carnosol and curcumin leads to the upregulation of HO-1, which mediates the downstream immunomodulatory activity of these polyphenols in human DC (Figure 4.18). These results are also suggestive that the anti-inflammatory phenotype characteristic of immune cells with higher catabolic metabolism and AMPK signalling may arise from increased expression of HO-1; this possibility is an interesting area for future research.

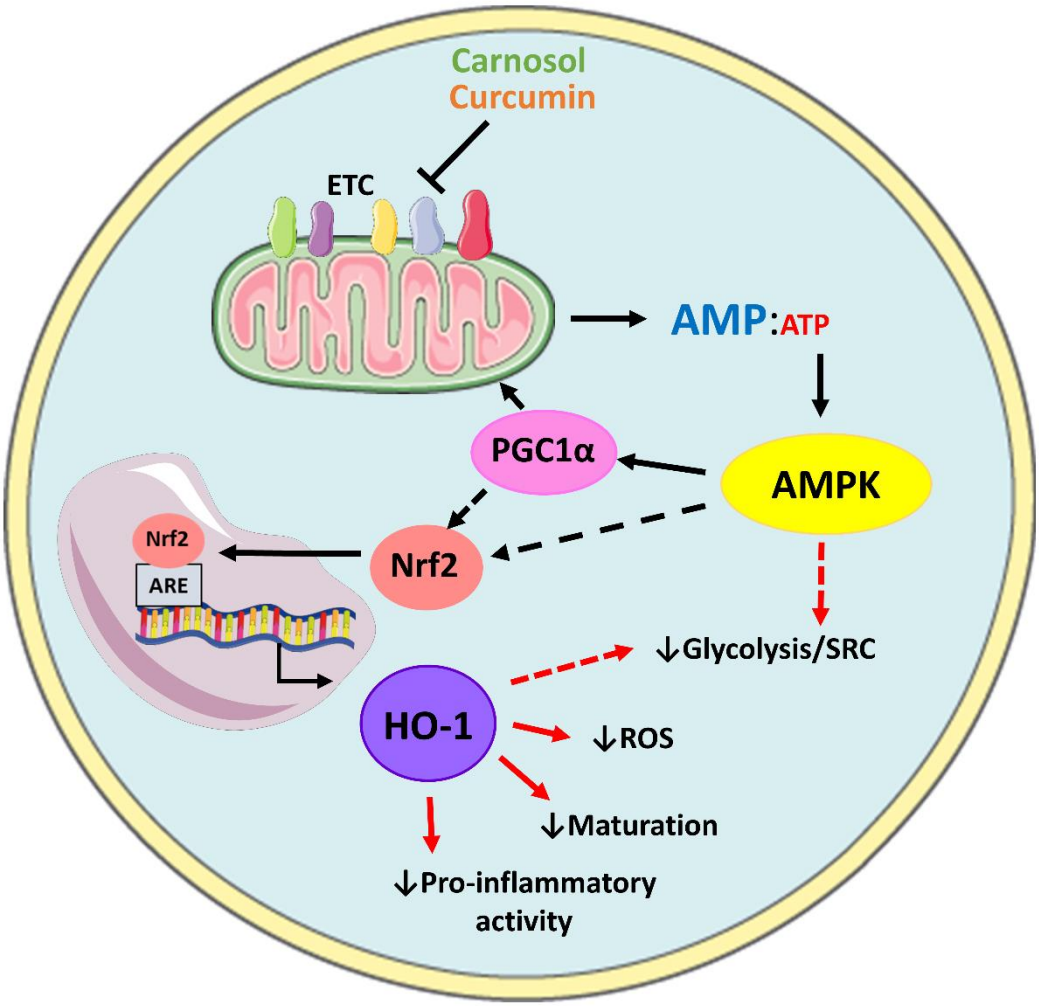

Figure 4.18. Model of AMPK-dependent induction of HO-1 by carnosol and curcumin in DC. Carnosol and curcumin are polyphenols which have been shown to inhibit components of the ETC, resulting in reduced ATP production and elevated AMP levels. AMP activates AMPK, which results in downstream activation of PGC1α and Nrf2. PGC1α promotes mitochondrial biogenesis and may also activate Nrf2 (black dashed arrows). Nrf2 translocates to the nucleus and induces transcription of HO-1. HO-1 and its products can then act as an antioxidant to neutralise ROS produced by mitochondrial metabolism, and downregulate DC maturation and pro-inflammatory functions. Additionally, AMPK or HO-1 may mediate the reduced rate of glycolysis and SRC observed in carnosol- and curcumin-treated DC (red dashed arrows).

Chapter 5:
Regulation of the adaptive immune response and psoriatic inflammation by carnosol and curcumin

5.1 Introduction

Autoimmunity occurs when dysregulated pro-inflammatory immune responses are mounted against the host's own tissues. This can be initiated by DC, which become inappropriately activated and present self-antigens alongside co-stimulatory signals to autoreactive T cells, resulting in their activation and expansion (39). It is the autoreactive T cells which cause the damaging inflammation characteristic of autoimmune diseases, through the production of potent pro-inflammatory cytokines such as IFNγ and IL-17. These cytokines trigger the recruitment and activation of other immune cells, as well as initiating the production of cytokines and chemokines by non-haematopoietic cells, creating an inflammatory loop which sustains and amplifies destructive inflammation within the affected tissue(s) (420,421). Thus, while targeting DC can prevent the activation of autoreactive T cells, inhibition of T cell proliferation and cytokine production, and promotion of regulatory T cells, is also an effective strategy in the treatment of autoimmune disease.

The regulatory role of HO-1 in innate immune cells such as DC is well established, however its function in the adaptive immune system is less certain. Some evidence exists to suggest that HO-1 can exert anti-inflammatory effects directly in T cells. Pae *et al.* first reported that $CD4^+CD25^+$ Tregs constitutively express HO-1, and that CD28 stimulation upregulates HO-1 expression in both $CD4^+CD25^+$ and $CD4^+CD25^-$ T cells. Furthermore, they found that overexpression of HO-1 prevented the proliferation of Jurkat T cells (183). This was supported by Choi *et al.* who found that upregulation of Foxp3 in Jurkat T cells induced expression of HO-1, which was required for their suppressive function (422), and Xia *et al.* who reported that HO-1 promoted expression of Foxp3, and the Treg-associated cytokines IL-10 and TGF-β, in murine splenocytes (423). Additionally, Zhang *et al.* found that treatment of naïve murine T cells with hemin, a HO-1 inducer, inhibited their proliferation and differentiation into Th17 cells (424). Suppressive effects for the HO-1 products BV and CO have also been described within T cell populations (184,185,318,425). Conversely, Zelenay *et al.* and Biburger *et al.* have reported that HO-1 expression is dispensable for the suppressive function of murine and human Tregs (187,426), and others have suggested that the anti-inflammatory effects of HO-1 in T cells are mediated by its activity in APCs rather than T cells themselves (180,186,188,189). Interestingly, HO-1 expression/activity has been reported to ameliorate the Th17/Treg imbalance in various murine models of T cell-mediated disease (232,360,427,428). Whether this is achieved via HO-1 activity in APCs or T cells remains unclear, however, there clearly exists a solid rationale for the use of HO-1 inducers as modulators of T cell responses.

Similarly to other HO-1 inducers, investigation into the effects of the polyphenols, carnosol and curcumin, in adaptive immune cells has been limited. Kliem *et al.* previously reported that curcumin can inhibit the activation of and cytokine production by T cells via inhibition of intracellular Ca^{2+} mobilisation after TCR stimulation, resulting in reduced nuclear translocation of NFAT (397). This was supported by Kim *et al.* who found that treatment of human $CD4^{+}$ T cells with curcumin limited their activation, proliferation and production of pro-inflammatory cytokines. Furthermore, they found that curcumin treatment increased the frequency of Tregs at later stages of culture, in a manner partially dependent on TGF-β (283). Interestingly, curcumin treatment was also observed to improve the ratio of Th17 cells to Tregs in a murine model of graft-versus-host disease (282), and in *ex vivo* T cells from SLE patients (429). There is, therefore, some evidence to support the use of curcumin to inhibit pro-inflammatory T cell responses, although further research into its activity in human cells is warranted. Comparatively, there are no studies to date investigating the effects of carnosol in T cells.

Psoriasis is an autoimmune disease characterised by extensive infiltration of immune cells into the skin and excessive proliferation of keratinocytes, resulting in the formation of red, scaly plaques associated with considerable pruritus and pain (251). Therefore, successful treatment of psoriasis requires that the activation of both infiltrating immune cells and local skin cells be halted; often inhibition of the immune response in psoriasis is sufficient to resolve the hyperproliferation of keratinocytes, as this appears to be caused by the action of Th17 cell cytokines including IL-17 and IL-22 (62,64,430). Interestingly, treatment of keratinocytes with HO-1 inducers *in vitro* has been reported to protect them from oxidative damage, and also limit their proliferation and production of cytokines (169,431,432). These studies are supported by animal models of psoriasis which have identified anti-psoriatic activity for HO-1 in keratinocytes and DC. Both Ma *et al.* and Zhang *et al.* observed that treatment with HO-1 inducers reduced epidermal hyperplasia in psoriaform lesions, while the latter also reported that HO-1 limits keratinocyte proliferation in response to IL-17 or IL-22, via inhibition of STAT3 signalling (257,258). Meanwhile, Listopad *et al.* found that HO-1 induction inhibited T-cell mediated psoriatic inflammation in mice by restricting antigen-presentation and cytokine production by APCs (179). Therefore, while these pre-clinical studies indicate that HO-1 induction can effectively protect against psoriasis through its action in innate cells and keratinocytes, it is unknown whether it can also act on pro-inflammatory T cells within psoriasis.

Clinical translation of HO-1 as a treatment for psoriasis is supported by existing therapies, such as phototherapy and DMF, which are associated with upregulation of HO-1 expression (260–263,433). However, direct administration of HO-1 inducers in psoriasis is currently limited as the

metalloporphyrins, CoPP and hemin, which have been utilised in animal models, are unsuitable for clinical use. Curcumin and carnosol were previously observed to induce HO-1 in human DC and PBMC, attenuate pro-inflammatory responses in DC and inhibit the metabolic changes associated with DC and T cell activation. Hence, they may represent attractive alternatives to metalloporphyrins as HO-1 inducers for the treatment of psoriasis. Accordingly, curcumin has shown efficacy in various psoriasis models. Treatment of keratinocytes with curcumin *in vitro* was found to cause cell cycle arrest, via inhibition of cyclin D1 expression (434). Meanwhile, both Kang *et al.* and Sun *et al.* observed that curcumin improved psoriatic lesions and inhibited the production of innate and adaptive cytokines in mice (288,289). Curcumin has additionally been investigated in a number of small clinical trials of psoriasis. Heng *et al.* reported that topical administration of curcumin effectively reduced epidermal hyperplasia and parakeratosis, as well as the infiltration and activation of immune cells (297). Conversely, Kurd *et al.* found little effect of orally-administered curcumin in an open-label trial (293), however, a lecithin-based oral preparation of curcumin used as an adjuvant therapy in psoriasis was found to effectively reduce psoriasis scores and serum IL-22 levels (298). While curcumin shows promise as a treatment for psoriasis, as is the case with other HO-1 inducers, there is a similar lack of information about its effects on psoriatic T cells. Furthermore, there have been no previous studies investigating the effects of carnosol in the context of psoriasis, either on keratinocytes or immune cells.

In summary, while HO-1, and the polyphenols carnosol and curcumin, have potential as treatments for autoimmune diseases such as psoriasis, their effects on adaptive immune cells are uncertain. This question is important as adaptive immune cells, particularly Th17 cells, are the primary pathogenic cells in many autoimmune diseases, while breakdown of Treg-mediated peripheral immune tolerance is also a precipitating event in autoimmunity. Therefore, the purpose of this chapter was to characterise the immunomodulatory effects of carnosol and curcumin in human PBMC, and determine their ability to limit psoriatic inflammation.

5.2 Aims

- To investigate if carnosol or curcumin can inhibit adaptive immune responses by human PBMC/T cells.
- To determine if carnosol or curcumin treatment can promote Tregs within PBMC.
- To characterise the anti-psoriatic effects of carnosol and curcumin in human keratinocytes and *ex vivo* PBMC from psoriasis patients.

5.3 Results

5.3.1 Treatment of PBMC with carnosol or curcumin inhibits T cell proliferation

In the previous chapter, both carnosol and curcumin were found to be non-toxic and capable of inducing HO-1 expression in human PBMC. Furthermore, these polyphenols effectively inhibited the upregulation of cellular metabolism by PBMC in response to anti-CD3 stimulation. Therefore, it was determined whether carnosol or curcumin treatment would also inhibit the proliferation of T cells after mitogenic stimulation. Human PBMC, labelled with CTV, were treated with carnosol (2.5-10 µM) or curcumin (1-5 µM) for 6 hours prior to stimulation with anti-CD3. After 3-4 days the proliferation of $CD4^+$ T cells within PBMC was assessed by flow cytometry. Stimulation of PBMC with anti-CD3 significantly increased T cell proliferation ($p<0.001$), however, both carnosol- and curcumin-treated PBMC displayed reduced T cell proliferation compared to control PBMC (Figure 5.1A). This effect was found to be dose dependent, with curcumin treatment at 2.5 µM and 5 µM resulting in significant inhibition of T cell proliferation ($p<0.05$ – $p<0.01$; Figure 5.1B).

5.3.2 Carnosol and curcumin are non-toxic to purified $CD4^+$ T cells

It was previously observed that carnosol and curcumin were well-tolerated by human PBMC, up to 10 µM and 5 µM, respectively. It was next determined whether the viability of purified $CD4^+$ T cells would be similarly unaffected by these polyphenols over the course of T cell activation. $CD4^+$ T cells were purified from human PBMC and treated with carnosol (2.5-10 µM) or curcumin (1-5 µM) for 6 hours prior to stimulation with anti-CD3 and anti-CD28. After 3-4 days cellular viability was assessed by flow cytometry using an amine-binding viability dye. The viability of PBMC treated with carnosol or curcumin at all concentrations was comparable to vehicle control treated PBMC, and was typically in the range of 80-90% (Figure 5.2). Therefore, both carnosol and curcumin were judged to be non-toxic to purified $CD4^+$ T cells at the same concentrations used in PBMC.

5.3.3 Carnosol and curcumin inhibit the proliferation of purified $CD4^+$ T cells

Carnosol and curcumin were observed to inhibit the proliferation of $CD4^+$ T cells within anti-CD3 stimulated PBMC. This effect could arise from either direct activity in T cells, or in APCs providing co-stimulation within PBMC. Having confirmed that carnosol and curcumin were well-tolerated by purified $CD4^+$ T cells it was next determined whether they would also affect T cell proliferation in the absence of APCs. $CD4^+$ T cells were purified from human PBMC, labelled with CTV, and treated with carnosol (2.5-10 µM) or curcumin (1-5 µM) for 6 hours prior to stimulation with anti-CD3 and anti-CD28. After 3-4 days, T cell proliferation was assessed by flow cytometry. $CD4^+$ T cells

stimulated with mitogens displayed significantly increased proliferation, which was inhibited in the presence of either carnosol or curcumin (Figure 5.3A). Furthermore, this inhibition was observed to be more potent than that previously observed in PBMC, with the highest concentrations of carnosol and curcumin tested resulting in almost complete attenuation of T cell proliferation (Figure 5.3B). Thus, carnosol and curcumin were confirmed to have inhibitory activity within human T cells separate from their effects in APCs.

5.3.4 Low-dose carnosol and curcumin treatment slightly increases the frequency of Tregs within human PBMC

HO-1 and curcumin have previously been reported to promote the generation of Tregs, and to improve Th17:Treg ratios in disease models (232,283,422,427). Therefore, it was next investigated whether treatment of human PBMC with carnosol or curcumin would increase the frequency of Tregs. PBMC were treated with carnosol (2.5-10 µM) or curcumin (1-5 µM) for 6 hours prior to stimulation with anti-CD3. After 3-4 days, the frequency of Tregs, designated as $CD4^+CD25^+Foxp3^+CD127^{lo}$, was determined by flow cytometry. A trend towards a slight increase in the frequency of Tregs among $CD4^+$ T cells was observed in PBMC treated with 2.5 µM of carnosol or curcumin, however this increase was not significant. Moreover, treatment of PBMC with higher doses of carnosol or curcumin trended towards a reduced frequency of Tregs (Figure 5.4). Therefore, neither carnosol nor curcumin were judged to substantially increase the frequency of Tregs within human PBMC.

5.3.5 Carnosol and curcumin do not alter CD39 or CTLA4 expression by Tregs

Although carnosol and curcumin were not found to substantially increase the frequency of Tregs within human PBMC, it was of interest to investigate whether they might instead alter the suppressive capacity of Tregs. CD39 is a surface enzyme expressed by Tregs which catalyses the conversion of ATP to ADP, and contributes to their suppressive activity (79–81). Furthermore, the CTLA4 receptor is essential for Treg-mediated suppression of T cells, as it removes the co-stimulatory receptors CD80 and CD86 expressed by APCs via trans-endocytosis (75–78). To determine whether carnosol or curcumin treatment could regulate expression of CD39 and CTLA4, human PBMC were treated and stimulated with anti-CD3 as before, and after 3-4 days the expression of CD39 and CTLA4 by Tregs was measured by flow cytometry. CD39 was found to be highly expressed by human Tregs, however neither carnosol nor curcumin altered CD39 expression at any concentration tested (Figure 5.5). Similarly, CTLA4 was also highly expressed in

Tregs, and again no concentration of carnosol or curcumin tested was found to alter this expression (Figure 5.6). Therefore, carnosol and curcumin do not appear to directly regulate the suppressive function of Tregs.

5.3.6 Carnosol and curcumin treatment preferentially inhibits proliferation of CD4⁺ effector cells versus Tregs

Carnosol and curcumin were previously found to inhibit the proliferation of both PBMC and purified $CD4^+$ T cells. However, although neither polyphenol was found to substantially increase the frequency of Tregs within human PBMC, a trend towards a slight increase in Treg frequencies was observed with low-dose carnosol and curcumin treatment. To elucidate the mechanism by which carnosol and curcumin might alter the frequency of Tregs within PBMC, the proliferation of Tregs was compared to that of effector T cells. Human PBMC were labelled with CTV, treated with increasing concentrations of carnosol or curcumin, and stimulated with anti-CD3 as before. After 3-4 days, the proliferation of $CD4^+Foxp3^-$ effector cells and $CD4^+CD25^+Foxp3^+CD127^{lo}$ Tregs was measured and compared. Both effector T cells and Tregs displayed similar levels of proliferation within control-treated PBMC. However, carnosol and curcumin treatment appeared to inhibit the proliferation of effector T cells to a greater degree than that of Tregs. (Figure 5.7A). This trend was most clearly observed in PBMC treated with curcumin at 2.5 and 5 μM (Figure 5.7B). Thus, the anti-proliferative activity of carnosol and curcumin may be greater in effector T cells than in Tregs, which could account for the small differences in Treg frequencies observed with carnosol and curcumin treatment.

5.3.7 Treatment of PBMC with carnosol and curcumin reduces the frequency of IL-17 and IFNγ producing T cells

Alongside promotion of Tregs, HO-1 and curcumin have previously been reported to reduce the frequency of pro-inflammatory T cell subsets such as Th17 and Th1 cells (232,283,360,427,428), which are characterised by their production of the cytokines IL-17 and IFNγ, respectively. Thus, it was next examined whether treatment of PBMC with carnosol or curcumin would alter the frequency of IL-17 and IFNγ producing helper T cells. Human PBMC were treated with increasing concentrations of carnosol or curcumin and stimulated with anti-CD3 as before. After 3-4 days, PBMC were re-stimulated with PMA and ionomycin, in the presence of brefeldin A, for 6 hours and cytokine production was analysed by flow cytometry.

The proportion of helper T cells ($CD3^+CD8^-$) which expressed IL-17 was observed to be greater in PBMC previously stimulated with anti-CD3 compared to unstimulated control PBMC. Furthermore, the frequency of IL-17^+ helper T cells was reduced among carnosol- and curcumin-treated PBMC, which displayed a frequency in between that of stimulated and unstimulated control PBMC (Figure 5.8). Similarly, anti-CD3 stimulated PBMC were also observed to upregulate the frequency of IFNγ^+ helper cells compared to unstimulated control PBMC. Again, carnosol and curcumin both inhibited the increased expression of IFNγ by stimulated PBMC, with carnosol- and curcumin-treated PBMC displaying an intermediate frequency of IFNγ^+ helper cells between that of stimulated and unstimulated control PBMC (Figure 5.9). The reduction of IL-17 and IFNγ producing helper T cells by carnosol and curcumin was similar between the different concentrations of each polyphenol tested, indicating that this effect may not be dose-dependent. In summary, these results indicate that carnosol and curcumin can reduce the frequencies of Th17 and Th1 cells in human PBMC.

5.3.8 Treatment of PBMC with carnosol or curcumin does not alter the frequency of TNFα or IL-2 producing T cells

Having observed that carnosol and curcumin inhibited the frequency of IL-17 and IFNγ producing helper T cells in anti-CD3 stimulated PBMC, it was important to distinguish whether this represented a specific effect on these T cell subsets, or if all cytokine production by T cells would be inhibited. Therefore, the frequency of TNFα and IL-2 producing helper T cells was also measured by flow cytometry, as previously described. TNFα is a pro-inflammatory cytokine broadly expressed by activated T cells; as expected, anti-CD3 stimulated PBMC displayed a higher frequency of TNFα^+ helper T cells compared to unstimulated PBMC. However, there was no discernible difference in the frequency of TNFα^+ cells within carnosol- or curcumin-treated PBMC (Figure 5.10). Similarly, IL-2 is a pleiotropic cytokine highly upregulated upon T cell activation, which has important roles in the growth and differentiation of T cell subsets, including Tregs (435). Stimulated PBMC possessed a much greater frequency of IL-2^+ helper T cells compared to unstimulated PBMC ($p<0.05$), which was similar to that observed with carnosol and curcumin treatment (Figure 5.11). Therefore, neither carnosol nor curcumin significantly reduced the proportion of TNFα or IL-2 producing T cells within PBMC, indicating that there is some specificity in their inhibition of T cell cytokine production.

5.3.9 Carnosol and curcumin treatment significantly reduces total IL-17 and IFNγ production by human PBMC and purified CD4⁺ T cells

Carnosol and curcumin were found to significantly inhibit T cell proliferation and reduce the frequency of IL-17 and IFNγ producing T helper cells within PBMC. Therefore, it was next determined whether this would be reflected in the total amounts of IL-17 and IFNγ produced by carnosol- and curcumin-treated PBMC. Human PBMC were treated with increasing concentrations of carnosol or curcumin and stimulated with anti-CD3 as before. After 3-4 days cell culture supernatants were removed and the concentrations of IL-17 and IFNγ were measured by ELISA. Both carnosol and curcumin significantly reduced the production of IL-17 and IFNγ by PBMC ($p<0.01$ – $p<0.0001$). Furthermore, this effect was dose dependent, with the highest doses of carnosol and curcumin tested almost completely abrogating the production of these pro-inflammatory cytokines (Figure 5.12).

Although the proliferation of purified $CD4^+$ T cells was also found to be inhibited by carnosol and curcumin, the frequency of IL-17 and IFNγ producing T helper cells was not analysed in carnosol- and curcumin-treated $CD4^+$ T cells. However, the total production of these cytokines was measured to indicate whether these polyphenols can also inhibit T cell cytokine production in the absence of APCs. $CD4^+$ T cells were purified from PBMC, treated with carnosol or curcumin and stimulated with anti-CD3 and anti-CD28, as described previously. After 3-4 days cell culture supernatants were removed and the concentrations of IL-17 and IFNγ were measured by ELISA. As was seen in PBMC, both carnosol and curcumin treatment resulted in a dose-dependent reduction of IL-17 and IFNγ production by $CD4^+$ T cells ($p<0.05$ – $p<0.001$). The concentrations of IL-17 and IFNγ were significantly reduced with the highest doses of carnosol and curcumin tested, which almost completely inhibited production of both cytokines (Figure 5.13). Taken together, these results support previous data demonstrating that carnosol and curcumin treatment inhibits T cell proliferation and modulates the frequency of Th17 and Th1 cell subsets, and suggest that these effects may be achieved through direct action on T cells.

5.3.10 Carnosol and curcumin are non-toxic to human keratinocytes

Carnosol and curcumin were found to have immunomodulatory effects in human T cells, which are relevant for the treatment of psoriasis. Therefore, it was also of interest to investigate their activity in keratinocytes. First, it was confirmed that carnosol and curcumin are non-toxic in these cells. HaCaT keratinocytes were treated with carnosol (2.5-10 μM) or curcumin (2.5-10 μM) for 24 hours, after which their viability was determined by alamarBlue assay. Neither carnosol nor

curcumin reduced the viability of keratinocytes compared to control-treated cells, at any concentration tested (Figure 5.14). Therefore, both polyphenols were judged to be well tolerated in HaCaT keratinocytes.

5.3.11 Keratinocyte proliferation is significantly reduced in the presence of carnosol or curcumin

Hyperproliferation of keratinocytes is a feature of psoriasis which contributes to the formation of psoriatic plaques. Therefore, inhibition of keratinocyte proliferation is required to improve the condition of psoriatic skin. Curcumin has previously been reported to prevent cell cycle progression in HaCaT keratinocytes (434), therefore it was next investigated whether curcumin and carnosol treatment would reduce the proliferation of these cells. HaCaT keratinocytes were treated with carnosol (2.5-10 µM) or curcumin (2.5-10 µM) and after 24 hours their proliferation was analysed by confocal microscopy. Carnosol treatment of keratinocytes produced a small but significant reduction in cell number compared to control-treated cells, which was similar across all concentrations tested ($p<0.01$ – $p<0.001$; Figure 5.15). Similarly, curcumin treatment also moderately inhibited keratinocyte proliferation at 2.5 µM and 5 µM, however, treatment with 10 µM curcumin resulted in a highly significant reduction of cell number ($p<0.0001$; Figure 5.16). These results indicate that carnosol and curcumin, while non-toxic to keratinocytes, effectively limit their basal proliferation.

5.3.12 Curcumin, but not carnosol, inhibits the production of IL-8 by keratinocytes

In addition to hyperproliferation, keratinocytes can contribute to the pathology of psoriasis by producing pro-inflammatory cytokines which amplify inflammation within the skin. IL-8 is a chemokine produced by keratinocytes in response to stimulation by other pro-inflammatory cytokines, which promotes the recruitment of neutrophils and increases vascularisation within the psoriatic plaque (436). Having observed that carnosol and curcumin both inhibit the proliferation of keratinocytes, it was next determined if they would also reduce their ability to produce IL-8 in response to inflammation. HaCaT keratinocytes were treated with carnosol (2.5-10 µM) or curcumin (2.5-10 µM) for 6 hours prior to stimulation with TNFα (100 ng/ml). After 24 hours, cell culture supernatants were removed and the concentration of IL-8 was measured by ELISA. Treatment of keratinocytes with curcumin produced a moderate dose-dependent reduction of IL-8 production, which was significant at the highest concentration of curcumin tested ($p<0.01$). Conversely, no reduction of IL-8 was observed in keratinocytes treated with any concentration of

carnosol (Figure 5.17). Taken together, these results indicate that curcumin is a more effective inhibitor of keratinocyte function than carnosol.

5.3.13 Treatment of ex vivo *PBMC from psoriasis patients with curcumin, but not carnosol, inhibits T cell proliferation*

Both curcumin and carnosol were observed to effectively inhibit T cell proliferation in PBMC and $CD4^+$ T cells obtained from healthy donors. However, it has previously been reported that psoriasis patients display increased levels of circulating pro-inflammatory T cells (437). Therefore, it was investigated whether carnosol or curcumin could also inhibit the proliferation of T cells from psoriasis patients. PBMC isolated from psoriasis patients were treated with carnosol (5 µM) or curcumin (5 µM) for 6 hours prior to stimulation with anti-CD3. After 4 days, PBMC were re-stimulated with PMA and ionomycin, in the presence of brefeldin A, for 6 hours and analysed for expression of the cellular proliferation marker, Ki67, by flow cytometry. $CD3^+CD8^-$ T cells from control-treated PBMC displayed strong expression of Ki67, which was similar to that of T cells from carnosol-treated PBMC. Conversely, curcumin treatment produced an approximate 50% reduction in Ki67 expression by T cells, which was statistically significant ($p<0.01$; Figure 5.18). Therefore, similar to previous results in healthy PBMC, curcumin was a more effective inhibitor of T cell proliferation in *ex vivo* psoriasis patient PBMC than carnosol.

5.3.14 Carnosol and curcumin minimally affect the frequency of TNFα or IL-2 producing T cells within ex vivo *PBMC from psoriasis patients*

Curcumin treatment was found to limit the proliferation of T cells within *ex vivo* PBMC from psoriasis patients. Previous work in healthy PBMC found that, despite their anti-proliferative activity, carnosol and curcumin did not compromise the expression of TNFα or IL-2 by T cells, indicating that these cells retain some capacity to respond to stimulation. Therefore, it was also determined whether this would be the case for carnosol- and curcumin-treated psoriasis patient PBMC. PBMC from psoriasis patients were treated with carnosol or curcumin and stimulated as described before. The expression of the cytokines TNFα and IL-2 by $CD3^+CD8^-$ T cells was measured by flow cytometry. TNFα was strongly expressed by T cells from psoriasis patients, and this expression was unaffected by either carnosol or curcumin treatment (Figure 5.19A,C). Similarly, IL-2 was also highly expressed by T cells, which was again unaffected by carnosol treatment. Curcumin did, however, produce a small but significant reduction in IL-2 expression by T cells, of approximately 10% ($p<0.01$). Despite this reduction, the overall frequency of $IL\text{-}2^+$ T cells in

curcumin-treated PBMC remained high, typically above 50% (Figure 5.19B,D). Therefore, these results confirm that neither carnosol nor curcumin exert broad inhibition of T cell cytokine production within *ex vivo* PBMC from psoriasis patients.

5.3.15 Curcumin, but not carnosol, significantly reduces the expression of psoriasis-associated cytokines by T cells within ex vivo *PBMC from psoriasis patients*

Although neither carnosol nor curcumin reduced the expression of TNFα or IL-2 in healthy human PBMC, they were found to reduce the frequencies of IL-17$^+$ and IFNγ$^+$ T cells, indicating that these polyphenols can specifically downregulate expression of certain pro-inflammatory cytokines. It has previously been reported that psoriasis patients display elevated serum levels of pro-inflammatory cytokines (438). Furthermore, it is known that these cytokines are key mediators in the pathology of psoriasis, particularly those of the Th17 axis (64,254). Therefore, it was next investigated whether carnosol or curcumin can specifically inhibit the expression of these psoriatic cytokines in *ex vivo* PBMC from psoriasis patients. The expression of IFNγ, IL-17, IL-22 and GM-CSF by CD3$^+$CD8$^-$ T cells within control, carnosol- or curcumin-treated PBMC was measured by flow cytometry, as previously described.

IFNγ was typically highly expressed by T cells from psoriasis patients, with an average of approximately 20% of T cells expressing this cytokine. Curcumin treatment resulted in a significant reduction in the frequency of IFNγ$^+$ T cells, as only 10% of T cells from curcumin-treated PBMC were found to express IFNγ ($p<0.01$). Conversely, carnosol had no effect on the frequency of IFNγ$^+$ T cells (Figure 5.20A,C). The frequency of IL-17$^+$ T cells was variable between individual patients, on average representing 3% of T cells within control- and carnosol-treated PBMC. Nonetheless, curcumin treatment significantly inhibited IL-17 expression by T cells in PBMC, with typically <1% of T cells expressing this important psoriasis-associated cytokine ($p<0.05$; Figure 5.20B,D). The expression of IL-22, another cytokine associated with Th17 cells, was similar to that of IL-17, as the frequency of IL-22$^+$ T cells within psoriasis patient PBMC was approximately 4%. Again, curcumin significantly reduced the expression of IL-22 by psoriasis patient T cells ($p<0.05$), while carnosol had no effect (Figure 5.21A,C). Finally, GM-CSF was highly expressed by T cells within psoriasis patient PBMC, with the average frequency of GM-CSF$^+$ T cells observed to be approximately 30%. Similar expression of this cytokine was observed within carnosol-treated PBMC, while curcumin treatment significantly reduced the frequency of GM-CSF$^+$ T cells to an average of 10% ($p<0.05$; Figure 5.21B,D). Taken together, these results indicate that curcumin can specifically inhibit the expression of pro-inflammatory cytokines relevant to psoriasis, while carnosol did not appear to modulate the activity of psoriasis patient T cells in this study.

5.3.16 Treatment of ex vivo *PBMC from psoriasis patients with curcumin, but not carnosol, reduces the frequency and IL-17 expression of γδ T cells*

Recent research has described an important role for γδ T cells in psoriasis pathogenesis within murine models, largely as a result of their strong expression of the psoriasis-associated cytokine IL-17 (439,440). Although it is not yet known whether this rare T cell subset is relevant in the context of human disease, it was of interest to determine whether carnosol or curcumin treatment would alter the frequency and cytokine expression of γδ T cells, as had been observed in $CD3^+CD8^-$ T cells. PBMC from psoriasis patients were treated with carnosol or curcumin and stimulated as previously described. The frequency of $CD3^+TCR\gamma\delta^+$ T cells was measured by flow cytometry. Control- and carnosol-treated PBMC displayed a similar frequency of γδ T cells, which varied considerably between individual patients but was, on average, approximately 4% of live cells. Interestingly, a significantly lower frequency of γδ T cells was observed in psoriasis patient PBMC treated with curcumin, which was typically in the range of ~0.2-1% of live cells ($p<0.05$; Figure 5.22A,B). γδ T cells from psoriasis patient PBMC also strongly expressed the pro-inflammatory cytokines IL-17, IFNγ and TNFα. A trend towards reduced IL-17, but not IFNγ or TNFα expression by γδ T cells was observed with curcumin treatment. Carnosol treatment did not reduce the expression of any cytokine by γδ T cells (Figure 5.22C). These results indicate that curcumin treatment can inhibit the expansion of γδ T cells, and their expression of the strongly psoriasis-associated cytokine, IL-17, in response to anti-CD3 stimulation, whereas carnosol treatment was found to be ineffective in this regard.

5.3.17 Treatment with carnosol or curcumin reduces the total production of IFNγ and IL-17 by ex vivo *PBMC from psoriasis patients*

Following the observation that *ex vivo* psoriasis patient PBMC treated with curcumin displayed significantly reduced T cell proliferation and pro-inflammatory cytokine expression, it was next investigated whether these effects would be reflected in the total production of IFNγ and IL-17 by these cells. PBMC from psoriasis patients were treated with carnosol or curcumin and stimulated with anti-CD3 as previously described. After 4 days, cell culture supernatants were removed and the concentrations of IFNγ and IL-17 were measured by ELISA. As expected, curcumin significantly reduced the production of IFNγ by psoriasis patient PBMC ($p<0.05$), while no significant reduction was observed with carnosol treatment. Interestingly, a trend towards reduced IL-17 production by psoriasis patient PBMC was observed with both carnosol and curcumin treatment (Figure 5.23). These results support the previously observed reduction of T cell proliferation and pro-

inflammatory T cell frequencies within curcumin-treated psoriasis patient PBMC, and additionally suggest that carnosol may have some, albeit limited, anti-inflammatory activity in psoriasis.

5.3.18 Curcumin reduces the poly-functionality of T cells in ex vivo *PBMC from psoriasis patients*

Given that one of the hallmarks of highly pro-inflammatory T cells is the capacity to produce multiple different cytokines, the poly-functionality of $CD3^{+}CD8^{-}$ T cells in control, carnosol- and curcumin-treated psoriasis patient PBMC was determined using SPICE analysis of flow cytometry data (Figure 5.24). The segments within the pie charts represent the proportion of cells producing 0 to 6 cytokines simultaneously, and are heat-map coded to indicate increasing cytokine poly-functionality (pie chart legend: white to red). The size of a pie segment corresponds to the frequency of that population. The arcs surrounding the pie charts correspond to the specific cytokines produced by the pie segments underneath (see pie arc legend). By comparing the poly-functionality profiles of control-treated to carnosol- and curcumin-treated psoriasis patient PBMC it was observed that carnosol treatment did not discernibly alter the frequency of poly-functional $CD3^{+}CD8^{-}$ T cells. In contrast, a clear increase in the frequency of T cells producing no cytokines (white pie segment) and decrease in the frequencies of T cells producing 3 or more cytokines (orange and red segments) was observed in curcumin-treated psoriasis patient PBMC compared to control. By examining the cytokine arcs it is evident that this decrease in T cell poly-functionality in curcumin-treated PBMC corresponds with a reduction in the frequencies of IFNγ, IL-17, GM-CSF and IL-22 producing cells, as was previously observed. This analysis provides greater insight into the action of curcumin on psoriatic T cells, indicating that its anti-inflammatory effects are greatest within highly pro-inflammatory poly-functional T cells.

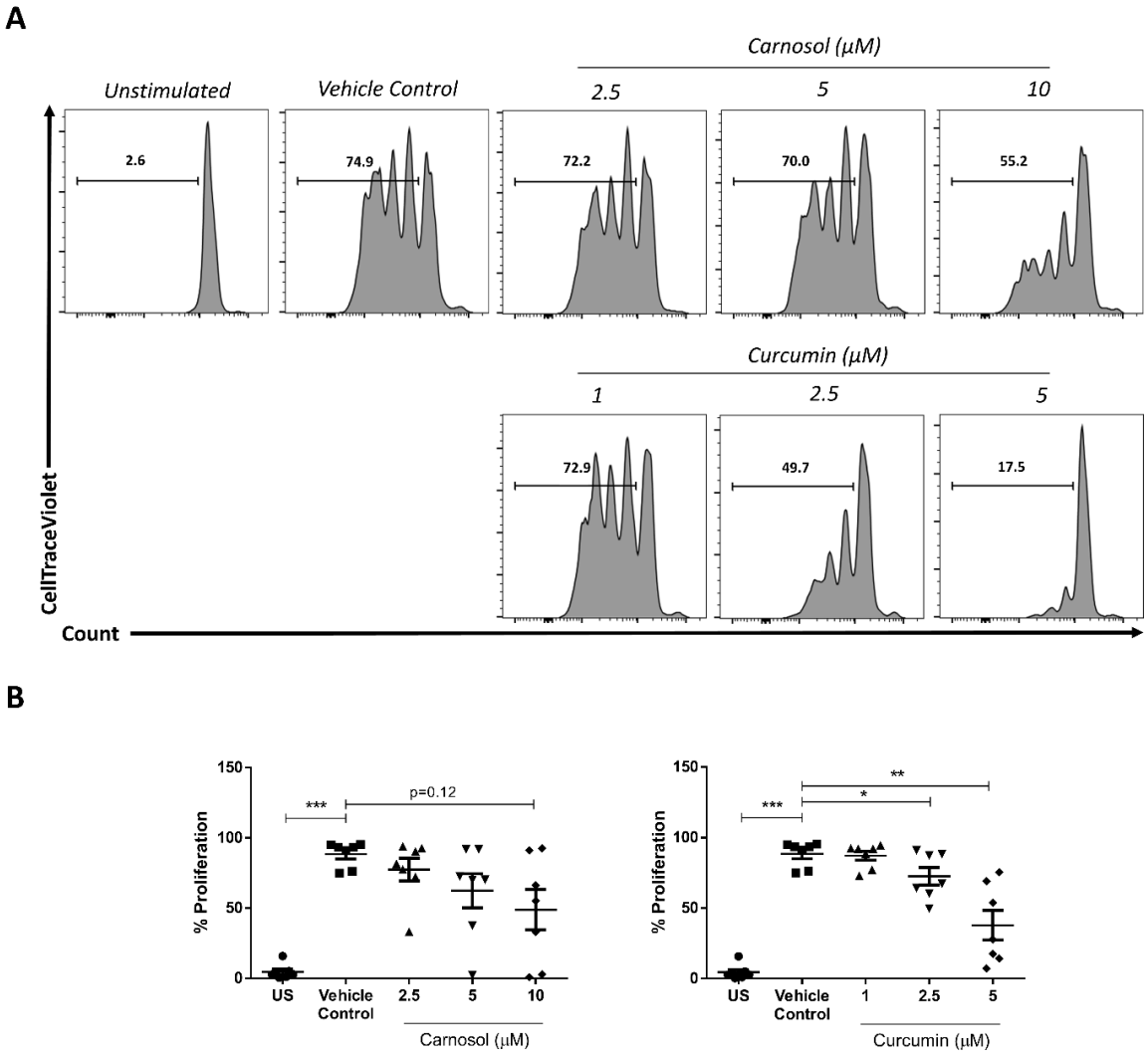

Figure 5.1. Carnosol and curcumin inhibit T cell proliferation in PBMC. PBMC labelled with CTV were either left unstimulated (US), or incubated with carnosol (2.5-10 μM), curcumin (1-5 μM), or a vehicle control for 6 hours prior to stimulation with anti-CD3. After 3-4 days, proliferation of $CD4^+$ T cells was measured by flow cytometry. **(A)** Histograms depicting proliferation of $CD4^+$ T cells (gated by scatter and viability) from unstimulated, and control-, carnosol- and curcumin-treated PBMC stimulated with anti-CD3. Data is from one donor and is representative of seven independent experiments. **(B)** Pooled data (n=7) depicting the mean (±SEM) percentage of proliferated $CD4^+$ T cells within PBMC. Statistical significance was determined by one-way ANOVA, with Dunnett's multiple comparisons post hoc test to compare treatment groups against the control group (***p<0.001, **p<0.01, *p<0.05).

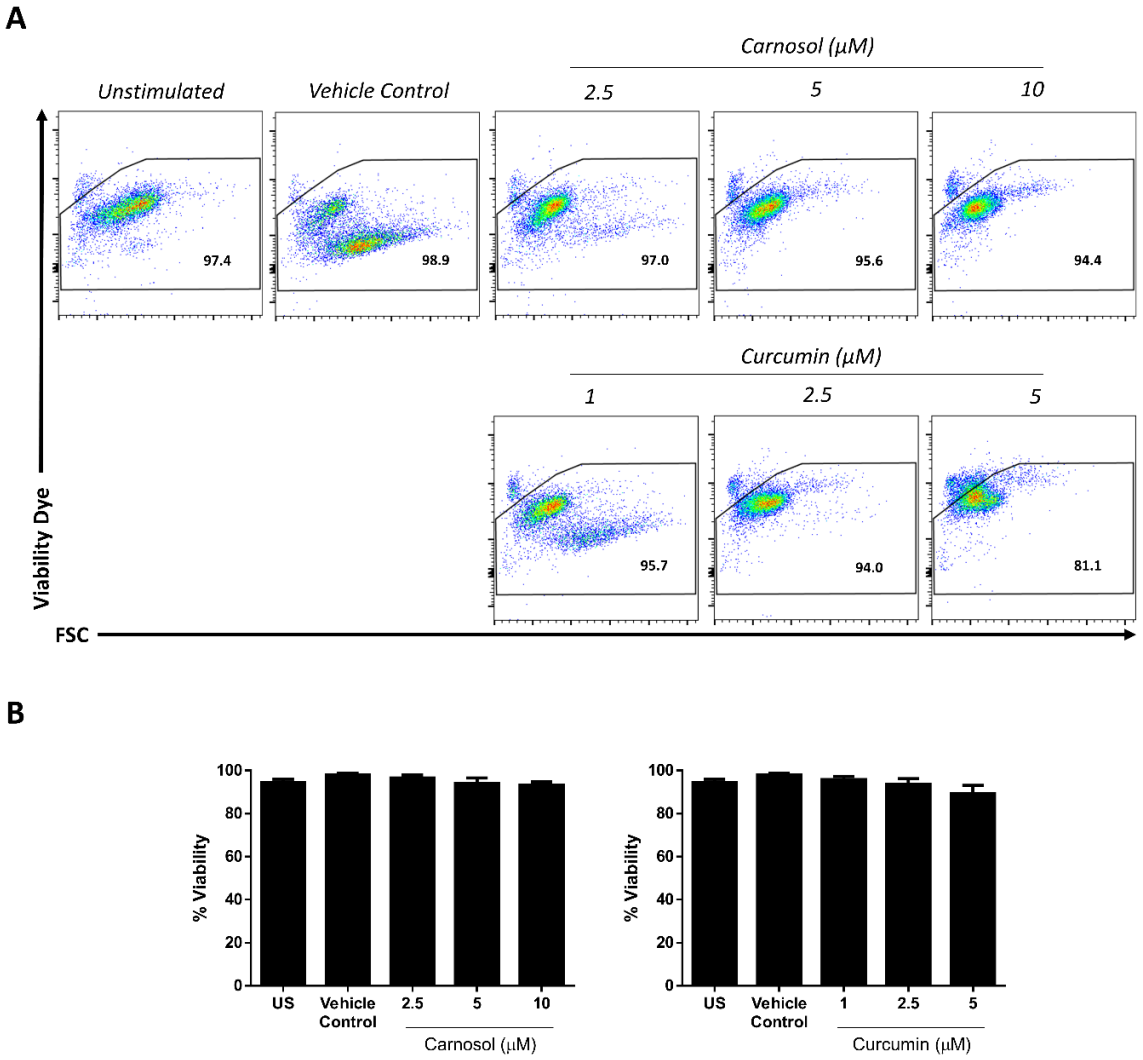

Figure 5.2. Carnosol and curcumin are non-toxic to purified CD4$^+$ T cells. CD4$^+$ T cells were either left unstimulated (US), or incubated with carnosol (2.5-10 μM), curcumin (1-5 μM), or a vehicle control for 6 hours prior to stimulation with anti-CD3 and anti-CD28 for 3-4 days. Cells were stained with an amine-binding viability dye and analysed by flow cytometry. **(A)** Dot plots depicting viability dye uptake of control-, carnosol- and curcumin-treated CD4$^+$ T cells (gated by forward and side scatter). Data is from one donor and is representative of four independent experiments. **(B)** Pooled data (n=4) depicting the mean (±SEM) percentage viable cells of lymphocytes (gated by forward and side scatter).

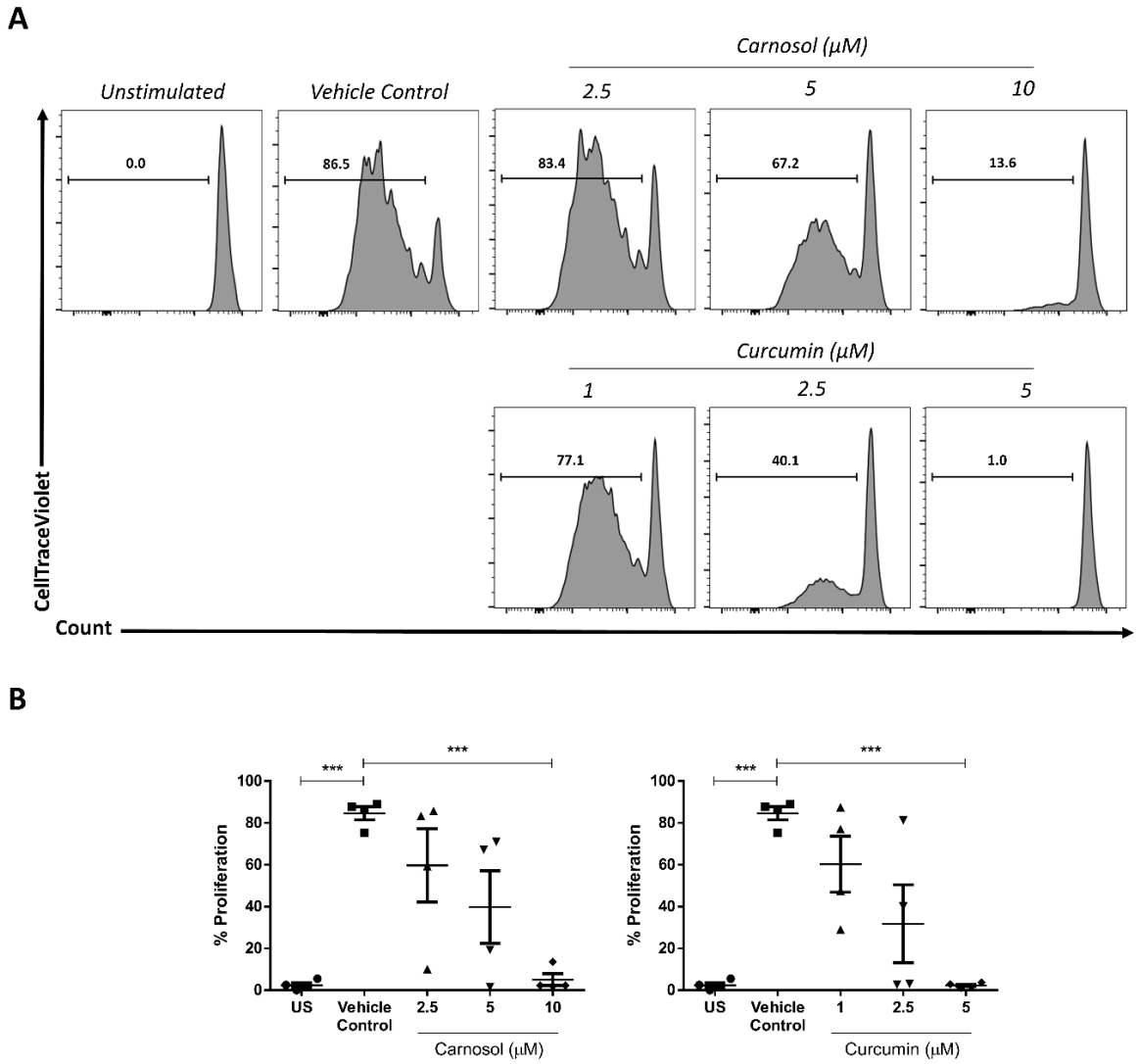

Figure 5.3. Carnosol and curcumin inhibit proliferation of purified CD4⁺ T cells. CD4⁺ T cells labelled with CTV were either left unstimulated (US), or incubated with carnosol (2.5-10 μM), curcumin (1-5 μM), or a vehicle control for 6 hours prior to stimulation with anti-CD3 and anti-CD28. After 3-4 days, proliferation of CD4⁺ T cells was measured by flow cytometry. **(A)** Histograms depicting proliferation of unstimulated, and control-, carnosol- and curcumin-treated CD4⁺ T cells (gated by scatter and viability) stimulated with anti-CD3 and anti-CD28. Data is from one donor and is representative of four independent experiments. **(B)** Pooled data (n=4) depicting the mean (±SEM) percentage of proliferated CD4⁺ T cells. Statistical significance was determined by one-way ANOVA, with Dunnett's multiple comparisons post hoc test to compare treatment groups against the control group (***p<0.001).

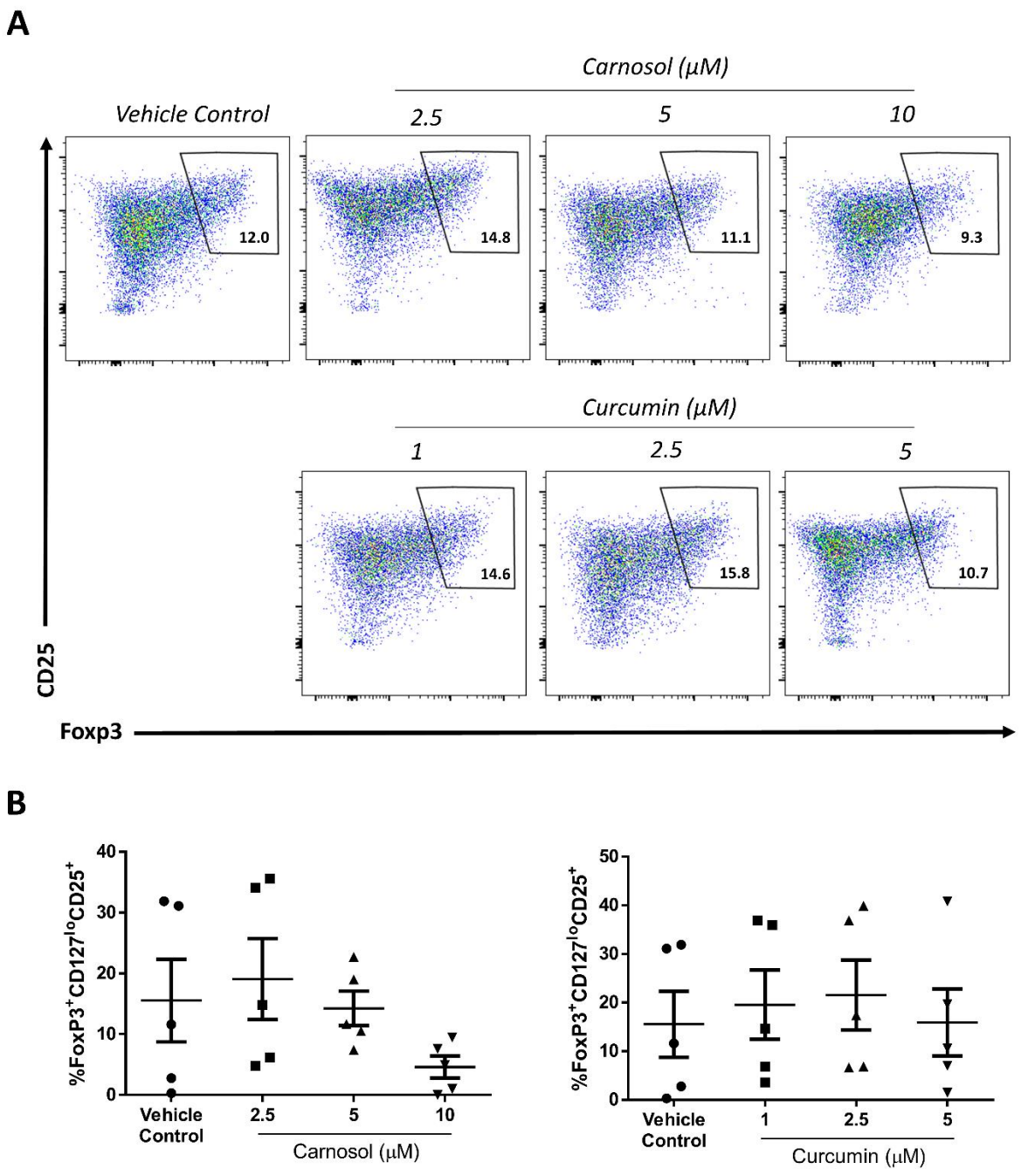

Figure 5.4. Low doses of carnosol and curcumin slightly increase the frequency of Tregs within PBMC. PBMC were incubated with carnosol (2.5-10 μM), curcumin (1-5 μM) or a vehicle control for 6 hours prior to stimulation with anti-CD3 for 3-4 days. The percentage of Treg cells was measured by flow cytometry, with Tregs identified as $CD4^+CD25^+Foxp3^+CD127^{lo}$. **(A)** Dot plots depicting the proportions of $CD25^+Foxp3^+$ cells within the $CD4^+$ population of carnosol- and curcumin-treated PBMC. Data is from one donor and is representative of five independent experiments. **(B)** Pooled data (n=5) depicting the mean (±SEM) percentage of $CD4^+CD25^+Foxp3^+CD127^{lo}$ Tregs within the $CD4^+$ population of carnosol- and curcumin-treated PBMC.

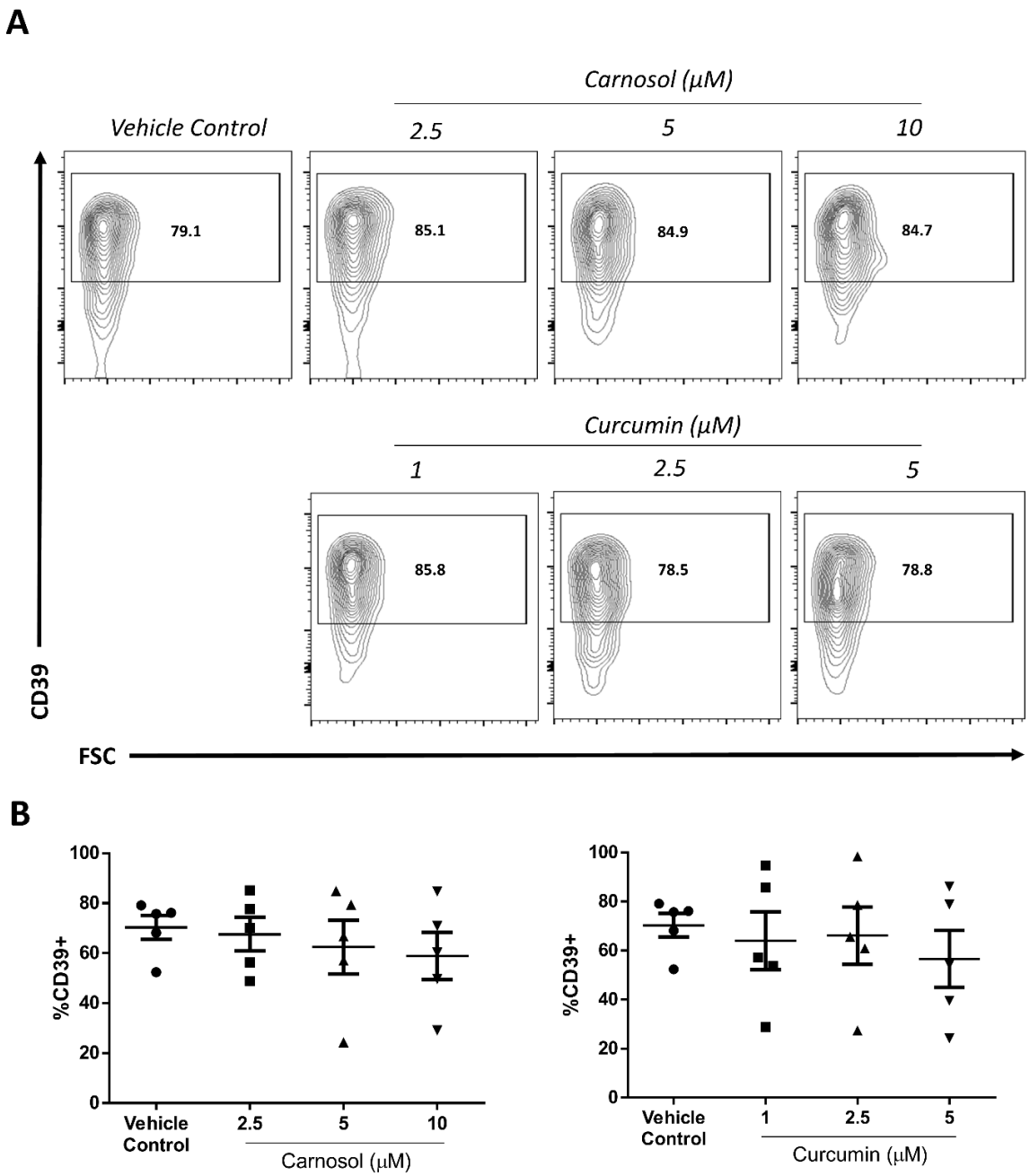

Figure 5.5. Carnosol and curcumin do not affect CD39 expression by Tregs. PBMC were incubated with carnosol (2.5-10 μM), curcumin (1-5 μM) or a vehicle control for 6 hours prior to stimulation with anti-CD3 for 3-4 days. Expression of CD39 by Tregs (identified as $CD4^+CD25^+Foxp3^+CD127^{lo}$) was measured by flow cytometry. **(A)** Dot plots depicting the proportions of $CD39^+$ Tregs within carnosol- and curcumin-treated PBMC. Data is from one donor and is representative of five independent experiments. **(B)** Pooled data (n=5) depicting the mean (±SEM) percentage of $CD39^+$ Tregs within carnosol- and curcumin-treated PBMC.

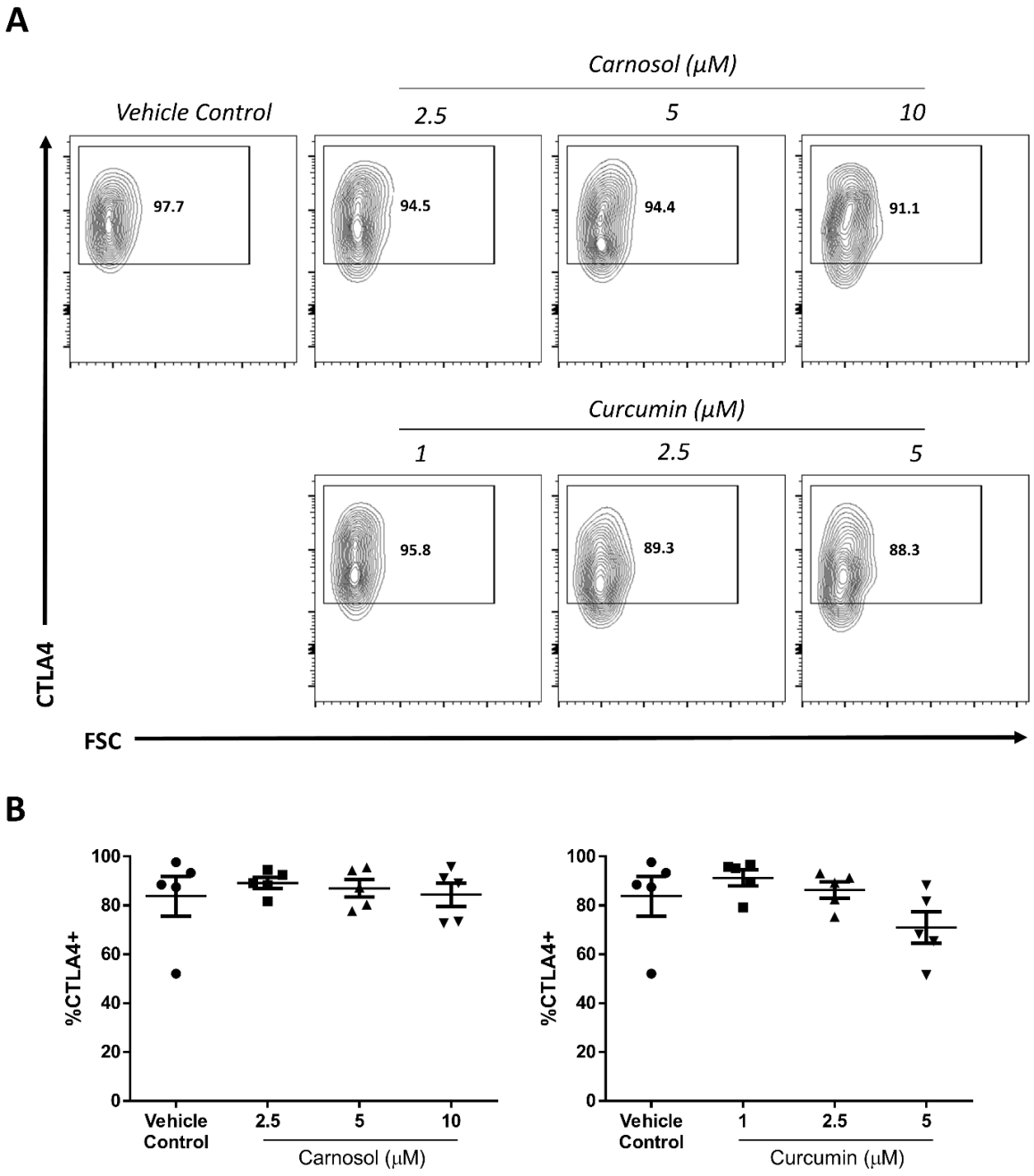

Figure 5.6. Carnosol and curcumin do not affect CTLA4 expression by Tregs. PBMC were incubated with carnosol (2.5-10 μM), curcumin (1-5 μM) or a vehicle control for 6 hours prior to stimulation with anti-CD3 for 3-4 days. Expression of CTLA4 by Tregs (identified as $CD4^+CD25^+Foxp3^+CD127^{lo}$) was measured by flow cytometry. **(A)** Dot plots depicting the proportions of $CTLA4^+$ Tregs within carnosol- and curcumin-treated PBMC. Data is from one donor and is representative of five independent experiments. **(B)** Pooled data (n=5) depicting the mean (±SEM) percentage of $CTLA4^+$ Tregs within carnosol- and curcumin-treated PBMC.

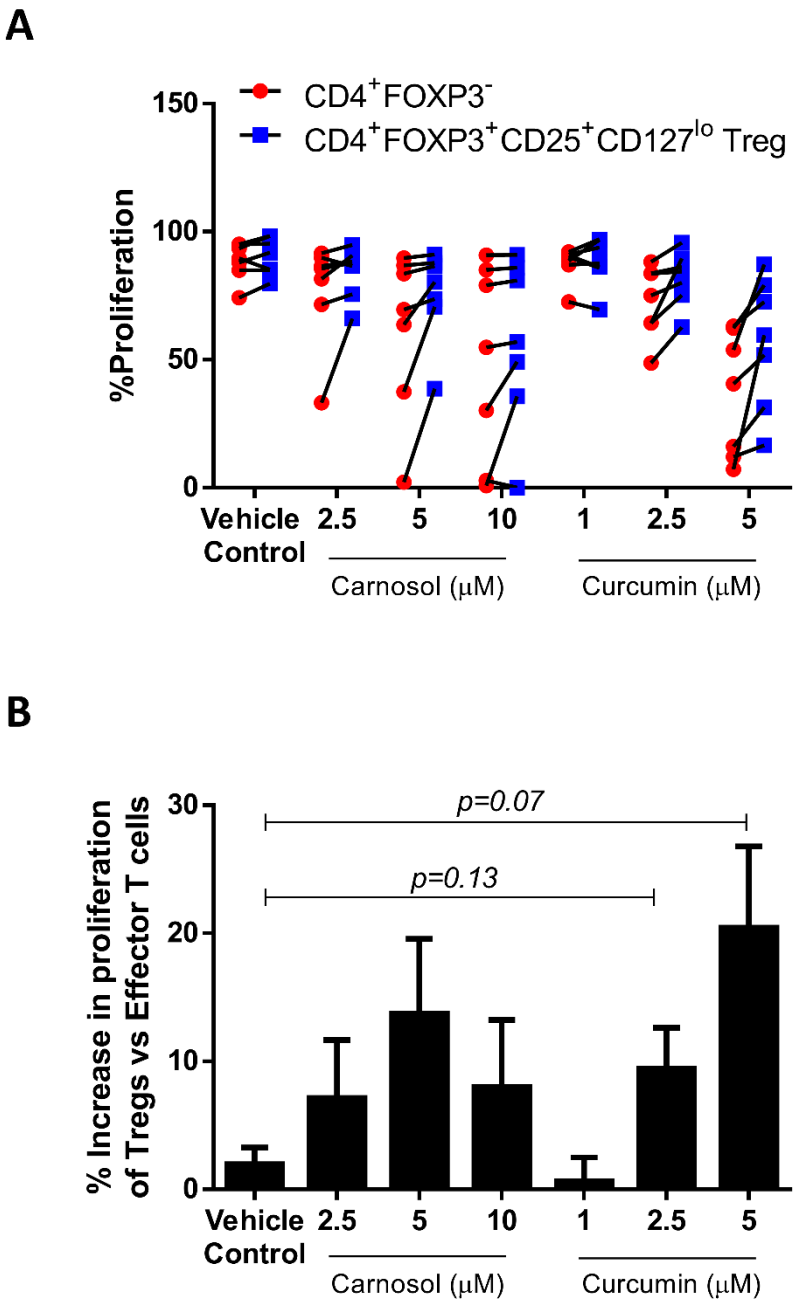

Figure 5.7. Carnosol and curcumin treatment preferentially inhibits proliferation of CD4$^+$ effector cells versus Tregs. PBMC labelled with CTV were incubated with carnosol (2.5-10 μM), curcumin (1-5 μM) or a vehicle control for 6 hours prior to stimulation with anti-CD3 for 3-4 days. The proliferation of Tregs versus non-Tregs was measured by flow cytometry, with Tregs identified as CD4$^+$CD25$^+$Foxp3$^+$CD127^{lo}, and non-Tregs as CD4$^+$FOXP3$^-$. **(A)** Results shown are paired percentages of proliferated non-Tregs versus Tregs from seven independent experiments. **(B)** Pooled data (n=7) depicting the mean (±SEM) percentage difference between the proliferation of Tregs and non-Tregs. Statistical significance was determined by one-way ANOVA, with Dunnett's multiple comparisons post hoc test to compare treatment groups against the control group.

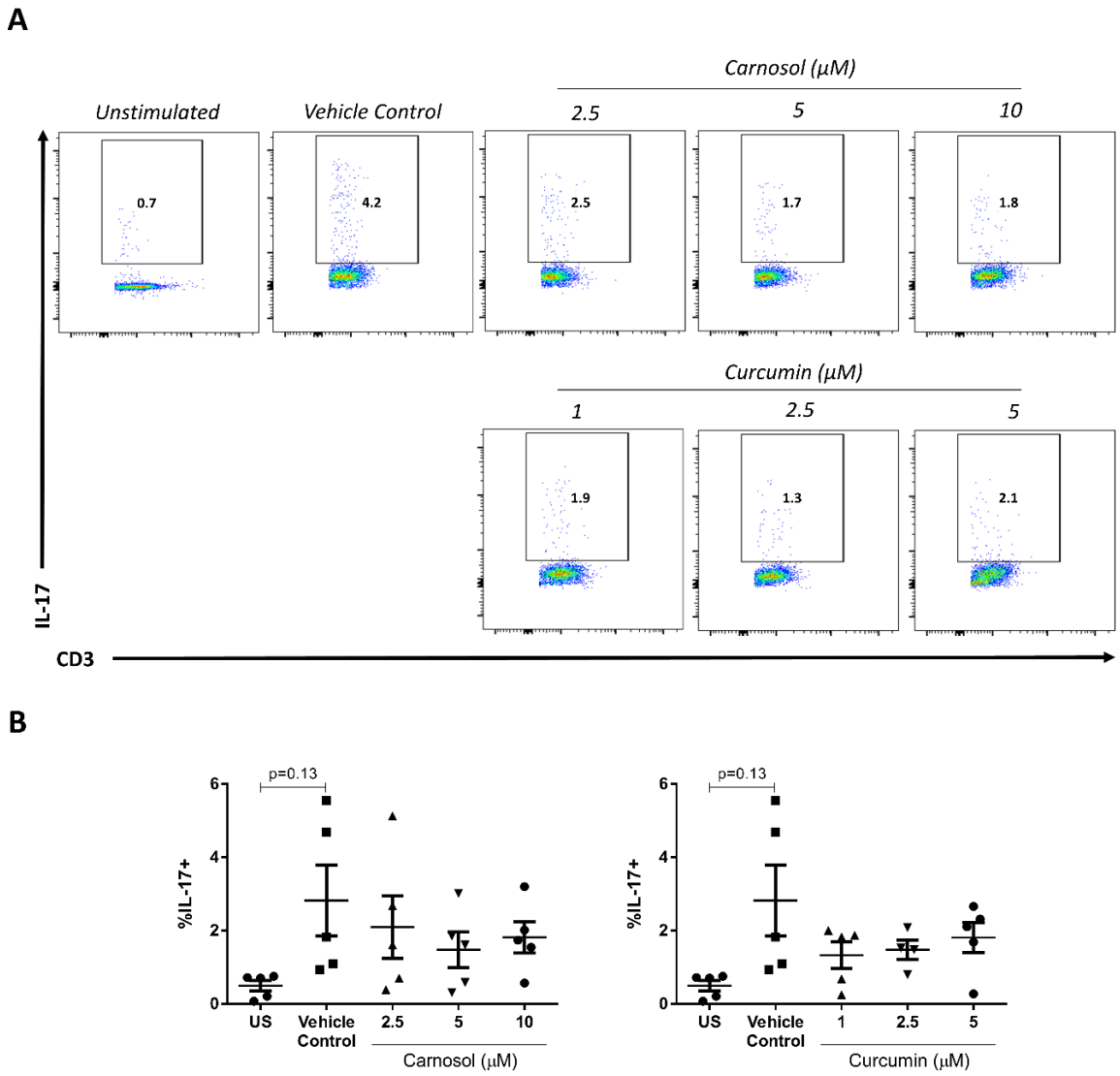

Figure 5.8. Carnosol and curcumin moderately reduce the frequency of IL-17 producing T cells. PBMC were either left unstimulated (US), or incubated with carnosol (2.5-10 µM), curcumin (1-5 µM) or a vehicle control for 6 hours prior to stimulation with anti-CD3 for 3-4 days. PBMC were then restimulated with PMA and ionomycin in the presence of brefeldin A for 6 hours and cytokine production by $CD3^+CD8^-$ T cells was analysed by flow cytometry. **(A)** Dot plots depicting the proportions of $IL\text{-}17^+$ cells within the $CD3^+CD8^-$ population of carnosol- and curcumin-treated PBMC. Data is from one donor and is representative of five independent experiments. **(B)** Pooled data (n=5) depicting the mean (±SEM) percentage of $IL\text{-}17^+$ cells within the $CD3^+CD8^-$ population of carnosol- and curcumin-treated PBMC. Statistical significance was determined by one-way ANOVA, with Dunnett's multiple comparisons post hoc test to compare treatment groups against the control group.

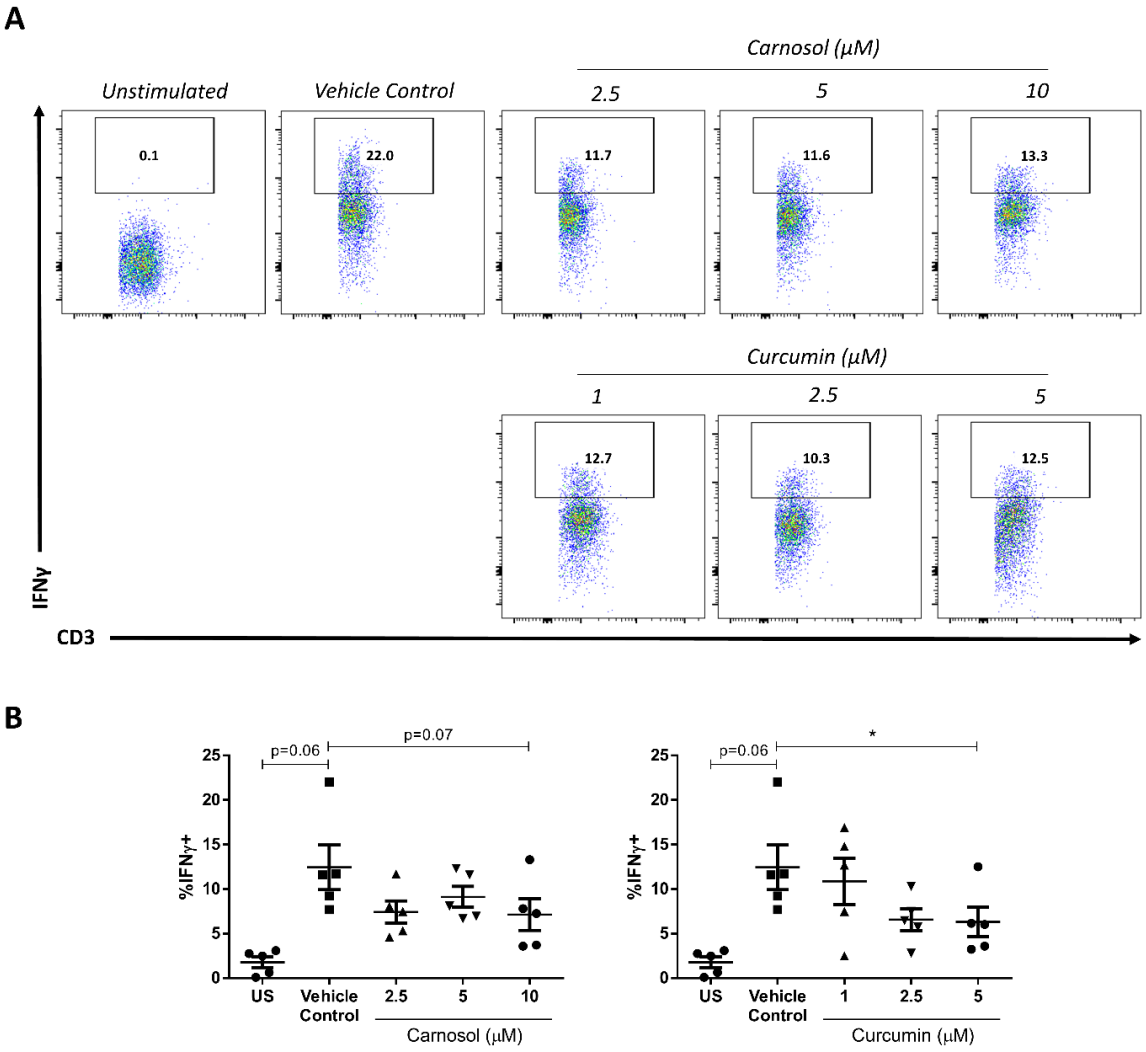

Figure 5.9. Carnosol and curcumin reduce the frequency of IFNγ producing T cells. PBMC were either left unstimulated (US), or incubated with carnosol (2.5-10 μM), curcumin (1-5 μM) or a vehicle control for 6 hours prior to stimulation with anti-CD3 for 3-4 days. PBMC were then restimulated with PMA and ionomycin in the presence of brefeldin A for 6 hours and cytokine production by $CD3^+CD8^-$ T cells was analysed by flow cytometry. **(A)** Dot plots depicting the proportion of $IFN\gamma^+$ cells within the $CD3^+CD8^-$ population of carnosol- and curcumin-treated PBMC. Data is from one donor and is representative of five independent experiments. **(B)** Pooled data (n=5) depicting the mean (±SEM) percentage of $IFN\gamma^+$ cells within the $CD3^+CD8^-$ population of carnosol- and curcumin-treated PBMC. Statistical significance was determined by one-way ANOVA, with Dunnett's multiple comparisons post hoc test to compare treatment groups against the control group (*p<0.05).

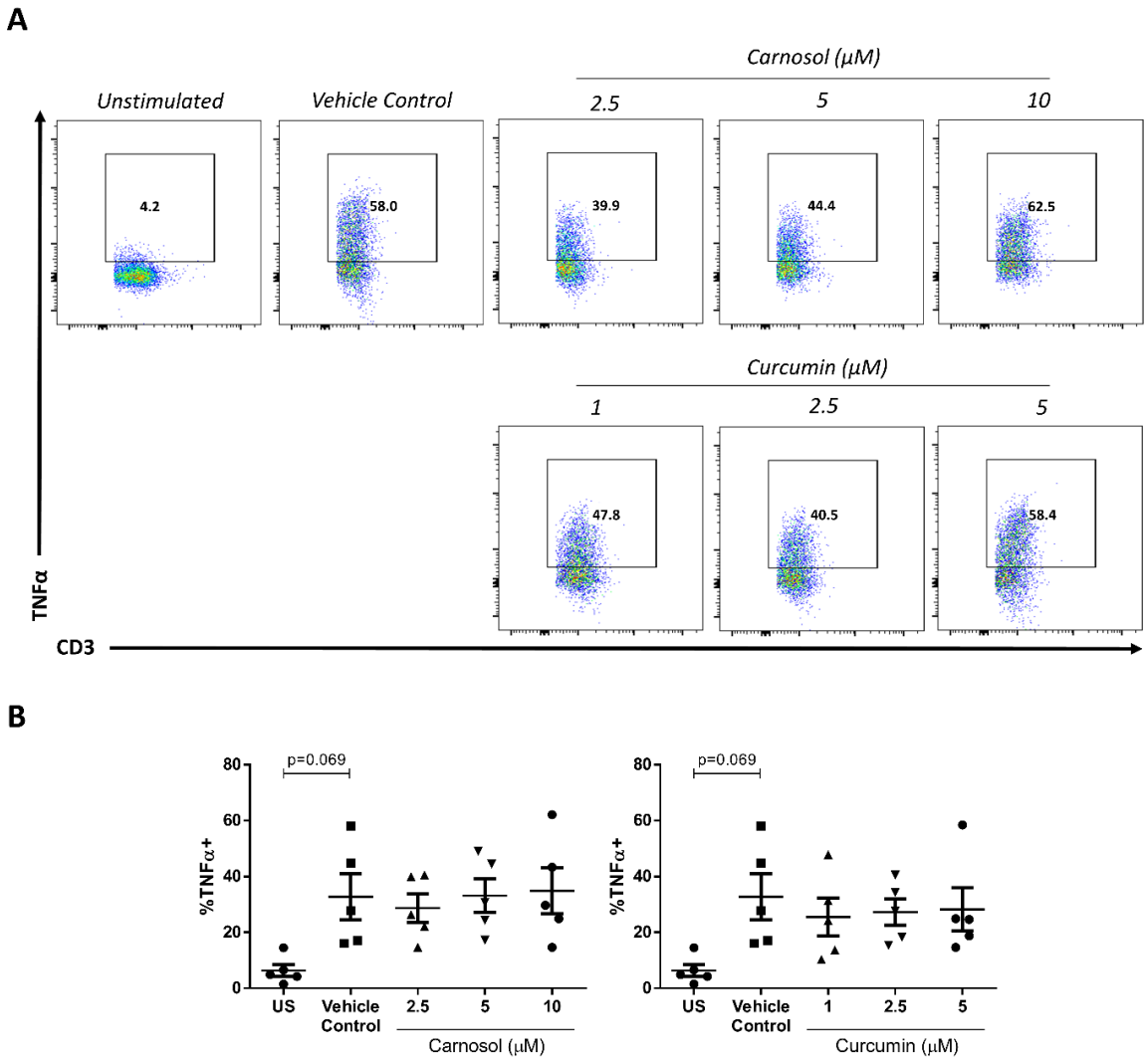

Figure 5.10. Carnosol and curcumin do not alter the frequency of TNFα producing T cells. PBMC were either left unstimulated (US), or incubated with carnosol (2.5-10 μM), curcumin (1-5 μM) or a vehicle control for 6 hours prior to stimulation with anti-CD3 for 3-4 days. PBMC were then restimulated with PMA and ionomycin in the presence of brefeldin A for 6 hours and cytokine production by $CD3^+CD8^-$ T cells was analysed by flow cytometry. **(A)** Dot plots depicting the proportion of $TNFα^+$ cells within the $CD3^+CD8^-$ population of carnosol- and curcumin-treated PBMC. Data is from one donor and is representative of five independent experiments. **(B)** Pooled data (n=5) depicting the mean (±SEM) percentage of $TNFα^+$ cells within the $CD3^+CD8^-$ population of carnosol- and curcumin-treated PBMC. Statistical significance was determined by one-way ANOVA, with Dunnett's multiple comparisons post hoc test to compare treatment groups against the control group.

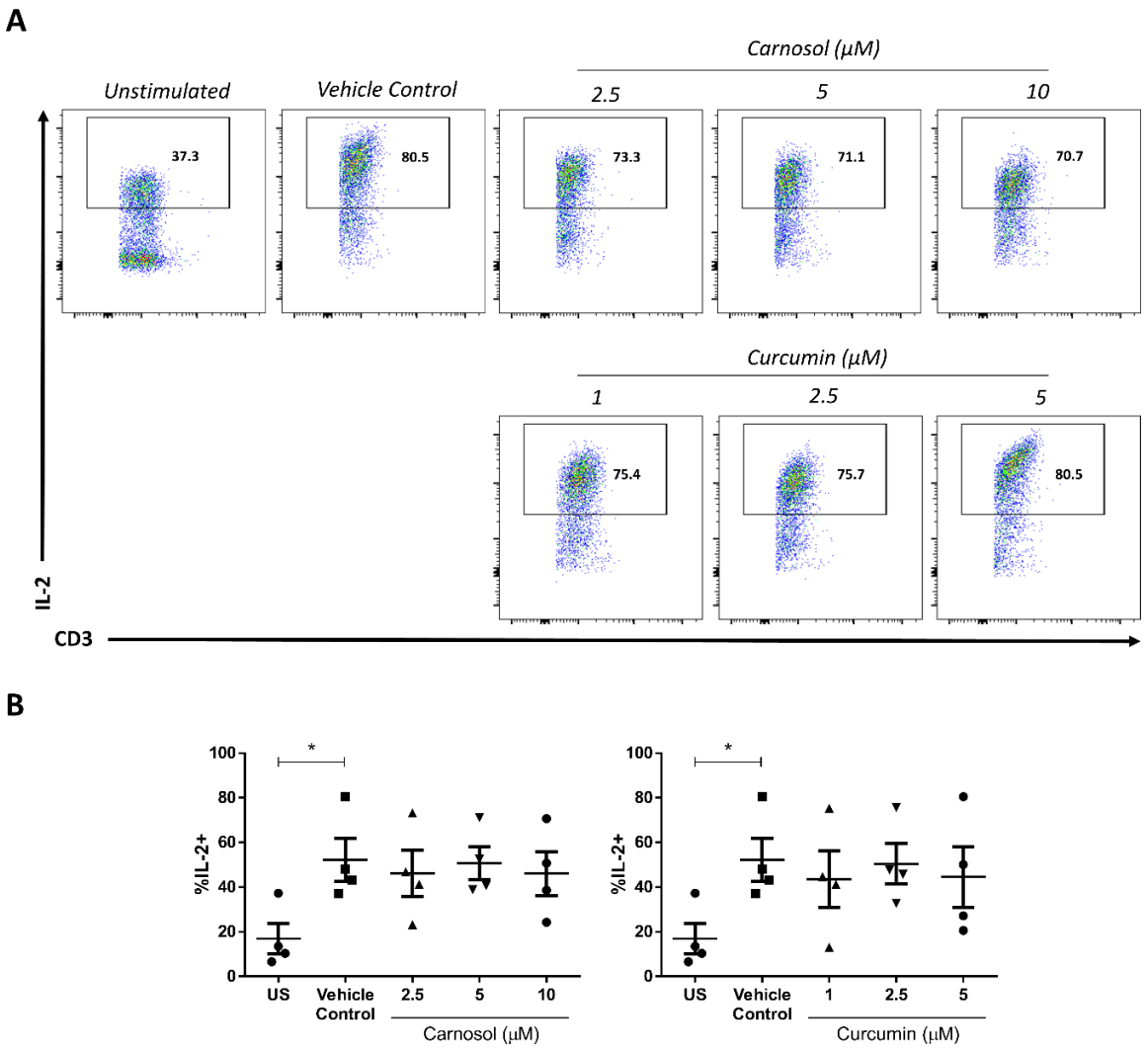

Figure 5.11. Carnosol and curcumin do not alter the frequency of IL-2 producing T cells. PBMC were either left unstimulated (US), or incubated with carnosol (2.5-10 μM), curcumin (1-5 μM) or a vehicle control for 6 hours prior to stimulation with anti-CD3 for 3-4 days. PBMC were then restimulated with PMA and ionomycin in the presence of brefeldin A for 6 hours and cytokine production by $CD3^+CD8^-$ T cells was analysed by flow cytometry. **(A)** Dot plots depicting the proportion of $IL\text{-}2^+$ cells within the $CD3^+CD8^-$ population of carnosol- and curcumin-treated PBMC. Data is from one donor and is representative of five independent experiments. **(B)** Pooled data (n=5) depicting the mean (±SEM) percentage of $IL\text{-}2^+$ cells within the $CD3^+CD8^-$ population of carnosol- and curcumin-treated PBMC. Statistical significance was determined by one-way ANOVA, with Dunnett's multiple comparisons post hoc test to compare treatment groups against the control group (*$p<0.05$).

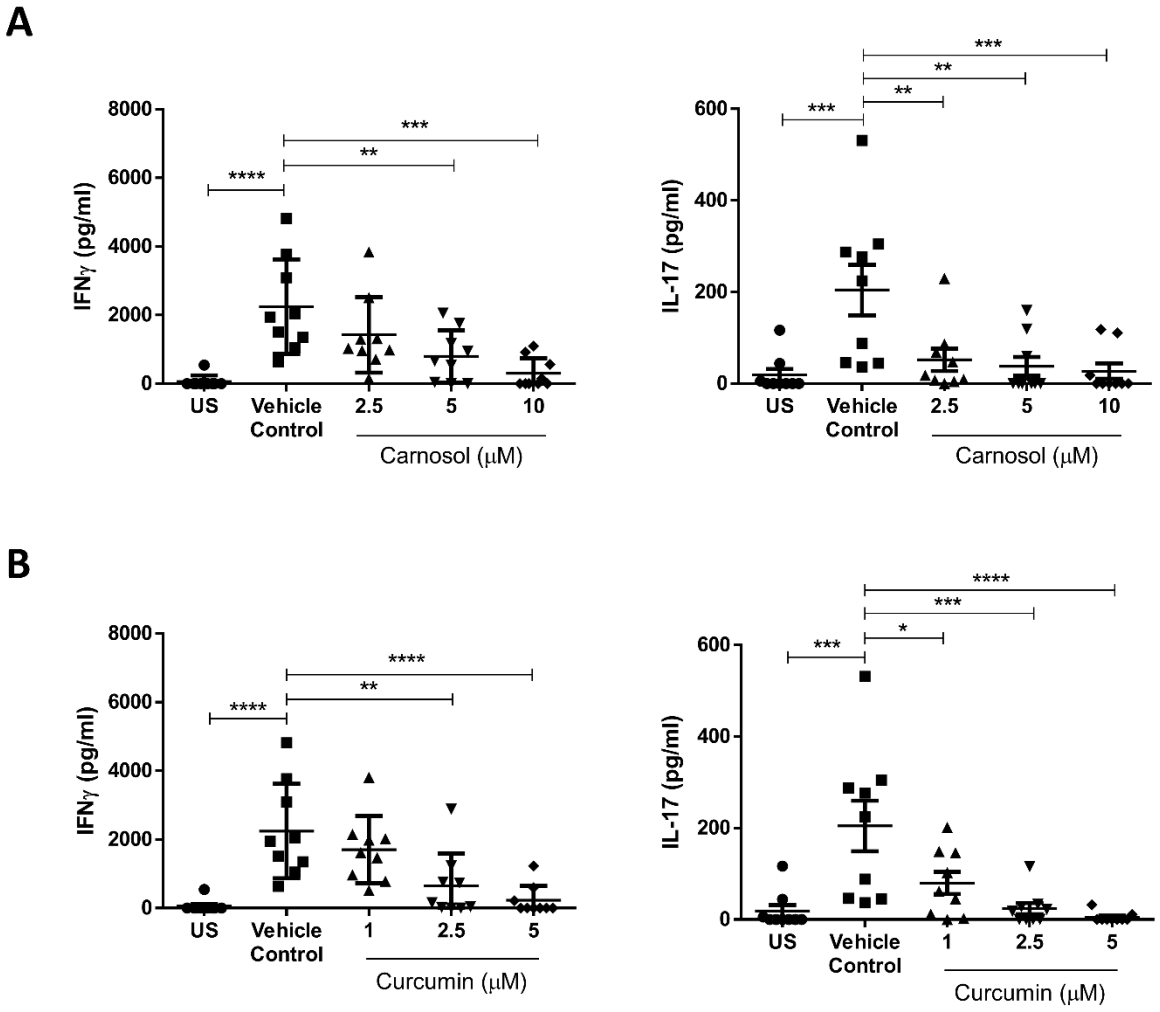

Figure 5.12. Carnosol and curcumin inhibit IFNγ and IL-17 production by PBMC. PBMC were either unstimulated (US) or incubated with carnosol (2.5-10 μM), curcumin (1-5 μM) or a vehicle control for 6 hours prior to stimulation with anti-CD3 for 3-4 days. The concentration of IFNγ and IL-17 in cell culture supernatants was measured by ELISA. Pooled data (n=9) depicts mean (±SEM) concentrations of IFNγ and IL-17 in PBMC treated with **(A)** carnosol or **(B)** curcumin (means of three technical replicates per donor). Statistical significance was determined by one-way ANOVA, with Dunnett's multiple comparisons post hoc test to compare treatment groups against the control group (****p<0.0001, ***p<0.001, **p<0.01, *p<0.05).

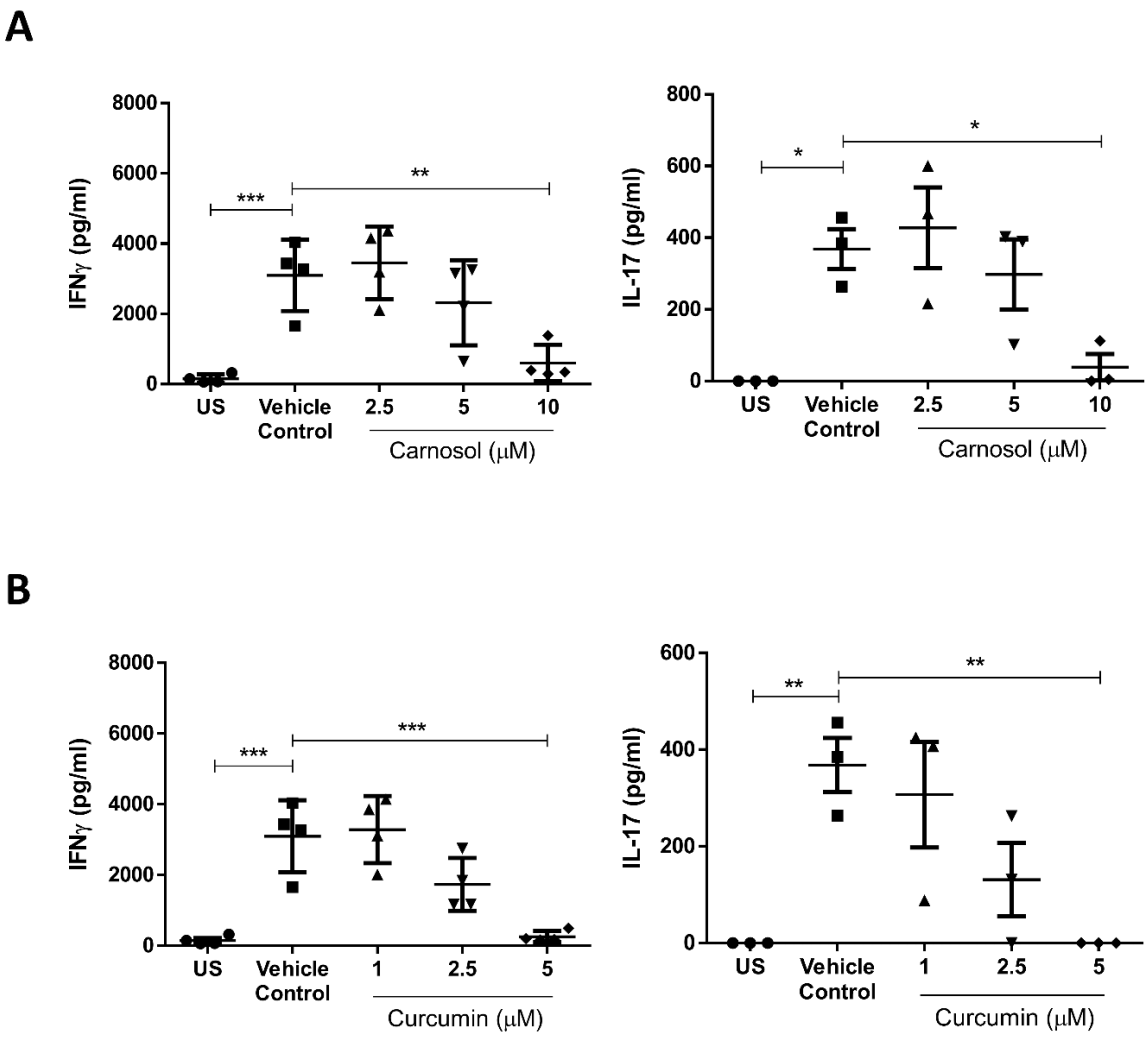

Figure 5.13. Carnosol and curcumin inhibit IFNγ and IL-17 production by CD4⁺ T cells. CD4⁺ T cells were either unstimulated (US) or incubated with carnosol (2.5-10 μM), curcumin (1-5 μM) or a vehicle control for 6 hours prior to stimulation with anti-CD3 and anti-CD28 for 3-4 days. The concentration of IFNγ and IL-17 in cell culture supernatants was measured by ELISA. Pooled data (n=3-4) depicts mean (±SEM) concentrations of IFNγ and IL-17 in CD4⁺ T cells treated with **(A)** carnosol or **(B)** curcumin (means of three technical replicates per donor). Statistical significance was determined by one-way ANOVA, with Dunnett's multiple comparisons post hoc test to compare treatment groups against the control group (***p<0.001, **p<0.01,*p<0.05).

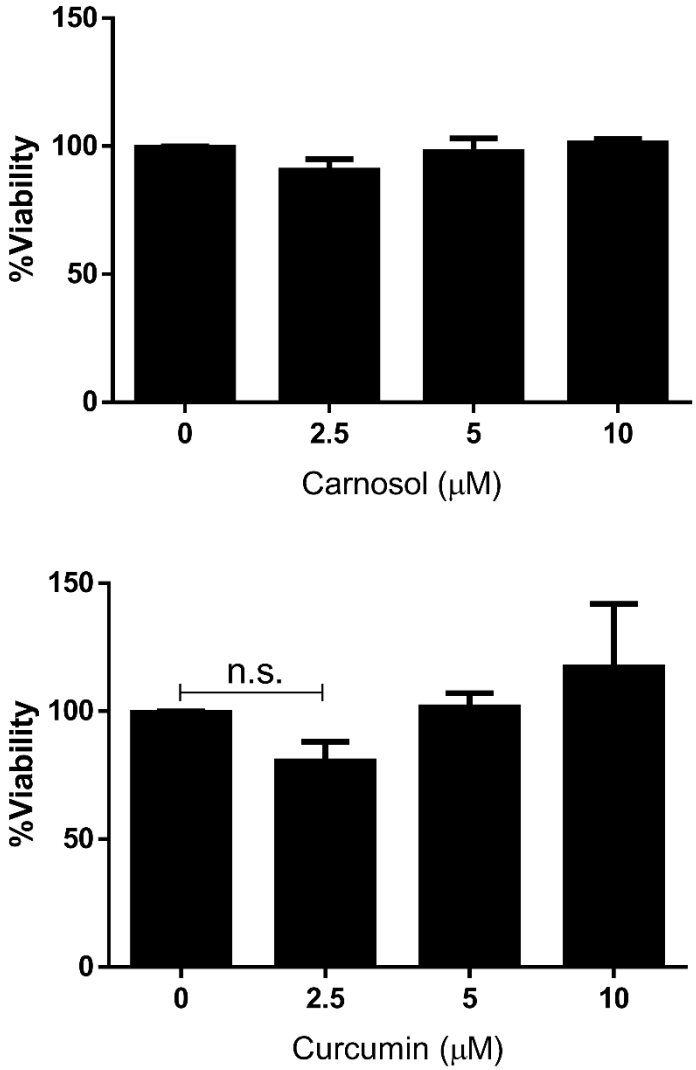

Figure 5.14. Carnosol and curcumin are non-toxic to HaCaT keratinocytes. HaCaT keratinocytes were treated with carnosol (2.5-10 μM), curcumin (2.5-10 μM) or a vehicle control for 24 hours. Viability was determined via alamarBlue reduction over 18 hours. Pooled data (n=3) depicts mean (±SEM) percentage viability of control, carnosol and curcumin treated HaCaTs (means of three technical replicates per experiment). Statistical significance was determined by one-way ANOVA, with Tukey's multiple comparisons post hoc test to compare the means of all treatment groups.

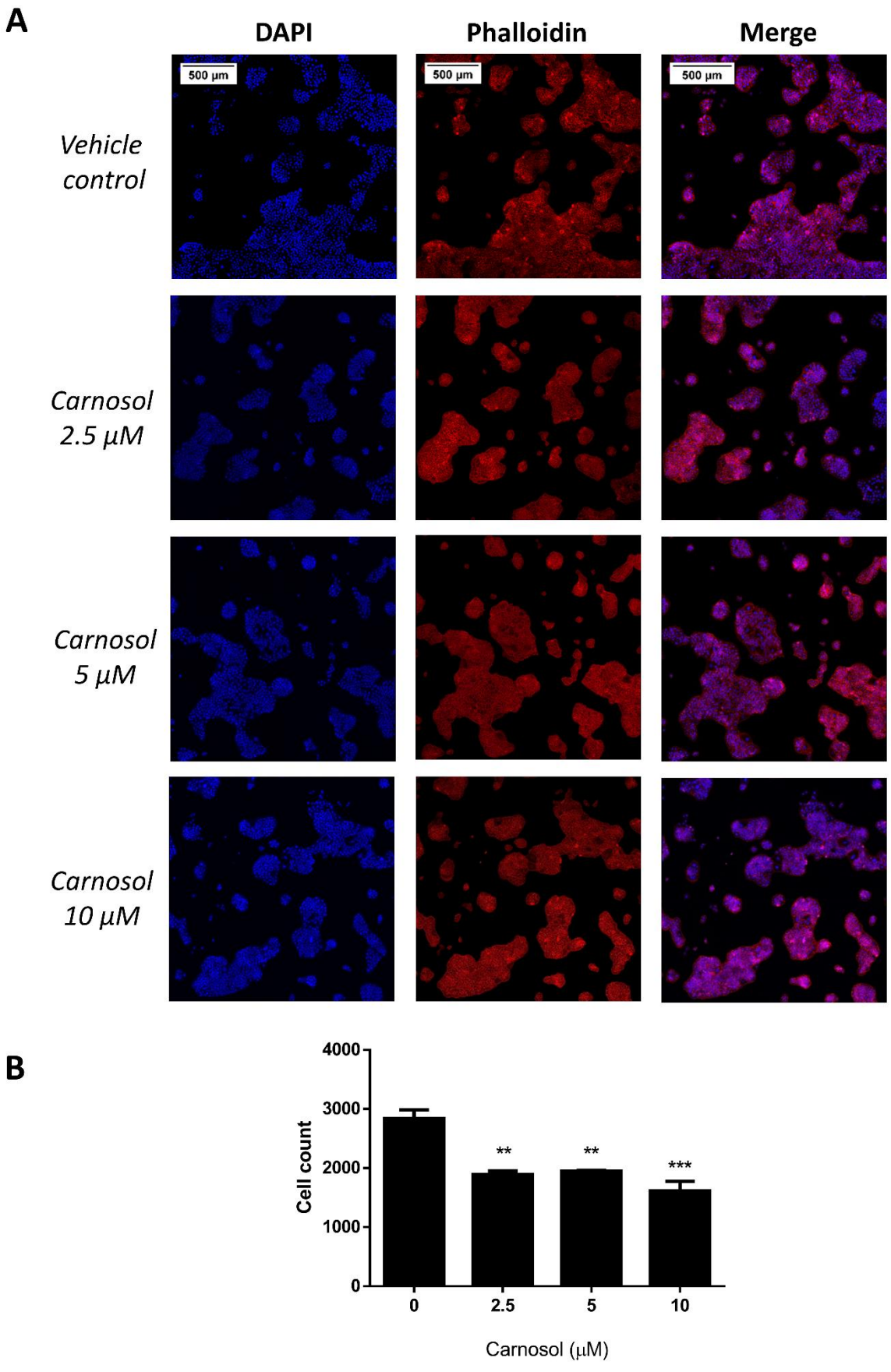
A
DAPI
Phalloidin
Merge
500 µm
Vehicle control
Carnosol 2.5 µM
Carnosol 5 µM
Carnosol 10 µM
B
Cell count
4000
3000
2000
1000
0
**
**
***
0
2.5
5
10
Carnosol (µM)

Figure 5.15. Carnosol reduces basal proliferation of HaCaT keratinocytes. HaCaT keratinocytes were treated with carnosol (2.5-10 μM) or a vehicle control for 24 hours. The nuclei and actin cytoskeleton were stained with DAPI and phalloidin, respectively. Cells were imaged by confocal microscopy, and cell proliferation was determined via cell count using ImageJ software. Each treatment group was imaged and counted in duplicate. **(A)** DAPI, phalloidin and composite images for each treatment group. Data shown is representative of two independent experiments. **(B)** Pooled data (n=2) depicting mean (±SEM) cell counts for each treatment group. Statistical significance was determined by one-way ANOVA with Dunnett's post hoc test to compare carnosol treatment groups to the vehicle control (***$p<0.001$, **$p<0.01$).

A

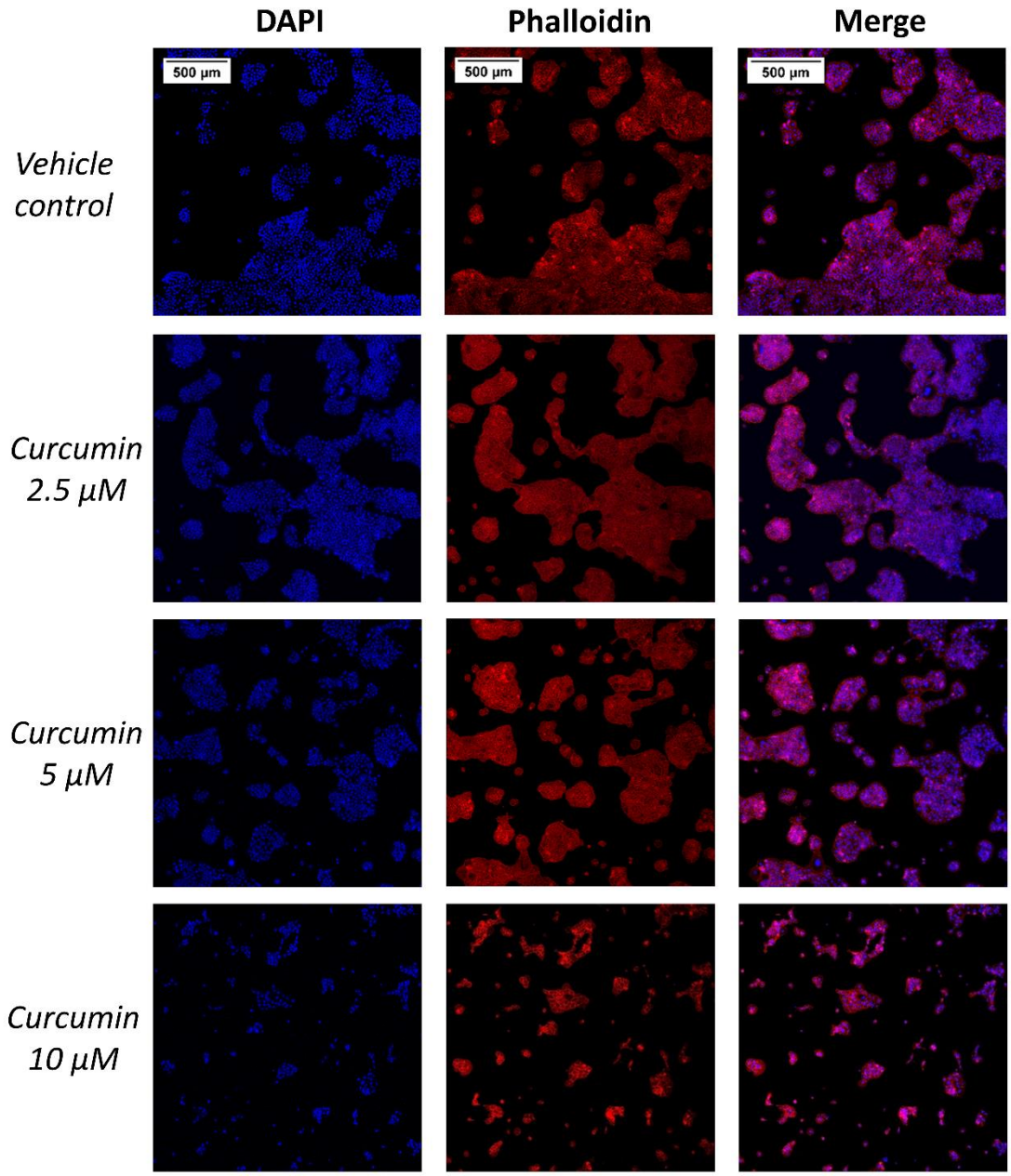
DAPI
Phalloidin
Merge
500 µm
Vehicle control
Curcumin 2.5 µM
Curcumin 5 µM
Curcumin 10 µM

B

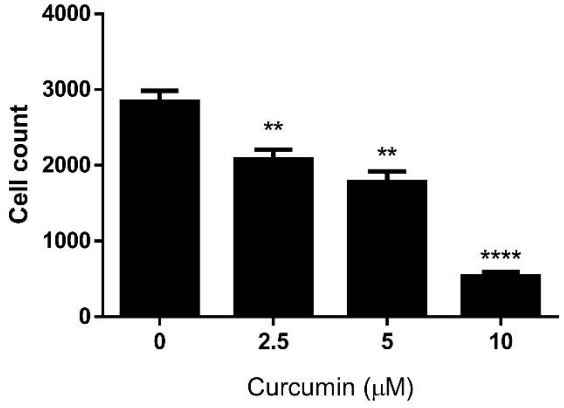
Cell count
4000
3000
2000
1000
0
**
**
****
0
2.5
5
10
Curcumin (µM)

Figure 5.16. Curcumin reduces basal proliferation of HaCaT keratinocytes. HaCaT keratinocytes were treated with curcumin (2.5-10 μM) or a vehicle control for 24 hours. The nuclei and actin cytoskeleton were stained with DAPI and phalloidin, respectively. Cells were imaged by confocal microscopy, and cell proliferation was determined via cell count using ImageJ software. Each treatment group was imaged and counted in duplicate. **(A)** DAPI, phalloidin and composite images for each treatment group. Data shown is representative of two independent experiments. **(B)** Pooled data (n=2) depicting mean (±SEM) cell counts for each treatment group. Statistical significance was determined by one-way ANOVA with Dunnett's post hoc test to compare curcumin treatment groups to the vehicle control (****$p<0.0001$, **$p<0.01$).

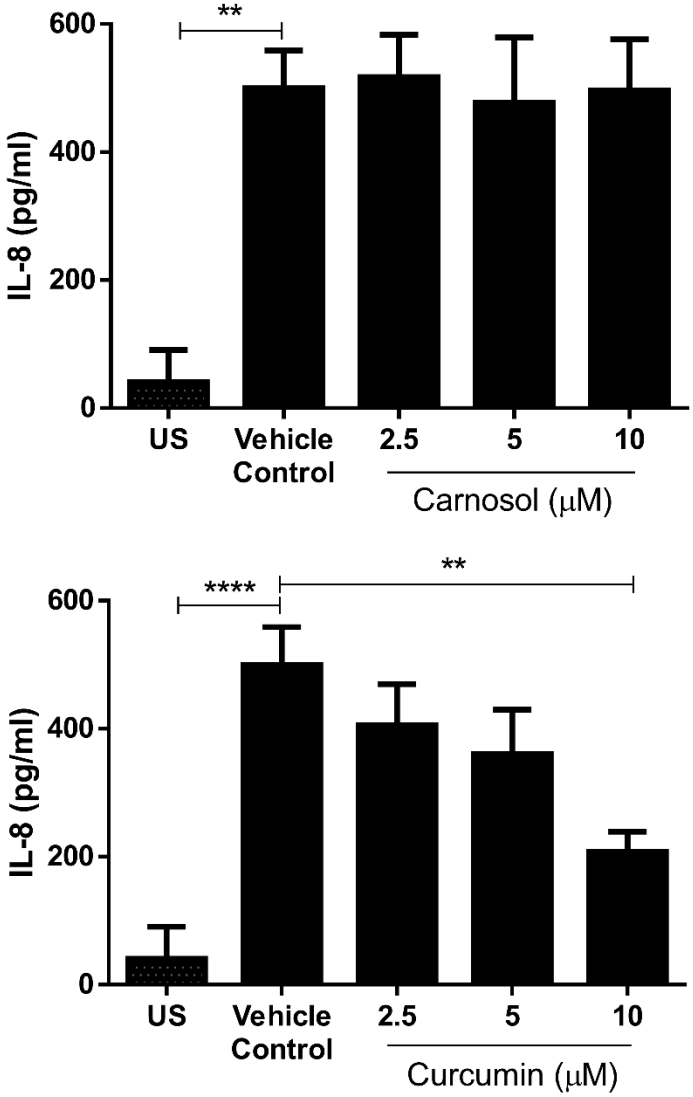

Figure 5.17. Curcumin, but not carnosol, significantly reduces IL-8 production by HaCaT keratinocytes. HaCaT keratinocytes were either unstimulated (US) or treated with carnosol (2.5-10 μM), curcumin (2.5-10 μM), or a vehicle control for 6 hours prior to stimulation with TNFα (100 ng/ml) for 24 hours. The concentration of IL-8 in cell culture supernatants was measured by ELISA. Pooled data (n=4) depicts mean (± SEM) concentration of IL-8 in carnosol, curcumin or control treated HaCaTs (means of three technical replicates per experiment). Statistical significance was determined by one-way ANOVA, with Dunnett's multiple comparisons post hoc test to compare means of all treatment groups to the control group (****$p<0.0001$, **$p<0.01$).

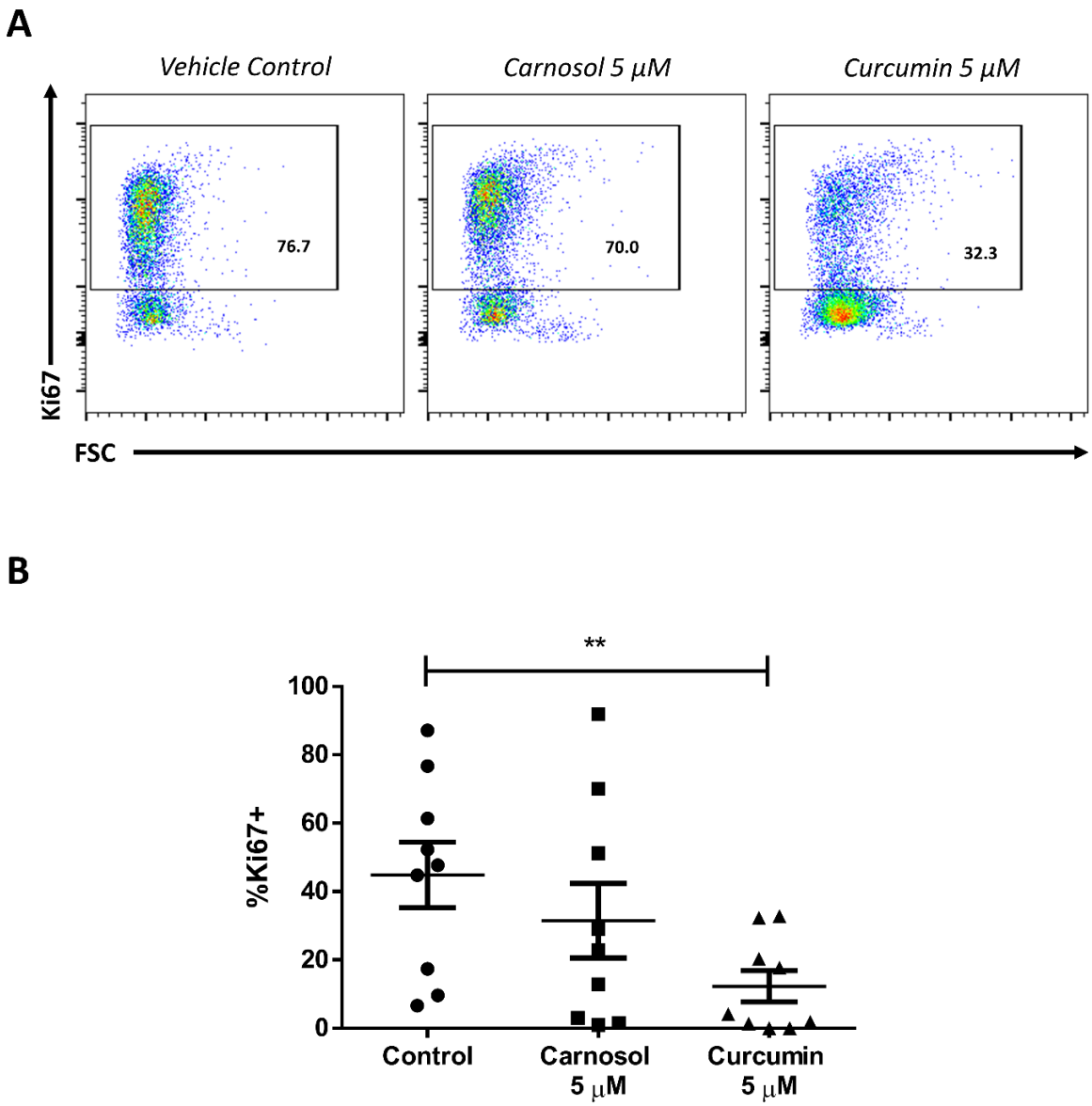

Figure 5.18. Curcumin, but not carnosol, significantly inhibits T cell proliferation in *ex vivo* PBMC from psoriasis patients. PBMC isolated from psoriasis patients (n=9) were treated with carnosol (5 µM), curcumin (5 µM) or a vehicle control for 6 hours prior to stimulation with anti-CD3. After 4 days, cells were restimulated with PMA and ionomycin in the presence of brefeldin A, and analysed by flow cytometry. **(A)** Dot plots depicting expression of the proliferation marker Ki67 in $CD3^{+}CD8^{-}$ T cells from control-, carnosol- or curcumin-treated PBMC. Data is from one patient and is representative of nine patient samples. **(B)** Pooled data (n=9) depicting mean (±SEM) percentage expression of the proliferation marker Ki67 in $CD3^{+}CD8^{-}$ T cells from control-, carnosol- or curcumin-treated PBMC. Statistical significance was determined by one-way ANOVA with Dunnett's post hoc test to compare carnosol and curcumin treatment to the control (**p<0.01).

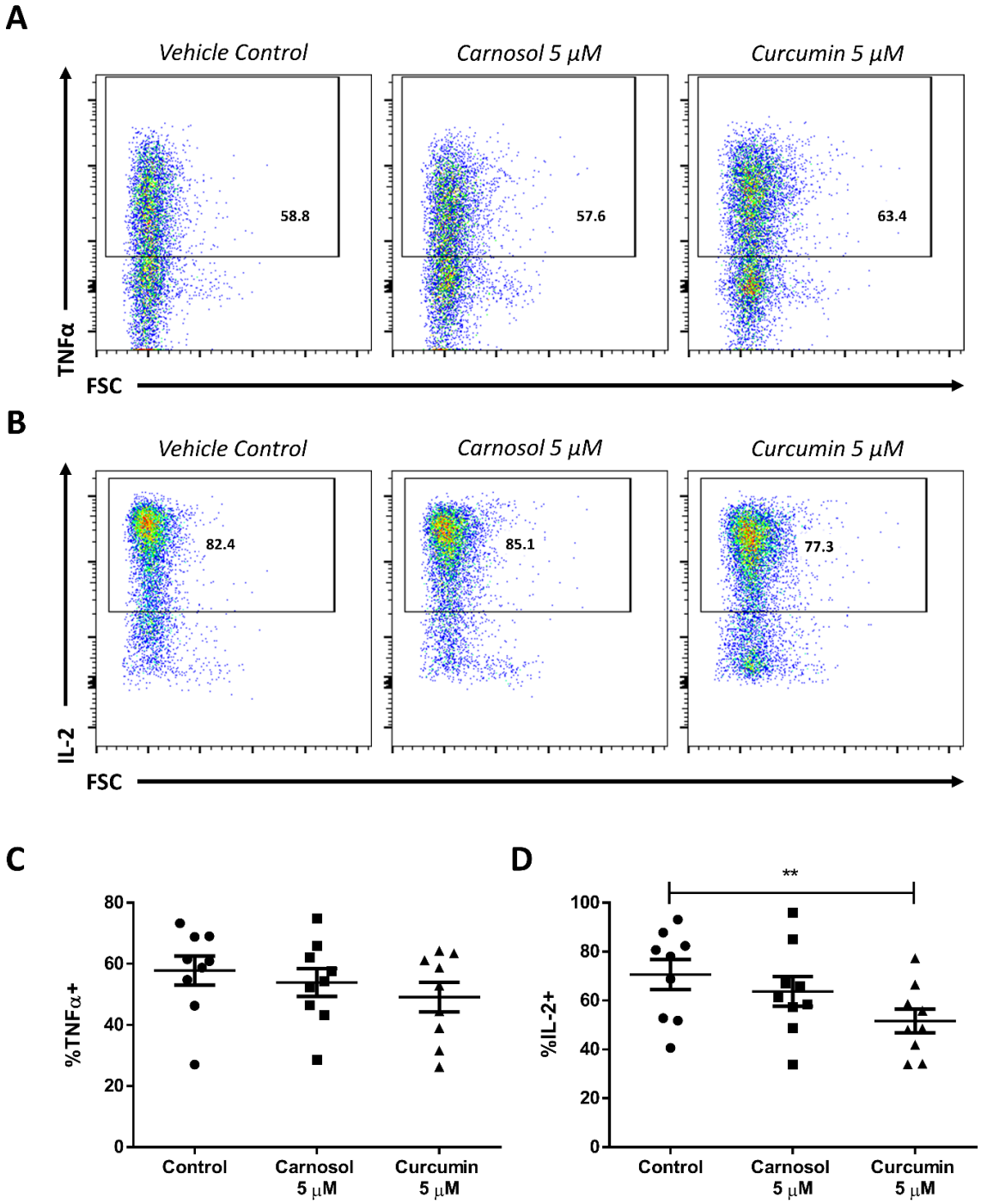

Figure 5.19. Curcumin slightly reduces IL-2, but not TNFα, expression in *ex vivo* PBMC from psoriasis patients. PBMC isolated from psoriasis patients (n=9) were treated with carnosol (5 μM), curcumin (5 μM) or a vehicle control for 6 hours prior to stimulation with anti-CD3. After 4 days, cells were restimulated with PMA and ionomycin in the presence of brefeldin A, and analysed by flow cytometry. Dot plots depict expression of TNFα **(A)** and IL-2 **(B)** by $CD3^+CD8^-$ T cells from control-, carnosol- or curcumin-treated PBMC. Data is from one patient and is representative of nine patient samples. Pooled data (n=9) depicts mean (±SEM) percentage expression of TNFα **(C)** and IL-2 **(D)** by $CD3^+CD8^-$ T cells from control-, carnosol- or curcumin-treated PBMC. Statistical significance was determined by one-way ANOVA with Dunnett's post hoc test to compare carnosol and curcumin treatment to the control (**p<0.01).

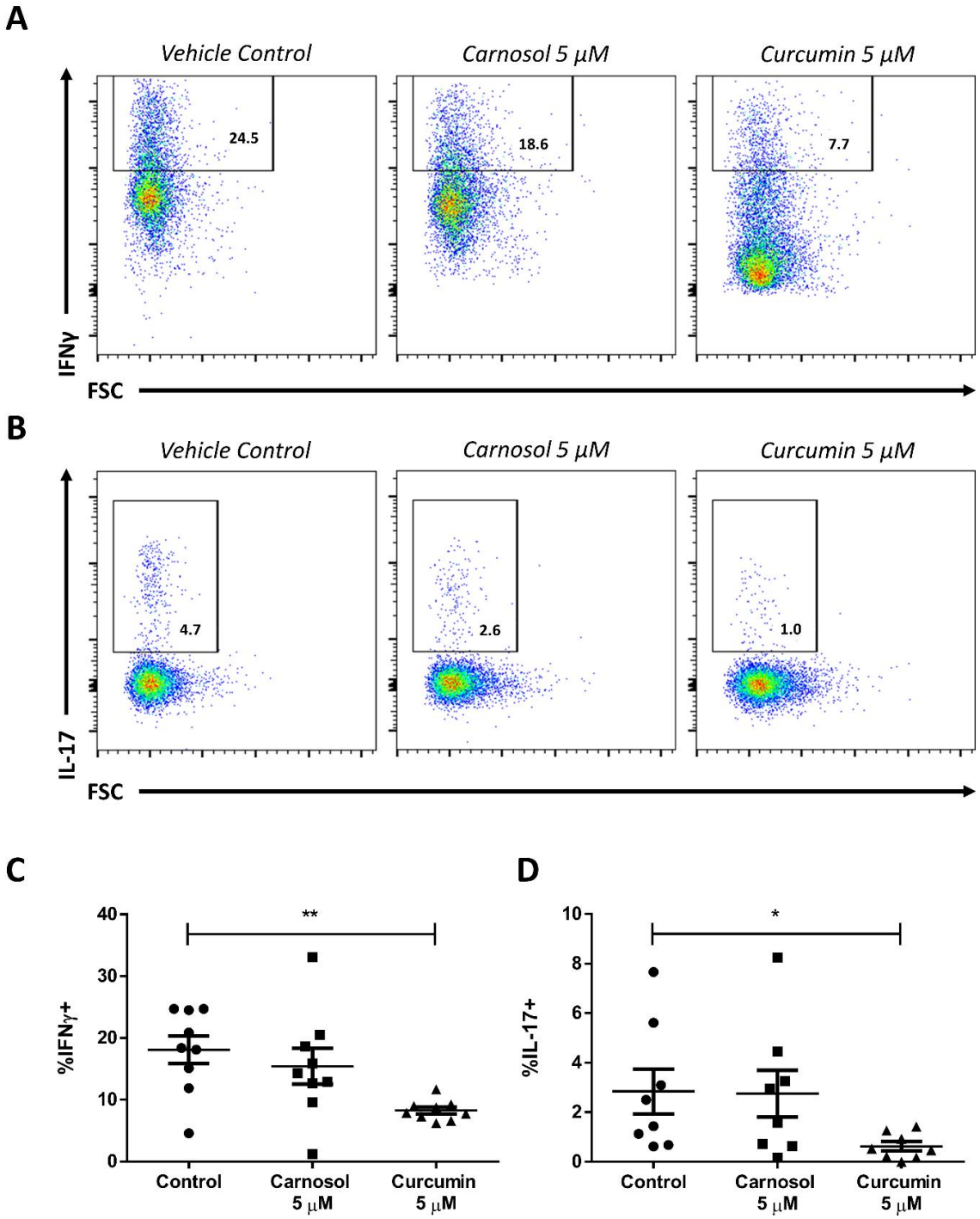

Figure 5.20. Curcumin, but not carnosol, significantly reduces expression of IFNγ and IL-17 in *ex vivo* PBMC from psoriasis patients. PBMC isolated from psoriasis patients (n=9) were treated with carnosol (5 μM), curcumin (5 μM) or a vehicle control for 6 hours prior to stimulation with anti-CD3. After 4 days, cells were restimulated with PMA and ionomycin in the presence of brefeldin A, and analysed by flow cytometry. Dot plots depict expression of IFNγ **(A)** and IL-17 **(B)** by $CD3^+CD8^-$ T cells from control-, carnosol- or curcumin-treated PBMC. Data is from one patient and is representative of nine patient samples. Pooled data (n=9) depicts mean (±SEM) percentage expression of IFNγ **(C)** and IL-17 **(D)** by $CD3^+CD8^-$ T cells from control-, carnosol- or curcumin-treated PBMC. Statistical significance was determined by one-way ANOVA with Dunnett's post hoc test to compare carnosol and curcumin treatment to the control (**p<0.01, *p<0.05).

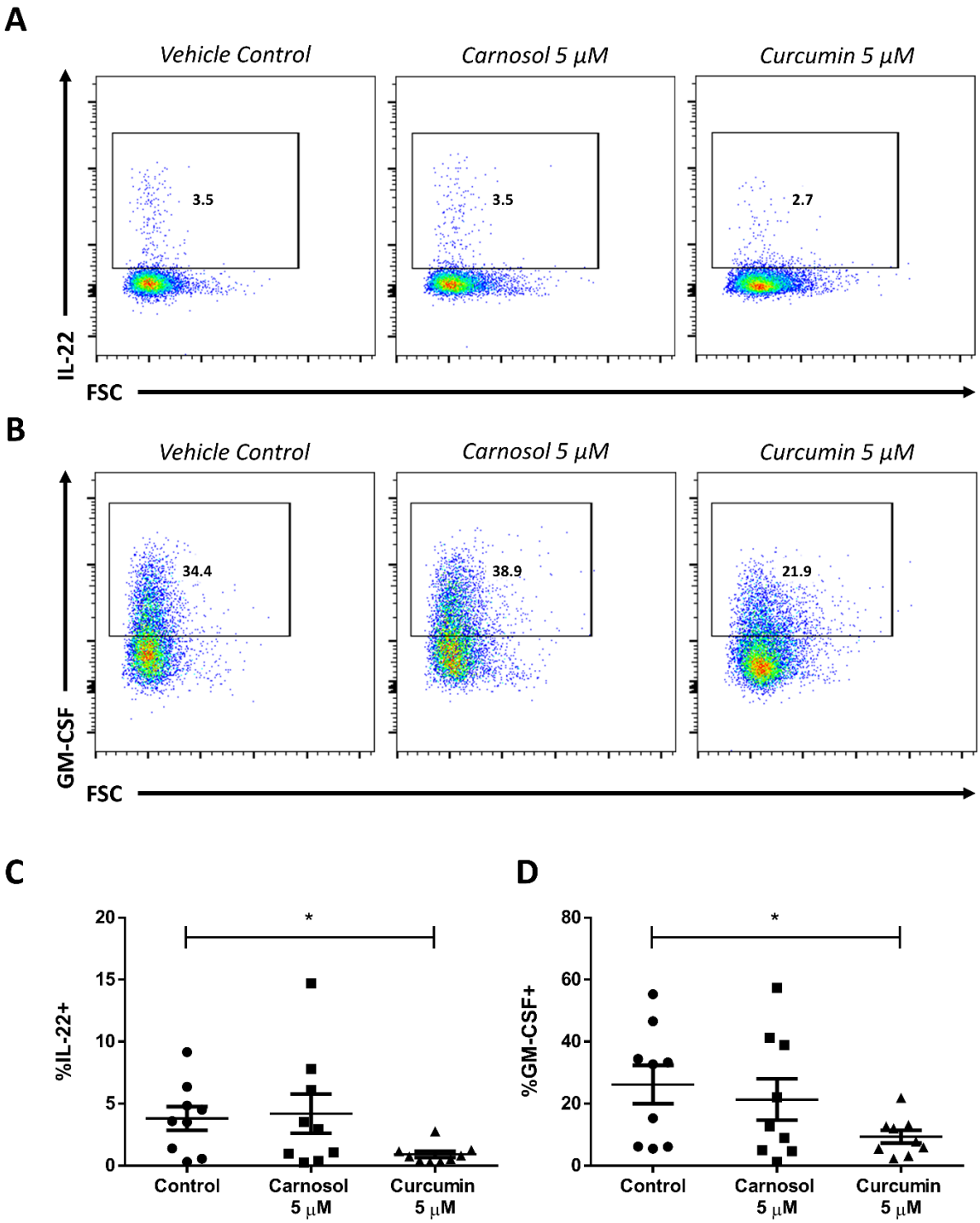

Figure 5.21. Curcumin, but not carnosol, significantly reduces expression of IL-22 and GM-CSF in *ex vivo* PBMC from psoriasis patients. PBMC isolated from psoriasis patients (n=9) were treated with carnosol (5 µM), curcumin (5 µM) or a vehicle control for 6 hours prior to stimulation with anti-CD3. After 4 days, cells were restimulated with PMA and ionomycin in the presence of brefeldin A, and analysed by flow cytometry. Dot plots depict expression of IL-22 **(A)** and GM-CSF **(B)** by $CD3^+CD8^-$ T cells from control-, carnosol- or curcumin-treated PBMC. Data is from one patient and is representative of nine patient samples. Pooled data (n=9) depicts mean (±SEM) percentage expression of IL-22 **(C)** and GM-CSF **(D)** by $CD3^+CD8^-$ T cells from control-, carnosol- or curcumin-treated PBMC. Statistical significance was determined by one-way ANOVA with Dunnett's post hoc test to compare carnosol and curcumin treatment to the control (*$p<0.05$).

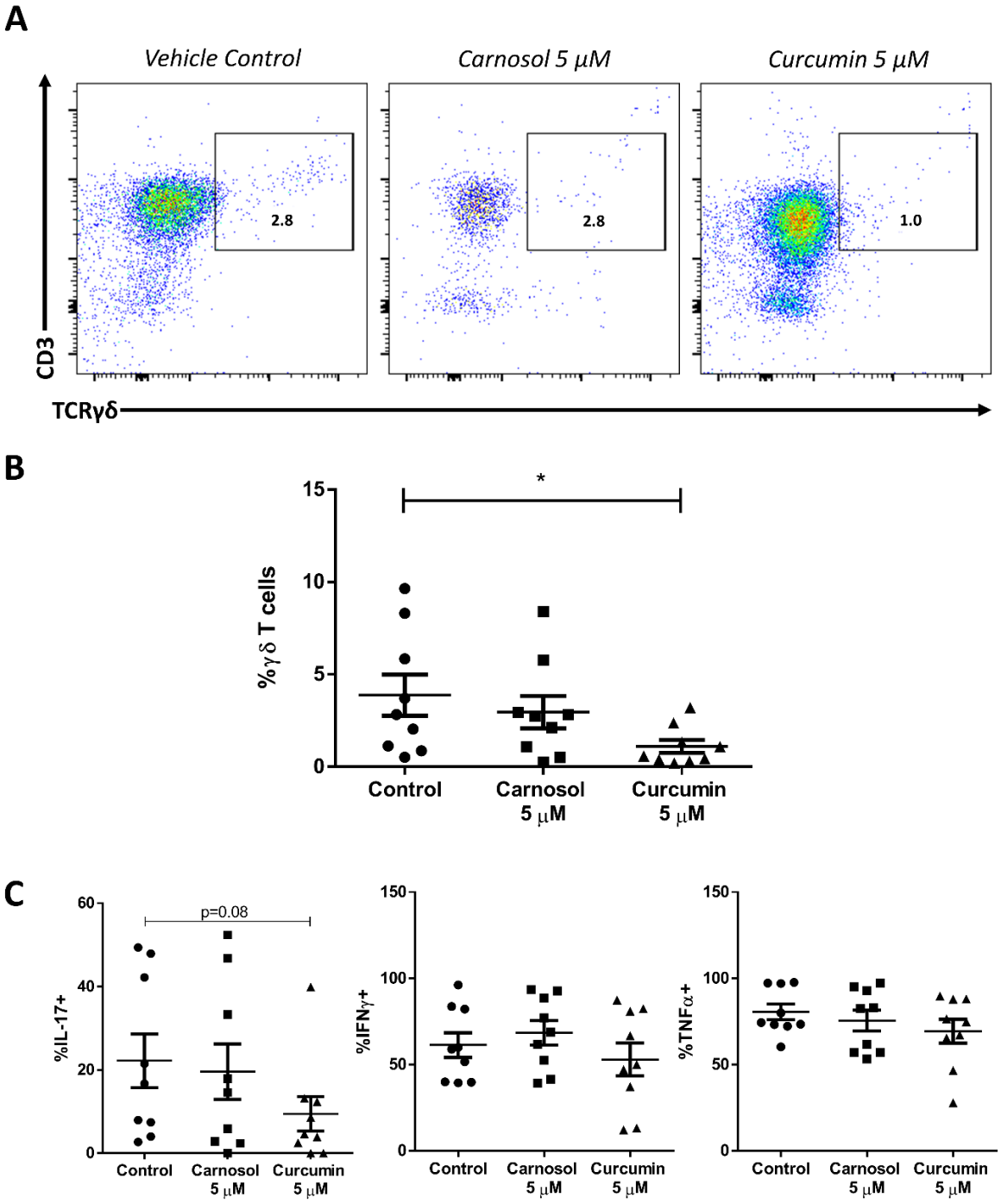

Figure 5.22. Curcumin, but not carnosol, significantly reduces the frequency of γδ T cells in *ex vivo* PBMC from psoriasis patients. PBMC isolated from psoriasis patients (n=9) were treated with carnosol (5 μM), curcumin (5 μM) or a vehicle control for 6 hours prior to stimulation with anti-CD3. After 4 days, cells were restimulated with PMA and ionomycin in the presence of brefeldin A, and analysed by flow cytometry. **(A)** Dot plots depicting the frequency of $CD3^+TCR\gamma\delta^+$ T cells from control-, carnosol- or curcumin-treated PBMC. Data is from one patient and is representative of nine patient samples. **(B)** Pooled data (n=9) depicting mean (±SEM) percentage frequency of $CD3^+TCR\gamma\delta^+$ T cells from control-, carnosol- or curcumin-treated psoriasis patient PBMC. **(C)** Pooled data (n=9) depicting mean (±SEM) percentage expression of IL-17, IFNγ and TNFα by $CD3^+TCR\gamma\delta^+$ T cells from control-, carnosol- or curcumin-treated PBMC. Statistical significance was determined by one-way ANOVA with Dunnett's post hoc test to compare carnosol and curcumin treatment to the control (*$p<0.05$).

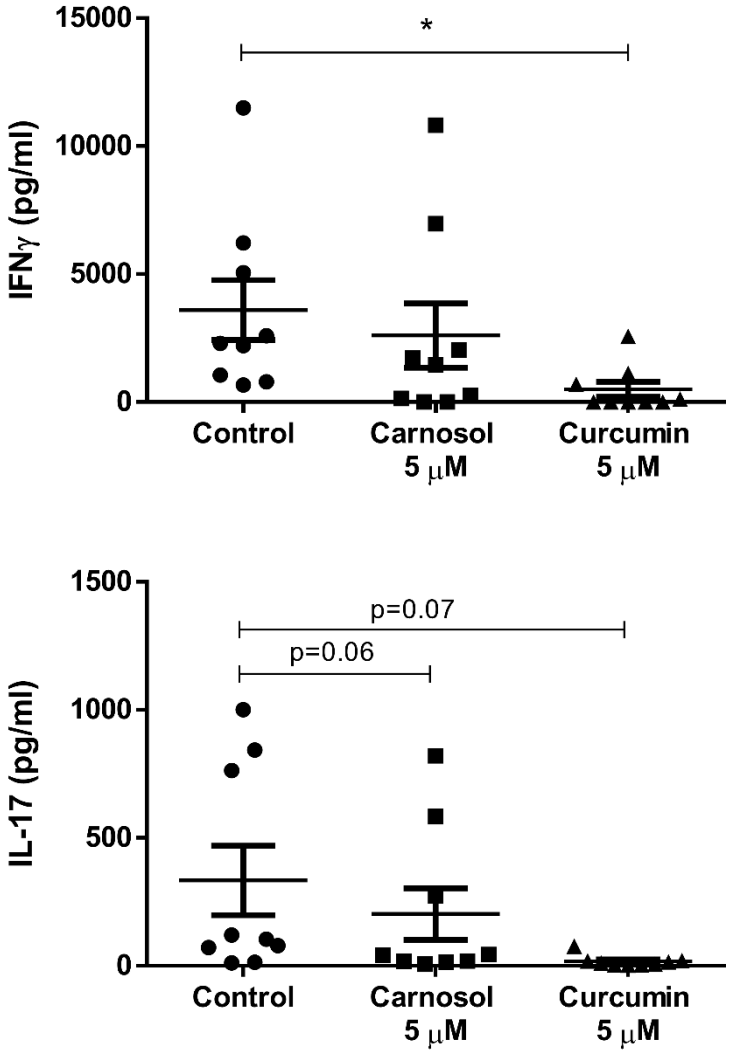

Figure 5.23. Curcumin reduces the production of IFNγ and IL-17 by *ex vivo* PBMC from psoriasis patients. PBMC isolated from psoriasis patients (n=9) were treated with carnosol (5 μM), curcumin (5 μM) or a vehicle control for 6 hours prior to stimulation with anti-CD3. After 4 days, the concentration of IFNγ and IL-17 in cell culture supernatants was measured by ELISA. Pooled data (n=9) depicts mean (±SEM) concentrations of IFNγ and IL-17 in cell culture supernatants of control, carnosol and curcumin treated PBMC (means of two or three technical replicates per patient). Statistical significance was determined by one-way ANOVA with Dunnett's post hoc test to compare carnosol and curcumin treatment to the control (*$p<0.05$).

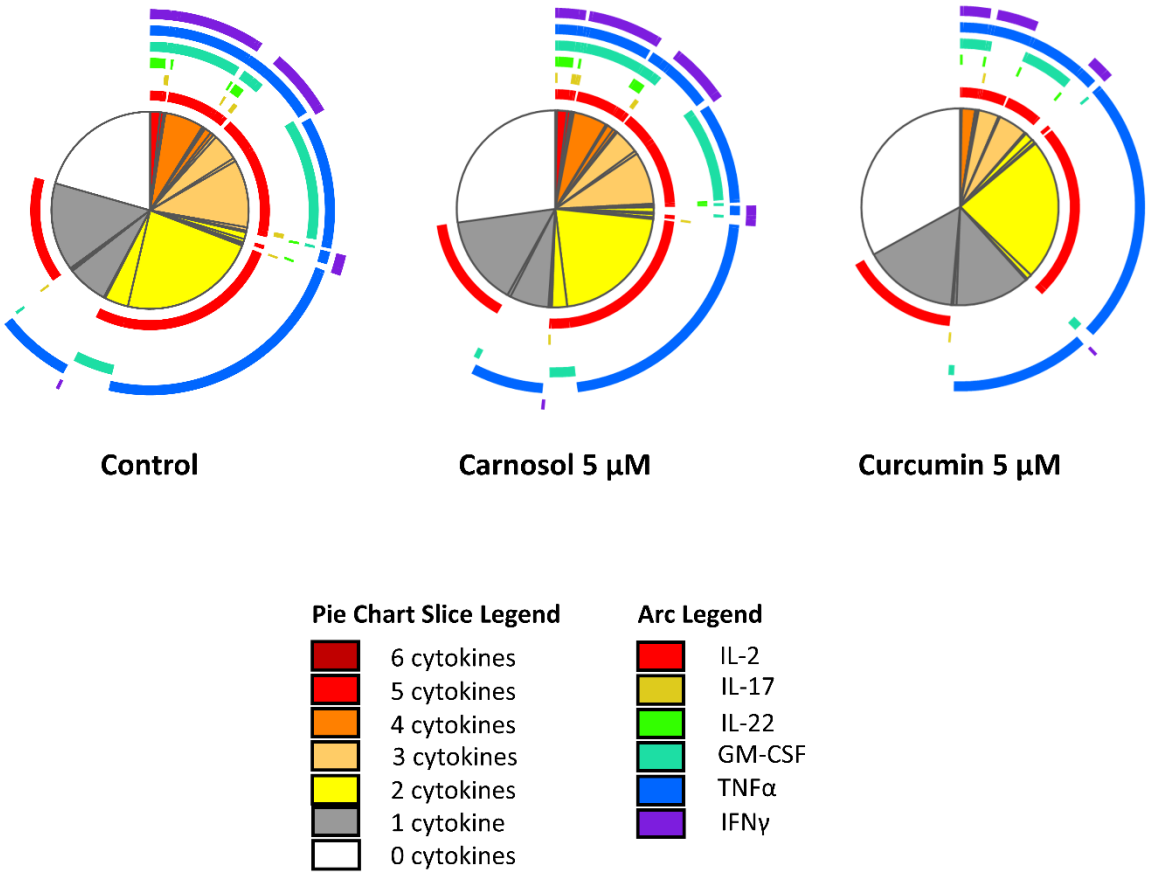

Figure 5.24. Curcumin reduces the poly-functionality of T cells in *ex vivo* PBMC from psoriasis patients. PBMC isolated from psoriasis patients (n=9) were treated with carnosol (5 µM), curcumin (5 µM) or a vehicle control for 6 hours prior to stimulation with anti-CD3. After 4 days, cells were restimulated with PMA and ionomycin in the presence of brefeldin A, and analysed by flow cytometry. The cytokine expression profiles of T cells from control-, carnosol- and curcumin-treated psoriasis patient PBMC were analysed using SPICE software. The pie charts represent the average frequencies of $CD3^{+}CD8^{-}$ T cells producing every combination of cytokines for multiple patients (n=9). The segments within the pie charts denote proportions of the $CD3^{+}CD8^{-}$ T cell population producing different combinations of cytokines, and are heat-map coded to indicate increasing cytokine production. The arcs surrounding the pie charts indicate the cytokine(s) produced by that proportion of cells.

5.4 Discussion

Management of autoimmune disease can be achieved by regulating pro-inflammatory immune responses initiated by APCs, propagated by adaptive immune cells, and exacerbated by bystander cells within the inflammatory microenvironment. Although the immunomodulatory effects of HO-1 in DC are well established, it is comparatively unclear whether this antioxidant and anti-inflammatory enzyme can also regulate the activity of adaptive immune cells and non-immune cells, especially in the context of autoimmunity. This question is of considerable relevance, as treatments for autoimmune diseases are most often administered after the onset of symptoms, when autoreactive T cells have already become activated and destructive inflammation is in place. Thus, an ideal therapy for autoimmunity would downregulate existing pro-inflammatory activity within autoreactive T cells and local tissues, prevent further activation of these cells via APCs, and re-establish peripheral tolerance by promoting Tregs and tolerogenic DC. The results of this chapter therefore aim to expand on previous work which described important anti-inflammatory effects for the HO-1 inducers, carnosol and curcumin, in human DC, by investigating their use in human PBMC/T cells. Furthermore, this chapter places the regulation of adaptive immune responses and bystander cells by carnosol and curcumin into the context of psoriasis, a prevalent autoimmune disease, by examining their activity within human keratinocytes and *ex vivo* PBMC isolated from psoriasis patients.

Although there have been a number of studies which have reported a role for HO-1 in the regulation of adaptive immune cells, it is currently thought that this is achieved through the action of HO-1 in APCs. In the present study, the HO-1 inducers carnosol and curcumin were found to inhibit T cell proliferation and expression of the pro-inflammatory cytokines IL-17 and IFNγ within healthy human PBMC stimulated with anti-CD3. These results are in agreement with those of Pae *et al.* who reported that HO-1 overexpression or CoPP treatment inhibits the proliferation of Jurkat T cells, human PBMC and human $CD4^+$ T cells (183,184). Conversely, Burt *et al.* previously reported that HO-1 inhibition results in the proliferation of T cells only when they are cultured in the presence of APCs (186). However, this discrepancy may be explained by differences in experimental conditions; Burt *et al.* assessed T cell proliferation in the steady state, i.e. without external stimulation (186), whereas in a study by Pae *et al.* (184), and the present study, proliferation in response to TCR stimulation was assessed. Inhibition of HO-1 in APCs may lead to increased activation of T cells in the absence of additional stimulation, whereas upregulation of HO-1 in T cells can inhibit proliferation and pro-inflammatory responses initiated by mitogenic stimulation. Indeed, while it was possible that the results obtained in PBMC were dependent on the presence of APCs, treatment of purified $CD4^+$ T cells with carnosol and curcumin also potently

inhibited their proliferation and pro-inflammatory cytokine production in response to stimulation. Therefore, it is evident that these polyphenols do regulate T cell responses independently of their activity in APCs.

This study presents data describing the anti-inflammatory effects of carnosol in adaptive immune cells for the first time. Interestingly, a study by Kim *et al.* which investigated the effects of curcumin in human $CD4^+$ T cells also reported that curcumin inhibits T cell proliferation and cytokine production in response to mitogenic stimulation. However, in addition to inhibition of Th1 and Th17 cytokines such as IFNγ and IL-17, curcumin was found to inhibit IL-2 and TNFα expression by T cells (283). In the present study, curcumin and carnosol treatment of healthy PBMC specifically reduced the frequency of $IFN\gamma^+$ and $IL\text{-}17^+$ T cells, without significant inhibition of either TNFα or IL-2. Other studies performed in murine and human splenocytes have additionally identified inhibition of IL-2 by curcumin as a contributor to the reduced proliferation observed in these cells (441,442). These differences may arise from the treatment of PBMC vs T cells alone; in this study, flow cytometry analysis of cytokine expression by T cells was performed in PBMC treated with carnosol/curcumin, while other studies have used purified $CD4^+$ T cells or splenocytes for their investigations. It is possible that the presence of APCs or other immune cells within PBMC partially suppresses the activity of these compounds in T cells. In support of this hypothesis, the inhibition of T cell proliferation by carnosol and curcumin was observed to be more potent in purified $CD4^+$ T cell populations than in PBMC. Further investigation into the action of carnosol and curcumin in mixed leukocyte populations is required to fully interpret these results.

The inhibitory effects of HO-1 in adaptive immune cells has previously been suggested to result from increased suppression by Tregs (232,423,424,427). This could occur through an increase in Treg frequency, or promotion of their suppressive function. Although Kim *et al.* reported that 5 μM curcumin treatment significantly increased the frequency of Tregs within human $CD4^+$ T cells (283), in the present study only a slight increase in Treg frequency was observed in PBMC treated with either curcumin or carnosol. Additionally, neither polyphenol altered the expression of CD39 or CTLA4 by Tregs, which contribute to their suppressive activity. Conflicting reports regarding HO-1/curcumin and Treg suppression currently exist in the literature; Forward *et al.* found that curcumin inhibited Treg-mediated suppression of murine effector T cells (441), while Choi *et al.* reported that HO-1 expression is required for the suppressive function of $Foxp3^+$ Jurkat T cells (422). Meanwhile, Zelenay *et al.* found that *HMOX1*$^{-/-}$ mice display normal levels of Tregs, with an intact suppressive capacity (187), and George *et al.* similarly observed that knockout of HO-1 in APCs, but not Tregs, impaired Treg-mediated suppression (188). Biburger *et al.* additionally

reported while HO-1 expression regulated the proliferation of human Tregs, it did not modify their suppressive function (426). In the present study it was observed that carnosol and curcumin inhibited the proliferation of effector T cells to a greater extent than that of Tregs. This may account for the slightly altered frequency of Tregs observed among carnosol- and curcumin-treated PBMC, as preferential inhibition of effector T cell proliferation would increase the overall proportion of Tregs. Furthermore, Zhang *et al.* previously reported that hemin treatment inhibited the differentiation of Th17 cells (424). Thus, while HO-1 may not be required for the expansion and function of Tregs, HO-1 upregulation may indirectly promote Tregs via inhibition of Th17 differentiation and effector T cell proliferation. This would ultimately enhance Treg-mediated suppression of pro-inflammatory T cells by increasing the Treg:effector ratio. It will be of interest in future studies to determine if carnosol and curcumin regulate the differentiation of Tregs from naïve T cells, and to assess the capability of carnosol- and curcumin-treated Tregs to suppress effector T cell responses.

While the results presented in this chapter describe important anti-inflammatory effects by carnosol and curcumin in human PBMC and T cells, the mechanism of action underlying the activity of these polyphenols in adaptive immune cells remains to be elucidated. Both carnosol and curcumin were previously observed to induce expression of HO-1 in PBMC, and many of the results described herein are similar to those previously reported for other HO-1 inducers and reaction products. Treatment of human PBMC with BV was found to inhibit their proliferation and cytokine production (318), while CO has been reported to limit T cell proliferation via inhibition of caspase 8 (185), and to reduce the production of IFNγ and IL-17 by murine lymph node cells (425). Interestingly, Pae *et al.* reported that CoPP treatment inhibited the proliferation of $CD4^+$ T cells via reduced production of IL-2, which was dependent on CO-mediated inhibition of ERK signalling (184). However, in the present study, the frequency of $IL\text{-}2^+$ T cells was unaltered in PBMC treated with carnosol or curcumin, hence it is unclear to what degree CO contributes to the immunomodulatory effects of these polyphenols in T cells. It is imperative that further research is undertaken to determine whether the anti-inflammatory effects of carnosol and curcumin in PBMC/T cells are dependent on the activity of HO-1. Furthermore, in the previous chapter it was observed that these polyphenols effectively limited the metabolic reprogramming associated with T cell activation. As the metabolism of T cells is known to greatly influence their differentiation and function, it would be of interest to investigate whether the metabolic effects of carnosol and curcumin mediate their observed reduction of T cell proliferation and Th1/Th17 cytokine production.

Although adaptive immune cells are the main instigators of autoimmunity, bystander cells within affected tissues can respond to and amplify pro-inflammatory immune responses, thereby contributing to disease pathology. Keratinocytes are the primary cell type in the skin affected by autoimmune inflammation in psoriasis. The clinical and histological features of psoriatic plaques including epidermal hyperplasia, parakeratosis, increased vascularisation and neutrophil infiltration all occur as a reaction of keratinocytes to the pro-inflammatory microenvironment created by activated immune cells (443). In this study, the effects of carnosol and curcumin were investigated in HaCaT cells, a commonly-used human keratinocyte cell line, to ascertain whether they may regulate keratinocyte activity relevant to psoriasis pathology. While curcumin has previously been reported to induce apoptosis in primary human keratinocytes at 20 μM (444), viability of HaCaT cells was unaffected by either curcumin or carnosol at concentrations ≤10 μM. Furthermore, both polyphenols significantly reduced the basal proliferation of keratinocytes, with curcumin displaying greater efficacy than carnosol in this regard. This is supported by previous studies which have reported that curcumin can downregulate the expression of cell cycle regulatory proteins in both primary and HaCaT keratinocytes (434,444). However, the hyperproliferation of keratinocytes in psoriasis occurs as a response to the pro-inflammatory cytokines IL-17 and IL-22, therefore, future work should assess whether carnosol and curcumin can also inhibit inflammatory proliferation in these cells.

In addition to increased levels of proliferation, keratinocytes produce certain cytokines and chemokines in response to inflammation; IL-8 is one such chemokine which causes the increased vascularisation and neutrophil accumulation seen in psoriatic plaques (436). Curcumin, but not carnosol, was observed to reduce the production of IL-8 by HaCaT keratinocytes in response to TNFα stimulation. This result appears to mirror the efficacy of these polyphenols as inhibitors of keratinocyte proliferation, therefore it should be determined whether the reduced IL-8 observed in curcumin-treated keratinocytes results from inhibition of cytokine production, or a reduction in cell number. Furthermore, although the anti-inflammatory effects of these polyphenols in DC were previously observed to be dependent on HO-1, their modulation of the HO-1 system was not assessed in keratinocytes during this study. Interestingly, HO-1 is expressed during the normal differentiation of primary keratinocytes, and is further upregulated by IL-1β and IL-17, indicating that it may be involved in regulating the response to inflammation in these cells (255). Treatment of HaCaT keratinocytes with the HO-1 inducers hemin and CoPP has additionally been reported to inhibit keratinocyte proliferation in response to IL-6 and IL-22 (258). Therefore, it should also be confirmed whether these polyphenols upregulate HO-1 expression in keratinocytes, and whether their anti-proliferative and anti-inflammatory effects are dependent on HO-1 activity. Taken

together, these results indicate that curcumin possesses greater efficacy over carnosol as an anti-psoriatic agent in keratinocytes.

Finally, the immunomodulatory activity of carnosol and curcumin observed in healthy human PBMC was applied to psoriasis via the *ex vivo* treatment of PBMC isolated from psoriasis patients. Patients with psoriasis are known to present with greater circulating numbers of pro-inflammatory T cells (437), and also display increased serum levels of psoriatic cytokines (438). Given this elevated inflammatory state that occurs with autoimmunity, it was important to confirm that immune cells from psoriasis patients would not be refractory to the anti-inflammatory effects of carnosol and curcumin observed in healthy donors. During this study, curcumin was found to significantly downregulate markers of T cell activation and inflammation relevant to psoriasis. The proliferation of T cells within curcumin-treated PBMC was significantly reduced, as was the frequency of γδ T cells, a rare T cell population which has recently been described to contribute to the pathology of psoriasis through its production of IL-17 (439,440). Furthermore, while there was minimal effect on the frequency of IL-2 and TNFα producing T cells within curcumin-treated PBMC, significant reductions in the expression of IFNγ, IL-17, IL-22 and GM-CSF were observed. Conversely, despite displaying some efficacy in healthy PBMC, carnosol treatment did not effectively limit pro-inflammatory responses by PBMC from psoriasis patients. However, due to the limited cell numbers available within patient samples, only a single concentration of each polyphenol was tested during this study; it is possible that the concentration of carnosol used (5 μM) did not reach therapeutic efficacy, and a higher concentration may be more effective in future studies. Nonetheless, this study demonstrated that curcumin is a more potent inhibitor of pro-inflammatory T cells than carnosol, in *ex vivo* PBMC from psoriasis patients.

The specific inhibition of Th1 and Th17 cytokine production by curcumin is highly relevant to psoriasis treatment, as these cytokines are the central driving force behind psoriatic inflammation. IFNγ has previously been identified as a prognostic factor for psoriasis severity (445), while blockade of GM-CSF was protective in a mouse model of psoriasis (446). Moreover, the Th17 cytokines, IL-17 and IL-22, are highly significant within psoriasis pathology, as both induce the abnormal keratinocyte responses seen in psoriatic plaques (64,430), and blockade of IL-17 alone has been clinically proven to resolve psoriatic symptoms (357). The effects of curcumin on pro-inflammatory cytokine production by T cells were further highlighted by SPICE analysis, which revealed that curcumin-treated PBMC from psoriasis patients displayed a reduced frequency of poly-functional T cells. Poly-functionality, i.e. the expression of multiple pro-inflammatory cytokines, has been identified in recent years as a hallmark of highly inflammatory pathogenic cells in immune-mediated disease (59,447). Therefore, the reduction of poly-functional T cells by

curcumin indicates that it can specifically inhibit the activity of pathogenic cells in autoimmunity, without compromising global immune function. Furthermore, the inhibition of cytokines relevant to psoriasis pathology, especially those associated with Th17 cells, by curcumin supports its use as an immunomodulatory treatment for psoriasis.

The results of this study support previous investigations which have demonstrated efficacy for curcumin in psoriasis; both Kang *et al.* and Sun *et al.* reported that curcumin treatment inhibited the production of pro-inflammatory cytokines, including IL-17, IL-22 and IFNγ, in murine models of psoriasis, while Sun *et al.* additionally observed that curcumin treatment downregulated the presence of γδ T cells in the skin of psoriatic mice (288,289). Furthermore, Heng *et al.* found that topical application of curcumin inhibited the proliferation of keratinocytes and T cell infiltration into the skin of psoriasis patients (297), while Antiga *et al.* reported that use of curcumin as an adjuvant therapy improved psoriasis symptoms and significantly reduced serum IL-22 concentrations (298). However, the present study represents the first extensive analysis of the effects of curcumin on adaptive immune cells in human psoriasis patients. It will be of interest in future research to assess whether curcumin is similarly effective at inhibiting the activity of T cells isolated from psoriatic plaques, as these cells are likely to be more pro-inflammatory than circulating T cells. Additionally, while curcumin was observed to slightly increase the frequency of Tregs within healthy PBMC, it was not possible to perform this analysis within psoriasis patient PBMC due to limiting cell numbers. Re-balancing the Th17/Treg axis in psoriasis via downregulation of Th17 cells and increasing the frequency of Tregs would hopefully contribute to the generation of long-lived therapeutic responses with curcumin treatment.

In conclusion, the polyphenols carnosol and curcumin have demonstrable immunomodulatory activity within human PBMC and T cells, which appears to be mediated by specific inhibition of proliferation and cytokine production in pro-inflammatory T cell subsets. Although it remains to be elucidated whether these effects are dependent on the upregulation of HO-1 by carnosol and curcumin, these results indicate that HO-1 can regulate immune function in both innate and adaptive immune cells, as well as non-immune cells, with important implications for the treatment of autoimmune disease (Figure 5.25). Furthermore, this study provides compelling evidence to support the use of curcumin as a treatment for psoriasis, through its anti-proliferative and anti-inflammatory effects in human keratinocytes and *ex vivo* psoriasis patient PBMC.

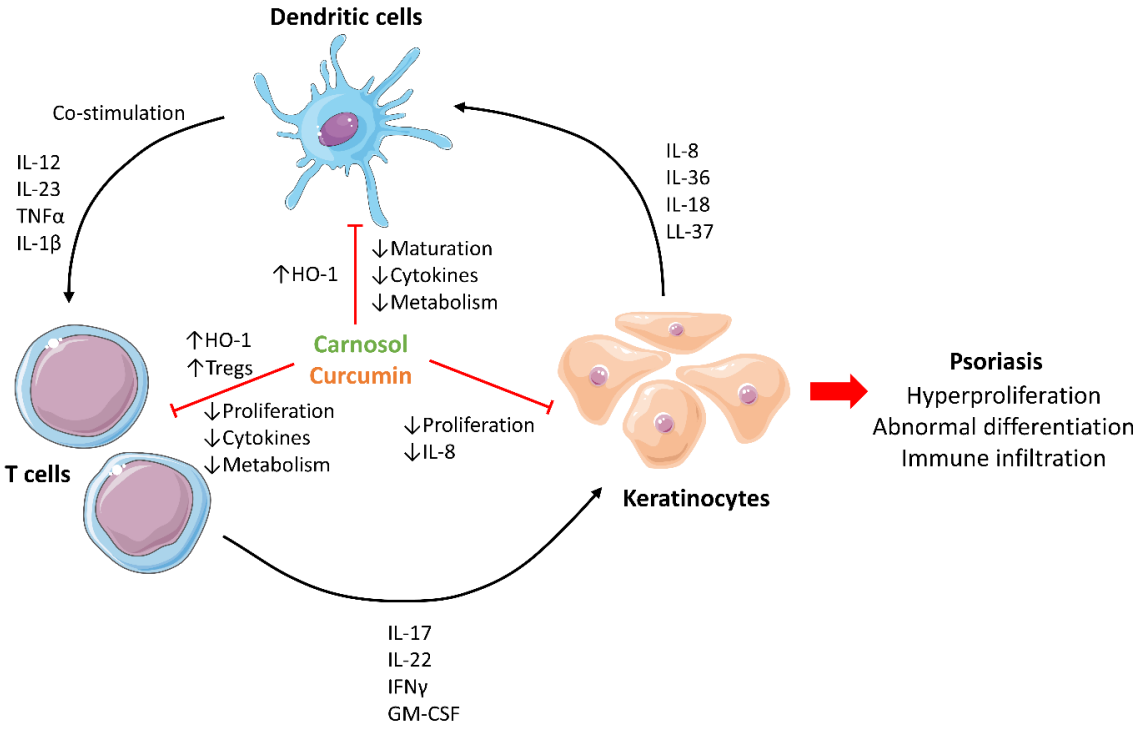

Figure 5.25. Effects of carnosol and curcumin on the cell types involved in psoriasis pathology. Psoriasis is an autoimmune disease where an inflammatory loop between DC, T cells and keratinocytes sustains and amplifies disease pathology. DC activate T cells and promote their differentiation into pro-inflammatory subsets via the production of polarising cytokines. T cells are the primary pathogenic cells within psoriasis, and produce pro-inflammatory cytokines such as IL-17 and IL-22. Keratinocytes react to T cell cytokines by increasing their rate of proliferation and producing cytokines and chemokines which further attract and activate infiltrating immune cells. This activity by keratinocytes results in the development of psoriatic plaques. Carnosol and curcumin can inhibit the activities of DC, T cells and keratinocytes, and thereby limit psoriatic inflammation.

Chapter 6:
General Discussion

The advent of immunotherapy has allowed for advances in our understanding of the immune system to be translated into sophisticated treatments for diseases characterised by inappropriate or insufficient immune activation. Autoimmunity occurs where immune tolerance mechanisms fail, resulting in deleterious immune responses directed against host tissues. It is estimated that there are over 80 different autoimmune diseases, with an overall global prevalence of ~5% (448). Although some of these diseases can be managed with the use of immunosuppressants, or more recently developed biologics against specific cytokines/receptors, many are resistant to currently available treatments, and there remains no cure for the majority of autoimmune diseases. Thus, there is a great unmet need to identify new treatment strategies which can modify the activity of immune cells that contribute to, or protect against, autoimmunity, as well as manage the local tissue response to autoimmune inflammation. Efforts to regulate the immune system in autoimmune disease have focused on DC, as the 'gatekeepers' of adaptive immunity, and T cells, particularly Th17 cells and Tregs which are often imbalanced in autoimmunity.

As outlined in chapter 1, the HO-1 system provides important antioxidant and anti-inflammatory protection to cells and tissues, and is increasingly appreciated as a significant regulator of immune cell function. Numerous pre-clinical studies have indicated that upregulation of HO-1 expression is protective in models of autoimmune diseases including EAE, colitis and psoriasis (179,210,232,257,258). However, translation of these studies to the clinic has been hindered by a lack of suitable HO-1 inducers, and inadequate analysis of the HO-1 system in human immune cells. The goal of this study was to address the above issues by investigating the efficacy of two plant-derived polyphenols, carnosol and curcumin, as HO-1 inducers and immunomodulators in primary human DC and PBMC. The results presented herein confirm that these polyphenols act as effective HO-1 inducers in human immune cells, and can downregulate pro-inflammatory immune responses relevant to autoimmune pathology. Furthermore, important insight into the mechanism of action of HO-1 in human DC, and its relationship to immunometabolism, was gained during the course of this investigation. Cumulatively, these data provide evidence to support the use of carnosol and curcumin as alternative HO-1 inducers in the treatment of autoimmune disease.

The results of chapter 3 demonstrate that carnosol and curcumin can promote tolerogenic DC by inhibiting DC maturation and pro-inflammatory functions in response to LPS stimulation. DC are instrumental in the pathogenesis of autoimmunity due to their ability to activate T cells and direct their polarisation. The requirement for DC in the initiation of EAE was first illustrated by Greter *et al.* who reported that MHC Class II expression by DC, but not CNS APCs, was essential for T cell invasion of the CNS and disease development (334). This was further supported by Bailey *et al.*,

who reported that peripheral DC migrate to the CNS during inflammation and present myelin antigens to autoreactive $CD4^+$ T cells, additionally promoting their polarisation into pathogenic Th17 cells via the production of IL-6 and IL-23 (331). Additional studies have also highlighted the importance of IL-23 production by DC in establishing the Th17-dominant inflammatory program in EAE (332,333,337). Furthermore, Sutton *et al.* reported that IL-23 and IL-1β also promoted the activation of pathogenic γδ T cells, which cooperated with Th17 cells in the production of IL-17 and EAE development. Interestingly, they also observed that IL-17 enhanced the production of IL-23 and IL-1β by LPS-stimulated DC, creating a positive feedback loop which supports further activation of pathogenic Th17 and γδ T cells (336). These results indicate that inhibition of DC activation and pro-inflammatory cytokine production can limit the generation of autoimmune inflammation by both conventional Th17 cells and γδ T cells in EAE and MS. Similarly, the contribution of DC to the inflammatory loop of psoriasis is now well appreciated, with IL-23 again identified as a key DC cytokine which promotes IL-17-dependent psoriatic inflammation (449). Indeed, monoclonal antibodies targeting IL-23 in psoriasis have been met with similar success rates as those which directly target IL-17 (357). Treatment of human DC with carnosol or curcumin in the present study was found to significantly reduce their expression of co-stimulatory molecules in response to maturation by LPS, which limited their ability to stimulate allogeneic $CD4^+$ T cells. Furthermore, the expression of IL-23, among other pro-inflammatory cytokines, was almost completely abrogated in carnosol- and curcumin-treated DC. These data indicate that carnosol and curcumin have considerable potential as treatments for autoimmune diseases where the provision of co-stimulation and pro-inflammatory cytokines, such as IL-23, by DC is established within disease pathology.

The polyphenols carnosol and curcumin were chosen for investigation in this study due to their previously established ability to upregulate expression of HO-1 (303,304,347). Both polyphenols robustly increased HO-1 expression in human DC, and moreover, their immunomodulatory effects in DC were found to be dependent on HO-1 activity. These results were anticipated given previous reports of the pivotal role played by HO-1 in the regulation of DC immunobiology (176–178). However, despite these reports it was unclear which of the HO-1 products mediates its effects in DC. The results of chapter 3 additionally aimed to answer this question via analysis of the effects of BV and PCB, a marine-derived LTP analogous to BV, in human DC, as well as the contribution of CO to the immunomodulatory effects of carnosol and curcumin. Interestingly, both BV and PCB moderately reduced the expression of DC maturation markers, and also strongly inhibited the production of pro-inflammatory cytokines. However, no effect was found with either LTP on the antigen uptake capacity of DC. Meanwhile, CO scavenging was found to partially limit the

reduction of DC maturation markers, cytokines and the maintenance of antigen uptake by carnosol and curcumin treatment in LPS-stimulated DC. Although previous studies have suggested that CO is the primary downstream effector of HO-1 in DC (173,206–208), aside from limited investigation by Rémy *et al.* (207), there has been no analysis of the role of BV in this context. Therefore, this study is the first to report that BV, alongside CO, exerts immunomodulatory effects in human DC. Taken together, these results suggest that all of the HO-1 products contribute to its activity in DC, and while some effects appear to be product-specific (e.g. antigen uptake), there exists considerable redundancy between them. Furthermore, although not investigated in the course of this study, the HO-1 protein itself has been reported to directly interact with transcription factors and thereby regulate downstream gene expression (359,360). Thus, while the current study supports the use of PCB as an alternative antioxidant/anti-inflammatory LTP to BV, it is likely that HO-1 inducers such as carnosol and curcumin will prove more effective immunomodulators as they can make use of the full spectrum of immunoregulation mediated by the HO-1 system.

In addition to elucidating the contribution of CO and BV to the regulation of DC maturation and function by HO-1, this study also provided mechanistic insight into the HO-1 dependent effects of carnosol and curcumin in human DC. MAPKs such as ERK and p38 integrate pro-inflammatory stimuli and maturation signals and activate downstream signalling pathways and transcription factors which initiate DC maturation and the production of pro-inflammatory cytokines (355). Treatment of DC with either carnosol or curcumin was found to inhibit the activation of ERK, its upstream kinase MEK, and p38 in response to LPS stimulation, in a HO-1 dependent manner. This result provides an explanation for the wide-ranging immunoregulatory effects of these polyphenols and HO-1 observed in human DC, which appear to be achieved through inhibition of signal transduction. Furthermore, these data expand the current understanding of HO-1 function in DC; HO-1 has previously been reported to inhibit p38 activation in BMDC and endothelial cells (178,367), and to inhibit MEK/ERK activation by IL-1β in human intervertebral cells (450), yet there have been no reports to date of the effects of HO-1 on MAPK signalling in human DC. Interestingly, MAPK signalling in DC is associated with their ability to initiate autoimmunity. Brereton *et al.* previously reported that inhibition of MEK/ERK signalling in BMDC significantly reduced their production of IL-1β and IL-23, and consequently, their ability to promote Th17 cells and neuroinflammation within EAE (337). Signalling via p38 in DC also appears to be required for the induction of EAE; Huang *et al.* reported that deletion of p38 in DC protected mice from EAE, again as a result of impaired Th17 activation due to reduced expression of CD86, IL-6 and IL-27 by DC (333). Importantly, HO-1 induction has previously been reported to protect against EAE via its

activity in DC (210,240); in light of the results described above, it is likely that this is achieved by HO-1 dependent inhibition of MEK/ERK and p38 signalling in DC. This study therefore reports for the first time that the polyphenols carnosol and curcumin can inhibit MAPK signalling and downstream immune responses in DC via their upregulation of HO-1, with important implications for the treatment of MS and other Th17-mediated autoimmune diseases.

One of the strategies currently under investigation to regulate the activity of immune cells in autoimmunity is alteration of their metabolic function. The results of chapter 4 provide new data which develops the under-explored study of human immune cell metabolism. Activation of primary human T cells populations in PBMC was observed to coincide with significant increases in their rate of glycolysis and SRC, which was also supported by an expansion of their mitochondrial compartment. This result is in agreement with a previous study by Renner *et al.* who reported that human $CD4^+$ and $CD8^+$ T cells upregulate both glycolytic and mitochondrial metabolism in response to TCR stimulation (139). Interestingly, both Renner *et al.* and Tripmacher *et al.* observed that inhibition of glycolysis alone was sufficient to prevent human T cell proliferation, but that cytokine production was affected only when both glycolysis and oxidative phosphorylation were inhibited (139,141). In the present study, carnosol and curcumin treatment of PBMC limited the upregulation of glycolysis and SRC in response to anti-CD3 stimulation, and also reduced mitochondrial biogenesis in these cells. Furthermore, and as shown in chapter 5, carnosol and curcumin treatment of PBMC was found to inhibit T cell proliferation and the production of IFNγ and IL-17, but not IL-2 or TNFα. It is possible that the reduced rate of glycolysis and SRC in these cells contributes to the observed inhibition of proliferation and pro-inflammatory cytokine production. One potential explanation for the specific downregulation of pro-inflammatory cytokines seen in carnosol- and curcumin-treated PBMC is that the inhibition of glycolytic metabolism by these polyphenols is felt most acutely in certain T cell subsets such as Th17 cells, which have been reported to be dependent on glycolysis for their effector function (129,372,373). However, further research into the relationship between the metabolic and immunologic effects of carnosol and curcumin in human PBMC/T cells is required to confirm this hypothesis.

Chapter 4 also provided insight into the metabolism of human DC under LPS stimulation. Primary human DC were found to increase their rate of both glycolysis and oxidative phosphorylation in response to LPS, and additionally showed a temporal upregulation of their glycolytic reserve and SRC early after activation. To date there has been only one previous study which has investigated the metabolism of human DC: Malinarich *et al.* similarly observed that glycolysis and oxidative phosphorylation are increased in LPS-stimulated DC, however, their study assessed the metabolism of DC too late after LPS stimulation to observe the temporal increase in glycolytic

reserve and SRC reported here (138). Therefore, the present study is the first to report that human DC undergo time-dependent changes in glycolytic and oxidative metabolism during maturation. This is in contrast to previous work in murine systems, in which activated BMDC undergo a switch to Warburg metabolism, with a concomitant decrease in oxidative phosphorylation (120–122). As previously discussed, this difference between murine and human DC likely results from divergent iNOS expression between the two cell types (132). The results of this study therefore have important implications for the targeting of DC metabolism in human disease, as these cells may prove more metabolically plastic than their murine counterparts. However, these results are limited by the use of *in vitro* generated human DC and the DC subsets, which exist *in vivo,* may display different metabolic properties as a result of their ontogeny or environment (403). Nonetheless, inhibition of glycolysis early during DC activation has potential to prevent increased flux into the TCA cycle, reduce downstream expansion of ER/Golgi membranes, and effectively inhibit DC maturation. In this study, carnosol and curcumin were found to inhibit the upregulation of glycolysis and the increased glycolytic reserve and SRC in LPS-stimulated DC. It remains to be determined if these metabolic effects contribute to the reduced maturation and pro-inflammatory function of carnosol- and curcumin-treated DC observed in chapter 3, and if so, whether this occurs independently of their HO-1 dependent inhibition of MAPK signalling. Interestingly, as a result of their role in cell growth and differentiation, signalling through MAPKs is associated with the promotion of anabolic metabolism in various cell types (92,451,452). In particular, Través *et al.* reported that inhibition of MEK/ERK in RAW264.7 macrophages inhibited their upregulation of glycolytic metabolism in response to LPS (453). Therefore, it is exciting to speculate that carnosol and curcumin regulate human DC via their upregulation of HO-1, which inhibits MAPK signalling to prevent both the activation of downstream pro-inflammatory transcription factors/signalling pathways and the metabolic changes which occur in response to LPS stimulation, thereby limiting DC maturation and function.

Aside from uncovering a potential role for HO-1 in the regulation of DC metabolism, a novel relationship between metabolic signalling and HO-1 induction by carnosol and curcumin in DC was discovered during this study. Carnosol and curcumin were both found to activate AMPK in primary human DC, which was required for their upregulation of HO-1 expression in these cells. Furthermore, the immunomodulatory activity of these polyphenols was attenuated by AMPK inhibition, providing a clear connection between the activation of AMPK by carnosol and curcumin and their HO-1 dependent effects in DC. Although carnosol and curcumin have previously been reported to activate AMPK in cancer and skeletal muscle cell lines (405–408), this study is the first to report this effect in immune cells. Similarly, while previous studies have reported that signalling

through AMPK can promote Nrf2 activation/HO-1 induction (392,393,404,412,413), this association has not been made in DC, nor with carnosol or curcumin treatment.

These results have a number of important implications for both HO-1 and immunometabolism research. Firstly, identification of a novel signalling pathway which can promote HO-1 upregulation in DC (and presumably other immune cells) opens up new possibilities in the search for HO-1 inducers which can regulate the immune response. Existing HO-1 inducers are believed to increase HO-1 expression due to their similarity to heme, the substrate of HO-1 (as is case with many metalloporphyrins), or by the induction of oxidative stress/inflammation which activate transcription factors including Nrf2, AP-1 and NF-κB (159). Activation of AMPK may serve as an effective mechanism to upregulate HO-1 in an anti-inflammatory setting without the associated toxicities of the aforementioned metalloporphyrins or ROS. Secondly, the induction of HO-1 by AMPK links its well-characterised regulation of catabolic metabolism with its more recently described anti-inflammatory activity. Engagement of oxidative phosphorylation and fatty acid oxidation is associated with tolerogenic/anti-inflammatory immune responses, and this metabolic program is coordinated by high AMPK activity (120,123,129). It is possible that the anti-inflammatory phenotype of AMPK-active immune cells is achieved not only though the inhibition of anabolic/pro-inflammatory signalling pathways such as mTOR, but also through the upregulation of HO-1, which, as is evident from this study and others, has wide-ranging anti-inflammatory effects in immune cells. As the field of immunometabolism continues to evolve, it will be interesting to explore the role of HO-1 in the relationship between AMPK, catabolic metabolism and the promotion of anti-inflammatory immune cells. Finally, AMPK has recently become a target of interest due to its 'health promoting' properties. AMPK activation is believed to promote overall cellular health by inducing a state of 'pseudo-starvation' that not only improves the bio-energetic fitness of the cell, but limits energy-intensive processes such as cell division and pro-inflammatory immune responses (454). Evidence that AMPK activation may be beneficial for certain health outcomes has largely arisen from laboratory investigations and epidemiological studies of the drug metformin, which is used as first-line treatment for type II diabetes. Metformin activates AMPK by inhibition of the ETC, similar to polyphenols such as curcumin, and has been associated with reduced levels of inflammation and cancer incidence (107,410,454,455). Additionally, salicylate, one of the active ingredients of the anti-inflammatory drug aspirin, has also been reported to activate AMPK (456). Low dose aspirin is prescribed as a preventative measure against cardiovascular disease and stroke, and like metformin, has been associated with reduced inflammation and cancer incidence (457,458). Although these associations remain hypothetical at present, it would be interesting to determine if patients receiving metformin or

aspirin treatment display increased expression of HO-1 as a result of AMPK activation by these drugs, and whether HO-1 contributes to their potential anti-inflammatory and anti-cancer effects.

As discussed previously, the results of chapter 5 described the anti-inflammatory effects of carnosol and curcumin in human PBMC/T cells, which complemented the inhibition of T cell metabolism by these polyphenols observed in chapter 4. The present study is the first to report that carnosol treatment can inhibit the adaptive immune response by human PBMC/T cells. Furthermore, these results add to previous studies which have investigated the effects of curcumin in T cells (283,397,441,442), and support a potential role for HO-1 in the regulation of the adaptive immune response. Both carnosol and curcumin reduced the proliferation of T cells and their expression of the pro-inflammatory cytokines IL-17 and IFNγ in healthy human PBMC. Although a number of *in vivo* disease models have indicated that HO-1 can reduce pro-inflammatory responses by T cells (210,232,244,360,427,459), it has been difficult to separate these effects from the suppressive activity of HO-1 in APCs. The results presented herein support previous studies which have reported that HO-1 has direct anti-inflammatory activity in T cells *in vitro* (183,424), and lend credence to the hypothesis that at least some of its effects on the adaptive immune response *in vivo* are mediated through regulation of these cells, in addition to APCs. Interestingly, the inhibition of T cell proliferation by carnosol and curcumin was observed to be greater in purified $CD4^+$ T cell cultures compared to PBMC; while this result rules out APCs within PBMC as the primary target for HO-1 in these experiments, it is not immediately clear why the presence of other immune cells suppresses the activity of these polyphenols in $CD4^+$ T cells. Furthermore, while supporting evidence exists to suggest that the effects of carnosol and curcumin in human PBMC/T cells are dependent on their upregulation of HO-1, this mechanism of action requires verification. These outstanding questions are currently under investigation in follow up studies in the Dunne lab. Promisingly, recent research has indicated that inhibition of HO-1 attenuates the anti-proliferative effects of these polyphenols in human PBMC (Hannah Fitzgerald, unpublished observations).

One of the mechanisms by which HO-1 has been suggested to regulate the adaptive immune response is through the promotion of Tregs. In chapter 5, low doses of carnosol and curcumin were observed to slightly increase the frequency of Tregs in PBMC, however, there was no effect on the expression of CD39 or CTLA4 by these Tregs. Upregulation of HO-1 has previously been observed to result in increased Treg frequencies *in vivo* (233,460–463). However, how this increase in Treg frequency is achieved is largely unknown. A number of studies have suggested that the upregulation of HO-1 in DC promotes the differentiation of iTregs from naïve T cells (180,188,189), while others have reported that HO-1 expression in T cells inhibits Th17 cell

differentiation (360,424), thereby favouring the generation of Tregs. Meanwhile, Zelenay *et al*. previously reported that *HMOX1*$^{-/-}$ mice display a normal frequency of Tregs, indicating that HO-1 is not required for Treg development (187). The results of this study suggest that HO-1 induction in T cells may inhibit the proliferation of effector T cell subsets to a greater degree than that of Tregs, thus increasing the relative frequency of these cells. While this effect has not been reported before, for either carnosol/curcumin or HO-1, it remains possible that the slight increase in Treg frequency observed with carnosol and curcumin treatment occurs through promotion of Treg differentiation, or inhibition of Th17 cell differentiation, as described above. Therefore, further research is required to determine if HO-1 alters the Th17/Treg cell balance through direct regulation of signalling in APCs and/or T cells, indirectly through manipulation of cellular proliferation, or via a combination of these mechanisms. Furthermore, debate also exists within the literature whether HO-1 expression contributes to the suppressive function of Tregs. It has previously been reported by Pae *et al.* and Choi *et al.* that human $CD4^{+}CD25^{+}$ Tregs constitutively express HO-1 (183,422). Choi *et al.* also observed that inhibition of HO-1 in a co-culture of Tregs and responder cells attenuated Treg-mediated suppression of T cell proliferation, however, given that HO-1 inhibition was applied to both Tregs and effector cells in this system, it is possible that this effect arose through increased proliferation of T cells in response to HO-1 inhibition rather than a failure of Treg suppression (422). In support of this hypothesis, Biburger *et al.* reported that inhibition of HO-1 increased the proliferation of Tregs, but did not compromise their suppressive capacity (426), while Zelenay *et al.* and George *et al.* also found that HO-1 expression by Tregs was not required for their ability to suppress T cell responses (187,188). The results of this study agree with the above studies which suggest that HO-1 does not directly mediate Treg suppression, as CD39 and CTLA4 expression by Tregs was unaffected by carnosol or curcumin treatment. However, this must be confirmed by analysis of the suppressive capacity of carnosol- and curcumin-treated Tregs in a co-culture setting. Taken together, the results of chapter 5 add valuable new data which increase our understanding of immunoregulation by HO-1 in effector T cells and Tregs. It is hoped that these results can also provide a foundation for the future use of carnosol and curcumin as modulators of the HO-1 system in adaptive immune cells.

The suppression of pro-inflammatory innate and adaptive immune responses by carnosol and curcumin described in this study provided encouragement that these (or similar) polyphenols may be useful as immunomodulators in the context of autoimmunity. Therefore, a translational study was performed to assess the capability of carnosol and curcumin to regulate the activity of cells relevant to the pathology of psoriasis, a common autoimmune disease. The results presented in chapter 5 support the use of curcumin as a treatment for psoriasis as it is capable of reducing

proliferation and inflammatory responses by human keratinocytes and *ex vivo* psoriasis patient PBMC.

Keratinocytes are both victims and accomplices in psoriatic inflammation; cytokines produced by infiltrating pro-inflammatory immune cells trigger the aberrant proliferation and differentiation of keratinocytes which results in plaque formation, yet keratinocytes themselves are involved in the initiation and amplification of inflammation in psoriasis (464). Curcumin was observed to significantly reduce the basal proliferation and production of IL-8 by human keratinocytes. This result is supported by a previous study by Heng *et al.* who observed that topical application of curcumin reduced expression of the proliferation marker Ki67 in the skin of psoriasis patients (297). Hyperproliferation of keratinocytes is a major contributor to the histological appearance of psoriatic skin (251), thus inhibition of proliferation in these cells acts to improve psoriasis symptoms. Meanwhile, IL-8 production by keratinocytes promotes plaque vascularisation and the infiltration and activation of neutrophils (436). Neutrophils are highly volatile innate immune cells which contribute to the inflammatory loop of psoriasis via the production of numerous pro-inflammatory cytokines which stimulate downstream responses by DC, T cells and keratinocytes (465). Furthermore, recent research has identified a role for neutrophil extracellular traps (NETs) in psoriasis pathology. NETosis is a unique type of cell death in which neutrophils release nucleic acids alongside pro-inflammatory mediators. Through the release of NETs, neutrophils have been suggested as major sources of IL-17 in psoriasis, while nucleic acids can form complexes with auto-antigens and increase PRR activation in DC (449,465). However, previous efforts to target IL-8 in psoriasis have been unsuccessful, therefore it is unlikely that inhibition of this cytokine and neutrophil activity in isolation is sufficient to ameliorate psoriatic inflammation (466,467). Although these preliminary results suggest that curcumin can effectively regulate the activity of keratinocytes in psoriasis, the range of keratinocyte responses investigated here is limited. Auto-antigens such as the antimicrobial peptide LL37 released by keratinocytes have been suggested to be triggers of psoriasis pathogenesis; a recent study identified LL37-specific T cells in up to 46% of psoriasis patients, and up to 75% of patients with moderate/severe disease (468). Thus, it would be useful for future research to investigate whether curcumin treatment can also inhibit the expression of auto-antigens such as LL37 by keratinocytes, as well as other pro-inflammatory cytokines relevant to psoriasis pathology including IL-36, IL-1β and IL-18 (62,464).

While keratinocytes can contribute and respond to psoriatic inflammation, as in many other autoimmune diseases, T cells are the primary pathogenic cells in psoriasis. Following from observations that carnosol and curcumin can limit proliferation and expression of pro-inflammatory cytokines by T cells in healthy PBMC, curcumin was also found to be an effective

inhibitor of inflammatory poly-functional T cells in *ex vivo* psoriasis patient PBMC. Psoriasis patient PBMC were observed to display robust expression of pro-inflammatory cytokines associated with psoriatic inflammation, including IL-17, IFNγ, IL-22 and GM-CSF, with IL-17 expression positively correlating with patient PASI scores (Appendix 2). Curcumin treatment was found to specifically reduce expression of these cytokines, without undue inhibition of general cytokine production by T cells. Interestingly, SPICE analysis of the cytokine expression profiles of T cells within *ex vivo* psoriasis patient PBMC indicated that the inhibitory activity of curcumin was most effective in poly-functional T cells which concurrently expressed multiple pro-inflammatory cytokines. This novel analytic tool has been utilised in recent studies to identify populations of highly pro-inflammatory and pathogenic cells in diseases such as RA and hidradenitis suppurativa (59,447). Although this study lacked a matched healthy control group for comparison of poly-functionality with psoriasis patients, these results indicate that the production of pro-inflammatory cytokines in psoriasis is largely mediated by these poly-functional cells. Thus, these results show promise for the ability of curcumin treatment to target pathogenic T cells in psoriasis without inducing global immunosuppression, which is an issue associated with some currently available immunosuppressants (469). In addition to its effects on T cell cytokine production, curcumin treatment also significantly inhibited T cell proliferation and reduced the frequency of γδ T cells among *ex vivo* psoriasis patient PBMC. Given that many existing psoriasis therapies function through the inhibition of T cell proliferation (470), this result is again encouraging for the prospective efficacy of curcumin in this context. Furthermore, γδ T cells have been identified as major producers of IL-17 important to the pathogenesis of psoriasis in murine models (439,440,471). While their contribution to human disease has yet to be fully elucidated, a population of skin-homing Vγ9Vδ2 T cells has been identified in psoriasis patients (472). Should this γδ T cell subset prove relevant to psoriasis pathology, it would be interesting to determine whether its expansion can also be inhibited by curcumin treatment.

The results of this study indicate that curcumin can act as an effective HO-1 inducer in the treatment of psoriasis. Importantly, curcumin appears to be capable of regulating the Th17 axis, which is critical to the pathology of psoriasis and other autoimmune diseases. This regulation is implemented at multiple points in the Th17 axis, including DC, keratinocytes and T cells themselves. Targeting of cytokines involved in this axis, particularly IL-23 and IL-17, has already been demonstrated to be highly effective in the treatment of psoriasis (357), and it is hoped that this strategy might also prove effective in other Th17-mediated diseases. These results therefore place curcumin (or curcumin analogues) in an excellent position for application as a treatment for psoriasis, with potential for further investigation into its use in other autoimmune and

inflammatory diseases. In particular, it is likely that curcumin will be most useful as an adjuvant therapy in psoriasis. An oral preparation of curcumin, Meriva™, has already found success as an adjuvant therapy alongside topical glucocorticosteroids in a recent phase III clinical trial (298). Additionally, recently-developed biologics have revolutionised the treatment of psoriasis, and it has been suggested that certain subsets of patients may benefit from combination therapy of biologics with other systemic or topical treatments (473). One of the limitations of the present study is that the clinical history of enrolled psoriasis patients was unavailable, therefore it is unknown which existing drugs or therapies were administered to these patients. Furthermore, while psoriasis patients display elevated levels of circulating inflammatory cells (437), the majority of pathogenic cells are localised to the skin, and therefore the results presented here may not accurately reflect the true inflammatory environment of psoriasis. Nonetheless, curcumin treatment reduced inflammatory responses in *ex vivo* PBMC from all patients enrolled in this study, indicating that it is an effective immunomodulator regardless of, or indeed, alongside, existing treatment regimens. It is hoped that these results can be replicated in T cells isolated from psoriatic plaques. Additionally, while carnosol treatment was ineffective at regulating immune responses in keratinocytes and psoriasis patient PBMC at the concentrations used in this study, it was observed to have significant immunomodulatory activity in human DC. Therefore, it is recommended that future studies continue to investigate the potential for this naturally-derived HO-1 inducer as a treatment for autoimmune disease, including psoriasis.

Finally, while this study provides evidence that carnosol and curcumin are effective modulators of the HO-1 system in human immune cells, and have anti-inflammatory activity which positions them as potential treatments for autoimmune and inflammatory diseases, translation of these results to a clinical setting requires careful consideration regarding drug formulation and administration. One of the caveats associated with these polyphenols is their poor solubility in aqueous solutions, which may limit their bioavailability by certain routes of administration. While both polyphenols are naturally-occurring in common herbs and spices, it is uncertain that they can reach an effective concentration through nutritional consumption alone. A recent study by Brück *et al.* reported that inclusion of 2% curcumin in the food pellets of mice effectively protected them from EAE (286). However, it is unclear whether dietary consumption represents a realistic mode of administration in humans, as previous studies have failed to detect HO-1 upregulation or clinical efficacy with large doses of oral curcumin in healthy volunteers and psoriasis patients, respectively (291,293). This is an especially relevant limitation to be aware of, as curcumin and its source, turmeric, have become popularised as ‘nutraceuticals’ and promoted for their supposed health benefits in recent years. However, due to the extensive interest in curcumin as an anti-

inflammatory agent, efforts made to improve its oral bioavailability, or to utilise alternative routes of administration, have been met with success in pre-clinical studies and clinical trials (287,297–299). Moreover, oral administration of curcumin may be useful in the treatment of gastrointestinal inflammation in IBD, in which drug absorption would not be required for it to reach its target tissue; indeed, oral curcumin has been reported to both induce and maintain disease remission as an adjuvant therapy in ulcerative colitis patients (294,295). While it is possible that carnosol has greater oral bioavailability than curcumin (316), there have been no studies to date examining the absorption or clinical efficacy of oral carnosol *in vivo*. However, topical administration of carnosol-rich sage extract was found to be effective as a treatment for erythema in a clinical trial (315). In summary, while this study presents important data demonstrating that these polyphenols are effective HO-1 inducers and immunomodulators in human immune cells, forethought should be paid to the route and mechanism of drug delivery when considering the application of these results.

Inflammation, while necessary for host defence, is a significant contributor to global morbidity and mortality as a feature of numerous diseases which threaten human health. Alongside an aging population, the rising incidence of inflammation-associated diseases including obesity, cancer and autoimmunity highlight the ongoing need to develop new anti-inflammatory and immunomodulatory therapies (235,474–476). The results presented herein highlight the potential of the HO-1 system to regulate the immune response in human immune cells, with particular relevance for the treatment of autoimmune diseases such as psoriasis. Insight into the mechanism of action of HO-1 in human DC, and its relationship to the emerging field of immunometabolism has also been gained in the course of this study. Furthermore, this study proposes use of the plant-derived polyphenols, carnosol and curcumin, as effective alternatives to existing HO-1 inducers which can harness the therapeutic potential of the HO-1 system in human disease. A summary of the major findings of this study is presented in Figure 6.1.

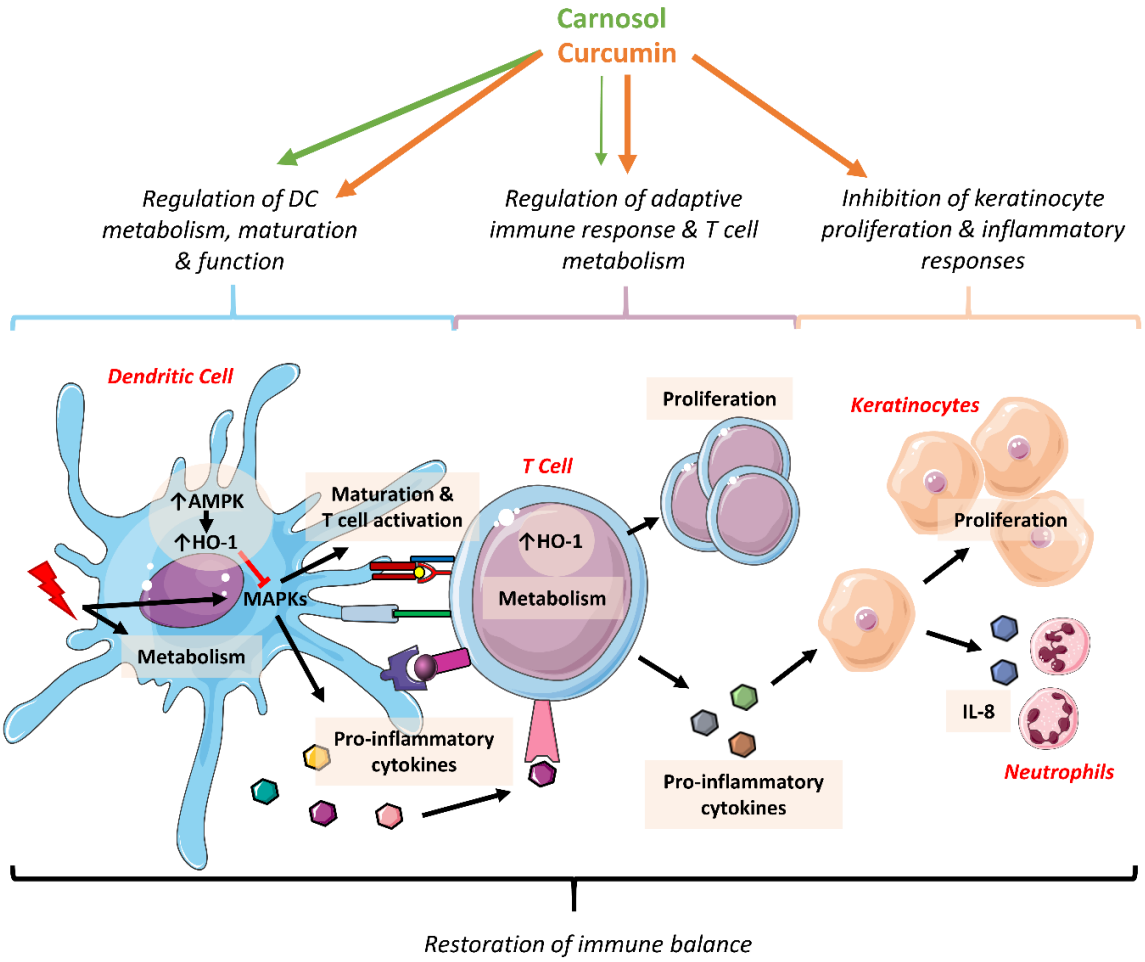

Figure 6.1. Immunoregulation by carnosol and curcumin and HO-1. The naturally-derived HO-1 inducers, carnosol and curcumin, regulate the immune response in human cells. Both polyphenols activate AMPK in human DC, which upregulates the expression of HO-1. HO-1 inhibits maturation, cytokine production and T cell activation by DC in response to pro-inflammatory stimuli, through inhibition of MAPK signalling. Carnosol and curcumin additionally inhibit metabolic changes arising from the activation of DC and T cells. In T cells, carnosol and curcumin upregulate HO-1, and inhibit proliferation and pro-inflammatory cytokine production in response to mitogens, with curcumin displaying greater potency over carnosol. Finally, curcumin can also regulate the proliferation of keratinocytes, and inhibit their production of the neutrophil attractant, IL-8, in response to pro-inflammatory cytokines. Together, immunoregulation by these polyphenols can reduce harmful immune activation and promote tolerogenic immune responses, with the goal of restoring immune balance in autoimmune diseases such as psoriasis.

References

1. Buchmann, K. Evolution of Innate Immunity: Clues from Invertebrates via Fish to Mammals. *Front. Immunol.* **5,** 459 (2014).

2. Litman, G. W., Rast, J. P. & Fugmann, S. D. The origins of vertebrate adaptive immunity. *Nat. Rev. Immunol.* **10,** 543–553 (2010).

3. Pancer, Z. & Cooper, M. D. The Evolution of Adaptive Immunity. *Annu. Rev. Immunol.* **24,** 497–518 (2006).

4. Dempsey, P. W., Vaidya, S. A. & Cheng, G. The Art of War: Innate and adaptive immune responses. *Cell. Mol. Life Sci. C.* **60,** 2604–2621 (2003).

5. Chen, G. Y. & Nuñez, G. Sterile inflammation: sensing and reacting to damage. *Nat. Rev. Immunol.* **10,** 826–837 (2010).

6. Matzinger, P., Koshland, D. E., Heidt, P. J., Vossen, J. M., Hill, G. R., Matzinger, P., Matzinger, P., Gallucci, S., Matzinger, P., Owen, R., Billingham, R. E., Brent, L., Medawar, P. B., Bretscher, P., Cohn, M., Lafferty, K. J., Cunningham, A., Jenkins, M. K., Schwartz, R. H., *et al.* The danger model: a renewed sense of self. *Science* **296,** 301–5 (2002).

7. Kumar, H., Kawai, T. & Akira, S. Pathogen recognition by the innate immune system. *Int. Rev. Immunol.* **30,** 16–34 (2011).

8. Takeda, K. & Akira, S. Toll-like receptors in innate immunity. *Int. Immunol.* **17,** 1–14 (2005).

9. Kawasaki, T. & Kawai, T. Toll-like receptor signaling pathways. *Front. Immunol.* **5,** 461 (2014).

10. Akira, S. & Takeda, K. Toll-like receptor signalling. *Nat. Rev. Immunol.* **4,** 499–511 (2004).

11. Latz, E., Xiao, T. S. & Stutz, A. Activation and regulation of the inflammasomes. *Nat. Rev. Immunol.* **13,** 397–411 (2013).

12. Shao, B. Z., Xu, Z. Q., Han, B. Z., Su, D. F. & Liu, C. NLRP3 inflammasome and its inhibitors: A review. *Front. Pharmacol.* **6,** (2015).

13. Tschopp, J. & Schroder, K. NLRP3 inflammasome activation: the convergence of multiple signalling pathways on ROS production? *Nat. Rev. Immunol.* **10,** 210–215 (2010).

14. Duewell, P., Kono, H., Rayner, K. J., Sirois, C. M., Vladimer, G., Bauernfeind, F. G., Abela, G. S., Franchi, L., Nuñez, G., Schnurr, M., Espevik, T., Lien, E., Fitzgerald, K. A., Rock, K. L., Moore, K. J., Wright, S. D., Hornung, V. & Latz, E. NLRP3 inflammasomes are required for atherogenesis and activated by cholesterol crystals. *Nature* **464,** 1357–1361 (2010).

15. Pazar, B., Ea, H.-K., Narayan, S., Kolly, L., Bagnoud, N., Chobaz, V., Roger, T., Liote, F., So, A. & Busso, N. Basic Calcium Phosphate Crystals Induce Monocyte/Macrophage IL-1 Secretion through the NLRP3 Inflammasome In Vitro. *J. Immunol.* **186,** 2495–2502 (2011).

16. Liu, K. & Nussenzweig, M. C. Origin and development of dendritic cells. *Immunol. Rev.* **234,** 45–54 (2010).

17. Merad, M., Sathe, P., Helft, J., Miller, J. & Mortha, A. The Dendritic Cell Lineage: Ontogeny and Function of Dendritic Cells and Their Subsets in the Steady State and the Inflamed Setting. *Annu. Rev. Immunol* **31,** 563–604 (2013).

18. Reizis, B., Bunin, A., Ghosh, H. S., Lewis, K. L. & Sisirak, V. Plasmacytoid dendritic cells: recent progress and open questions. *Annu. Rev. Immunol.* **29,** 163–83 (2011).

19. Banchereau, J., Briere, F., Caux, C., Davoust, J., Lebecque, S., Liu, Y.-J., Pulendran, B. & Palucka, K. Immunobiology of Dendritic Cells. *Annu. Rev. Immunol.* **18,** 767–811 (2000).

20. Riol-Blanco, L., Sanchez-Sanchez, N., Torres, A., Tejedor, A., Narumiya, S., Corbi, A. L., Sanchez-Mateos, P. & Rodriguez-Fernandez, J. L. The Chemokine Receptor CCR7 Activates in Dendritic Cells Two Signaling Modules That Independently Regulate Chemotaxis and Migratory Speed. *J. Immunol.* **174,** 4070–4080 (2005).

21. Mildner, A. & Jung, S. Development and Function of Dendritic Cell Subsets. *Immunity* **40,** 642–656 (2014).

22. Kapsenberg, M. L. Dendritic-cell control of pathogen-driven T-cell polarization. *Nat. Rev. Immunol.* **3,** 984–993 (2003).

23. Kambayashi, T. & Laufer, T. M. Atypical MHC class II-expressing antigen-presenting cells: Can anything replace a dendritic cell? *Nat. Rev. Immunol.* **14,** 719–730 (2014).

24. Kronenberg, M. & Rudensky, A. Regulation of immunity by self-reactive T cells. *Nature* **435,** 598–604 (2005).

25. Goodnow, C. C., Sprent, J., de St Groth, B. F. & Vinuesa, C. G. Cellular and genetic mechanisms of self tolerance and autoimmunity. *Nature* **435,** 590–597 (2005).

26. Fathman, C. G. & Lineberry, N. B. Molecular mechanisms of CD4+ T-cell anergy. *Nat. Rev. Immunol.* **7,** 599–609 (2007).

27. Lewis, K. L. & Reizis, B. Dendritic Cells: Arbiters of Immunity and Immunological Tolerance. *Cold Spring Harb. Perspect. Biol.* **4,** a007401 (2012).

28. Lipscomb, M. F. & Masten, B. J. Dendritic Cells: Immune Regulators in Health and Disease. *Physiol Rev* **82,** 97–130 (2002).

29. Lutz, M. B. & Schuler, G. Immature, semi-mature and fully mature dendritic cells: which signals induce tolerance or immunity? *Trends Immunol.* **23,** 445–449 (2002).

30. Steinman, R. M., Hawiger, D. & Nussenzweig, M. C. Tolerogenic dendritic cells. *Annu. Rev. Immunol.* **21,** 685–711 (2003).

31. Cools, N., Ponsaerts, P., Tendeloo, V. F. I. Van & Berneman, Z. N. Balancing between immunity and tolerance: an interplay between dendritic cells, regulatory T cells, and effector T cells. *J. Leukoc. Biol.* **82,** 1365–1374 (2007).

32. Belkaid, Y. & Oldenhove, G. Tuning Microenvironments: Induction of Regulatory T Cells by Dendritic Cells. *Immunity* **29,** 362–371 (2008).

33. Dalod, M., Chelbi, R., Malissen, B. & Lawrence, T. Dendritic cell maturation: functional specialization through signaling specificity and transcriptional programming. *EMBO J.* **33,** 1104–16 (2014).

34. Probst, H. C., McCoy, K., Okazaki, T., Honjo, T. & van den Broek, M. Resting dendritic cells induce peripheral CD8+ T cell tolerance through PD-1 and CTLA-4. *Nat. Immunol.* **6,** 280–286 (2005).

35. Carter, L. L., Fouser, L. A., Jussif, J., Fitz, L., Deng, B., Wood, C. R., Collins, M., Honjo, T., Freeman, G. J. & Carreno, B. M. PD-1:PD-L inhibitory pathway affects both CD4+ and CD8+ T cells and is overcome by IL-2. *Eur. J. Immunol.* **32,** 634 (2002).

36. Blanco, P., Palucka, A. K., Pascual, V. & Banchereau, J. Dendritic cells and cytokines in

human inflammatory and autoimmune diseases. *Cytokine Growth Factor Rev.* **19,** 41–52 (2008).

37. Weisenseel, P., Laumbacher, B., Besgen, P., Ludolph-Hauser, D., Herzinger, T., Roecken, M., Wank, R. & Prinz, J. C. Streptococcal infection distinguishes different types of psoriasis. *J. Med. Genet.* **39,** 767–768 (2002).

38. Palucka, A. K., Banchereau, J., Blanco, P. & Pascual, V. The interplay of dendritic cell subsets in systemic lupus erythematosus. *Immunol. Cell Biol.* **80,** 484–488 (2002).

39. Ganguly, D., Haak, S., Sisirak, V. & Reizis, B. The role of dendritic cells in autoimmunity. *Nat. Rev. Immunol.* **13,** 566–77 (2013).

40. Boltjes, A. & van Wijk, F. Human Dendritic Cell Functional Specialization in Steady-State and Inflammation. *Front. Immunol.* **5,** 131 (2014).

41. Whiteside, T. L. Regulatory T cell subsets in human cancer: are they regulating for or against tumor progression? *Cancer Immunol. Immunother.* **63,** 67–72 (2014).

42. Tran Janco, J. M., Lamichhane, P., Karyampudi, L. & Knutson, K. L. Tumor-Infiltrating Dendritic Cells in Cancer Pathogenesis. *J. Immunol.* **194,** 2985–2991 (2015).

43. Callahan, M. K. & Wolchok, J. D. At the Bedside: CTLA-4- and PD-1-blocking antibodies in cancer immunotherapy. *J. Leukoc. Biol.* **94,** 41–53 (2013).

44. Weber, J. Immune checkpoint proteins: a new therapeutic paradigm for cancer--preclinical background: CTLA-4 and PD-1 blockade. *Semin. Oncol.* **37,** 430–439 (2010).

45. Hamid, O., Robert, C., Daud, A., Hodi, F. S., Hwu, W.-J., Kefford, R., Wolchok, J. D., Hersey, P., Joseph, R. W., Weber, J. S., Dronca, R., Gangadhar, T. C., Patnaik, A., Zarour, H., Joshua, A. M., Gergich, K., Elassaiss-Schaap, J., Algazi, A., Mateus, C., *et al.* Safety and Tumor Responses with Lambrolizumab (Anti–PD-1) in Melanoma. *N. Engl. J. Med.* **369,** 134–144 (2013).

46. John, L. B., Devaud, C., Duong, C. P. M., Yong, C. S., Beavis, P. A., Haynes, N. M., Chow, M. T., Smyth, M. J., Kershaw, M. H. & Darcy, P. K. Anti-PD-1 antibody therapy potently enhances the eradication of established tumors by gene-modified T cells. *Clin. Cancer Res.* **19,** 5636–5646 (2013).

47. Beroukhim, K., Danesh, M. J., Nguyen, C., Austin, A., Koo, J. & Levin, E. Anti-IL-23 Phase II Data for Psoriasis: A Review. *J. Drugs Dermatol.* **14,** 1093–6 (2015).

48. Morelli, A. E. & Thomson, A. W. Tolerogenic dendritic cells and the quest for transplant tolerance. *Nat. Rev. Immunol.* **7,** 610–621 (2007).

49. Palucka, K. & Banchereau, J. Cancer immunotherapy via dendritic cells. *Nat. Rev. Cancer* **12,** 265–277 (2012).

50. Germain, R. N. T-cell development and the CD4–CD8 lineage decision. *Nat. Rev. Immunol.* **2,** 309–322 (2002).

51. Bonneville, M., O'Brien, R. L. & Born, W. K. γδ T cell effector functions: a blend of innate programming and acquired plasticity. *Nat. Rev. Immunol.* **10,** 467–478 (2010).

52. Maddur, M. S., Miossec, P., Kaveri, S. V. & Bayry, J. Th17 Cells: Biology, Pathogenesis of Autoimmune and Inflammatory Diseases, and Therapeutic Strategies. *Am. J. Pathol.* **181,** 8–18 (2012).

53. Korn, T., Bettelli, E., Oukka, M. & Kuchroo, V. K. IL-17 and Th17 Cells. *Annu. Rev. Immunol.* **27,** 485–517 (2009).

54. Burkett, P. R., Meyer zu Horste, G. & Kuchroo, V. K. Pouring fuel on the fire: Th17 cells, the environment, and autoimmunity. *J. Clin. Invest.* **125,** 2211–2219 (2015).

55. Komiyama, Y., Nakae, S., Matsuki, T., Nambu, A., Ishigame, H., Kakuta, S., Sudo, K. & Iwakura, Y. IL-17 Plays an Important Role in the Development of Experimental Autoimmune Encephalomyelitis. *J. Immunol.* **177,** 566–573 (2006).

56. Langrish, C. L., Chen, Y., Blumenschein, W. M., Mattson, J., Basham, B., Sedgwick, J. D., McClanahan, T., Kastelein, R. A. & Cua, D. J. IL-23 drives a pathogenic T cell population that induces autoimmune inflammation. *J. Exp. Med.* **201,** 233–240 (2005).

57. Zhu, S. & Qian, Y. IL-17/IL-17 receptor system in autoimmune disease: mechanisms and therapeutic potential. *Clin. Sci.* **122,** 487–511 (2012).

58. Gaffen, S. L. The Role of Interleukin-17 in the Pathogenesis of Rheumatoid Arthritis. *Curr. Rheumatol. Reports Curr. Med. Gr. LLC ISSN* **11,** 365–370 (2009).

59. Basdeo, S. A., Moran, B., Cluxton, D., Canavan, M., McCormick, J., Connolly, M., Orr, C., Mills, K. H. G., Veale, D. J., Fearon, U. & Fletcher, J. M. Polyfunctional, Pathogenic CD161+ Th17 Lineage Cells Are Resistant to Regulatory T Cell-Mediated Suppression in the Context of Autoimmunity. *J. Immunol.* **195,** 528–540 (2015).

60. Martin, D. A., Towne, J. E., Kricorian, G., Klekotka, P., Gudjonsson, J. E., Krueger, J. G. & Russell, C. B. The Emerging Role of IL-17 in the Pathogenesis of Psoriasis: Preclinical and Clinical Findings. *J. Invest. Dermatol.* **133,** 17–26 (2013).

61. Cai, Y., Fleming, C. & Yan, J. New insights of T cells in the pathogenesis of psoriasis. *Cell. Mol. Immunol.* **9,** 302–9 (2012).

62. Tortola, L., Rosenwald, E., Abel, B., Blumberg, H., Schäfer, M., Coyle, A. J., Renauld, J.-C., Werner, S., Kisielow, J. & Kopf, M. Psoriasiform dermatitis is driven by IL-36-mediated DC-keratinocyte crosstalk. *J. Clin. Invest.* **122,** 3965–76 (2012).

63. Henry, C. M., Sullivan, G. P., Clancy, D. M., Afonina, I. S., Kulms, D. & Martin, S. J. Neutrophil-Derived Proteases Escalate Inflammation through Activation of IL-36 Family Cytokines. *Cell Rep.* **14,** 708–22 (2016).

64. Cho, K.-A., Suh, J. W., Lee, K. H., Kang, J. L. & Woo, S.-Y. IL-17 and IL-22 enhance skin inflammation by stimulating the secretion of IL-1β by keratinocytes via the ROS-NLRP3-caspase-1 pathway. *Int. Immunol.* **24,** 147–58 (2012).

65. Baliwag, J., Barnes, D. H. & Johnston, A. Cytokines in psoriasis. *Cytokine* **73,** 342–350 (2015).

66. Mease, P. J. Inhibition of interleukin-17, interleukin-23 and the TH17 cell pathway in the treatment of psoriatic arthritis and psoriasis. *Curr. Opin. Rheumatol.* **27,** 127–33 (2015).

67. Elloso, M. M., Gomez-Angelats, M. & Fourie, A. M. Targeting the Th17 pathway in psoriasis. *J. Leukoc. Biol.* **92,** 1187–97 (2012).

68. Johnson-Huang, L. M., Lowes, M. A. & Krueger, J. G. Putting together the psoriasis puzzle: an update on developing targeted therapies. *Dis. Model. Mech.* **5,** 423–33 (2012).

69. Hori, S., Nomura, T. & Sakaguchi, S. Control of Regulatory T Cell Development by the Transcription Factor Foxp3. *Science (80-.).* **299,** 1057–1061 (2003).

70. Sakaguchi, S., Yamaguchi, T., Nomura, T. & Ono, M. Regulatory T Cells and Immune Tolerance. *Cell* **133,** 775–787 (2008).

71. Sakaguchi, S., Miyara, M., Costantino, C. M. & Hafler, D. A. FOXP3+ regulatory T cells in the human immune system. *Nat. Rev. Immunol.* **10,** 490–500 (2010).

72. Yadav, M., Stephan, S. & Bluestone, J. A. Peripherally induced Tregs-role in immune homeostasis and autoimmunity. *Front. Immunol.* **4,** (2013).

73. Vignali, D. A. A., Collison, L. W. & Workman, C. J. How regulatory T cells work. *Nat. Rev. Immunol.* **8,** 523–532 (2008).

74. Bluestone, J. A. & Abbas, A. K. Natural versus adaptive regulatory T cells. *Nat. Rev. Immunol.* **3,** 253–7 (2003).

75. Hou, T. Z., Qureshi, O. S., Wang, C. J., Baker, J., Young, S. P., Walker, L. S. K. & Sansom, D. M. A transendocytosis model of CTLA-4 function predicts its suppressive behavior on regulatory T cells. *J. Immunol.* **194,** 2148–59 (2015).

76. Qureshi, O. S., Zheng, Y., Nakamura, K., Attridge, K., Manzotti, C., Schmidt, E. M., Baker, J., Jeffery, L. E., Kaur, S., Briggs, Z., Hou, T. Z., Futter, C. E., Anderson, G., Walker, L. S. K. & Sansom, D. M. Trans-endocytosis of CD80 and CD86: a molecular basis for the cell-extrinsic function of CTLA-4. *Science* **332,** 600–3 (2011).

77. Sansom, D. M. Moving CTLA-4 from the trash to recycling. *Science (80-.).* **349,** 377–378 (2015).

78. Walker, L. S. K. Treg and CTLA-4: two intertwining pathways to immune tolerance. *J. Autoimmun.* **45,** 49–57 (2013).

79. Dwyer, K. M., Deaglio, S., Gao, W., Friedman, D., Strom, T. B. & Robson, S. C. CD39 and control of cellular immune responses. *Purinergic Signal.* **3,** 171–180 (2007).

80. Antonioli, L., Pacher, P., Vizi, E. S. & Haskó, G. CD39 and CD73 in immunity and inflammation. *Trends Mol. Med.* **19,** 355–367 (2013).

81. Borsellino, G., Kleinewietfeld, M., Di Mitri, D., Sternjak, A., Diamantini, A., Giometto, R., Höpner, S., Centonze, D., Bernardi, G., Dell'Acqua, M. L., Rossini, P. M., Battistini, L., Rötzschke, O. & Falk, K. Expression of ectonucleotidase CD39 by Foxp3+ Treg cells: Hydrolysis of extracellular ATP and immune suppression. *Blood* **110,** 1225–1232 (2007).

82. Haskó, G., Linden, J., Cronstein, B. & Pacher, P. Adenosine receptors: therapeutic aspects for inflammatory and immune diseases. *Nat. Rev. Drug Discov.* **7,** 759–770 (2008).

83. Haskó, G. & Cronstein, B. N. Adenosine: an endogenous regulator of innate immunity. *Trends Immunol.* **25,** 33–39 (2004).

84. Fletcher, J. M., Lonergan, R., Costelloe, L., Kinsella, K., Moran, B., O'Farrelly, C., Tubridy, N. & Mills, K. H. G. CD39+Foxp3+ regulatory T Cells suppress pathogenic Th17 cells and are impaired in multiple sclerosis. *J. Immunol. (Baltimore, Md. 1950)* **183,** 7602–7610 (2009).

85. Tang, Y., Jiang, L., Zheng, Y., Ni, B. & Wu, Y. Expression of CD39 on FoxP3+ T regulatory cells correlates with progression of HBV infection. *BMC Immunol.* **13,** 17 (2012).

86. Künzli, B. M., Bernlochner, M.-I., Rath, S., Käser, S., Csizmadia, E., Enjyoji, K., Cowan, P., d'Apice, A., Dwyer, K., Rosenberg, R., Perren, A., Friess, H., Maurer, C. A., Robson, S. C., Kunzli, B. M., Bernlochner, M.-I., Rath, S., Kaser, S., Csizmadia, E., *et al.* Impact of CD39 and purinergic signalling on the growth and metastasis of colorectal cancer. *Purinergic Signal.*

7, 231–241 (2011).

87. Nikolova, M., Carriere, M., Jenabian, M. A., Limou, S., Younas, M., K??k, A., Hu??, S., Seddiki, N., Hulin, A., Delaneau, O., Schuitemaker, H., Herbeck, J. T., Mullins, J. I., Muhtarova, M., Bensussan, A., Zagury, J. F., Lelievre, J. D. & L??vy, Y. CD39/adenosine pathway is involved in AIDS progression. *PLoS Pathog.* **7,** e1002110 (2011).

88. Sun, X., Wu, Y., Gao, W., Enjyoji, K., Csizmadia, E., Müller, C. E., Murakami, T. & Robson, S. C. CD39/ENTPD1 expression by CD4+Foxp3+regulatory T cells promotes hepatic metastatic tumor growth in mice. *Gastroenterology* **139,** 1030–1040 (2010).

89. Stagg, J. & Smyth, M. J. Extracellular adenosine triphosphate and adenosine in cancer. *Oncogene* **29,** 5346–5358 (2010).

90. Couper, K. N., Blount, D. G. & Riley, E. M. IL-10: The Master Regulator of Immunity to Infection. *J. Immunol.* **180,** 5771–5777 (2008).

91. Akram, M. Citric Acid Cycle and Role of its Intermediates in Metabolism. *Cell Biochem. Biophys.* **68,** 475–478 (2014).

92. O'Neill, L. A. J., Kishton, R. J. & Rathmell, J. A guide to immunometabolism for immunologists. *Nat Rev Immunol* **16,** 553–565 (2016).

93. Glatz, J. F. C. & Luiken, J. J. F. P. Fatty acids in cell signaling: Historical perspective and future outlook. *Prostaglandins Leukot. Essent. Fat. Acids* **92,** 57–62 (2015).

94. Stincone, A., Prigione, A., Cramer, T., Wamelink, M. M. C., Campbell, K., Cheung, E., Olin-Sandoval, V., Grüning, N. M., Krüger, A., Tauqeer Alam, M., Keller, M. A., Breitenbach, M., Brindle, K. M., Rabinowitz, J. D. & Ralser, M. The return of metabolism: Biochemistry and physiology of the pentose phosphate pathway. *Biol. Rev.* **90,** 927–963 (2015).

95. Wu, G. Amino acids: Metabolism, functions, and nutrition. *Amino Acids* **37,** 1–17 (2009).

96. Saxton, R. A. & Sabatini, D. M. mTOR Signaling in Growth, Metabolism, and Disease. *Cell* **168,** 960–976 (2017).

97. Düvel, K., Yecies, J. L., Menon, S., Raman, P., Lipovsky, A. I., Souza, A. L., Triantafellow, E., Ma, Q., Gorski, R., Cleaver, S., Vander Heiden, M. G., MacKeigan, J. P., Finan, P. M., Clish, C. B., Murphy, L. O. & Manning, B. D. Activation of a metabolic gene regulatory network downstream of mTOR complex 1. *Mol. Cell* **39,** 171–183 (2010).

98. Majmundar, A. J., Wong, W. J. & Simon, M. C. Hypoxia-Inducible Factors and the Response to Hypoxic Stress. *Mol. Cell* **40,** 294–309 (2010).

99. Lee, M. N., Ha, S. H., Kim, J., Koh, A., Lee, C. S., Kim, J. H., Jeon, H., Kim, D.-H., Suh, P.-G. & Ryu, S. H. Glycolytic flux signals to mTOR through glyceraldehyde-3-phosphate dehydrogenase-mediated regulation of Rheb. *Mol. Cell. Biol.* **29,** 3991–4001 (2009).

100. Sancak, Y., Bar-Peled, L., Zoncu, R., Markhard, A. L., Nada, S. & Sabatini, D. M. Ragulator-rag complex targets mTORC1 to the lysosomal surface and is necessary for its activation by amino acids. *Cell* **141,** 290–303 (2010).

101. Pópulo, H., Lopes, J. M. & Soares, P. The mTOR signalling pathway in human cancer. *Int. J. Mol. Sci.* **13,** 1886–1918 (2012).

102. Hardie, D. G., Ross, F. A. & Hawley, S. A. AMPK: A nutrient and energy sensor that maintains energy homeostasis. *Nat. Rev. Mol. Cell Biol.* **13,** 251–262 (2012).

103. Jager, S., Handschin, C., St.-Pierre, J. & Spiegelman, B. M. AMP-activated protein kinase (AMPK) action in skeletal muscle via direct phosphorylation of PGC-1 . *Proc. Natl. Acad. Sci.* **104,** 12017–12022 (2007).

104. Egan, D. F., Shackelford, D. B., Mihaylova, M. M., Gelino, S., Kohnz, R. A., Mair, W., Vasquez, D. S., Joshi, A., Gwinn, D. M., Taylor, R., Asara, J. M., Fitzpatrick, J., Dillin, A., Viollet, B., Kundu, M., Hansen, M. & Shaw, R. J. Phosphorylation of ULK1 (hATG1) by AMP-activated protein kinase connects energy sensing to mitophagy. *Science (80-.).* **331,** 456–461 (2011).

105. Day, E. A., Ford, R. J. & Steinberg, G. R. AMPK as a Therapeutic Target for Treating Metabolic Diseases. *Trends Endocrinol. Metab.* **28,** 545–560 (2017).

106. Rizos, C. V. & Elisaf, M. S. Metformin and cancer. *Eur. J. Pharmacol.* **705,** 96–108 (2013).

107. Saisho, Y. Metformin and Inflammation: Its Potential Beyond Glucose-lowering Effect. *Endocr. Metab. Immune Disord. Drug Targets* **15,** 196–205 (2015).

108. Rodriguez-Prados, J.-C., Traves, P. G., Cuenca, J., Rico, D., Aragones, J., Martin-Sanz, P., Cascante, M. & Bosca, L. Substrate Fate in Activated Macrophages: A Comparison between Innate, Classic, and Alternative Activation. *J. Immunol.* **185,** 605–614 (2010).

109. Warburg, O. On the Origin of Cancer Cells. *Source Sci. New Ser.* **123,** 309–314 (1956).

110. Tannahill, G. M., Curtis, A. M., Adamik, J., Palsson-McDermott, E. M., McGettrick, A. F., Goel, G., Frezza, C., Bernard, N. J., Kelly, B., Foley, N. H., Zheng, L., Gardet, A., Tong, Z., Jany, S. S., Corr, S. C., Haneklaus, M., Caffrey, B. E., Pierce, K., Walmsley, S., *et al.* Succinate is an inflammatory signal that induces IL-1β through HIF-1α. *Nature* **496,** 238–242 (2013).

111. Cramer, T., Yamanishi, Y., Clausen, B. E., Förster, I., Pawlinski, R., Mackman, N., Haase, V. H., Jaenisch, R., Corr, M., Nizet, V., Firestein, G. S., Gerber, H.-P., Ferrara, N. & Johnson, R. S. HIF-1α Is Essential for Myeloid Cell-Mediated Inflammation. *Cell* **112,** 645–657 (2003).

112. Byles, V., Covarrubias, A. J., Ben-Sahra, I., Lamming, D. W., Sabatini, D. M., Manning, B. D. & Horng, T. The TSC-mTOR pathway regulates macrophage polarization. *Nat. Commun.* **4,** 2834 (2013).

113. Lunt, S. Y. & Vander Heiden, M. G. Aerobic Glycolysis: Meeting the Metabolic Requirements of Cell Proliferation. *Annu. Rev. Cell Dev. Biol.* **27,** 441–464 (2011).

114. Taylor, C. T. & Colgan, S. P. Regulation of immunity and inflammation by hypoxia in immunological niches. *Nat. Rev. Immunol.* **17,** 774–785 (2017).

115. Ecker, J., Liebisch, G., Englmaier, M., Grandl, M., Robenek, H. & Schmitz, G. Induction of fatty acid synthesis is a key requirement for phagocytic differentiation of human monocytes. *Proc. Natl. Acad. Sci.* **107,** 7817–7822 (2010).

116. Vats, D., Mukundan, L., Odegaard, J. I., Zhang, L., Smith, K. L., Morel, C. R., Greaves, D. R., Murray, P. J. & Chawla, A. Oxidative metabolism and PGC-1β attenuate macrophage-mediated inflammation. *Cell Metab.* **4,** 13–24 (2006).

117. Huang, S. C. C., Everts, B., Ivanova, Y., O'Sullivan, D., Nascimento, M., Smith, A. M., Beatty, W., Love-Gregory, L., Lam, W. Y., O'Neill, C. M., Yan, C., Du, H., Abumrad, N. A., Urban, J. F., Artyomov, M. N., Pearce, E. L. & Pearce, E. J. Cell-intrinsic lysosomal lipolysis is essential for alternative activation of macrophages. *Nat. Immunol.* **15,** 846–855 (2014).

118. Galván-Peña, S. & O'Neill, L. A. Metabolic Reprograming in Macrophage Polarization. *Front. Immunol.* **5,** 420 (2014).

119. Sag, D., Carling, D., Stout, R. D. & Suttles, J. Adenosine 5'-Monophosphate-Activated Protein Kinase Promotes Macrophage Polarization to an Anti-Inflammatory Functional Phenotype. *J. Immunol.* **181,** 8633–8641 (2008).

120. Krawczyk, C. M., Holowka, T., Sun, J., Blagih, J., Amiel, E., DeBerardinis, R. J., Cross, J. R., Jung, E., Thompson, C. B., Jones, R. G. & Pearce, E. J. Toll-like receptor-induced changes in glycolytic metabolism regulate dendritic cell activation. *Blood* **115,** 4742–9 (2010).

121. Jantsch, J., Chakravortty, D., Turza, N., Prechtel, A. T., Buchholz, B., Gerlach, R. G., Volke, M., Gläsner, J., Warnecke, C., Wiesener, M. S., Eckardt, K.-U., Steinkasserer, A., Hensel, M. & Willam, C. Hypoxia and hypoxia-inducible factor-1 alpha modulate lipopolysaccharide-induced dendritic cell activation and function. *J. Immunol.* **180,** 4697–705 (2008).

122. Everts, B., Amiel, E., Huang, S. C.-C., Smith, A. M., Chang, C.-H., Lam, W. Y., Redmann, V., Freitas, T. C., Blagih, J., van der Windt, G. J. W., Artyomov, M. N., Jones, R. G., Pearce, E. L. & Pearce, E. J. TLR-driven early glycolytic reprogramming via the kinases TBK1-IKKε supports the anabolic demands of dendritic cell activation. *Nat. Immunol.* **15,** 323–332 (2014).

123. Carroll, K. C., Viollet, B. & Suttles, J. AMPKα1 deficiency amplifies proinflammatory myeloid APC activity and CD40 signaling. *J. Leukoc. Biol.* **94,** 1113–21 (2013).

124. Fox, C. J., Hammerman, P. S. & Thompson, C. B. Fuel feeds function: Energy metabolism and the T-cell response. *Nat. Rev. Immunol.* **5,** 844–852 (2005).

125. Pearce, E. L. & Pearce, E. J. Metabolic Pathways in Immune Cell Activation and Quiescence. *Immunity* **38,** 633–643 (2013).

126. Gubser, P. M., Bantug, G. R., Razik, L., Fischer, M., Dimeloe, S., Hoenger, G., Durovic, B., Jauch, A. & Hess, C. Rapid effector function of memory CD8+ T cells requires an immediate-early glycolytic switch. *Nat. Immunol.* **14,** 1064–1072 (2013).

127. Menk, A. V., Scharping, N. E., Moreci, R. S., Zeng, X., Guy, C., Salvatore, S., Bae, H., Xie, J., Young, H. A., Wendell, S. G. & Delgoffe, G. M. Early TCR Signaling Induces Rapid Aerobic Glycolysis Enabling Distinct Acute T Cell Effector Functions. *Cell Rep.* **22,** 1509–1521 (2018).

128. Finlay, D. K., Rosenzweig, E., Sinclair, L. V, Feijoo-Carnero, C., Hukelmann, J. L., Rolf, J., Panteleyev, A. A., Okkenhaug, K. & Cantrell, D. A. PDK1 regulation of mTOR and hypoxia-inducible factor 1 integrate metabolism and migration of CD8+ T cells. *J. Exp. Med.* **209,** 2441–53 (2012).

129. Michalek, R. D., Gerriets, V. A., Jacobs, S. R., Macintyre, A. N., MacIver, N. J., Mason, E. F., Sullivan, S. A., Nichols, A. G. & Rathmell, J. C. Cutting Edge: Distinct Glycolytic and Lipid Oxidative Metabolic Programs Are Essential for Effector and Regulatory CD4+ T Cell Subsets. *J. Immunol.* **186,** 3299–3303 (2011).

130. Demetrius, L. Of mice and men. *EMBO Rep.* **6,** S39-44 (2005).

131. Van den Bossche, J., Baardman, J., Otto, N. A., van der Velden, S., Neele, A. E., van den Berg, S. M., Luque-Martin, R., Chen, H.-J., Boshuizen, M. C. S., Ahmed, M., Hoeksema, M. A., de Vos, A. F. & de Winther, M. P. J. Mitochondrial Dysfunction Prevents Repolarization of Inflammatory Macrophages. *Cell Rep.* **17,** 684–696 (2016).

132. Everts, B., Amiel, E., Van Der Windt, G. J. W., Freitas, T. C., Chott, R., Yarasheski, K. E., Pearce, E. L. & Pearce, E. J. Commitment to glycolysis sustains survival of NO-producing inflammatory dendritic cells. *Blood* **120,** 1422–1431 (2012).

133. Weinberg, J. B., Misukonis, M. A., Shami, P. J., Mason, S. N., Sauls, D. L., Dittman, W. A., Wood, E. R., Smith, G. K., McDonald, B., Bachus, K. E. & et al. Human mononuclear phagocyte inducible nitric oxide synthase (iNOS): analysis of iNOS mRNA, iNOS protein, biopterin, and nitric oxide production by blood monocytes and peritoneal macrophages. *Blood* **86,** 1184–1195 (1995).

134. Thomas, A. C. & Mattila, J. T. 'Of mice and men': Arginine metabolism in macrophages. *Front. Immunol.* **5,** 479 (2014).

135. Gleeson, L. E., Sheedy, F. J., Palsson-McDermott, E. M., Triglia, D., O'Leary, S. M., O'Sullivan, M. P., O'Neill, L. A. J. & Keane, J. Cutting Edge: Mycobacterium tuberculosis Induces Aerobic Glycolysis in Human Alveolar Macrophages That Is Required for Control of Intracellular Bacillary Replication. *J. Immunol.* **196,** 2444–2449 (2016).

136. Cheng, S. C., Scicluna, B. P., Arts, R. J. W., Gresnigt, M. S., Lachmandas, E., Giamarellos-Bourboulis, E. J., Kox, M., Manjeri, G. R., Wagenaars, J. A. L., Cremer, O. L., Leentjens, J., Van Der Meer, A. J., Van De Veerdonk, F. L., Bonten, M. J., Schultz, M. J., Willems, P. H. G. M., Pickkers, P., Joosten, L. A. B., Van Der Poll, T., *et al.* Broad defects in the energy metabolism of leukocytes underlie immunoparalysis in sepsis. *Nat. Immunol.* **17,** 406–413 (2016).

137. Papathanassiu, A. E., Ko, J.-H., Imprialou, M., Bagnati, M., Srivastava, P. K., Vu, H. A., Cucchi, D., McAdoo, S. P., Ananieva, E. A., Mauro, C. & Behmoaras, J. BCAT1 controls metabolic reprogramming in activated human macrophages and is associated with inflammatory diseases. *Nat. Commun.* **8,** 16040 (2017).

138. Malinarich, F., Duan, K., Hamid, R. A., Bijin, A., Lin, W. X., Poidinger, M., Fairhurst, A.-M. & Connolly, J. E. High Mitochondrial Respiration and Glycolytic Capacity Represent a Metabolic Phenotype of Human Tolerogenic Dendritic Cells. *J. Immunol.* **194,** 5174–5186 (2015).

139. Renner, K., Geiselhöringer, A. L., Fante, M., Bruss, C., Färber, S., Schönhammer, G., Peter, K., Singer, K., Andreesen, R., Hoffmann, P., Oefner, P., Herr, W. & Kreutz, M. Metabolic plasticity of human T cells: Preserved cytokine production under glucose deprivation or mitochondrial restriction, but 2-deoxy-glucose affects effector functions. *Eur. J. Immunol.* **45,** 2504–2516 (2015).

140. Dziurla, R., Gaber, T., Fangradt, M., Hahne, M., Tripmacher, R., Kolar, P., Spies, C. M., Burmester, G. R. & Buttgereit, F. Effects of hypoxia and/or lack of glucose on cellular energy metabolism and cytokine production in stimulated human CD4+ T lymphocytes. *Immunol. Lett.* **131,** 97–105 (2010).

141. Tripmacher, R., Gaber, T., Dziurla, R., Häupl, T., Erekul, K., Grützkau, A., Tschirschmann, M., Scheffold, A., Radbruch, A., Burmester, G. R. & Buttgereit, F. Human CD4+T cells maintain specific functions even under conditions of extremely restricted ATP production. *Eur. J. Immunol.* **38,** 1631–1642 (2008).

142. Procaccini, C., Carbone, F., Di Silvestre, D., Brambilla, F., De Rosa, V., Galgani, M., Faicchia, D., Marone, G., Tramontano, D., Corona, M., Alviggi, C., Porcellini, A., La Cava, A., Mauri, P. & Matarese, G. The Proteomic Landscape of Human Ex Vivo Regulatory and Conventional T Cells Reveals Specific Metabolic Requirements. *Immunity* **44,** 406–21 (2016).

143. Gatza, E., Wahl, D. R., Opipari, A. W., Sundberg, T. B., Reddy, P., Liu, C., Glick, G. D. & Ferrara, J. L. M. Manipulating the Bioenergetics of Alloreactive T Cells Causes Their Selective Apoptosis and Arrests Graft-Versus-Host Disease. *Sci. Transl. Med.* **3,** 67ra8-67ra8 (2011).

144. Franchi, L., Monteleone, I., Hao, L.-Y., Spahr, M. A., Zhao, W., Liu, X., Demock, K., Kulkarni, A., Lesch, C. A., Sanchez, B., Carter, L., Marafini, I., Hu, X., Mashadova, O., Yuan, M., Asara, J. M., Singh, H., Lyssiotis, C. A., Monteleone, G., *et al.* Inhibiting Oxidative Phosphorylation In Vivo Restrains Th17 Effector Responses and Ameliorates Murine Colitis. *J. Immunol.* **198,** 1600810 (2017).

145. Everse, J. & Hsia, N. The Toxicities of Native and Modified Hemoglobins. *Free Radic. Biol. Med.* **22,** 1075–1099 (1997).

146. Jeney, V., Balla, J., Yachie, A., Varga, Z., Vercellotti, G. M., Eaton, J. W., Balla, G., Halliwell, B., Gutteridge, J., Weiss, S., Repine, J., Fox, R., Berger, E., Gannon, D., Varani, J., Phan, S., Schraufstatter, I., Hyslop, P., Jackson, J., *et al.* Pro-oxidant and cytotoxic effects of circulating heme. *Blood* **100,** 879–87 (2002).

147. Larsen, R., Gouveia, Z., Soares, M. P. & Gozzelino, R. Heme cytotoxicity and the pathogenesis of immune-mediated inflammatory diseases. *Front. Pharmacol.* **3,** 77 (2012).

148. Baranano, D. E., Rao, M., Ferris, C. D. & Snyder, S. H. Biliverdin reductase: a major physiologic cytoprotectant. *Proc. Natl. Acad. Sci. U. S. A.* **99,** 16093–8 (2002).

149. Wegiel, B. & Otterbein, L. E. Go green: the anti-inflammatory effects of biliverdin reductase. *Front. Pharmacol.* **3,** 47 (2012).

150. Sedlak, T. W., Saleh, M., Higginson, D. S., Paul, B. D., Juluri, K. R. & Snyder, S. H. Bilirubin and glutathione have complementary antioxidant and cytoprotective roles. *Proc. Natl. Acad. Sci. U. S. A.* **106,** 5171–5176 (2009).

151. Sedlak, T. W. & Snyder, S. H. Bilirubin benefits: cellular protection by a biliverdin reductase antioxidant cycle. *Pediatrics* **113,** 1776–82 (2004).

152. Maines, M. D. The Heme Oxygenase System: A Regulator of Second Messenger Gases. *Annu. Rev. Pharmacol. Toxicol* **37,** 517–54 (1997).

153. Verma, A., Hirsch, D., Glatt, C., Ronnett, G. & Snyder, S. Carbon monoxide: a putative neural messenger. *Science (80-.).* **259,** 381–384 (1993).

154. Ma, Q. Role of Nrf2 in Oxidative Stress and Toxicity. *Annu. Rev. Pharmacol. Toxicol* **53,** 401–26 (2013).

155. Kansanen, E., Kuosmanen, S. M., Leinonen, H. & Levonen, A.-L. The Keap1-Nrf2 pathway: Mechanisms of activation and dysregulation in cancer. *Redox Biol.* **1,** 45–49 (2013).

156. Taguchi, K., Motohashi, H. & Yamamoto, M. Molecular mechanisms of the Keap1-Nrf2 pathway in stress response and cancer evolution. *Genes to Cells* **16,** 123–140 (2011).

157. Zenke-Kawasaki, Y., Dohi, Y., Katoh, Y., Ikura, T., Ikura, M., Asahara, T., Tokunaga, F., Iwai, K. & Igarashi, K. Heme Induces Ubiquitination and Degradation of the Transcription Factor Bach1. *Mol. Cell. Biol.* **27,** 6962–6971 (2007).

158. Lavrovsky, Y., Schwartzman, M. L., Levere, R. D., Kappas, A. & Abraham, N. G. Identification of binding sites for transcription factors NF-kappa B and AP-2 in the promoter region of the human heme oxygenase 1 gene. *Proc. Natl. Acad. Sci. U. S. A.* **91,** 5987–91 (1994).

159. Paine, A., Eiz-Vesper, B., Blasczyk, R. & Immenschuh, S. Signaling to heme oxygenase-1 and its anti-inflammatory therapeutic potential. *Biochem. Pharmacol.* **80,** 1895–903 (2010).

160. Rushworth, S. A. & O'Connell, M. A. Haem oxygenase-1 in inflammation. *Biochem. Soc. Trans.* **32,** 1093–1094 (2004).

161. Alam, J. & Cook, J. L. How Many Transcription Factors Does It Take to Turn On the Heme Oxygenase-1 Gene? *Am. J. Respir. Cell Mol. Biol.* **36,** 166–174 (2007).

162. Morgan, M. J. & Liu, Z. Crosstalk of reactive oxygen species and NF-κB signaling. *Cell Res.* **21,** 103–15 (2011).

163. Lian, K.-C., Chuang, J.-J., Hsieh, C.-W., Wung, B.-S., Huang, G.-D., Jian, T.-Y. & Sun, Y.-W. Dual mechanisms of NF-kappaB inhibition in carnosol-treated endothelial cells. *Toxicol. Appl. Pharmacol.* **245,** 21–35 (2010).

164. Bellezza, I., Tucci, A., Galli, F., Grottelli, S., Mierla, A. L., Pilolli, F. & Minelli, A. Inhibition of NF-κB nuclear translocation via HO-1 activation underlies α-tocopheryl succinate toxicity. *J. Nutr. Biochem.* **23,** 1583–1591 (2012).

165. McNally, S. J., Harrison, E. M., Ross, J. A., Garden, O. J. & Wigmore, S. J. Curcumin induces heme oxygenase 1 through generation of reactive oxygen species, p38 activation and phosphatase inhibition. *Int. J. Mol. Med.* **19,** 165–172 (2007).

166. Lin, C.-C., Chiang, L.-L., Lin, C.-H., Shih, C.-H., Liao, Y.-T., Hsu, M.-J. & Chen, B.-C. Transforming growth factor-β1 stimulates heme oxygenase-1 expression via the PI3K/Akt and NF-κB pathways in human lung epithelial cells. *Eur. J. Pharmacol.* **560,** 101–109 (2007).

167. Martin, D., Rojo, A. I., Salinas, M., Diaz, R., Gallardo, G., Alam, J., De Galarreta, C. M. R. & Cuadrado, A. Regulation of heme oxygenase-1 expression through the phosphatidylinositol 3-kinase/Akt pathway and the Nrf2 transcription factor in response to the antioxidant phytochemical carnosol. *J. Biol. Chem.* **279,** 8919–29 (2004).

168. Ryter, S. W. & Choi, A. M. K. Targeting heme oxygenase-1 and carbon monoxide for therapeutic modulation of inflammation. *Transl. Res.* **167,** 7–34 (2016).

169. Seo, S. H. & Jeong, G. S. Fisetin inhibits TNF-alpha-induced inflammatory action and hydrogen peroxide-induced oxidative damage in human keratinocyte HaCaT cells through PI3K/AKT/Nrf-2-mediated heme oxygenase-1 expression. *Int. Immunopharmacol.* **29,** 246–253 (2015).

170. Lee, T.-S. & Chau, L.-Y. Heme oxygenase-1 mediates the anti-inflammatory effect of interleukin-10 in mice. *Nat. Med.* **8,** 240–6 (2002).

171. Ricchetti, G. A., Williams, L. M. & Foxwell, B. M. J. Heme oxygenase 1 expression induced by IL-10 requires STAT-3 and phosphoinositol-3 kinase and is inhibited by lipopolysaccharide. *J. Leukoc. Biol.* **76,** 719–26 (2004).

172. Nakahira, K., Kim, H. P., Geng, X. H., Nakao, A., Wang, X., Murase, N., Drain, P. F., Wang, X., Sasidhar, M., Nabel, E. G., Takahashi, T., Lukacs, N. W., Ryter, S. W., Morita, K. & Choi, A. M. K. Carbon monoxide differentially inhibits TLR signaling pathways by regulating ROS-induced trafficking of TLRs to lipid rafts. *J. Exp. Med.* **203,** 2377–89 (2006).

173. Riquelme, S. A., Bueno, S. M. & Kalergis, A. M. Carbon monoxide down-modulates Toll-like receptor 4/MD2 expression on innate immune cells and reduces endotoxic shock susceptibility. *Immunology* **144,** 321–332 (2015).

174. Kapturczak, M. H., Wasserfall, C., Brusko, T., Campbell-Thompson, M., Ellis, T. M., Atkinson, M. A. & Agarwal, A. Heme oxygenase-1 modulates early inflammatory responses: evidence from the heme oxygenase-1-deficient mouse. *Am. J. Pathol.* **165,** 1045–53 (2004).

175. Hull, T. D., Agarwal, A. & George, J. F. The mononuclear phagocyte system in homeostasis and disease: a role for heme oxygenase-1. *Antioxid. Redox Signal.* **20,** 1770–88 (2014).

176. Chauveau, C., Rémy, S., Royer, P. J., Hill, M., Tanguy-Royer, S., Hubert, F.-X., Tesson, L., Brion, R., Beriou, G., Gregoire, M., Josien, R., Cuturi, M. C. & Anegon, I. Heme oxygenase-1 expression inhibits dendritic cell maturation and proinflammatory function but conserves IL-10 expression. *Blood* **106,** 1694–702 (2005).

177. Moreau, A., Hill, M., Thébault, P., Deschamps, J. Y., Chiffoleau, E., Chauveau, C., Moullier, P., Anegon, I., Alliot-Licht, B. & Cuturi, M. C. Tolerogenic dendritic cells actively inhibit T cells through heme oxygenase-1 in rodents and in nonhuman primates. *FASEB J.* **23,** 3070–7 (2009).

178. Al-Huseini, L. M. A., Aw Yeang, H. X., Hamdam, J. M., Sethu, S., Alhumeed, N., Wong, W. & Sathish, J. G. Heme oxygenase-1 regulates dendritic cell function through modulation of p38 MAPK-CREB/ATF1 signaling. *J. Biol. Chem.* **289,** 16442–51 (2014).

179. Listopad, J., Asadullah, K., Sievers, C., Ritter, T., Meisel, C., Sabat, R. & Döcke, W.-D. Heme oxygenase-1 inhibits T cell-dependent skin inflammation and differentiation and function of antigen-presenting cells. *Exp. Dermatol.* **16,** 661–70 (2007).

180. Schumacher, A., Wafula, P. O., Teles, A., El-Mousleh, T., Linzke, N., Zenclussen, M. L., Langwisch, S., Heinze, K., Wollenberg, I., Casalis, P. A., Volk, H.-D., Fest, S. & Zenclussen, A. C. Blockage of heme oxygenase-1 abrogates the protective effect of regulatory T cells on murine pregnancy and promotes the maturation of dendritic cells. *PLoS One* **7,** e42301 (2012).

181. Wegiel, B., Hedblom, A., Li, M., Gallo, D., Csizmadia, E., Harris, C., Nemeth, Z., Zuckerbraun, B. S., Soares, M., Persson, J. L. & Otterbein, L. E. Heme oxygenase-1 derived carbon monoxide permits maturation of myeloid cells. *Cell Death Dis.* **5,** e1139 (2014).

182. Naito, Y., Takagi, T. & Higashimura, Y. Heme oxygenase-1 and anti-inflammatory M2 macrophages. *Arch. Biochem. Biophys.* **564C,** 83–88 (2014).

183. Pae, H.-O., Oh, G.-S., Choi, B.-M., Chae, S.-C. & Chung, H.-T. Differential expressions of heme oxygenase-1 gene in CD25− and CD25+ subsets of human CD4+ T cells. *Biochem. Biophys. Res. Commun.* **306,** 701–705 (2003).

184. Pae, H.-O., Oh, G.-S., Choi, B.-M., Chae, S.-C., Kim, Y.-M., Chung, K.-R. & Chung, H.-T. Carbon Monoxide Produced by Heme Oxygenase-1 Suppresses T Cell Proliferation via Inhibition of IL-2 Production. *J. Immunol.* **172,** 4744–4751 (2004).

185. Song, R., Mahidhara, R. S., Zhou, Z., Hoffman, R. A., Seol, D.-W., Flavell, R. A., Billiar, T. R., Otterbein, L. E. & Choi, A. M. K. Carbon Monoxide Inhibits T Lymphocyte Proliferation via Caspase-Dependent Pathway. *J. Immunol.* **172,** 1220–1226 (2004).

186. Burt, T. D., Seu, L., Mold, J. E., Kappas, A. & McCune, J. M. Naive human T cells are activated and proliferate in response to the heme oxygenase-1 inhibitor tin mesoporphyrin. *J. Immunol.* **185,** 5279–88 (2010).

187. Zelenay, S., Chora, A., Soares, M. P. & Demengeot, J. Heme oxygenase-1 is not required for mouse regulatory T cell development and function. *Int. Immunol.* **19,** 11–8 (2007).

188. George, J. F., Braun, A., Brusko, T. M., Joseph, R., Bolisetty, S., Wasserfall, C. H., Atkinson, M. A., Agarwal, A. & Kapturczak, M. H. Suppression by CD4+CD25+ regulatory T cells is dependent on expression of heme oxygenase-1 in antigen-presenting cells. *Am. J. Pathol.* **173,** 154–60 (2008).

189. Wong, T.-H., Chen, H.-A., Gau, R.-J., Yen, J.-H. & Suen, J.-L. Heme Oxygenase-1-Expressing Dendritic Cells Promote Foxp3+ Regulatory T Cell Differentiation and Induce Less Severe

Airway Inflammation in Murine Models. *PLoS One* **11,** e0168919 (2016).

190. Vítek, L. The role of bilirubin in diabetes, metabolic syndrome, and cardiovascular diseases. *Front. Pharmacol.* **3 APR,** 55 (2012).

191. Dennery, P. A. Evaluating the Beneficial and Detrimental Effects of Bile Pigments in Early and Later Life. *Front. Pharmacol.* **3,** 115 (2012).

192. Wang, W. W., Smith, D. L. H. & Zucker, S. D. Bilirubin inhibits iNOS expression and NO production in response to endotoxin in rats. *Hepatology* **40,** 424–33 (2004).

193. Wu, J., Ma, J., Fan, S.-T., Schlitt, H. J. & Tsui, T.-Y. Bilirubin derived from heme degradation suppresses MHC class II expression in endothelial cells. *Biochem. Biophys. Res. Commun.* **338,** 890–896 (2005).

194. Vogel, M. E. Bilirubin acts as an endogenous regulator of inflammation by disrupting adhesion molecule-mediated leukocyte migration. *Inflamm. Cell Signal.* **3,** (2016).

195. Joshi, V., Umashankara, M., Ramakrishnan, C., Nanjaraj Urs, A. N., Suvilesh, K. N., Velmurugan, D., Rangappa, K. S. & Vishwanath, B. S. Dimethyl ester of bilirubin exhibits anti-inflammatory activity through inhibition of secretory phospholipase A2, lipoxygenase and cyclooxygenase. *Arch. Biochem. Biophys.* **598,** 28–39 (2016).

196. Sarady-Andrews, J. K., Liu, F., Gallo, D., Nakao, A., Overhaus, M., Öllinger, R., Choi, A. M. & Otterbein, L. E. Biliverdin administration protects against endotoxin-induced acute lung injury in rats. *Am. J. Physiol. Cell. Mol. Physiol.* **289,** L1131–L1137 (2005).

197. Li, J.-J., Zou, Z.-Y., Liu, J., Xiong, L.-L., Jiang, H.-Y., Wang, T.-H. & Shao, J.-L. Biliverdin administration ameliorates cerebral ischemia reperfusion injury in rats and is associated with proinflammatory factor downregulation. *Exp. Ther. Med.* **14,** 671–679 (2017).

198. Bellner, L., Vitto, M., Patil, K. A., Dunn, M. W., Regan, R. & Laniado-Schwartzman, M. Exacerbated corneal inflammation and neovascularization in the HO-2 null mice is ameliorated by biliverdin. *Exp. Eye Res.* **87,** 268–278 (2008).

199. Bellner, L., Wolstein, J., Patil, K. A., Dunn, M. W. & Laniado-Schwartzman, M. Biliverdin Rescues the HO-2 Null Mouse Phenotype of Unresolved Chronic Inflammation Following Corneal Epithelial Injury. *Invest. Ophthalmol. Vis. Sci.* **52,** 3246–53 (2011).

200. Wegiel, B., Baty, C. J., Gallo, D., Csizmadia, E., Scott, J. R., Akhavan, A., Chin, B. Y., Kaczmarek, E., Alam, J., Bach, F. H., Zuckerbraun, B. S. & Otterbein, L. E. Cell surface biliverdin reductase mediates biliverdin-induced anti-inflammatory effects via phosphatidylinositol 3-kinase and Akt. *J. Biol. Chem.* **284,** 21369–78 (2009).

201. Wegiel, B., Gallo, D., Csizmadia, E., Roger, T., Kaczmarek, E., Harris, C., Zuckerbraun, B. S. & Otterbein, L. E. Biliverdin inhibits Toll-like receptor-4 (TLR4) expression through nitric oxide-dependent nuclear translocation of biliverdin reductase. *Proc. Natl. Acad. Sci. U. S. A.* **108,** 18849–54 (2011).

202. Ahmad, Z., Salim, M. & Maines, M. D. Human biliverdin reductase is a leucine zipper-like DNA-binding protein and functions in transcriptional activation of heme oxygenase-1 by oxidative stress. *J. Biol. Chem.* **277,** 9226–9232 (2002).

203. Otterbein, L. E., Bach, F. H., Alam, J., Soares, M., Tao Lu, H., Wysk, M., Davis, R. J., Flavell, R. A. & Choi, A. M. K. Carbon monoxide has anti-inflammatory effects involving the mitogen-activated protein kinase pathway. *Nat Med* **6,** 422–428 (2000).

204. Sarady, J. K., Otterbein, S. L., Liu, F., Otterbein, L. E. & Choi, A. M. K. Carbon Monoxide

Modulates Endotoxin-Induced Production of Granulocyte Macrophage Colony-Stimulating Factor in Macrophages. *Am. J. Respir. Cell Mol. Biol.* **27,** 739–745 (2002).

205. Sawle, P., Foresti, R., Mann, B. E., Johnson, T. R., Green, C. J. & Motterlini, R. Carbon monoxide-releasing molecules (CO-RMs) attenuate the inflammatory response elicited by lipopolysaccharide in RAW264.7 murine macrophages. *Br. J. Pharmacol.* **145,** 800–810 (2005).

206. Tardif, V., Riquelme, S. A., Remy, S., Carreño, L. J., Cortés, C. M., Simon, T., Hill, M., Louvet, C., Riedel, C. A., Blancou, P., Bach, J.-M., Chauveau, C., Bueno, S. M., Anegon, I. & Kalergis, A. M. Carbon monoxide decreases endosome-lysosome fusion and inhibits soluble antigen presentation by dendritic cells to T cells. *Eur. J. Immunol.* **43,** 2832–44 (2013).

207. Rémy, S., Blancou, P., Tesson, L., Tardif, V., Brion, R., Royer, P. J., Motterlini, R., Foresti, R., Painchaut, M., Pogu, S., Gregoire, M., Bach, J. M., Anegon, I. & Chauveau, C. Carbon monoxide inhibits TLR-induced dendritic cell immunogenicity. *J. Immunol.* **182,** 1877–84 (2009).

208. Riquelme, S. A., Pogu, J., Anegon, I., Bueno, S. M. & Kalergis, A. M. Carbon monoxide impairs mitochondria-dependent endosomal maturation and antigen presentation in dendritic cells. *Eur. J. Immunol.* **45,** 3269–88 (2015).

209. Chung, S. W., Liu, X., Macias, A. A., Baron, R. M. & Perrella, M. A. Heme oxygenase-1–derived carbon monoxide enhances the host defense response to microbial sepsis in mice. *J. Clin. Invest.* **118,** 239–247 (2008).

210. Chora, Â. A., Fontoura, P., Cunha, A., Pais, T. F., Cardoso, S., Ho, P. P., Lee, L. Y., Sobel, R. A., Steinman, L. & Soares, M. P. Heme oxygenase–1 and carbon monoxide suppress autoimmune neuroinflammation. *J. Clin. Invest.* **117,** 438–447 (2007).

211. Uddin, M. J., Jeong, S., Zheng, M., Chen, Y., Cho, G. J., Chung, H. T. & Joe, Y. Carbon monoxide attenuates dextran sulfate sodium-induced colitis via inhibition of GSK-3β signaling. *Oxid. Med. Cell. Longev.* **2013,** 210563 (2013).

212. Hettiarachchi, N., Dallas, M., Al-Owais, M., Griffiths, H., Hooper, N., Scragg, J., Boyle, J. & Peers, C. Heme oxygenase-1 protects against Alzheimer's amyloid-β1-42-induced toxicity via carbon monoxide production. *Cell Death Dis.* **5,** e1569 (2014).

213. Sahara, H., Shimizu, A., Setoyama, K., Okumi, M., Oku, M., Samelson-Jones, E. & Yamada, K. Carbon monoxide reduces pulmonary ischemia–reperfusion injury in miniature swine. *J. Thorac. Cardiovasc. Surg.* **139,** 1594–1601 (2010).

214. Ozaki, K. S., Kimura, S. & Murase, N. Use of carbon monoxide in minimizing ischemia/reperfusion injury in transplantation. *Transplant. Rev. (Orlando).* **26,** 125–39 (2012).

215. Sato, K., Balla, J., Otterbein, L., Smith, R. N., Brouard, S., Lin, Y., Csizmadia, E., Sevigny, J., Robson, S. C., Vercellotti, G., Choi, A. M., Bach, F. H. & Soares, M. P. Carbon monoxide generated by heme oxygenase-1 suppresses the rejection of mouse-to-rat cardiac transplants. *J Immunol* **166,** 4185–4194 (2001).

216. Lin, C.-C., Yang, C.-C., Hsiao, L.-D., Chen, S.-Y. & Yang, C.-M. Heme Oxygenase-1 Induction by Carbon Monoxide Releasing Molecule-3 Suppresses Interleukin-1β-Mediated Neuroinflammation. *Front. Mol. Neurosci.* **10,** 387 (2017).

217. Song, L., Li, J., Yuan, X., Liu, W., Chen, Z., Guo, D., Yang, F., Guo, Q. & Song, H. Carbon monoxide-releasing molecule suppresses inflammatory and osteoclastogenic cytokines in

nicotine- and lipopolysaccharide-stimulated human periodontal ligament cells via the heme oxygenase-1 pathway. *Int. J. Mol. Med.* **40,** 1591–1601 (2017).

218. Mangano, K., Cavalli, E., Mammana, S., Basile, M. S., Caltabiano, R., Pesce, A., Puleo, S., Atanasov, A. G., Magro, G., Nicoletti, F. & Fagone, P. Involvement of the Nrf2/HO-1/CO axis and therapeutic intervention with the CO-releasing molecule CORM-A1, in a murine model of autoimmune hepatitis. *J. Cell. Physiol.* **233,** 4156–4165 (2018).

219. Morse, D., Pischke, S. E., Zhou, Z., Davis, R. J., Flavell, R. A., Loop, T., Otterbein, S. L., Otterbein, L. E. & Choi, A. M. K. Suppression of Inflammatory Cytokine Production by Carbon Monoxide Involves the JNK Pathway and AP-1. *J. Biol. Chem.* **278,** 36993–36998 (2003).

220. Ryter, S. W., Alam, J. & Choi, A. M. K. Heme oxygenase-1/carbon monoxide: from basic science to therapeutic applications. *Physiol. Rev.* **86,** 583–650 (2006).

221. Ryter, S. W. & Otterbein, L. E. Carbon monoxide in biology and medicine. *BioEssays* **26,** 270–280 (2004).

222. Jung, S.-S., Moon, J.-S., Xu, J.-F., Ifedigbo, E., Ryter, S. W., Choi, A. M. K. & Nakahira, K. Carbon monoxide negatively regulates NLRP3 inflammasome activation in macrophages. *Am. J. Physiol. - Lung Cell. Mol. Physiol.* **308,** L1058–L1067 (2015).

223. Wang, X. M., Kim, H. P., Nakahira, K., Ryter, S. W. & Choi, A. M. K. The heme oxygenase-1/carbon monoxide pathway suppresses TLR4 signaling by regulating the interaction of TLR4 with caveolin-1. *J. Immunol.* **182,** 3809–18 (2009).

224. Kim, K. M., Pae, H.-O., Zheng, M., Park, R., Kim, Y.-M. & Chung, H.-T. Carbon Monoxide Induces Heme Oxygenase-1 via Activation of Protein Kinase R Like Endoplasmic Reticulum Kinase and Inhibits Endothelial Cell Apoptosis Triggered by Endoplasmic Reticulum Stress. *Circ. Res.* **101,** 919–927 (2007).

225. Yang, Y. C., Huang, Y. T., Hsieh, C. W., Yang, P. M. & Wung, B. S. Carbon monoxide induces heme oxygenase-1 to modulate STAT3 activation in endothelial cells via S-glutathionylation. *PLoS One* **9,** e100677 (2014).

226. Wang, B., Cao, W., Biswal, S. & Doré, S. Carbon monoxide-activated Nrf2 pathway leads to protection against permanent focal cerebral ischemia. *Stroke.* **42,** 2605–10 (2011).

227. Chiang, N., Shinohara, M., Dalli, J., Mirakaj, V., Kibi, M., Choi, A. M. K. & Serhan, C. N. Inhaled carbon monoxide accelerates resolution of inflammation via unique proresolving mediator-heme oxygenase-1 circuits. *J. Immunol.* **190,** 6378–88 (2013).

228. Motterlini, R., Clark, J. E., Foresti, R., Sarathchandra, P., Mann, B. E. & Green, C. J. Carbon Monoxide-Releasing Molecules: Characterization of Biochemical and Vascular Activities. *Circ. Res.* **90,** 17e–24 (2002).

229. Motterlini, R. & Otterbein, L. E. The therapeutic potential of carbon monoxide. *Nat Rev Drug Discov* **9,** 728–743 (2010).

230. Fagone, P., Patti, F., Mangano, K., Mammana, S., Coco, M., Touil-Boukoffa, C., Chikovani, T., Di Marco, R. & Nicoletti, F. Heme oxygenase-1 expression in peripheral blood mononuclear cells correlates with disease activity in multiple sclerosis. *J. Neuroimmunol.* **261,** 82–6 (2013).

231. Hanselmann, C., Mauch, C. & Werner, S. Haem oxygenase-1: a novel player in cutaneous wound repair and psoriasis? *Biochem. J.* **353,** 459–66 (2001).

232. Zhang, L., Zhang, Y., Zhong, W., Di, C., Lin, X. & Xia, Z. Heme oxygenase-1 ameliorates dextran sulfate sodium-induced acute murine colitis by regulating Th17/Treg cell balance. *J. Biol. Chem.* **289,** 26847–58 (2014).

233. Schulz, S., Chisholm, K. M., Zhao, H., Kalish, F., Yang, Y., Wong, R. J. & Stevenson, D. K. Heme oxygenase-1 confers protection and alters T-cell populations in a mouse model of neonatal intestinal inflammation. *Pediatr. Res.* **77,** 640–648 (2015).

234. Benallaoua, M., François, M., Batteux, F., Thelier, N., Shyy, J. Y.-J., Fitting, C., Tsagris, L., Boczkowski, J., Savouret, J.-F., Corvol, M.-T., Poiraudeau, S. & Rannou, F. Pharmacologic induction of heme oxygenase 1 reduces acute inflammatory arthritis in mice. *Arthritis Rheum.* **56,** 2585–94 (2007).

235. Lerner, A., Jeremias, P. & Matthias, T. The World Incidence and Prevalence of Autoimmune Diseases is Increasing. *Int. J. Celiac Dis.* **3,** 151–155 (2016).

236. Schipper, H. M. Heme oxygenase expression in human central nervous system disorders. *Free Radic. Biol. Med.* **37,** 1995–2011 (2004).

237. Fagone, P., Mangano, K., Quattrocchi, C., Motterlini, R., Di Marco, R., Magro, G., Penacho, N., Romao, C. C. & Nicoletti, F. Prevention of clinical and histological signs of proteolipid protein (PLP)-induced experimental allergic encephalomyelitis (EAE) in mice by the water-soluble carbon monoxide-releasing molecule (CORM)-A1. *Clin. Exp. Immunol.* **163,** 368–74 (2011).

238. Liu, Y., Zhu, B., Wang, X., Luo, L., Li, P., Paty, D. W. & Cynader, M. S. Bilirubin as a potent antioxidant suppresses experimental autoimmune encephalomyelitis: implications for the role of oxidative stress in the development of multiple sclerosis. *J. Neuroimmunol.* **139,** 27–35 (2003).

239. Liu, Y., Liu, J., Tetzlaff, W., Paty, D. W. & Cynader, M. S. Biliverdin reductase, a major physiologic cytoprotectant, suppresses experimental autoimmune encephalomyelitis. *Free Radic. Biol. Med.* **40,** 960–967 (2006).

240. Simon, T., Pogu, J., Rémy, S., Brau, F., Pogu, S., Maquigneau, M., Fonteneau, J.-F., Poirier, N., Vanhove, B., Blancho, G., Piaggio, E., Anegon, I. & Blancou, P. Inhibition of effector antigen-specific T cells by intradermal administration of heme oxygenase-1 inducers. *J. Autoimmun.* **81,** 44–55 (2017).

241. Neurath, M. Current and emerging therapeutic targets for IBD. *Nat. Rev. Gastroenterol. Hepatol.* **14,** 688–688 (2017).

242. Paul, G., Bataille, F., Obermeier, F., Bock, J., Klebl, F., Strauch, U., Lochbaum, D., Rummele, P., Farkas, S., Scholmerich, J., Fleck, M., Rogler, G. & Herfarth, H. Analysis of intestinal haem-oxygenase-1 (HO-1) in clinical and experimental colitis. *Clin. Exp. Immunol.* **140,** 547–555 (2005).

243. Takagi, T., Naito, Y., Mizushima, K., Nukigi, Y., Okada, H., Suzuki, T., Hirata, I., Omatsu, T., Okayama, T., Handa, O., Kokura, S., Ichikawa, H. & Yoshikawa, T. Increased intestinal expression of heme oxygenase-1 and its localization in patients with ulcerative colitis. *J. Gastroenterol. Hepatol.* **23,** S229–S233 (2008).

244. Zhong, W., Xia, Z., Hinrichs, D., Rosenbaum, J. T., Wegmann, K. W., Meyrowitz, J. & Zhang, Z. Hemin Exerts Multiple Protective Mechanisms and Attenuates Dextran Sulfate Sodium–induced Colitis. *J. Pediatr. Gastroenterol. Nutr.* **50,** 132–139 (2010).

245. Berberat, P. O., A-Rahim, Y. I., Yamashita, K., Warny, M. M., Csizmadia, E., Robson, S. C. &

Bach, F. H. Heme Oxygenase-1-Generated Biliverdin Ameliorates Experimental Murine Colitis. *Inflamm. Bowel Dis.* **11,** 350–359 (2005).

246. Uddin, M. J., Jeong, S., Zheng, M., Chen, Y., Cho, G. J., Chung, H. T. & Joe, Y. Carbon Monoxide Attenuates Dextran Sulfate Sodium-Induced Colitis via Inhibition of GSK-3 *β* Signaling. *Oxid. Med. Cell. Longev.* **2013,** 1–9 (2013).

247. Hegazi, R. A. F., Rao, K. N., Mayle, A., Sepulveda, A. R., Otterbein, L. E. & Plevy, S. E. Carbon monoxide ameliorates chronic murine colitis through a heme oxygenase 1–dependent pathway. *J. Exp. Med.* **202,** 1703–1713 (2005).

248. Onyiah, J. C., Sheikh, S. Z., Maharshak, N., Steinbach, E. C., Russo, S. M., Kobayashi, T., Mackey, L. C., Hansen, J. J., Moeser, A. J., Rawls, J. F., Borst, L. B., Otterbein, L. E. & Plevy, S. E. Carbon Monoxide and Heme Oxygenase-1 Prevent Intestinal Inflammation in Mice by Promoting Bacterial Clearance. *Gastroenterology* **144,** 789–798 (2013).

249. Sheikh, S. Z., Hegazi, R. A., Kobayashi, T., Onyiah, J. C., Russo, S. M., Matsuoka, K., Sepulveda, A. R., Li, F., Otterbein, L. E. & Plevy, S. E. An anti-inflammatory role for carbon monoxide and heme oxygenase-1 in chronic Th2-mediated murine colitis. *J. Immunol.* **186,** 5506–13 (2011).

250. Parisi, R., Symmons, D. P. M., Griffiths, C. E. M. & Ashcroft, D. M. Global Epidemiology of Psoriasis: A Systematic Review of Incidence and Prevalence. *J. Invest. Dermatol.* **133,** 377–385 (2013).

251. Griffiths, C. E. M. & Barker, J. N. W. N. Pathogenesis and clinical features of psoriasis. *Lancet* **370,** 263–271 (2007).

252. Jariwala, S. P. The role of dendritic cells in the immunopathogenesis of psoriasis. *Arch. Dermatol. Res.* **299,** 359–66 (2007).

253. Eyerich, K., Dimartino, V. & Cavani, A. IL-17 and IL-22 in immunity: Driving protection and pathology. *Eur. J. Immunol.* **47,** 607–614 (2017).

254. Benham, H., Norris, P., Goodall, J., Wechalekar, M. D., FitzGerald, O., Szentpetery, A., Smith, M., Thomas, R. & Gaston, H. Th17 and Th22 cells in psoriatic arthritis and psoriasis. *Arthritis Res. Ther.* **15,** R136 (2013).

255. Numata, I., Okuyama, R., Memezawa, A., Ito, Y., Takeda, K., Furuyama, K., Shibahara, S. & Aiba, S. Functional expression of heme oxygenase-1 in human differentiated epidermis and its regulation by cytokines. *J. Invest. Dermatol.* **129,** 2594–603 (2009).

256. Grochot-Przeczek, A., Lach, R., Mis, J., Skrzypek, K., Gozdecka, M., Sroczynska, P., Dubiel, M., Rutkowski, A., Kozakowska, M., Zagorska, A., Walczynski, J., Was, H., Kotlinowski, J., Drukala, J., Kurowski, K., Kieda, C., Herault, Y., Dulak, J. & Jozkowicz, A. Heme oxygenase-1 accelerates cutaneous wound healing in mice. *PLoS One* **4,** e5803 (2009).

257. Ma, L. J., You, Y., Bai, B. X. & Li, Y.-Z. Therapeutic effects of heme oxygenase-1 on psoriasiform skin lesions in guinea pigs. *Arch. Dermatol. Res.* **301,** 459–66 (2009).

258. Zhang, B., Xie, S., Su, Z., Song, S., Xu, H., Chen, G., Cao, W., Yin, S., Gao, Q. & Wang, H. Heme oxygenase-1 induction attenuates imiquimod-induced psoriasiform inflammation by negative regulation of Stat3 signaling. *Sci. Rep.* **6,** 21132 (2016).

259. Nisar, M. F., Parsons, K. S. G., Bian, C. X. & Zhong, J. L. UVA irradiation induced heme oxygenase-1: a novel phototherapy for morphea. *Photochem. Photobiol.* **91,** 210–20

260. Xiang, Y., Liu, G., Yang, L. & Zhong, J. L. UVA-induced protection of skin through the

induction of heme oxygenase-1. *Biosci. Trends* **5,** 239–44 (2011).

261. Allanson, M. & Reeve, V. E. Immunoprotective UVA (320-400 nm) irradiation upregulates heme oxygenase-1 in the dermis and epidermis of hairless mouse skin. *J. Invest. Dermatol.* **122,** 1030–6 (2004).

262. Lehmann, J. C. U., Listopad, J. J., Rentzsch, C. U., Igney, F. H., von Bonin, A., Hennekes, H. H., Asadullah, K. & Docke, W.-D. F. Dimethylfumarate induces immunosuppression via glutathione depletion and subsequent induction of heme oxygenase 1. *J. Invest. Dermatol.* **127,** 835–45 (2007).

263. Ghoreschi, K., Brück, J., Kellerer, C., Deng, C., Peng, H., Rothfuss, O., Hussain, R. Z., Gocke, A. R., Respa, A., Glocova, I., Valtcheva, N., Alexander, E., Feil, S., Feil, R., Schulze-Osthoff, K., Rupec, R. A., Lovett-Racke, A. E., Dringen, R., Racke, M. K., *et al.* Fumarates improve psoriasis and multiple sclerosis by inducing type II dendritic cells. *J. Exp. Med.* **208,** 2291–303 (2011).

264. Schulz, S., Wong, R. J., Vreman, H. J. & Stevenson, D. K. Metalloporphyrins - an update. *Front. Pharmacol.* **3,** 68 (2012).

265. Schmidt, R. Cobalt protoporphyrin as a potential therapeutic agent? *FASEB J.* **21,** 2639; author reply 2640 (2007).

266. Linker, R. A. & Gold, R. Dimethyl Fumarate for Treatment of Multiple Sclerosis: Mechanism of Action, Effectiveness, and Side Effects. *Curr. Neurol. Neurosci. Rep.* **13,** 394 (2013).

267. Chen, D., Brown, J. D., Kawasaki, Y., Bommer, J., Takemoto, J. Y., McDonagh, A., Sedlak, T., Snyder, S., Soares, M., Bach, F., Baranano, D., Rao, M., Ferris, C., Snyder, S., Maghzal, G., Leck, M., Collinson, E., Li, C., Stocker, R., *et al.* Scalable production of biliverdin IXα by Escherichia coli. *BMC Biotechnol.* **12,** 89 (2012).

268. Basnet, P. & Skalko-Basnet, N. Curcumin: An Anti-Inflammatory Molecule from a Curry Spice on the Path to Cancer Treatment. *Molecules* **16,** 4567–4598 (2011).

269. Menon, V. P. & Sudheer, A. R. Antioxidant and anti-inflammatory properties of curcumin. *Adv. Exp. Med. Biol.* **595,** 105–25 (2007).

270. Salem, M., Rohani, S., Gillies, E. R., Hatcher, H., Planalp, R., Cho, J., Torti, F. M., Torti, S. V., Tiwari, B. K., Agrawal, G. P., Aggarwal, B. B., Sundaram, C., Malani, N., Ichikawa, H., Aggarwal, B. B., Shishodia, S., Payton, F., Sandusky, P., Alworth, W. L., *et al.* Curcumin, a promising anti-cancer therapeutic: a review of its chemical properties, bioactivity and approaches to cancer cell delivery. *RSC Adv.* **4,** 10815 (2014).

271. Wilken, R., Veena, M. S., Wang, M. B. & Srivatsan, E. S. Curcumin: A review of anti-cancer properties and therapeutic activity in head and neck squamous cell carcinoma. *Mol. Cancer* **10,** 12 (2011).

272. Kumari, N., Kulkarni, A. A., Lin, X., McLean, C., Ammosova, T., Ivanov, A., Hipolito, M., Nekhai, S. & Nwulia, E. Inhibition of HIV-1 by curcumin A, a novel curcumin analog. *Drug Des. Devel. Ther.* **9,** 5051–60 (2015).

273. Motterlini, R., Foresti, R., Bassi, R. & Green, C. J. Curcumin, an antioxidant and anti-inflammatory agent, induces heme oxygenase-1 and protects endothelial cells against oxidative stress. *Free Radic. Biol. Med.* **28,** 1303–1312 (2000).

274. Farombi, E. O., Shrotriya, S., Na, H.-K., Kim, S.-H. & Surh, Y.-J. Curcumin attenuates dimethylnitrosamine-induced liver injury in rats through Nrf2-mediated induction of heme

oxygenase-1. *Food Chem. Toxicol.* **46,** 1279–87 (2008).

275. Boyanapalli, S. S. S., Paredes-Gonzalez, X., Fuentes, F., Zhang, C., Guo, Y., Pung, D., Saw, C. L. L. & Kong, A.-N. T. Nrf2 knockout attenuates the anti-inflammatory effects of phenethyl isothiocyanate and curcumin. *Chem. Res. Toxicol.* **27,** 2036–43 (2014).

276. Hsu, H.-Y., Chu, L.-C., Hua, K.-F. & Chao, L. K. Heme oxygenase-1 mediates the anti-inflammatory effect of Curcumin within LPS-stimulated human monocytes. *J. Cell. Physiol.* **215,** 603–12 (2008).

277. Kim, G.-Y., Kim, K.-H., Lee, S.-H., Yoon, M.-S., Lee, H.-J., Moon, D.-O., Lee, C.-M., Ahn, S.-C., Park, Y. C. & Park, Y.-M. Curcumin Inhibits Immunostimulatory Function of Dendritic Cells: MAPKs and Translocation of NF- B as Potential Targets. *J. Immunol.* **174,** 8116–8124 (2005).

278. Cong, Y., Wang, L., Konrad, A., Schoeb, T. & Elson, C. O. Curcumin induces the tolerogenic dendritic cell that promotes differentiation of intestine-protective regulatory T cells. *Eur. J. Immunol.* **39,** 3134–3146 (2009).

279. Rogers, N. M., Kireta, S. & Coates, P. T. H. Curcumin induces maturation-arrested dendritic cells that expand regulatory T cells in vitro and in vivo. *Clin. Exp. Immunol.* **162,** 460–73 (2010).

280. Shirley, S. A., Montpetit, A. J., Lockey, R. F. & Mohapatra, S. S. Curcumin prevents human dendritic cell response to immune stimulants. *Biochem. Biophys. Res. Commun.* **374,** 431–6 (2008).

281. Gao, X., Kuo, J., Jiang, H., Deeb, D., Liu, Y., Divine, G., Chapman, R. A., Dulchavsky, S. A. & Gautam, S. C. Immunomodulatory activity of curcumin: suppression of lymphocyte proliferation, development of cell-mediated cytotoxicity, and cytokine production in vitro. *Biochem. Pharmacol.* **68,** 51–61 (2004).

282. Park, M.-J., Moon, S.-J., Lee, S.-H., Yang, E.-J., Min, J.-K., Cho, S.-G., Yang, C.-W., Park, S.-H., Kim, H.-Y. & Cho, M.-L. Curcumin Attenuates Acute Graft-versus-Host Disease Severity via In Vivo Regulations on Th1, Th17 and Regulatory T Cells. *PLoS One* **8,** e67171 (2013).

283. Kim, G., Jang, M. S., Son, Y. M., Seo, M. J., Ji, S. Y., Han, S. H., Jung, I. D., Park, Y. M., Jung, H. J. & Yun, C. H. Curcumin Inhibits CD4+ T Cell Activation, but Augments CD69 Expression and TGF-β1-Mediated Generation of Regulatory T Cells at Late Phase. *PLoS One* **8,** e62300 (2013).

284. Liu, L., Liu, Y. L., Liu, G. X., Chen, X., Yang, K., Yang, Y. X., Xie, Q., Gan, H. K., Huang, X. L. & Gan, H. T. Curcumin ameliorates dextran sulfate sodium-induced experimental colitis by blocking STAT3 signaling pathway. *Int. Immunopharmacol.* **17,** 314–20 (2013).

285. Zhao, H. M., Xu, R., Huang, X. Y., Cheng, S. M., Huang, M. F., Yue, H. Y., Wang, X., Zou, Y., Lu, A. P. & Liu, D. Y. Curcumin suppressed activation of dendritic cells via JAK/STAT/SOCS signal in mice with experimental colitis. *Front. Pharmacol.* **7,** 1–1 (2016).

286. Brück, J., Holstein, J., Glocova, I., Seidel, U., Geisel, J., Kanno, T., Kumagai, J., Mato, N., Sudowe, S., Widmaier, K., Sinnberg, T., Yazdi, A. S., Eberle, F. C., Hirahara, K., Nakayama, T., Röcken, M. & Ghoreschi, K. Nutritional control of IL-23/Th17-mediated autoimmune disease through HO-1/STAT3 activation. *Sci. Rep.* **7,** 44482 (2017).

287. Capini, C., Jaturanpinyo, M., Chang, H.-I., Mutalik, S., McNally, A., Street, S., Steptoe, R., O'Sullivan, B., Davies, N. & Thomas, R. Antigen-specific suppression of inflammatory arthritis using liposomes. *J. Immunol.* **182,** 3556–65 (2009).

288. Kang, D., Li, B., Luo, L., Jiang, W., Lu, Q., Rong, M. & Lai, R. Curcumin shows excellent therapeutic effect on psoriasis in mouse model. *Biochimie* **123,** 73–80 (2016).

289. Sun, J., Zhao, Y. & Hu, J. Curcumin Inhibits Imiquimod-Induced Psoriasis-Like Inflammation by Inhibiting IL-1beta and IL-6 Production in Mice. *PLoS One* **8,** e67078 (2013).

290. Mancuso, C. & Barone, E. Curcumin in clinical practice: myth or reality? *Trends Pharmacol. Sci.* **30,** 333–334 (2009).

291. Klickovic, U., Doberer, D., Gouya, G., Aschauer, S., Weisshaar, S., Storka, A., Bilban, M. & Wolzt, M. Human Pharmacokinetics of High Dose Oral Curcumin and Its Effect on Heme Oxygenase-1 Expression in Healthy Male Subjects. *Biomed Res. Int.* **2014,** 1–7 (2014).

292. Anand, P., Kunnumakkara, A. B., Newman, R. A., Aggarwal, B. B., Anand, P., Kunnumakkara, A. B. & Newman, R. A. Bioavailability of Curcumin : Problems and Promises. *Mol. Pharm.* **4,** 807–818 (2007).

293. Kurd, S. K., Smith, N., VanVoorhees, A., Troxel, A. B., Badmaev, V., Seykora, J. T. & Gelfand, J. M. Oral curcumin in the treatment of moderate to severe psoriasis vulgaris: A prospective clinical trial. *J. Am. Acad. Dermatol.* **58,** 625–31 (2008).

294. Hanai, H., Iida, T., Takeuchi, K., Watanabe, F., Maruyama, Y., Andoh, A., Tsujikawa, T., Fujiyama, Y., Mitsuyama, K., Sata, M., Yamada, M., Iwaoka, Y., Kanke, K., Hiraishi, H., Hirayama, K., Arai, H., Yoshii, S., Uchijima, M., Nagata, T., *et al.* Curcumin Maintenance Therapy for Ulcerative Colitis: Randomized, Multicenter, Double-Blind, Placebo-Controlled Trial. *Clin. Gastroenterol. Hepatol.* **4,** 1502–1506 (2006).

295. Lang, A., Salomon, N., Wu, J. C. Y., Kopylov, U., Lahat, A., Har-Noy, O., Ching, J. Y. L., Cheong, P. K., Avidan, B., Gamus, D., Kaimakliotis, I., Eliakim, R., Ng, S. C. & Ben-Horin, S. Curcumin in Combination With Mesalamine Induces Remission in Patients With Mild-to-Moderate Ulcerative Colitis in a Randomized Controlled Trial. *Clin. Gastroenterol. Hepatol.* **13,** 1444–1449.e1 (2015).

296. Pulikkotil, S. & Nath, S. Effects of curcumin on crevicular levels of IL-1β and CCL28 in experimental gingivitis. *Aust. Dent. J.* **60,** 317–327 (2015).

297. Heng, M. C. Y., Song, M. K., Harker, J. & Heng, M. K. Drug-induced suppression of phosphorylase kinase activity correlates with resolution of psoriasis as assessed by clinical, histological and immunohistochemical parameters. *Br. J. Dermatol.* **143,** 937–949 (2000).

298. Antiga, E., Bonciolini, V., Volpi, W., Del Bianco, E., Caproni, M., Antiga, E., Bonciolini, V., Volpi, W., Del Bianco, E. & Caproni, M. Oral Curcumin (Meriva) Is Effective as an Adjuvant Treatment and Is Able to Reduce IL-22 Serum Levels in Patients with Psoriasis Vulgaris. *Biomed Res. Int.* **2015,** 283634 (2015).

299. Mohanty, C. & Sahoo, S. K. Curcumin and its topical formulations for wound healing applications. *Drug Discov. Today* **22,** 1582–1592 (2017).

300. Chainani-wu, N. Safety and anti-inflammatory activity of curcumin: A component of tumeric (curcuma longa). *J. Altern. Complement. Med.* **9,** 161–168 (2003).

301. Burgos-Morón, E., Calderón-Montaño, J. M., Salvador, J., Robles, A. & López-Lázaro, M. The dark side of curcumin. *Int. J. Cancer* **126,** 1771–5 (2010).

302. Johnson, J. J. Carnosol: a promising anti-cancer and anti-inflammatory agent. *Cancer Lett.* **305,** 1–7 (2011).

303. Foresti, R., Bains, S. K., Pitchumony, T. S., de Castro Brás, L. E., Drago, F., Dubois-Randé, J.-

L., Bucolo, C. & Motterlini, R. Small molecule activators of the Nrf2-HO-1 antioxidant axis modulate heme metabolism and inflammation in BV2 microglia cells. *Pharmacol. Res.* **76,** 132–48 (2013).

304. Rücker, H. & Amslinger, S. Identification of heme oxygenase-1 stimulators by a convenient ELISA-based bilirubin quantification assay. *Free Radic. Biol. Med.* **78,** 135–46 (2015).

305. Petiwala, S. M. & Johnson, J. J. Diterpenes from rosemary (Rosmarinus officinalis): Defining their potential for anti-cancer activity. *Cancer Lett.* **367,** 93–102 (2015).

306. Kyung-Soo Chun, R., Kundu, J., Gyeong Chae, I. & Kumar Kundu, J. Carnosol: A Phenolic Diterpene With Cancer Chemopreventive Potential. *J Cancer Prev* **1919,** 103–110 (2014).

307. Lo, A.-H., Liang, Y.-C., Lin-Shiau, S.-Y., Ho, C.-T. & Lin, J.-K. Carnosol, an antioxidant in rosemary, suppresses inducible nitric oxide synthase through down-regulating nuclear factor-κB in mouse macrophages. *Carcinogenesis* **23,** 983–991 (2002).

308. Tong, L. & Wu, S. The Mechanisms of Carnosol in Chemoprevention of Ultraviolet B-Light-Induced Non-Melanoma Skin Cancer Formation. *Sci. Rep.* **8,** 3574 (2018).

309. Schwager, J., Richard, N., Fowler, A., Seifert, N. & Raederstorff, D. Carnosol and related substances modulate chemokine and cytokine production in macrophages and chondrocytes. *Molecules* **21,** 465 (2016).

310. Sanchez, C., Horcajada, M. N., Scalfo, F. M., Ameye, L., Offord, E. & Henrotin, Y. Carnosol inhibits pro-inflammatory and catabolic mediators of cartilage breakdown in human osteoarthritic chondrocytes and mediates cross-talk between subchondral bone osteoblasts and chondrocytes. *PLoS One* **10,** e0136118 (2015).

311. Wang, Z. H., Xie, Y. X., Zhang, J. W., Qiu, X. H., Cheng, A. Bin, Tian, L., Ma, B. Y. & Hou, Y. B. Carnosol protects against spinal cord injury through Nrf-2 upregulation. *J. Recept. Signal Transduct.* **36,** 72–78 (2016).

312. Emami, F., Ali-Beig, H., Farahbakhsh, S., Mojabi, N., Rastegar-Moghadam, B., Arbabian, S., Kazemi, M., Tekieh, E., Golmanesh, L., Ranjbaran, M., Jalili, C., Noroozzadeh, A. & Sahraei, H. Hydroalcoholic extract of Rosemary (Rosmarinus officinalis L.) and its constituent carnosol inhibit formalin-induced pain and inflammation in mice. *Pakistan J. Biol. Sci. PJBS* **16,** 309–16 (2013).

313. Maione, F., Cantone, V., Pace, S., Chini, M. G., Bisio, A., Romussi, G., Pieretti, S., Werz, O., Koeberle, A., Mascolo, N. & Bifulco, G. Anti-inflammatory and analgesic activity of carnosol and carnosic acid *in vivo* and *in vitro* and *in silico* analysis of their target interactions. *Br. J. Pharmacol.* **174,** 1497–1508 (2017).

314. Lee, D. Y., Hwang, C. J., Choi, J. Y., Park, M. H., Song, M. J., Oh, K. W., Son, D. J., Lee, S. H., Han, S. B. & Hong, J. T. Inhibitory effect of carnosol on phthalic anhydride-induced atopic dermatitis via inhibition of STAT3. *Biomol. Ther.* **25,** 535–544 (2017).

315. Reuter, J., Jocher, A., Hornstein, S., Mönting, J. & Schempp, C. Sage Extract Rich in Phenolic Diterpenes Inhibits Ultraviolet-Induced Erythema *in Vivo*. *Planta Med.* **73,** 1190–1191 (2007).

316. Arranz, E., Guri, A., Fornari, T., Mendiola, J. A., Reglero, G. & Corredig, M. In vitro uptake and immune functionality of digested Rosemary extract delivered through food grade vehicles. *Food Res. Int.* **97,** 71–77 (2017).

317. McCarty, M. F. Clinical potential of Spirulina as a source of phycocyanobilin. *J. Med. Food*

10, 566–70 (2007).

318. Basdeo, S. A., Campbell, N. K., Sullivan, L. M., Flood, B., Creagh, E. M., Mantle, T. J., Fletcher, J. M. & Dunne, A. Suppression of human alloreactive T cells by linear tetrapyrroles; relevance for transplantation. *Transl. Res.* **178,** 81–94.e2 (2016).

319. Ku, C. S., Pham, T. X., Park, Y., Kim, B., Shin, M. S., Kang, I. & Lee, J. Edible blue-green algae reduce the production of pro-inflammatory cytokines by inhibiting NF-κB pathway in macrophages and splenocytes. *Biochim. Biophys. Acta - Gen. Subj.* **1830,** 2981–2988 (2013).

320. Rasool, M., Sabina, E. P. & Lavanya, B. Anti-inflammatory effect of Spirulina fusiformis on adjuvant-induced arthritis in mice. *Biol. Pharm. Bull.* **29,** 2483–7 (2006).

321. Mao, T. K., Van de Water, J. & Gershwin, M. E. Effects of a Spirulina-based dietary supplement on cytokine production from allergic rhinitis patients. *J. Med. Food* **8,** 27–30 (2005).

322. Deng, R. & Chow, T.-J. Hypolipidemic, antioxidant, and anti-inflammatory activities of microalgae Spirulina. *Cardiovasc. Ther.* **28,** e33-45 (2010).

323. Liu, J., Zhang, Q.-Y., Yu, L.-M., Liu, B., Li, M.-Y. & Zhu, R.-Z. Phycocyanobilin accelerates liver regeneration and reduces mortality rate in carbon tetrachloride-induced liver injury mice. *World J. Gastroenterol.* **21,** 5465–72 (2015).

324. Zheng, J., Inoguchi, T., Sasaki, S., Maeda, Y., McCarty, M. F., Fujii, M., Ikeda, N., Kobayashi, K., Sonoda, N. & Takayanagi, R. Phycocyanin and phycocyanobilin from Spirulina platensis protect against diabetic nephropathy by inhibiting oxidative stress. *Am. J. Physiol. Regul. Integr. Comp. Physiol.* **304,** R110-20 (2013).

325. Marín-Prida, J., Pavón-Fuentes, N., Llópiz-Arzuaga, A., Fernández-Massó, J. R., Delgado-Roche, L., Mendoza-Marí, Y., Santana, S. P., Cruz-Ramírez, A., Valenzuela-Silva, C., Nazábal-Gálvez, M., Cintado-Benítez, A., Pardo-Andreu, G. L., Polentarutti, N., Riva, F., Pentón-Arias, E. & Pentón-Rol, G. Phycocyanobilin promotes PC12 cell survival and modulates immune and inflammatory genes and oxidative stress markers in acute cerebral hypoperfusion in rats. *Toxicol. Appl. Pharmacol.* **272,** 49–60 (2013).

326. Pentón-Rol, G., Martínez-Sánchez, G., Cervantes-Llanos, M., Lagumersindez-Denis, N., Acosta-Medina, E. F., Falcón-Cama, V., Alonso-Ramírez, R., Valenzuela-Silva, C., Rodríguez-Jiménez, E., Llópiz-Arzuaga, A., Marín-Prida, J., López-Saura, P. A., Guillén-Nieto, G. E. & Pentón-Arias, E. C-Phycocyanin ameliorates experimental autoimmune encephalomyelitis and induces regulatory T cells. *Int. Immunopharmacol.* **11,** 29–38 (2011).

327. Cervantes-Llanos, M., Lagumersindez-Denis, N., Marín-Prida, J., Pavón-Fuentes, N., Falcon-Cama, V., Piniella-Matamoros, B., Camacho-Rodríguez, H., Fernández-Massó, J. R., Valenzuela-Silva, C., Raíces-Cruz, I., Pentón-Arias, E., Teixeira, M. M. & Pentón-Rol, G. Beneficial effects of oral administration of C-Phycocyanin and Phycocyanobilin in rodent models of experimental autoimmune encephalomyelitis. *Life Sci.* **194,** 130–138 (2018).

328. Pentón-Rol, G., Marín-Prida, J. & Falcón-Cama, V. C-Phycocyanin and Phycocyanobilin as Remyelination Therapies for Enhancing Recovery in Multiple Sclerosis and Ischemic Stroke: A Preclinical Perspective. *Behav. Sci. (Basel).* **8,** 15 (2018).

329. Strasky, Z., Zemankova, L., Nemeckova, I., Rathouska, J., Wong, R. J., Muchova, L., Subhanova, I., Vanikova, J., Vanova, K., Vitek, L. & Nachtigal, P. Spirulina platensis and phycocyanobilin activate atheroprotective heme oxygenase-1: a possible implication for

atherogenesis. *Food Funct.* **4,** 1586–94 (2013).

330. Minic, S. L., Stanic-Vucinic, D., Mihailovic, J., Krstic, M., Nikolic, M. R. & Cirkovic Velickovic, T. Digestion by pepsin releases biologically active chromopeptides from C-phycocyanin, a blue-colored biliprotein of microalga Spirulina. *J. Proteomics* **147,** 132–139 (2015).

331. Bailey, S. L., Schreiner, B., McMahon, E. J. & Miller, S. D. CNS myeloid DCs presenting endogenous myelin peptides 'preferentially' polarize CD4+ TH-17 cells in relapsing EAE. *Nat. Immunol.* **8,** 172–180 (2007).

332. El-Behi, M., Ciric, B., Dai, H., Yan, Y., Cullimore, M., Safavi, F., Zhang, G.-X., Dittel, B. N. & Rostami, A. The encephalitogenicity of TH17 cells is dependent on IL-1- and IL-23-induced production of the cytokine GM-CSF. *Nat. Immunol.* **12,** 568–575 (2011).

333. Huang, G., Wang, Y., Vogel, P., Kanneganti, T.-D., Otsu, K. & Chi, H. Signaling via the kinase p38α programs dendritic cells to drive TH17 differentiation and autoimmune inflammation. *Nat. Immunol.* **13,** 152–161 (2012).

334. Greter, M., Heppner, F. L., Lemos, M. P., Odermatt, B. M., Goebels, N., Laufer, T., Noelle, R. J. & Becher, B. Dendritic cells permit immune invasion of the CNS in an animal model of multiple sclerosis. *Nat. Med.* **11,** 328–334 (2005).

335. Karni, A., Abraham, M., Monsonego, A., Cai, G., Freeman, G. J., Hafler, D., Khoury, S. J. & Weiner, H. L. Innate immunity in multiple sclerosis: myeloid dendritic cells in secondary progressive multiple sclerosis are activated and drive a proinflammatory immune response. *J. Immunol.* **177,** 4196–202 (2006).

336. Sutton, C. E., Lalor, S. J., Sweeney, C. M., Brereton, C. F., Lavelle, E. C. & Mills, K. H. G. Interleukin-1 and IL-23 induce innate IL-17 production from gammadelta T cells, amplifying Th17 responses and autoimmunity. *Immunity* **31,** 331–41 (2009).

337. Brereton, C. F., Sutton, C. E., Lalor, S. J., Lavelle, E. C. & Mills, K. H. G. Inhibition of ERK MAPK suppresses IL-23- and IL-1-driven IL-17 production and attenuates autoimmune disease. *J. Immunol.* **183,** 1715–23 (2009).

338. Yogev, N., Frommer, F., Lukas, D., Kautz-Neu, K., Karram, K., Ielo, D., von Stebut, E., Probst, H.-C., van den Broek, M., Riethmacher, D., Birnberg, T., Blank, T., Reizis, B., Korn, T., Wiendl, H., Jung, S., Prinz, M., Kurschus, F. C. & Waisman, A. Dendritic Cells Ameliorate Autoimmunity in the CNS by Controlling the Homeostasis of PD-1 Receptor+ Regulatory T Cells. *Immunity* **37,** 264–275 (2012).

339. Dann, A., Poeck, H., Croxford, A. L., Gaupp, S., Kierdorf, K., Knust, M., Pfeifer, D., Maihoefer, C., Endres, S., Kalinke, U., Meuth, S. G., Wiendl, H., Knobeloch, K.-P., Akira, S., Waisman, A., Hartmann, G. & Prinz, M. Cytosolic RIG-I–like helicases act as negative regulators of sterile inflammation in the CNS. *Nat. Neurosci.* **15,** 98–106 (2012).

340. Kuruvilla, A. P., Shah, R., Hochwald, G. M., Liggitt, H. D., Palladino, M. A., Thorbecke, G. J. & Flavell, R. A. Protective effect of transforming growth factor beta 1 on experimental autoimmune diseases in mice. *Proc. Natl. Acad. Sci. U. S. A.* **88,** 2918–21 (1991).

341. Nestle, F. O., Turka, L. A. & Nickoloff, B. J. Characterization of dermal dendritic cells in psoriasis. Autostimulation of T lymphocytes and induction of Th1 type cytokines. *J. Clin. Invest.* **94,** 202–9 (1994).

342. Lowes, M. A., Chamian, F., Abello, M. V., Fuentes-Duculan, J., Lin, S.-L., Nussbaum, R., Novitskaya, I., Carbonaro, H., Cardinale, I., Kikuchi, T., Gilleaudeau, P., Sullivan-Whalen, M., Wittkowski, K. M., Papp, K., Garovoy, M., Dummer, W., Steinman, R. M. & Krueger, J. G.

Increase in TNF-alpha and inducible nitric oxide synthase-expressing dendritic cells in psoriasis and reduction with efalizumab (anti-CD11a). *Proc. Natl. Acad. Sci. U. S. A.* **102,** 19057–62 (2005).

343. Zaba, L. C., Cardinale, I., Gilleaudeau, P., Sullivan-Whalen, M., Suárez-Fariñas, M., Fuentes-Duculan, J., Novitskaya, I., Khatcherian, A., Bluth, M. J., Lowes, M. A. & Krueger, J. G. Amelioration of epidermal hyperplasia by TNF inhibition is associated with reduced Th17 responses. *J. Exp. Med.* **204,** 3183–3194 (2007).

344. Yawalkar, N., Tscharner, G. G., Hunger, R. E. & Hassan, A. S. Increased expression of IL-12p70 and IL-23 by multiple dendritic cell and macrophage subsets in plaque psoriasis. *J. Dermatol. Sci.* **54,** 99–105 (2009).

345. Kim, I. H., West, C. E., Kwatra, S. G., Feldman, S. R. & O'Neill, J. L. Comparative Efficacy of Biologics in Psoriasis. *Am. J. Clin. Dermatol.* **13,** 365–374 (2012).

346. Glitzner, E., Korosec, A., Brunner, P. M., Drobits, B., Amberg, N., Schonthaler, H. B., Kopp, T., Wagner, E. F., Stingl, G., Holcmann, M. & Sibilia, M. Specific roles for dendritic cell subsets during initiation and progression of psoriasis. *EMBO Mol. Med.* **6,** 1312–27 (2014).

347. Son, Y., Lee, J. H., Chung, H.-T. & Pae, H.-O. Therapeutic roles of heme oxygenase-1 in metabolic diseases: curcumin and resveratrol analogues as possible inducers of heme oxygenase-1. *Oxid. Med. Cell. Longev.* **2013,** 639541 (2013).

348. Yamashita, K., McDaid, J., Ollinger, R., Tsui, T. Y., Berberat, P. O., Usheva, A., Csizmadia, E., Smith, R. N., Soares, M. P. & Bach, F. H. Biliverdin, a natural product of heme catabolism, induces tolerance to cardiac allografts. *FASEB J.* **18,** 765–767 (2004).

349. Galvao, J., Davis, B., Tilley, M., Normando, E., Duchen, M. R. & Cordeiro, M. F. Unexpected low-dose toxicity of the universal solvent DMSO. *FASEB J.* **28,** 1317–1330 (2014).

350. Park, Y., Ryu, H. S., Lee, H. K., Kim, J. S., Yun, J., Kang, J. S., Hwang, B. Y., Hong, J. T., Kim, Y. & Han, S.-B. Tussilagone inhibits dendritic cell functions via induction of heme oxygenase-1. *Int. Immunopharmacol.* **22,** 400–8 (2014).

351. Kantengwa, S., Jornot, L., Devenoges, C. & Nicod, L. P. Superoxide anions induce the maturation of human dendritic cells. *Am. J. Respir. Crit. Care Med.* **167,** 431–7 (2003).

352. Lyakh, L., Trinchieri, G., Provezza, L., Carra, G. & Gerosa, F. Regulation of interleukin-12/interleukin-23 production and the T-helper 17 response in humans. *Immunol. Rev.* **226,** 112–31 (2008).

353. Chung, Y., Chang, S. H., Martinez, G. J., Yang, X. O., Nurieva, R., Kang, H. S., Ma, L., Watowich, S. S., Jetten, A. M., Tian, Q. & Dong, C. Critical Regulation of Early Th17 Cell Differentiation by Interleukin-1 Signaling. *Immunity* **30,** 576–587 (2009).

354. Lawrence, T. The nuclear factor NF-kappaB pathway in inflammation. *Cold Spring Harb. Perspect. Biol.* **1,** (2009).

355. Nakahara, T., Moroi, Y., Uchi, H. & Furue, M. Differential role of MAPK signaling in human dendritic cell maturation and Th1/Th2 engagement. *J. Dermatol. Sci.* **42,** 1–11 (2006).

356. Applegate, L. A., Luscher, P. & Tyrrell, R. M. Induction of heme oxygenase: a general response to oxidant stress in cultured mammalian cells. *Cancer Res.* **51,** 974–8 (1991).

357. Dong, J. & Goldenberg, G. New Biologics in Psoriasis: An Update on IL-23 and IL-17 Inhibitors. *Cutis* **99,** 123–7 (2017).

358. Mucha, O., Podkalicka, P., Czarnek, M., Biela, A., Mieczkowski, M., Kachamakova-Trojanowska, N., Stepniewski, J., Jozkowicz, A., Dulak, J. & Loboda, A. Pharmacological versus genetic inhibition of heme oxygenase-1 - the comparison of metalloporphyrins, shRNA and CRISPR/Cas9 system. *Acta Biochim. Pol.* **65,** 277–286 (2018).

359. Lin, Q., Weis, S., Yang, G., Weng, Y. H., Helston, R., Rish, K., Smith, A., Bordner, J., Polte, T., Gaunitz, F. & Dennery, P. A. Heme oxygenase-1 protein localizes to the nucleus and activates transcription factors important in oxidative stress. *J. Biol. Chem.* **282,** 20621–20633 (2007).

360. Lin, X. L., Lv, J. J., Lv, J., Di, C. X., Zhang, Y. J., Zhou, T., Liu, J. L. & Xia, Z. W. Heme oxygenase-1 directly binds STAT3 to control the generation of pathogenic Th17 cells during neutrophilic airway inflammation. *Allergy Eur. J. Allergy Clin. Immunol.* **72,** 1972–1987 (2017).

361. Tas, S. W., de Jong, E. C., Hajji, N., May, M. J., Ghosh, S., Vervoordeldonk, M. J. & Tak, P. P. Selective inhibition of NF-κB in dendritic cells by the NEMO-binding domain peptide blocks maturation and prevents T cell proliferation and polarization. *Eur. J. Immunol.* **35,** 1164–1174 (2005).

362. Dalod, M., Chelbi, R., Malissen, B. & Lawrence, T. Dendritic cell maturation: functional specialization through signaling specificity and transcriptional programming. *EMBO J.* **33,** 1104–16 (2014).

363. Jobin, C., Bradham, C. A., Russo, M. P., Juma, B., Narula, A. S., Brenner, D. A. & Sartor, R. B. Curcumin Blocks Cytokine-Mediated NF-kB Activation and Proinflammatory Gene Expression by Inhibiting Inhibitory Factor I-kB Kinase Activity. *J. Immunol.* **163,** 3474–3483 (1999).

364. Singh, S. & Aggarwal, B. B. Activation of transcription factor NF-kappaB is suppressed by curcumin (diferulolylmethane). *J. Biol. Chem.* **270,** 24995–25000 (1995).

365. Plotnikov, A., Zehorai, E., Procaccia, S. & Seger, R. The MAPK cascades: Signaling components, nuclear roles and mechanisms of nuclear translocation. *Biochim. Biophys. Acta - Mol. Cell Res.* **1813,** 1619–1633 (2011).

366. Kyriakis, J. M. & Avruch, J. Mammalian Mitogen-Activated Protein Kinase Signal Transduction Pathways Activated by Stress and Inflammation. *Physiol. Rev.* **81,** 807–869 (2001).

367. Silva, G., Cunha, A., Gregoire, I. P., Seldon, M. P. & Soares, M. P. The Antiapoptotic Effect of Heme Oxygenase-1 in Endothelial Cells Involves the Degradation of p38 MAPK Isoform. *J. Immunol.* **177,** 1894–1903 (2006).

368. Freitag, J., Berod, L., Kamradt, T. & Sparwasser, T. Immunometabolism and autoimmunity. *Immunol. Cell Biol.* **94,** 925–934 (2016).

369. La Rocca, C., Carbone, F., De Rosa, V., Colamatteo, A., Galgani, M., Perna, F., Lanzillo, R., Brescia Morra, V., Orefice, G., Cerillo, I., Florio, C., Maniscalco, G. T., Salvetti, M., Centonze, D., Uccelli, A., Longobardi, S., Visconti, A. & Matarese, G. Immunometabolic profiling of T cells from patients with relapsing-remitting multiple sclerosis reveals an impairment in glycolysis and mitochondrial respiration. *Metabolism* **77,** 39–46 (2017).

370. Delgoffe, G. M., Kole, T. P., Zheng, Y., Zarek, P. E., Matthews, K. L., Xiao, B., Worley, P. F., Kozma, S. C. & Powell, J. D. The mTOR Kinase Differentially Regulates Effector and Regulatory T Cell Lineage Commitment. *Immunity* **30,** 832–844 (2009).

371. Zheng, Y., Delgoffe, G. M., Meyer, C. F., Chan, W. & Powell, J. D. Anergic T Cells Are Metabolically Anergic. *J. Immunol.* **183,** 6095–6101 (2009).

372. Shi, L. Z., Wang, R., Huang, G., Vogel, P., Neale, G., Green, D. R. & Chi, H. HIF1α–dependent glycolytic pathway orchestrates a metabolic checkpoint for the differentiation of TH17 and Treg cells. *J. Exp. Med.* **208,** 1367–1376 (2011).

373. Dang, E. V., Barbi, J., Yang, H. Y., Jinasena, D., Yu, H., Zheng, Y., Bordman, Z., Fu, J., Kim, Y., Yen, H. R., Luo, W., Zeller, K., Shimoda, L., Topalian, S. L., Semenza, G. L., Dang, C. V., Pardoll, D. M. & Pan, F. Control of TH17/Treg balance by hypoxia-inducible factor 1. *Cell* **146,** 772–784 (2011).

374. Berod, L., Friedrich, C., Nandan, A., Freitag, J., Hagemann, S., Harmrolfs, K., Sandouk, A., Hesse, C., Castro, C. N., BäHre, H., Tschirner, S. K., Gorinski, N., Gohmert, M., Mayer, C. T., Huehn, J., Ponimaskin, E., Abraham, W. R., MüLler, R., Lochner, M., *et al.* De novo fatty acid synthesis controls the fate between regulatory T and T helper 17 cells. *Nat. Med.* **20,** 1327–1333 (2014).

375. De Rosa, V., Galgani, M., Porcellini, A., Colamatteo, A., Santopaolo, M., Zuchegna, C., Romano, A., De Simone, S., Procaccini, C., La Rocca, C., Carrieri, P. B., Maniscalco, G. T., Salvetti, M., Buscarinu, M. C., Franzese, A., Mozzillo, E., La Cava, A. & Matarese, G. Glycolysis controls the induction of human regulatory T cells by modulating the expression of FOXP3 exon 2 splicing variants. *Nat. Immunol.* **16,** 1174–1184 (2015).

376. Wegiel, B., Nemeth, Z., Correa-Costa, M., Bulmer, A. C. & Otterbein, L. E. Heme Oxygenase-1: A Metabolic Nike. *Antioxid. Redox Signal.* **20,** 1709–1722 (2014).

377. Ahlström, K., Biber, B., Åberg, A., Waldenström, A., Ronquist, G., Abrahamsson, P., StrandÉn, P., Johansson, G. & Haney, M. F. Metabolic responses in ischemic myocardium after inhalation of carbon monoxide. *Acta Anaesthesiol. Scand.* **53,** 1036–1042 (2009).

378. Lancel, S., Montaigne, D., Marechal, X., Marciniak, C., Hassoun, S. M., Decoster, B., Ballot, C., Blazejewski, C., Corseaux, D., Lescure, B., Motterlini, R. & Neviere, R. Carbon Monoxide Improves Cardiac Function and Mitochondrial Population Quality in a Mouse Model of Metabolic Syndrome. *PLoS One* **7,** e41836 (2012).

379. Suliman, H. B., Carraway, M. S., Ali, A. S., Reynolds, C. M., Welty-Wolf, K. E. & Piantadosi, C. A. The CO/HO system reverses inhibition of mitochondrial biogenesis and prevents murine doxorubicin cardiomyopathy. *J. Clin. Invest.* **117,** 3730–41 (2007).

380. Almeida, A. S., Queiroga, C. S. F., Sousa, M. F. Q., Alves, P. M. & Vieira, H. L. A. Carbon Monoxide Modulates Apoptosis by Reinforcing Oxidative Metabolism in Astrocytes. *J. Biol. Chem.* **287,** 10761–10770 (2012).

381. Huang, J., Simcox, J., Mitchell, T. C., Jones, D., Cox, J., Luo, B., Cooksey, R. C., Boros, L. G. & McClain, D. A. Iron regulates glucose homeostasis in liver and muscle via AMP-activated protein kinase in mice. *FASEB J.* **27,** 2845–2854 (2013).

382. Frezza, C., Zheng, L., Folger, O., Rajagopalan, K. N., MacKenzie, E. D., Jerby, L., Micaroni, M., Chaneton, B., Adam, J., Hedley, A., Kalna, G., Tomlinson, I. P. M., Pollard, P. J., Watson, D. G., Deberardinis, R. J., Shlomi, T., Ruppin, E. & Gottlieb, E. Haem oxygenase is synthetically lethal with the tumour suppressor fumarate hydratase. *Nature* **477,** 225–228 (2011).

383. Brennan, M. S., Matos, M. F., Li, B., Hronowski, X., Gao, B., Juhasz, P., Rhodes, K. J. & Scannevin, R. H. Dimethyl fumarate and monoethyl fumarate exhibit differential effects on

KEAP1, NRF2 activation, and glutathione depletion in vitro. *PLoS One* **10,** e0120254 (2015).

384. Mills, E. L., Ryan, D. G., Prag, H. A., Dikovskaya, D., Menon, D., Zaslona, Z., Jedrychowski, M. P., Costa, A. S. H., Higgins, M., Hams, E., Szpyt, J., Runtsch, M. C., King, M. S., McGouran, J. F., Fischer, R., Kessler, B. M., McGettrick, A. F., Hughes, M. M., Carroll, R. G., *et al.* Itaconate is an anti-inflammatory metabolite that activates Nrf2 via alkylation of KEAP1. *Nature* **556,** 113–117 (2018).

385. Lin, H., Yu, C.-H., Jen, C.-Y., Cheng, C.-F., Chou, Y., Chang, C.-C. & Juan, S.-H. Adiponectin-Mediated Heme Oxygenase-1 Induction Protects Against Iron-Induced Liver Injury via a PPARα-Dependent Mechanism. *Am. J. Pathol.* **177,** 1697–1709 (2010).

386. Frauwirth, K. A., Riley, J. L., Harris, M. H., Parry, R. V., Rathmell, J. C., Plas, D. R., Elstrom, R. L., June, C. H. & Thompson, C. B. The CD28 signaling pathway regulates glucose metabolism. *Immunity* **16,** 769–777 (2002).

387. Jacobs, S. R., Herman, C. E., MacIver, N. J., Wofford, J. A., Wieman, H. L., Hammen, J. J. & Rathmell, J. C. Glucose Uptake Is Limiting in T Cell Activation and Requires CD28-Mediated Akt-Dependent and Independent Pathways. *J. Immunol.* **180,** 4476–4486 (2008).

388. Tan, H., Yang, K., Li, Y., Shaw, T. I., Wang, Y., Blanco, D. B., Wang, X., Cho, J.-H., Wang, H., Rankin, S., Guy, C., Peng, J. & Chi, H. Integrative Proteomics and Phosphoproteomics Profiling Reveals Dynamic Signaling Networks and Bioenergetics Pathways Underlying T Cell Activation. *Immunity* **46,** 488–503 (2017).

389. Baixauli, F., Acín-Pérez, R., Villarroya-Beltrí, C., Mazzeo, C., Nuñez-Andrade, N., Gabandé-Rodriguez, E., Ledesma, M. D., Blázquez, A., Martin, M. A., Falcón-Pérez, J. M., Redondo, J. M., Enríquez, J. A. & Mittelbrunn, M. Mitochondrial Respiration Controls Lysosomal Function during Inflammatory T Cell Responses. *Cell Metab.* **22,** 485–498 (2015).

390. D'Souza, A. D., Parikh, N., Kaech, S. M. & Shadel, G. S. Convergence of multiple signaling pathways is required to coordinately up-regulate mtDNA and mitochondrial biogenesis during T cell activation. *Mitochondrion* **7,** 374–385 (2007).

391. Desdín-Micó, G., Soto-Heredero, G. & Mittelbrunn, M. Mitochondrial activity in T cells. *Mitochondrion* **41,** 51–57 (2018).

392. Cho, R.-L., Lin, W.-N., Wang, C.-Y., Yang, C.-C., Hsiao, L.-D., Lin, C.-C. & Yang, C.-M. Heme oxygenase-1 induction by rosiglitazone via PKCα/AMPKα/p38 MAPKα/SIRT1/PPARγ pathway suppresses lipopolysaccharide-mediated pulmonary inflammation. *Biochem. Pharmacol.* **148,** 222–237 (2018).

393. Liu, X., Peyton, K. J., Shebib, A. R., Wang, H., Korthuis, R. J. & Durante, W. Activation of AMPK stimulates heme oxygenase-1 gene expression and human endothelial cell survival. *Am. J. Physiol. Circ. Physiol.* **300,** H84–H93 (2011).

394. Chang, C.-H., Curtis, J. D., Maggi, L. B., Faubert, B., Villarino, A. V., O'Sullivan, D., Huang, S. C.-C., van der Windt, G. J. W., Blagih, J., Qiu, J., Weber, J. D., Pearce, E. J., Jones, R. G. & Pearce, E. L. Posttranscriptional Control of T Cell Effector Function by Aerobic Glycolysis. *Cell* **153,** 1239–1251 (2013).

395. Klein Geltink, R. I., O'Sullivan, D., Corrado, M., Bremser, A., Buck, M. D., Buescher, J. M., Firat, E., Zhu, X., Niedermann, G., Caputa, G., Kelly, B., Warthorst, U., Rensing-Ehl, A., Kyle, R. L., Vandersarren, L., Curtis, J. D., Patterson, A. E., Lawless, S., Grzes, K., *et al.* Mitochondrial Priming by CD28. *Cell* **171,** 385–397.e11 (2017).

396. Wahl, D. R., Byersdorfer, C. A., Ferrara, J. L. M., Opipari, A. W., Glick, G. D. & Glick, G. D.

Distinct metabolic programs in activated T cells: opportunities for selective immunomodulation. *Immunol. Rev.* **249,** 104–15 (2012).

397. Kliem, C., Merling, A., Giaisi, M., Köhler, R., Krammer, P. H. & Li-Weber, M. Curcumin suppresses T cell activation by blocking Ca2+ mobilization and nuclear factor of activated T cells (NFAT) activation. *J. Biol. Chem.* **287,** 10200–9 (2012).

398. Hardie, D. G. AMP-activated protein kinase: an energy sensor that regulates all aspects of cell function. *Genes Dev.* **25,** 1895–908 (2011).

399. Reznick, R. M. & Shulman, G. I. The role of AMP-activated protein kinase in mitochondrial biogenesis. *J. Physiol.* **574,** 33–9 (2006).

400. MacIver, N. J., Blagih, J., Saucillo, D. C., Tonelli, L., Griss, T., Rathmell, J. C. & Jones, R. G. The Liver Kinase B1 Is a Central Regulator of T Cell Development, Activation, and Metabolism. *J. Immunol.* **187,** 4187–4198 (2011).

401. Blagih, J., Coulombe, F., Vincent, E. E., Dupuy, F., Galicia-Vázquez, G., Yurchenko, E., Raissi, T. C., vanderWindt, G. J. W., Viollet, B., Pearce, E. L., Pelletier, J., Piccirillo, C. A., Krawczyk, C. M., Divangahi, M. & Jones, R. G. The Energy Sensor AMPK Regulates T Cell Metabolic Adaptation and Effector Responses InVivo. *Immunity* **42,** 41–54 (2015).

402. Tamás, P., Hawley, S. A., Clarke, R. G., Mustard, K. J., Green, K., Hardie, D. G. & Cantrell, D. A. Regulation of the energy sensor AMP-activated protein kinase by antigen receptor and Ca^{2+} in T lymphocytes. *J. Exp. Med.* **203,** 1665–1670 (2006).

403. Thwe, P. M. & Amiel, E. The role of nitric oxide in metabolic regulation of dendritic cell immune function. *Cancer Lett.* **412,** 236–242 (2018).

404. Mo, C., Wang, L., Zhang, J., Numazawa, S., Tang, H., Tang, X., Han, X., Li, J., Yang, M., Wang, Z., Wei, D. & Xiao, H. The Crosstalk Between Nrf2 and AMPK Signal Pathways Is Important for the Anti-Inflammatory Effect of Berberine in LPS-Stimulated Macrophages and Endotoxin-Shocked Mice. *Antioxid. Redox Signal.* **20,** 574–588 (2014).

405. Johnson, J. J., Syed, D. N., Heren, C. R., Suh, Y., Adhami, V. M. & Mukhtar, H. Carnosol, a dietary diterpene, displays growth inhibitory effects in human prostate cancer PC3 cells leading to G2-phase cell cycle arrest and targets the 5'-AMP-activated protein kinase (AMPK) pathway. *Pharm. Res.* **25,** 2125–2134 (2008).

406. Vlavcheski, F., Baron, D., Vlachogiannis, I., MacPherson, R. & Tsiani, E. Carnosol Increases Skeletal Muscle Cell Glucose Uptake via AMPK-Dependent GLUT4 Glucose Transporter Translocation. *Int. J. Mol. Sci.* **19,** 1321 (2018).

407. Kim, J. H., Park, J. M., Kim, E. K., Lee, J. O., Lee, S. K., Jung, J. H., You, G. Y., Park, S. H., Shu, P. G. & Kim, H. S. Curcumin stimulates glucose uptake through AMPK-p38 MAPK pathways in L6 myotube cells. *J. Cell. Physiol.* **223,** 771–778 (2010).

408. Kim, T., Davis, J., Zhang, A. J., He, X. & Mathews, S. T. Curcumin activates AMPK and suppresses gluconeogenic gene expression in hepatoma cells. *Biochem. Biophys. Res. Commun.* **388,** 377–382 (2009).

409. Zheng, J. & Ramirez, V. D. Inhibition of mitochondrial proton F0F1-ATPase/ATP synthase by polyphenolic phytochemicals. *Br. J. Pharmacol.* **130,** 1115–1123 (2000).

410. Kim, J., Yang, G., Kim, Y., Kim, J. & Ha, J. AMPK activators: mechanisms of action and physiological activities. *Exp. Mol. Med.* **48,** e224–e224 (2016).

411. Gledhill, J. R., Montgomery, M. G., Leslie, A. G. W. & Walker, J. E. Mechanism of inhibition

of bovine F1-ATPase by resveratrol and related polyphenols. *Proc. Natl. Acad. Sci.* **104,** 13632–13637 (2007).

412. Zimmermann, K., Baldinger, J., Mayerhofer, B., Atanasov, A. G., Dirsch, V. M. & Heiss, E. H. Activated AMPK boosts the Nrf2/HO-1 signaling axis - A role for the unfolded protein response. *Free Radic. Biol. Med.* **88,** 417–426 (2015).

413. Joo, M. S., Kim, W. D., Lee, K. Y., Kim, J. H., Koo, J. H. & Kim, S. G. AMPK Facilitates Nuclear Accumulation of Nrf2 by Phosphorylating at Serine 550. *Mol. Cell. Biol.* **36,** 1931–1942 (2016).

414. Dinkova-Kostova, A. T. & Abramov, A. Y. The emerging role of Nrf2 in mitochondrial function. *Free Radic. Biol. Med.* **88,** 179–188 (2015).

415. Austin, S. & St-Pierre, J. PGC1 and mitochondrial metabolism - emerging concepts and relevance in ageing and neurodegenerative disorders. *J. Cell Sci.* **125,** 4963–4971 (2012).

416. Baldelli, S., Aquilano, K. & Ciriolo, M. R. Punctum on two different transcription factors regulated by PGC-1α: Nuclear factor erythroid-derived 2-like 2 and nuclear respiratory factor 2. *Biochim. Biophys. Acta - Gen. Subj.* **1830,** 4137–4146 (2013).

417. Piantadosi, C. A. & Suliman, H. B. Redox regulation of mitochondrial biogenesis. *Free Radic. Biol. Med.* **53,** 2043–2053 (2012).

418. Tufekci, K. U., Civi Bayin, E., Genc, S. & Genc, K. The Nrf2/ARE Pathway: A Promising Target to Counteract Mitochondrial Dysfunction in Parkinson's Disease. *Parkinsons. Dis.* **2011,** 314082 (2011).

419. Zmijewski, J. W., Banerjee, S., Bae, H., Friggeri, A., Lazarowski, E. R. & Abraham, E. Exposure to hydrogen peroxide induces oxidation and activation of AMP-activated protein kinase. *J. Biol. Chem.* **285,** 33154–33164 (2010).

420. Lees, J. R. Interferon gamma in autoimmunity: A complicated player on a complex stage. *Cytokine* **74,** 18–26 (2015).

421. Kim, B.-S., Park, Y.-J. & Chung, Y. Targeting IL-17 in autoimmunity and inflammation. *Arch. Pharm. Res.* **39,** 1537–1547 (2016).

422. Choi, B. M., Pae, H. O., Jeong, Y. R., Kim, Y. M. & Chung, H. T. Critical role of heme oxygenase-1 in Foxp3-mediated immune suppression. *Biochem. Biophys. Res. Commun.* **327,** 1066–1071 (2005).

423. Xia, Z.-W., Xu, L.-Q., Zhong, W.-W., Wei, J.-J., Li, N.-L., Shao, J., Li, Y.-Z., Yu, S.-C. & Zhang, Z.-L. Heme Oxygenase-1 Attenuates Ovalbumin-Induced Airway Inflammation by Up-Regulation of Foxp3 T-Regulatory Cells, Interleukin-10, and Membrane-Bound Transforming Growth Factor-β1. *Am. J. Pathol.* **171,** 1904–1914 (2007).

424. Zhang, Y., Zhang, L., Wu, J., Di, C. & Xia, Z. Heme oxygenase-1 exerts a protective role in ovalbumin-induced neutrophilic airway inflammation by inhibiting Th17 cell-mediated immune response. *J. Biol. Chem.* **288,** 34612–26 (2013).

425. Nikolic, I., Vujicic, M., Stojanovic, I., Stosic-Grujicic, S. & Saksida, T. Carbon Monoxide-Releasing Molecule-A1 Inhibits Th1/Th17 and Stimulates Th2 Differentiation In vitro. *Scand. J. Immunol.* **80,** 95–100 (2014).

426. Biburger, M., Theiner, G., Schädle, M., Schuler, G. & Tiegs, G. Pivotal Advance: Heme oxygenase 1 expression by human CD4 + T cells is not sufficient for their development of immunoregulatory capacity. *J. Leukoc. Biol.* **87,** 193–202 (2010).

427. Chen, X., Su, W., Wan, T., Yu, J., Zhu, W., Tang, F., Liu, G., Olsen, N., Liang, D. & Zheng, S. G. Sodium butyrate regulates Th17/Treg cell balance to ameliorate uveitis via the Nrf2/HO-1 pathway. *Biochem. Pharmacol.* **142,** 111–119 (2017).

428. Yu, M., Wang, J., Fang, Q., Liu, P., Chen, S., Zhe, N., Lin, X., Zhang, Y., Zhao, J. & Zhou, Z. High expression of heme oxygenase-1 in target organs may attenuate acute graft-versus-host disease through regulation of immune balance of TH17/Treg. *Transpl. Immunol.* **37,** 10–17 (2016).

429. Handono, K., Pratama, M. Z., Endharti, A. T. & Kalim, H. Treatment of low doses curcumin could modulate Th17/Treg balance specifically on CD4+ T cell cultures of systemic lupus erythematosus patients. *Cent. Eur. J. Immunol.* **40,** 461–469 (2015).

430. Fujita, H. The role of IL-22 and Th22 cells in human skin diseases. *J. Dermatol. Sci.* **72,** 3–8 (2013).

431. Helwa, I., Patel, R., Karempelis, P., Kaddour-Djebbar, I., Choudhary, V. & Bollag, W. B. The Antipsoriatic Agent Monomethylfumarate Has Antiproliferative, Prodifferentiative, and Anti-Inflammatory Effects on Keratinocytes. *J. Pharmacol. Exp. Ther.* **352,** 90–97 (2014).

432. Zhu, W., Xu, J., Ge, Y., Cao, H., Ge, X., Luo, J., Xue, J., Yang, H., Zhang, S. & Cao, J. Epigallocatechin-3-gallate (EGCG) protects skin cells from ionizing radiation via heme oxygenase-1 (HO-1) overexpression. *J. Radiat. Res.* **55,** 1056–1065 (2014).

433. Nisar, M. F., Parsons, K. S. G., Bian, C. X. & Zhong, J. L. UVA Irradiation Induced Heme Oxygenase-1: A Novel Phototherapy for Morphea. *Photochem. Photobiol.* **91,** 210–220 (2015).

434. Hung, C. T., Huang, S. M., Cheng, H. C., Liu, S. T., Chang, Y. L., Liu, Y. C. & Wang, W. M. The inhibitory mechanism by curcumin on the Zac1-enhanced cyclin D1 expression in human keratinocytes. *J. Dermatol. Sci.* **79,** 262–267 (2015).

435. Liao, W., Lin, J. X. & Leonard, W. J. IL-2 family cytokines: New insights into the complex roles of IL-2 as a broad regulator of T helper cell differentiation. *Curr. Opin. Immunol.* **23,** 598–604 (2011).

436. Russo, R. C., Garcia, C. C., Teixeira, M. M. & Amaral, F. A. The CXCL8/IL-8 chemokine family and its receptors in inflammatory diseases. *Expert Rev. Clin. Immunol.* **10,** 593–619 (2014).

437. Kagami, S., Rizzo, H. L., Lee, J. J., Koguchi, Y. & Blauvelt, A. Circulating Th17, Th22, and Th1 cells are increased in psoriasis. *J. Invest. Dermatol.* **130,** 1373–1383 (2010).

438. Arican, O., Aral, M., Sasmaz, S. & Ciragil, P. Serum levels of TNF-α, IFN-γ, IL-6, IL-8, IL-12, IL-17, and IL-18 in patients with active psoriasis and correlation with disease severity. *Mediators Inflamm.* **2005,** 273–279 (2005).

439. Pantelyushin, S., Haak, S., Ingold, B., Kulig, P., Heppner, F. L., Navarini, A. A. & Becher, B. Rorγt + innate lymphocytes and γδ T cells initiate psoriasiform plaque formation in mice. *J. Clin. Invest.* **122,** 2252–2256 (2012).

440. Cai, Y., Shen, X., Ding, C., Qi, C., Li, K., Li, X., Jala, V. R., Zhang, H., Wang, T., Zheng, J. & Yan, J. Pivotal role of dermal IL-17-producing γδ T cells in skin inflammation. *Immunity* **35,** 596–610 (2011).

441. Forward, N. A., Conrad, D. M., Power Coombs, M. R., Doucette, C. D., Furlong, S. J., Lin, T.-J. & Hoskin, D. W. Curcumin blocks interleukin (IL)-2 signaling in T-lymphocytes by inhibiting IL-2 synthesis, CD25 expression, and IL-2 receptor signaling. *Biochem. Biophys. Res.*

Commun. **407,** 801–806 (2011).

442. Ranjan, D., Chen, C., Johnston, T. D., Jeon, H. & Nagabhushan, M. Curcumin inhibits mitogen stimulated lymphocyte proliferation, NFκB activation, and IL-2 signaling. *J. Surg. Res.* **121,** 171–177 (2004).

443. Lowes, M. A., Russell, C. B., Martin, D. A., Towne, J. E. & Krueger, J. G. The IL-23/T17 pathogenic axis in psoriasis is amplified by keratinocyte responses. *Trends Immunol.* **34,** 174–81 (2013).

444. Balasubramanian, S. & Eckert, R. L. Curcumin suppresses AP1 transcription factor-dependent differentiation and activates apoptosis in human epidermal keratinocytes. *J. Biol. Chem.* **282,** 6707–6715 (2007).

445. Abdallah, M. A., Abdel-Hamid, M. F., Kotb, A. M. & Mabrouk, E. A. Serum interferon-gamma is a psoriasis severity and prognostic marker. *Cutis* **84,** 163–8 (2009).

446. Scholz, T., Weigert, A., Brüne, B., Sadik, C. D., Böhm, B. & Burkhardt, H. GM-CSF in murine psoriasiform dermatitis: Redundant and pathogenic roles uncovered by antibody-induced neutralization and genetic deficiency. *PLoS One* **12,** e0182646 (2017).

447. Moran, B., Sweeney, C. M., Hughes, R., Malara, A., Kirthi, S., Tobin, A. M., Kirby, B. & Fletcher, J. M. Hidradenitis Suppurativa Is Characterized by Dysregulation of the Th17:Treg Cell Axis, Which Is Corrected by Anti-TNF Therapy. *J. Invest. Dermatol.* **137,** 2389–2395 (2017).

448. Hayter, S. M. & Cook, M. C. Updated assessment of the prevalence, spectrum and case definition of autoimmune disease. *Autoimmun. Rev.* **11,** 754–765 (2012).

449. Schön, M. P. & Erpenbeck, L. The Interleukin-23/Interleukin-17 Axis Links Adaptive and Innate Immunity in Psoriasis. *Front. Immunol.* **9,** 1323 (2018).

450. Hu, B., Shi, C., Xu, C., Cao, P., Tian, Y., Zhang, Y., Deng, L., Chen, H. & Yuan, W. Heme oxygenase-1 attenuates IL-1β induced alteration of anabolic and catabolic activities in intervertebral disc degeneration. *Sci. Rep.* **6,** 21190 (2016).

451. Gehart, H., Kumpf, S., Ittner, A. & Ricci, R. MAPK signalling in cellular metabolism: stress or wellness? *EMBO Rep.* **11,** 834–40 (2010).

452. Sozen, B., Ozturk, S., Yaba, A. & Demir, N. The p38 MAPK signalling pathway is required for glucose metabolism, lineage specification and embryo survival during mouse preimplantation development. *Mech. Dev.* **138,** 375–398 (2015).

453. Través, P. G., de Atauri, P., Marín, S., Pimentel-Santillana, M., Rodríguez-Prados, J.-C., Marín de Mas, I., Selivanov, V. A., Martín-Sanz, P., Boscá, L. & Cascante, M. Relevance of the MEK/ERK signaling pathway in the metabolism of activated macrophages: a metabolomic approach. *J. Immunol.* **188,** 1402–10 (2012).

454. O'Neill, L. A. J. & Hardie, D. G. Metabolism of inflammation limited by AMPK and pseudo-starvation. *Nature* **493,** 346–355 (2013).

455. Soranna, D., Scotti, L., Zambon, A., Bosetti, C., Grassi, G., Catapano, A., La Vecchia, C., Mancia, G. & Corrao, G. Cancer Risk Associated with Use of Metformin and Sulfonylurea in Type 2 Diabetes: A Meta-Analysis. *Oncologist* **17,** 813–822 (2012).

456. Hawley, S. A., Fullerton, M. D., Ross, F. A., Schertzer, J. D., Chevtzoff, C., Walker, K. J., Peggie, M. W., Zibrova, D., Green, K. A., Mustard, K. J., Kemp, B. E., Sakamoto, K., Steinberg, G. R. & Hardie, D. G. The ancient drug salicylate directly activates AMP-activated protein

kinase. *Science (80-.).* **336,** 918–922 (2012).

457. Rothwell, P. M., Price, J. F., Fowkes, F. G. R., Zanchetti, A., Roncaglioni, M. C., Tognoni, G., Lee, R., Belch, J. F., Wilson, M., Mehta, Z. & Meade, T. W. Short-term effects of daily aspirin on cancer incidence, mortality, and non-vascular death: analysis of the time course of risks and benefits in 51 randomised controlled trials. *Lancet* **379,** 1602–1612 (2012).

458. Steinberg, G. R., Dandapani, M. & Hardie, D. G. AMPK: mediating the metabolic effects of salicylate-based drugs? *Trends Endocrinol. Metab.* **24,** 481–7 (2013).

459. Yang, Y., Zhang, X., Xu, M., Wu, X., Zhao, F. & Zhao, C. Quercetin attenuates collagen-induced arthritis by restoration of Th17/Treg balance and activation of Heme Oxygenase 1-mediated anti-inflammatory effect. *Int. Immunopharmacol.* **54,** 153–162 (2018).

460. Karimi, K., Kandiah, N., Chau, J., Bienenstock, J. & Forsythe, P. A Lactobacillus rhamnosus Strain Induces a Heme Oxygenase Dependent Increase in Foxp3+ Regulatory T Cells. *PLoS One* **7,** e47556 (2012).

461. Sun, L., Shi, T., Qiao, H., Jiang, X., Jiang, H., Krissansen, G. W. & Sun, X. Hepatic Overexpression of Heme Oxygenase-1 Improves Liver Allograft Survival by Expanding T Regulatory Cells. *J. Surg. Res.* **166,** e187–e194 (2011).

462. Brandsma, C.-A., Hylkema, M. N., van der Strate, B. W., Slebos, D.-J., Luinge, M. A., Geerlings, M., Timens, W., Postma, D. S. & Kerstjens, H. A. Heme oxygenase-1 prevents smoke induced B-cell infiltrates: a role for regulatory T cells? *Respir. Res.* **9,** 17 (2008).

463. Lee, S. S., Gao, W., Mazzola, S., Thomas, M. N., Csizmadia, E., Otterbein, L. E., Bach, F. H. & Wang, H. Heme oxygenase-1, carbon monoxide, and bilirubin induce tolerance in recipients toward islet allografts by modulating T regulatory cells. *FASEB J.* **21,** 3450–3457 (2007).

464. Albanesi, C., Madonna, S., Gisondi, P. & Girolomoni, G. The Interplay Between Keratinocytes and Immune Cells in the Pathogenesis of Psoriasis. *Front. Immunol.* **9,** 1549 (2018).

465. Schön, M. P., Broekaert, S. M. C. & Erpenbeck, L. Sexy again: the renaissance of neutrophils in psoriasis. *Exp. Dermatol.* **26,** 305–311 (2017).

466. Skov, L., Beurskens, F. J., Zachariae, C. O. C., Reitamo, S., Teeling, J., Satijn, D., Knudsen, K. M., Boot, E. P. J., Hudson, D., Baadsgaard, O., Parren, P. W. H. I. & van de Winkel, J. G. J. IL-8 as antibody therapeutic target in inflammatory diseases: reduction of clinical activity in palmoplantar pustulosis. *J. Immunol.* **181,** 669–79 (2008).

467. Yan, L., Anderson, G. M., DeWitte, M. & Nakada, M. T. Therapeutic potential of cytokine and chemokine antagonists in cancer therapy. *Eur. J. Cancer* **42,** 793–802 (2006).

468. Lande, R., Botti, E., Jandus, C., Dojcinovic, D., Fanelli, G., Conrad, C., Chamilos, G., Feldmeyer, L., Marinari, B., Chon, S., Vence, L., Riccieri, V., Guillaume, P., Navarini, A. A., Romero, P., Costanzo, A., Piccolella, E., Gilliet, M. & Frasca, L. The antimicrobial peptide LL37 is a T-cell autoantigen in psoriasis. *Nat. Commun.* **5,** 5621 (2014).

469. Papoutsaki, M. & Costanzo, A. Treatment of psoriasis and psoriatic arthritis. *BioDrugs* **27,** 3–12 (2013).

470. Conrad, C. & Flatz. Role of T-cell-mediated inflammation in psoriasis: pathogenesis and targeted therapy. *Psoriasis Targets Ther.* **3,** 1 (2013).

471. Mabuchi, T., Takekoshi, T. & Hwang, S. T. Epidermal CCR6+ γδ T cells are major producers

of IL-22 and IL-17 in a murine model of psoriasiform dermatitis. *J. Immunol.* **187,** 5026–31 (2011).

472. Laggner, U., Di Meglio, P., Perera, G. K., Hundhausen, C., Lacy, K. E., Ali, N., Smith, C. H., Hayday, A. C., Nickoloff, B. J. & Nestle, F. O. Identification of a Novel Proinflammatory Human Skin-Homing Vγ9Vδ2 T Cell Subset with a Potential Role in Psoriasis. *J. Immunol.* **187,** 2783–2793 (2011).

473. Cather, J. C. & Crowley, J. J. Use of Biologic Agents in Combination with Other Therapies for the Treatment of Psoriasis. *Am. J. Clin. Dermatol.* **15,** 467–478 (2014).

474. Franceschi, C. & Campisi, J. Chronic Inflammation (Inflammaging) and Its Potential Contribution to Age-Associated Diseases. *Journals Gerontol. Ser. A Biol. Sci. Med. Sci.* **69,** S4–S9 (2014).

475. Torre, L. A., Siegel, R. L., Ward, E. M. & Jemal, A. Global Cancer Incidence and Mortality Rates and Trends- An Update. *Cancer Epidemiol. Biomarkers Prev.* **25,** 16 LP-27 (2015).

476. Hruby, A. & Hu, F. B. The Epidemiology of Obesity: A Big Picture. *Pharmacoeconomics* **33,** 673–89 (2015).

Appendix

1. HO-1 knockdown by siRNA

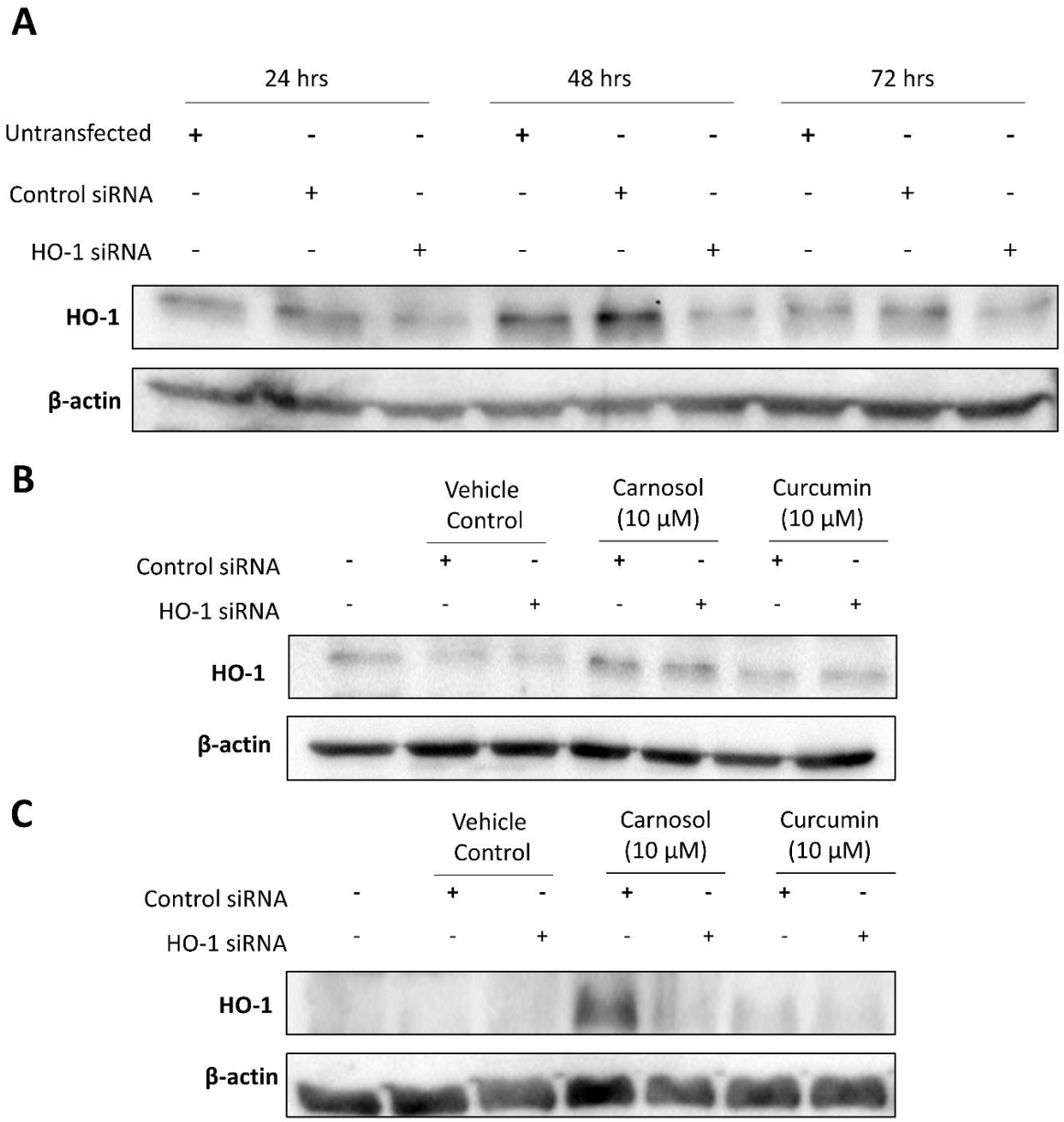

Figure app.1.1. Optimisation of siRNA knockdown of HO-1 in primary human DC. (A) Primary human DC were transfected with non-targeting siRNA or siRNA targeting HO-1 for 24, 48, or 72 hours. HO-1 expression was detected by Western blot. **(B)** DC were transfected with non-targeting siRNA or siRNA targeting HO-1 for 48 hours prior to treatment with carnosol (10 μM), curcumin (10 μM) or a vehicle control for 24 hours. HO-1 expression was detected by Western blot. **(C)** DC were transfected with non-targeting siRNA or siRNA targeting HO-1 for 24 hours, then transfected a second time for a further 24 hours prior to treatment with carnosol (10 μM), curcumin (10 μM) or a vehicle control for 24 hours. HO-1 expression was detected by Western blot.

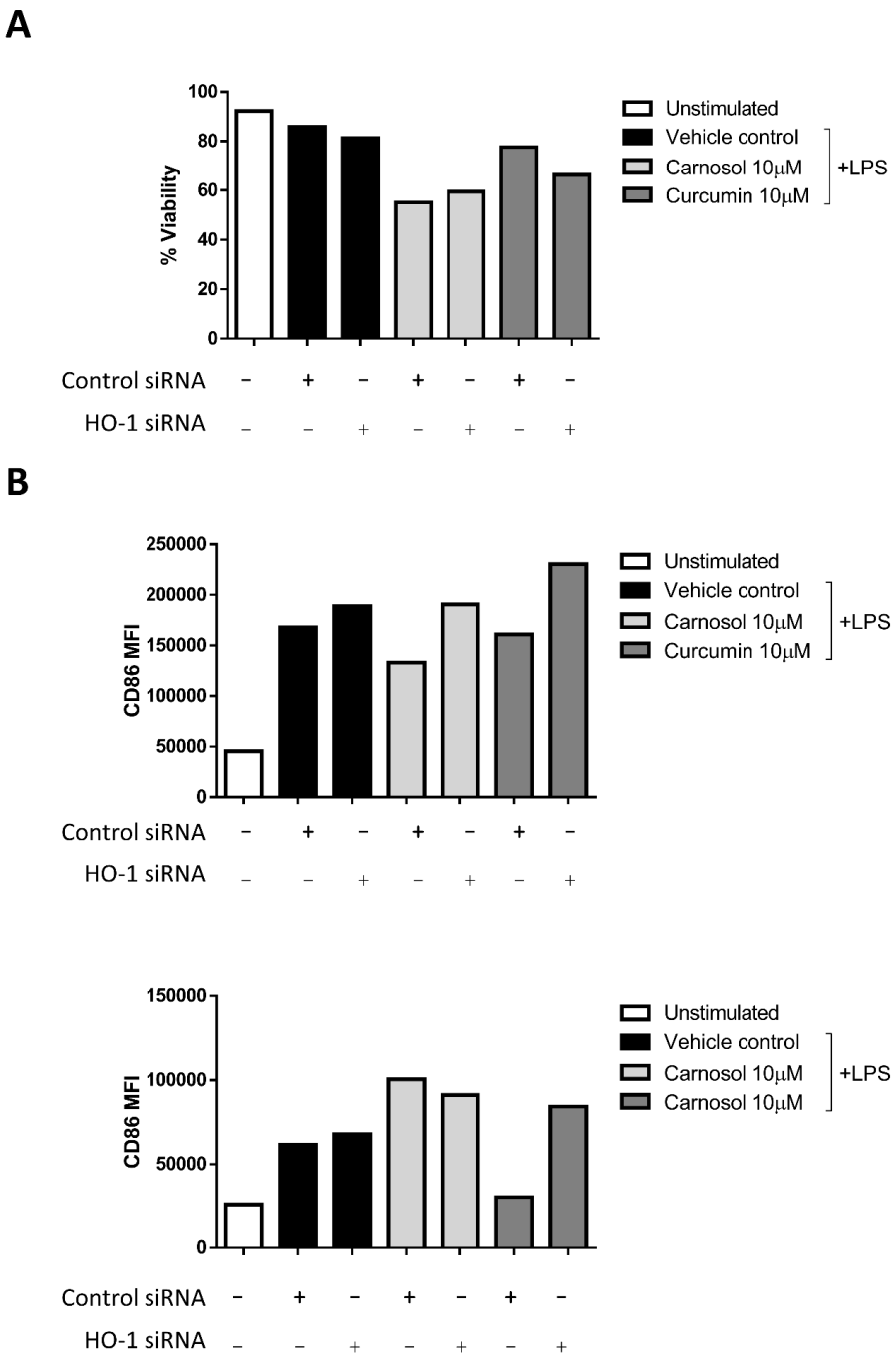

Figure app.1.2. siRNA transfection limits DC viability, but HO-1 knockdown may inhibit reduced CD86 expression in carnosol and curcumin treated DC. DC were transfected with non-targeting siRNA or siRNA targeting HO-1 for 24 hours, transfected a second time for a further 24 hours and treated with carnosol (10 μM), curcumin (10 μM) or a vehicle control for 6 hours prior to stimulation with LPS for 24 hours. Cells were stained with a fixable viability dye and a fluorescently-conjugated antibody against CD86. **(A)** Percentage viability of untransfected DC, and transfected DC treated with a vehicle control, carnosol or curcumin for 6 hours prior to stimulation with LPS for 24 hours. Data depicts one experiment in one donor. **(B)** Mean Fluorescence Intensity (MFI) of CD86 of untransfected DC, and transfected DC treated with a vehicle control, carnosol or curcumin for 6 hours prior to stimulation with LPS for 24 hours. Data depicts two experiments in two different donors.

2. PASI & IL-17 correlation

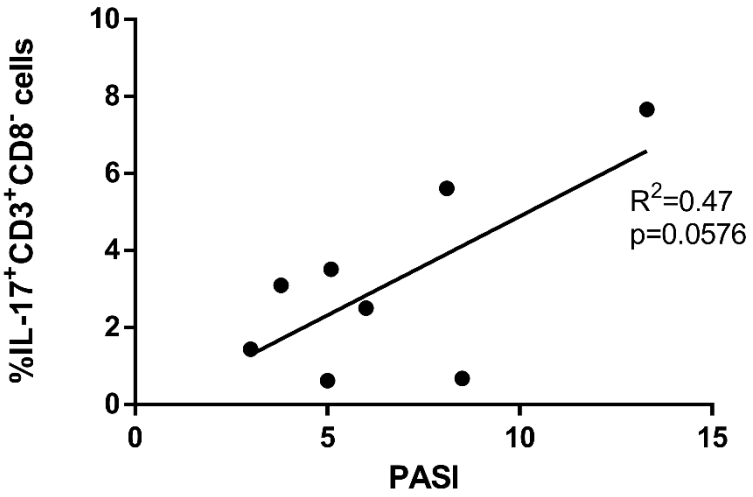

Figure app.2.1. Correlation of patient PASI scores with frequency of IL-17$^+$ T cells.

3. Full-length Western blots

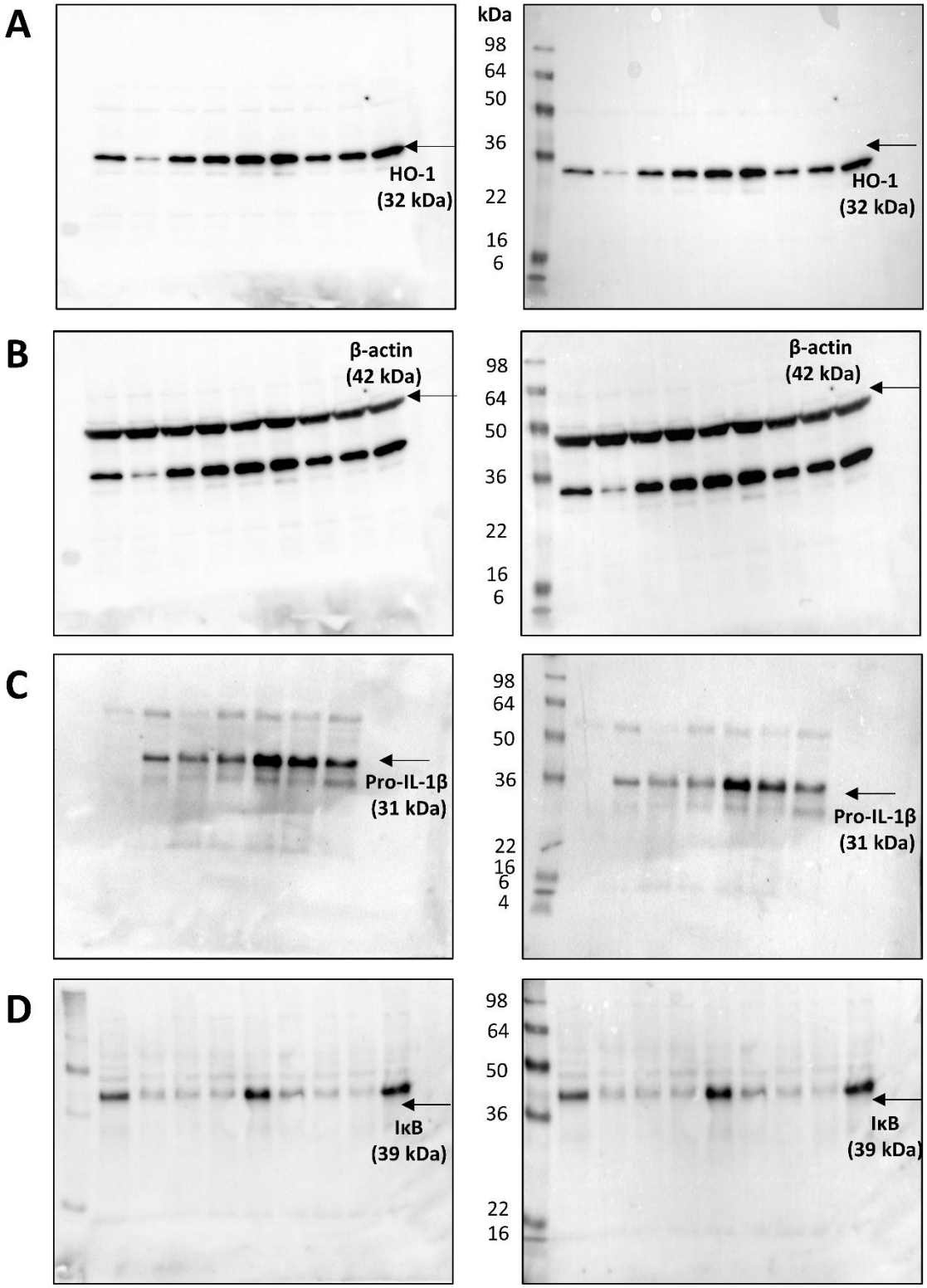

Figure app.3.1. Example full-length Western blots for HO-1, β-actin, pro-IL-1β and IκB. Full-length Western blots probed for **(A)** HO-1, **(B)** β-actin, **(C)** pro-IL-1β, and **(D)** IκB. Data shown depicts images of exposed bands alone (left) and merged images to include the protein ladder (right).

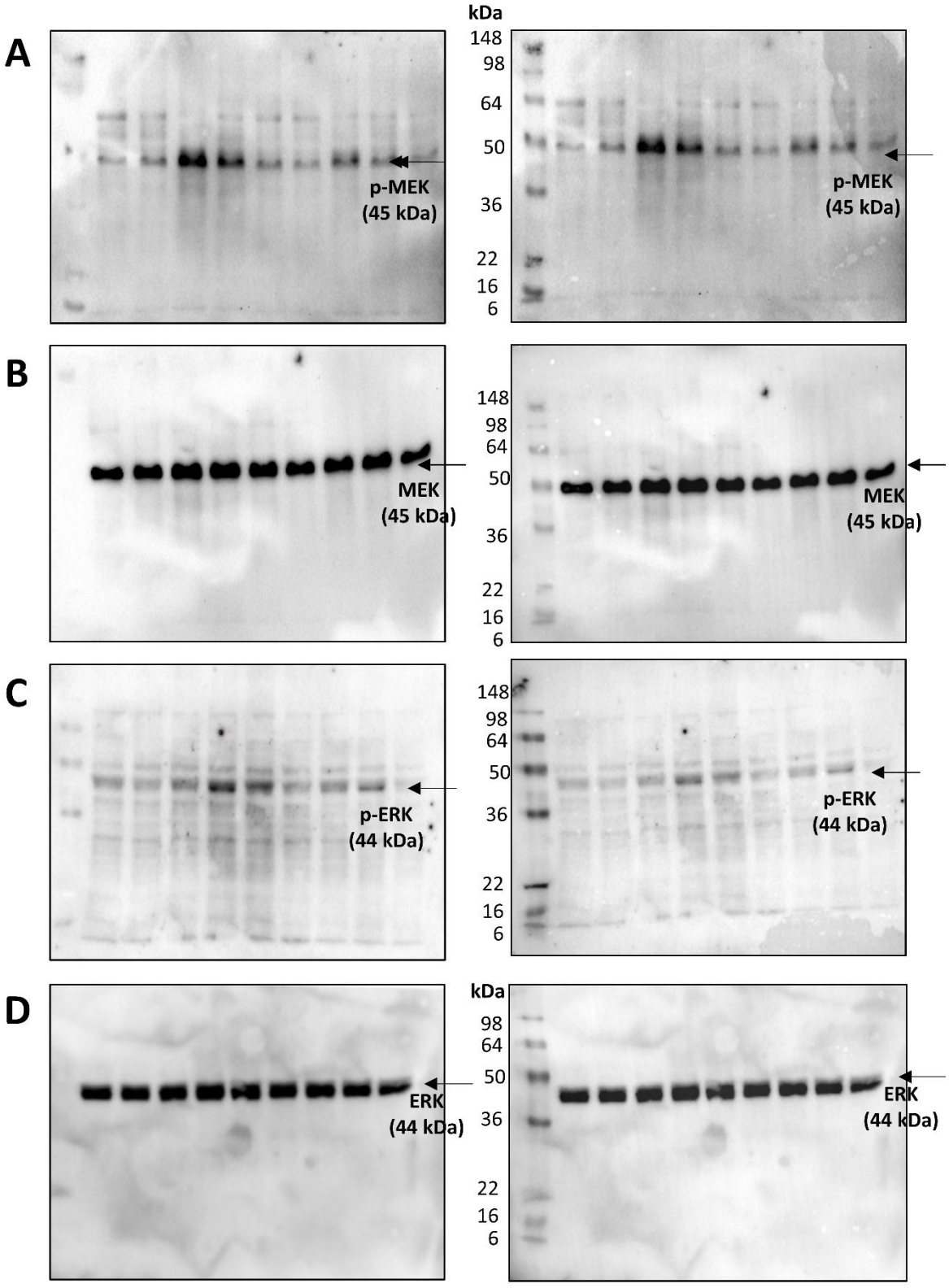

Figure app.3.2. Example full-length Western blots for p-MEK, MEK, p-ERK and ERK. Full-length Western blots probed for **(A)** p-MEK, **(B)** MEK, **(C)** p-ERK, and **(D)** ERK. Data shown depicts images of exposed bands alone (left) and merged images to include the protein ladder (right).

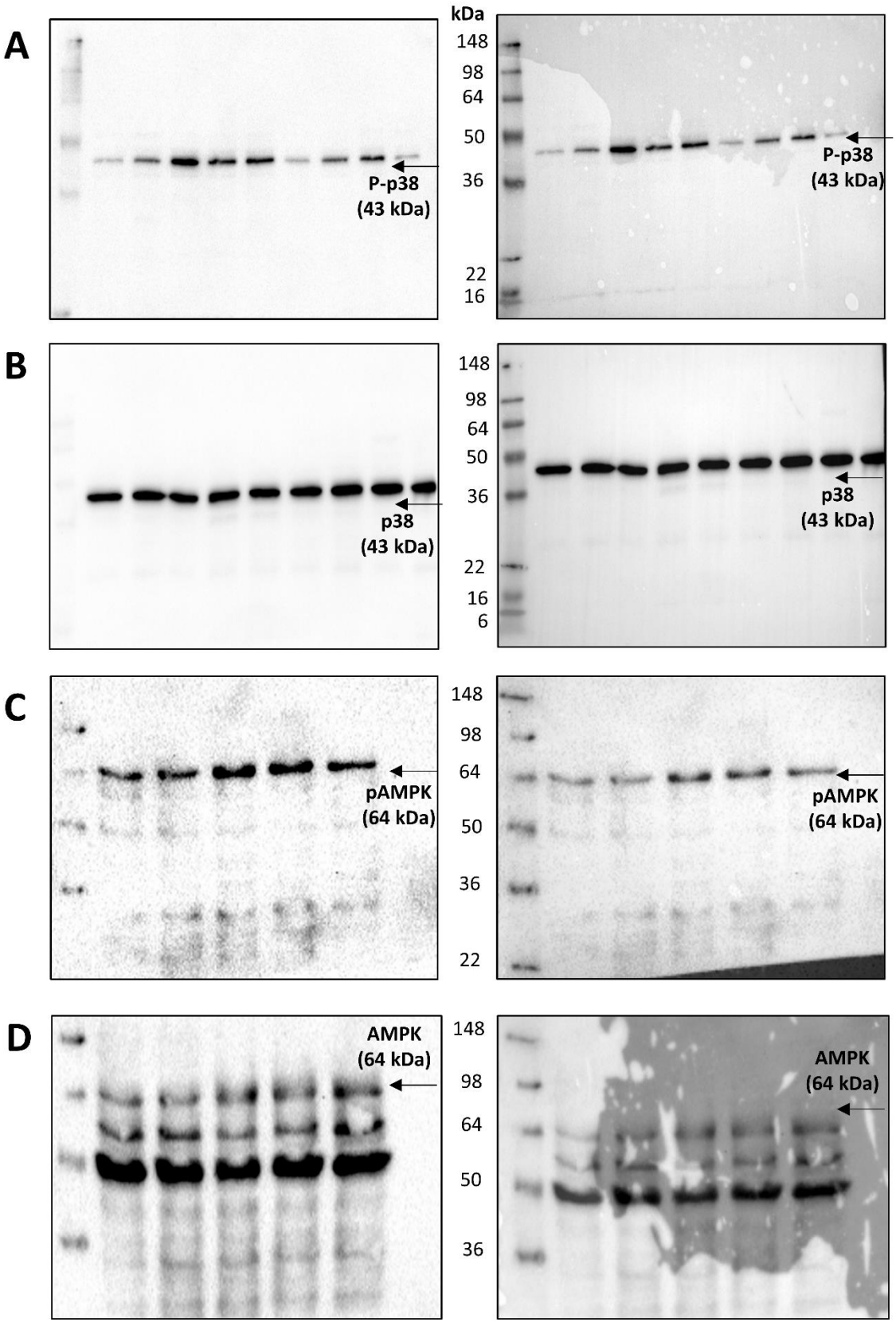

Figure app.3.3. Example full-length Western blots for p-p38, p38, p-AMPK and AMPK. Full-length Western blots probed for **(A)** p-p38, **(B)** p38, **(C)** p-AMPK, and **(D)** AMPK. Data shown depicts images of exposed bands alone (left) and merged images to include the protein ladder (right).

4. Flow cytometry gating strategies

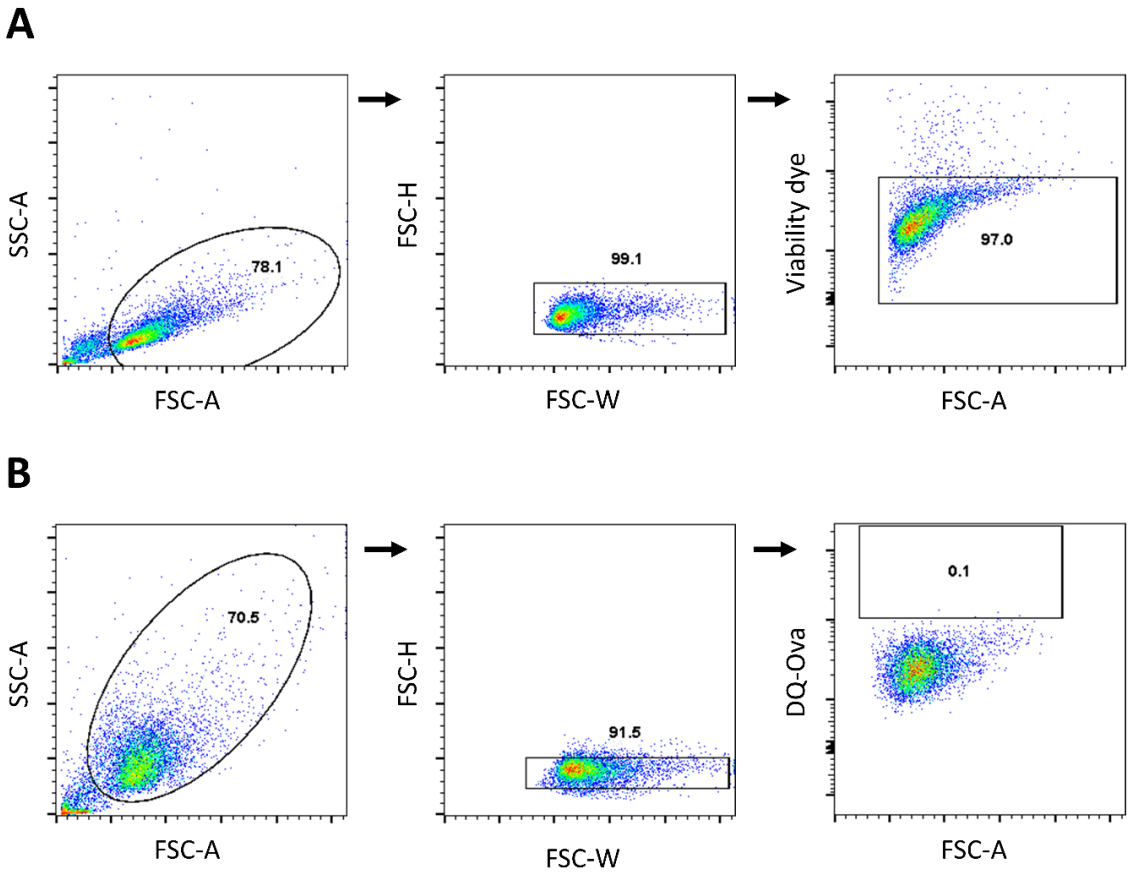

Figure app.4.1. Gating strategy for DC maturation and antigen uptake assays. (A) To assess expression of maturation markers by DC, the DC population was first selected by FSC and SSC. Single cells were then gated on by FSC width and height. Viable cells were then selected on the basis of viability dye exclusion. **(B)** To measure DQ-Ova uptake, the DC population was first selected on the basis of FSC and SSC in order to exclude debris and dying cells. Single cells were then selected on the basis of FSC width and height. The DQ-Ova+ cell gate was then drawn using control cells which were not incubated with DQ-Ova.

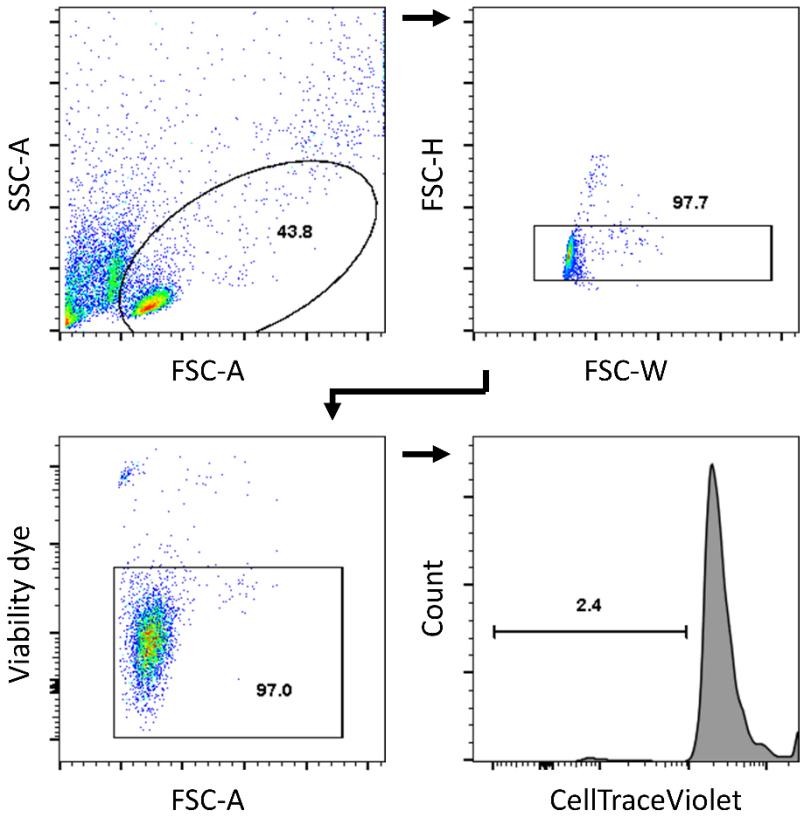

Figure app.4.2. Gating strategy for proliferation assays. To assess T cell proliferation, PBMC or $CD4^+$ T cells were labelled with CTV. Lymphocytes were first gated on the basis of FSC and SSC. Single cells were then gated on by FSC width and height. Viable cells were then selected on the basis of viability dye exclusion. The percentage of cell proliferation was determined using unstimulated control cells to draw the CTV histogram gate.

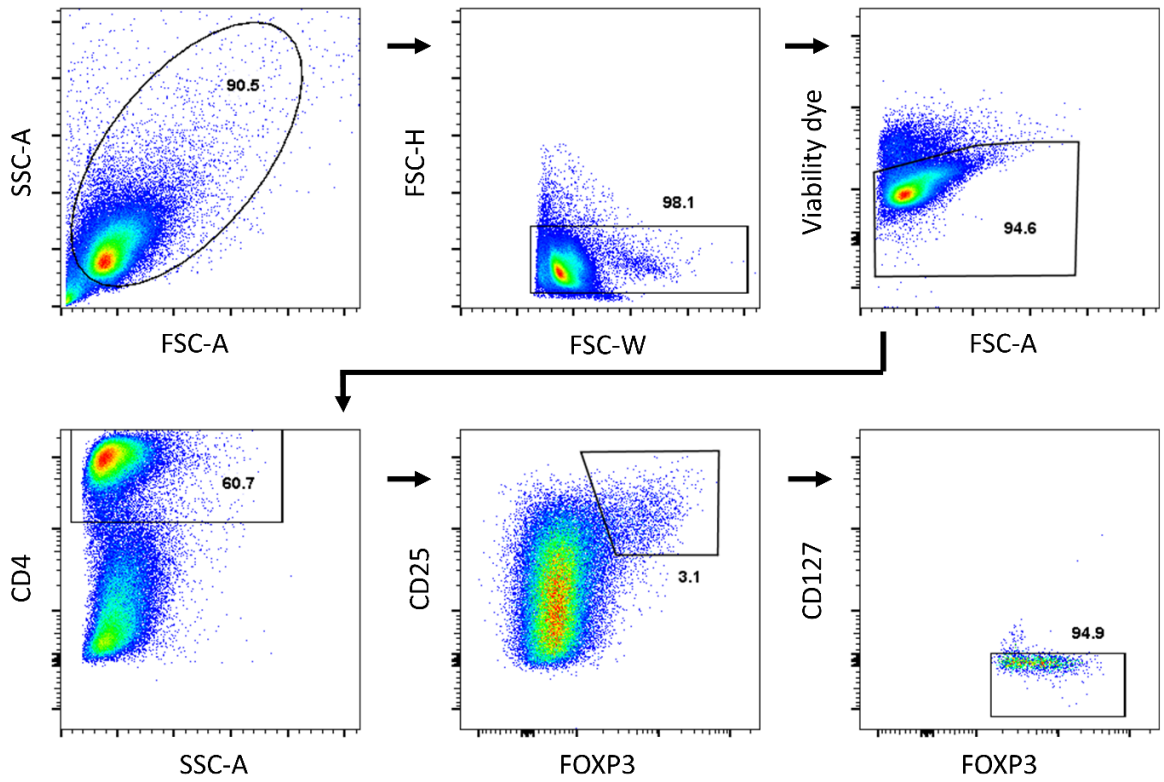

Figure app.4.3. Gating strategy for Tregs. To identify Treg cells, cells were stained with fluorochrome-conjugated antibodies against CD4, CD25, FOXP3 and CD127. Lymphocytes were gated on the basis of FSC and SSC. Single cells were then gated on by FSC width and height. Viable cells were then selected on the basis of viability dye exclusion. $CD4^+$ cells were selected from viable cells on the basis of high CD4 expression. $CD25^+Foxp3^+$ cells were then gated on within the $CD4^+$ population. Finally, $CD127^+$ cells were excluded to identify the population of $CD4^+CD25^+Foxp3^+CD127^{lo}$ Tregs.

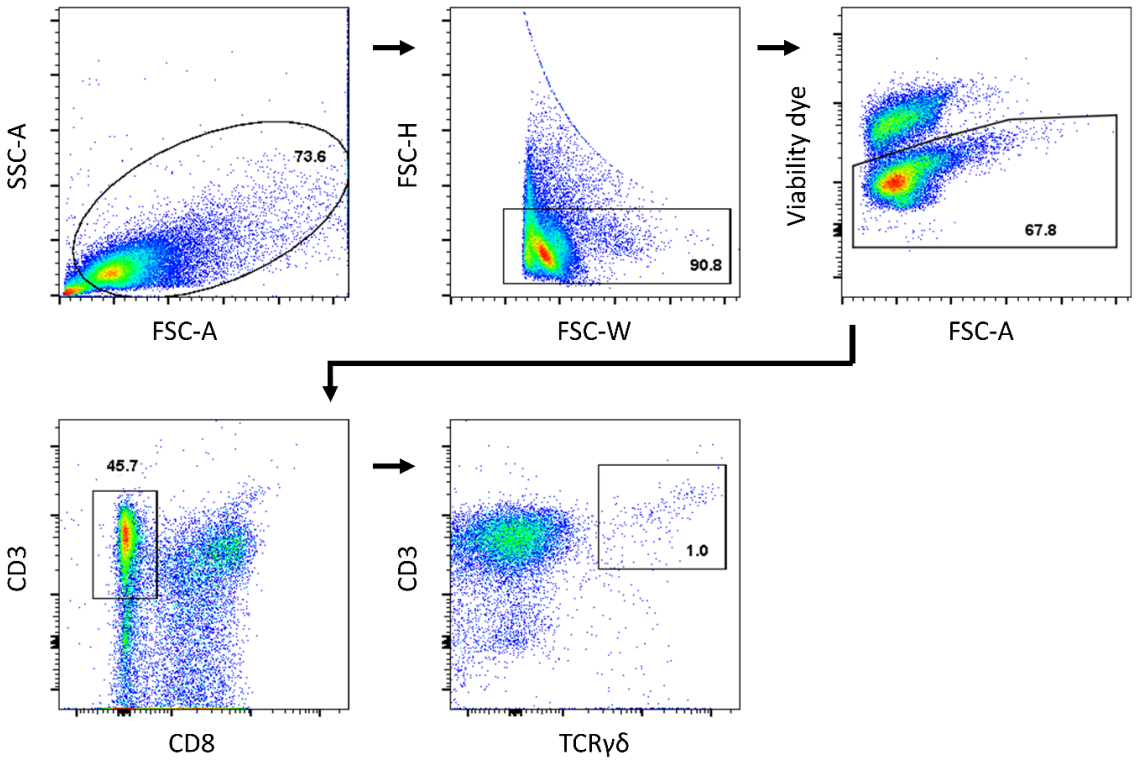

Figure app.4.4. Gating strategy for T cell cytokine assays. To assess cytokine production by T cells, cells were stimulated with PMA and ionomycin in the presence of brefeldin A prior to staining with fluorochrome-conjugated antibodies against T cell lineage markers and cytokines of interest. First, lymphocytes were gated on the basis of FSC and SSC. Single cells were then gated on by FSC width and height. Viable cells were then selected on the basis of viability dye exclusion. $CD3^{+}CD8^{-}$ cells were selected from the population of viable cells to identify helper T cells. Finally, $CD3^{+}TCR\gamma\delta^{+}$ cells were selected from the population of viable cells to identify γδ T cells.